JAERI 1300

JAERI 1300

THYDE-P2 : RCS (Reactor-Coolant System) Analysis Code

December 1986

日本原子力研究所

Japan Atomic Energy Research Institute

JAERI レポートは，日本原子力研究所が研究成果編集委員会の審査を経て不定期に公刊している研究報告書です。

入手の問合わせは，日本原子力研究所技術情報部情報資料課（〒319-11茨城県那珂郡東海村）あて，お申しこしください。なお，このほかに財団法人原子力弘済会資料センター（〒319-11 茨城県那珂郡東海村日本原子力研究所内）で複写による実費頒布をおこなっております。

JAERI reports are reviewed by the Board of Editors and issued irregularly.

Inquiries about availability of the reports should be addressed to Information Division Department of Technical Information, Japan Atomic Energy Research Institute, Tokai-mura, Naka-gun, Ibaraki-ken 319-11, Japan.

編集兼発行　日本原子力研究所

印　　刷　いばらき印刷㈱

THYDE-P2 Code : RCS (Reactor-Coolant System) Analysis Code

Yoshiro ASAHI, Masashi HIRANO and Kazuo SATO

Department of Reactor Safety Research
Tokai Research Establishment
Japan Atomic Energy Research Institute
Tokai-mura, Naka-gun, Ibaraki-ken

(Received March 24, 1986)

Abstract

THYDE-P2, being characterized by the new thermal-hydraulic network model, is applicable to analysis of RCS behaviors in response to various disturbances including LB (large break)-LOCA(loss-of-coolant accident). In LB-LOCA analysis, THYDE-P2 is capable of through calculation from its initiation to complete reflooding of the core without an artificial change in the methods and models.

The first half of the report is the description of the methods and models for use in the THYDE-P2 code, i.e., (1) the thermal-hydraulic network model, (2) the various RCS components models, (3) the heat sources in fuel, (4) the heat transfer correlations, (5) the mechanical behavior of clad and fuel, and (6) the steady state adjustment.

The second half of the report is the user's mannual for the THYDE-P2 code (version SV04L08A) containing items; (1) the program control (2) the input requirements, (3) the execution of THYDE-P2 job, (4) the output specifications and (5) the sample problem to demonstrate capability of the thermal-hydraulic network model, among other things.

Keywords: THYDE-P2 Code, RCS, Methods, Models, LOCA, Heat Transfer, Thermal-Hydraulic Network, Clad, Fuel, Version SV04L08A, User's Mannual, Sample Problem, RCS Transients

THYDE-P2：RCS（原子炉冷却材系）解析コード

日本原子力研究所東海研究所原子炉安全工学部

朝日　義郎・平野　雅司・佐藤　一男

（1986年3月24日受理）

要　　旨

THYDE－P2の特徴は新熱水力回路網モデルである．THYDE－P2は，LB－LOCA（大破断冷却材喪失事故）を含むところの種々の外乱に対して，RCSがいかに挙動するかを解析することができる．LB－LOCA解析に於いては，THYDE－P2は，方法とモデルの変更なしに，再冠水終了までの一貫解析をすることができる．

この報告書の前半では，THYDE－P2の方法とモデルとに関して，次のことが記述してある．(1) 熱水力回路網モデル，(2) 各種コンポーネントモデル，(3) 燃料中の熱源，(4) 熱伝達相関式，(5) 燃料と被覆管の機械的挙動，及び (6) 定常設定．

後半は，THYDE－P2（SV04L08A版）の使用手引書になっていて，次のことが記述してある．(1) プログラムコントロール，(2) インプットデータの入力方法，(3) THYDE－P2計算の実行方法，(4) 計算結果の出力方法と (5) 特に熱水力回路網モデルの性能を実証するサンプル問題．

CONTENTS

目　　次

List of Tables and Figures

List of Tables

List of Figures

1. Introduction

The subject matter of this document is the description of the computer code, THYDE-P2, concerned with LWR (light water reactor) plant dynamics, in response to various disturbances, including a break of a primary coolant system pipe, generally referred to as a loss-of-coolant accident (LOCA). LB(large break)-LOCA can be considered to be the most critical for testing the methods and models for plant dynamics, since thermal-hydraulic conditions in the system drastically change during the transient. Therefore, THYDE-P2 has intensively been applied to LOCA analysis to verify its methods and models. There are a number of computer codes[(2)-(8)] or code systems[(9),(10)] for use in LOCA analysis. But most of them tend to exhibit several difficulties such as mass imbalance and numerical instability.

First of all, mass or momentum or energy imbalance results from improper space differencing of the conservation equation. If space differencing is not correct, mass imbalance in LOCA analysis could be so large that a large amount of mass comparable to injected ECC water could "disapper" from the system. Secondly, even if the space differencing is correct, imbalance still could occur unless a non-linear implicit scheme were applied. Thirdly, various mode transitions, e.g., coolant phase change may bring about numerical instabilities.

These problems predominate especially at low pressure. This fact is the main reason why the secondary system of a PWR or the neiborhood of the turbine of a BWR, which is at low pressure already at steady state, has not been adequately included in transient analysis. In LOCA analysis, to avoid numerical instability induced by condensation ("water packing") and to somehow continue the reflood calculation, it has been customary in the existing LOCA analysis codes either to raise the ECC water enthalpy (RELAP-FLOOD[(9)]) or to neglect the time derivatives in the conservation equations (WREFLOOD[(6)]). These assumptions are not only unconvincing, but also are likely to lead to erroneous conclusions.

The main features of THYDE-P2 are (1) the complete steady state adjustment, (2) the new thermal-hydraulic network model, (3) the non-linear implicit scheme for thermal-hydraulics, (4) the non-equilibrium models, (5) the automatic time step width control and (6) vectorization of the program:

(1) THYDE-P2 carries out steady state adjustment, which is complete in the sense that the state obtained is the set of exact solutions to the null transient problem, i.e., the transient problem without an external disturbance, not only for thermal-hydraulics of the network, but also for all the other phenomena in the THYDE-P2 simulation of RCS.

(2) A new representation of a control volume has made it possible to develop a new thermal-hydraulic network model, which well matches our physical intuitions. The model reduces the flow equations by three steps, each of which is closely related to topological features of the hydraulic network. The new model does not depend on specific forms for the conservation equations, but is quite general. For example, the incorporation of thermal non-equilibrium effect in the model did not require substantial programming changes.

(3) To solve the equations of a network "exactly", an iterative method is applied based on the new network model. Applicability of a linear implicit method is questionable especially at low pressure when non-linearity of the flow equations predominates.

(4) Non-linear implicit scheme for use in the thermal-hydraulic network requires continuity of the various parameters involved in the flow equations. Physically, this amounts to taking into consideration non-equilibrium effects arising from various mode transitions.

(5) THYDE-P2 determines the time step width automatically as the calculation proceeds. The non-linear implicit method, the non-equilibrium model and the steady state adjustment are all combined to materialize the automatic time step width control of THYDE-P2.

These features have enabled THYDE-P2 to perform through calculation[43] of LB-LOCAs without an artificial change of the methods and models.

What is improved with THYDE-P2 as compared to THYDE-P1[44] is; (1) not only the mass and momentum equations but also the energy equation are included in the non-linear implicit scheme, (2) the valve model is implemented, (3) the relaxation equation for void fraction is theoretically derived, (4) vectorization of the program is implemented, (5) both EM (evaluation model) and BE (best estimate) calculations are possible and so on.

2. Thermal-Hydraulics

In this chapter, we will discuss the thermal-hydraulic network model of the THYDE-P2 code. Starting from the three conservation equations for two-phase mixture, we will develop the new calculation scheme for thermal-hydraulics such that mass, momentum and energy conserve. If we stay within the framework of the three conservation equations for two-phase mixture, however, it will be difficult to explain two major problems; (1) phase separation and (2) phase change. In order to solve these problems, we are obliged to resort to what is called UV (unequal velocity) and UT (unequal temperature) models. Thus, the UV effect will be accounted for on the basis of the drift flux model (see section 2.2.2), while the UT effect will be incorporated in the model by taking into consideration two other conservation equations for vapor (section 2.2.3).

In section 2.1, the various components for use in the THYDE-P2 thermal-hydraulic network modelling are defined. In section 2.2, we will derive the equations for the normal node and the various junctions from the conservation equations. In section 2.3, the new algorithm for a thermal-hydraulic system such as a PWR RCS is presented. It is the new node-and-junction representation of a thermal-hydraulic system that will enable us to construct the new thermal-hydraulic network model described in section 2.2. In THYDE-P2, the options are provided to model the steam generator (SG) secondary system, the pressurizer (PZR) and the accumulator (AC). They will be referred to as the special nodes, which are described in section 2.4 along with the pump model. In section 2.5, we will discuss the loss coefficient, the valve and the critical flow.

2.1 Network Components

In the THYDE-P2 code, a coolant system is regarded hydrodynamically as a network of various coolant components which may be classified into the nodes and the junctions as shown in **Tables 2–1** and **2–2**. In terms of these nodes and junctions, we will see, in the following discussions of this chapter, that a coolant system can be represented as a thermal-hydraulic network, in which a node and a junction appear alternately.

A normal node is a volume element to which the one-dimensional flow model may be applicable (see **Fig. 2–1–1**). It is the very representation of the conservation laws in such a volume element, i.e., a normal node, that will enable us to construct the new thermal-hydraulic network model to be described in section 2.2. We will see later that even a pump can be represented by a normal node. Let the positive direction of the flow be that of the steady state flow. For a node, the inlet and outlet of the steady state flow will be referred to as points A and E, respectively.

A normal junction serially connects two normal nodes possibly with a sudden area change (see **Fig. 2–1–2**). Among nodes and junctions in **Tables 2–1** and **2–2**, only mixing junctions are multiple-branched (see **Fig. 2–1–3**). Owing to this very feature, they play an essential role in forming a complex coolant network such as a reactor coolant system (see **Fig. 2–3–4**).

A boundary junction will be placed at an interface between our thermal-hydraulic network and its exterior. The dead end of a duct can be simulated by a boundary junction through which no interaction with the exterior takes place. We call the node adjacent to a boundary junction the boundary node, which are classified into the guillotine break node, the dead end node and the injection node. The boundary conditions of the system will be incorporated in the model by modifying the equations for the boundary node.

The duct connecting a boundary junction to a mixing junction of the network is called a linkage duct which is composed of a number of normal nodes called the linkage nodes (see **Fig. 2–1–4**). The steady state linkage flow can be stagnant. We let point E of a linkage flow be the end adjacent to the boundary junction, whereas point A be the other end adjacent to the mixing junction. Accordingly, points A and E of each linkage node can be determined. It should be noted that prior to a double-ended break, the break point is regarded as a normal junction, but after the break the break point will be considered as a boundary junction.

Finally, we note that a node and a mixing junction have volume whereas a normal or boundary junction is volumeless. We also note that in a power plant the thermal-hydraulic network can be regarded as medium which combines thermal-hydraulically the thermal, mechanical and neutronic behaviors of the system.

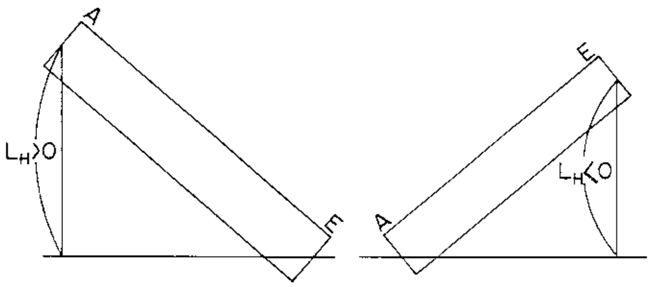

Fig. 2–1–1 Normal Node.

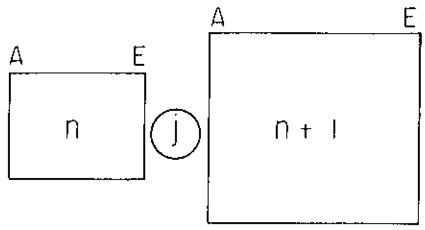

Fig. 2–1–2 Two Successive Normal Nodes Connected by Normal Junction.

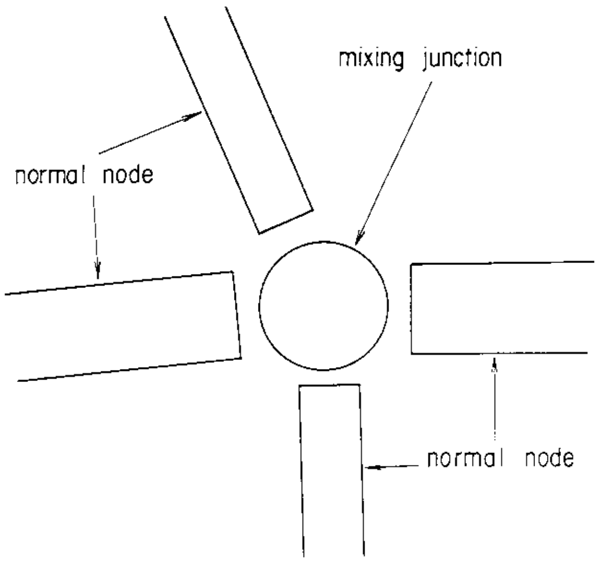

Fig. 2–1–3 Mixing Junction.

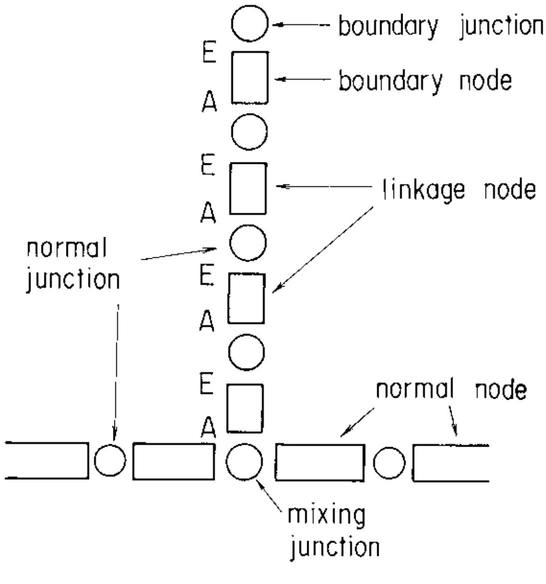

Fig. 2–1–4 Linkage Nodes.

Table 2–1 Nodes

node	normal node	duct
		flow channel
		pump
		others
	special node	SG 2ndry system
		pressurizer
		accumulator
		discharge tank

Table 2–2 Junctions

junction	normal junction	
	mixing junction	(a) lower plenum
		(b) upper plenum
		(c) downcomer top
		(d) others
	boundary junction	(a) hydraulic source
		(b) injection flow
		(c) dead end
		(d) break
		(e) others

2.2 Derivation of Network Equations

In this section, we will derive the equations for the network under the several assumptions. They would be subjected to improvements based on future progress in two-phase flow research.

2.2.1 Conservation Equations for Two-Phase Mixture

The one-dimensional mass, energy and momentum equations for the two-phase mixture(2-6) are given by

$$\frac{\partial}{\partial t} A\rho + \frac{\partial}{\partial z} AG = 0 \tag{2-2-1}$$

$$\frac{\partial}{\partial t} A\rho h + \frac{\partial}{\partial z} A\Lambda = Aq''' \tag{2-2-2}$$

and

$$\frac{\partial}{\partial t} AG + A\frac{\partial p}{\partial z} + \frac{\partial}{\partial z} A\Psi = -A\rho g - \frac{A}{2}\left(\frac{\kappa}{L} + \frac{f}{D}|G|G\right)\frac{\Phi^2}{\rho_f} \tag{2-2-3}$$

where

$$\begin{aligned} \kappa &= kG|G| & Re \geqq Re_t \\ &= (k\mu/D)Re_t G & Re \leqq Re_t \end{aligned} \tag{2-2-4}$$

$$\rho = \alpha\rho_g + (1-\alpha)\rho_f \tag{2-2-5}$$

$$G = \alpha\rho_g u_g + (1-\alpha)\rho_f u_f \tag{2-2-6}$$

$$\Psi = \alpha\rho_g u_g^2 + (1-\alpha)\rho_f u_f^2 \tag{2-2-7}$$

$$\Lambda = \alpha\rho_g h_g u_g + (1-\alpha)\rho_f h_f u_f \tag{2-2-8}$$

$$\rho h = \alpha\rho_g h_g + (1-\alpha)\rho_f h_f \tag{2-2-9}$$

We consider in the following way. The solution to the conservation equations for the mixture, i.e., Eqs. (2–2–1) to (2–2–3) defines the equilibrium state with the assumption that the two phases are at the saturation temperature. In general, the actual state is different from the equilibrium state. The actual (non-equilibrium) state will asymptotically approach the equilibrium by transferring energy between the phases, if the mixture is left without external disturbances.

2.2.2 Thermal-Hydraulic Quantities

We eliminate u_g and u_f in Eqs. (2–2–7) and (2–2–8) with the help of

$$u_f=\frac{G-\alpha\rho_g u_{rel}}{\rho}$$

and

$$u_g=\frac{G+(1-\alpha)\rho_f u_{rel}}{\rho}$$

Then, we obtain

$$\Psi=\frac{G^2}{\rho}+B \tag{2–2–10}$$

and

$$A=Gh+I \tag{2–2–11}$$

where

$$B=\frac{\alpha(1-\alpha)\rho_g\rho_f}{\rho}u_{rel}^2 \tag{2–2–12}$$

and

$$I=\frac{\alpha(1-\alpha)\rho_g\rho_f h_{gf}}{\rho^2}u_{rel} \tag{2–2–13}$$

The relative velocity u_{rel} may be given by the drift flux model(11) as

$$u_{rel}=\frac{u_{gj}}{1-\alpha} \tag{2–2–14}$$

where u_{gj} is the drift velocity(12),(13), and

$$u_{gj}=1.14\left[\frac{\sigma g(\rho_{fs}-\rho_{gs})}{\rho_{fs}^2}\right]^{1/4}S_\alpha^2 \tag{2–2–15}$$

for the "churn-turbulent" bubbly flow. The factor S_α^2 is used to avoid divergence of u_{rel} when α approaches unity such that

$$S_\alpha=1-e^{(1-\alpha)/(1-\alpha_c)} \tag{2–2–16}$$

with α_c =0.8. When α is large, the flow pattern becomes annular or stratified flow so that u_g and u_f could change independently. Momentum flux B has been found usually not effective, while enthalpy flux I may play an important role, for example, in phase separation under vertical low flow condition.

Next, we obtain equilibrium quantities. Equilibrium mass quality may be given by

$$x_1=\frac{h-h_{fs}(p)}{h_{gfs}(p)} \tag{2–2–17}$$

which, however, can become either greater than unity or less than zero. Therefore, we might define mass quality such that

$$
\begin{aligned}
x_c &= 1 & & h>h_{gs}\\
&= x_1 & & h_{fs}\leqq h\leqq h_{gs}\\
&= 0 & & h<h_{fs}
\end{aligned}
$$

But, since the derivatives of mass quality defined above are not continuous at x_1 = 0 or 1, we can not obtain the solution so that mass, energy and momentum conserve. This is one of the problems associated with phase change.

In order to overcome the difficulty, we will define the equilibrium mass quality x_c which is a smooth function of p and h and bounded between zero and unity such that

$$x_c = \begin{cases} ae^{-(a-x_1)/a} & x_1 < a \\ x_1 & a \leqq x_1 \leqq b \\ 1-(1-b)e^{-(x_1-b)/(1-b)} & x_1 > b \end{cases} \tag{2-2-18}$$

where $0 < a < b < 1$. In terms of x_c, we can define

$$\alpha_c = \frac{x_c \rho_{fs}}{x_c \rho_{fs} + (1-x_c)\rho_{gs}} \tag{2-2-19}$$

where $0 < \alpha_c < 1$. We will call the quantity α_c the void fraction in what is called the equilibrium model (see subsection 2.2.3).

Next, we discuss the implications of the modifications of x_1 for $x_1 < a$ and $x_1 > b$, i.e., Eq. (2–2–18). Consider the equilibrium state so that $\alpha = \alpha_c$. Then Eq. (2–2–9) gives

$$h = x_c h_g + (1-x_c)h_f \tag{2-2-20}$$

since $x_c = \frac{\alpha \rho_g}{\rho}$. On the other hand, Eq. (2–2–17) implies

$$h = x_1 h_{gs} + (1-x_1)h_{fs} \tag{2-2-21}$$

For $a \leqq x_1 \leqq b$, $x_1 = x_c$ so that we can define

$$h_g = h_{gs} \quad \text{and} \quad h_f = h_{fs} \tag{2-2-22}$$

For $x_1 < a$, assuming $h_g = h_{gs}$ in Eq. (2–2–20), we obtain

$$h_f = \frac{h - x_c h_{gs}}{1 - x_c} \tag{2-2-23}$$

and

$$h_g = h_{gs}. \tag{2-2-24}$$

For $x_1 > b$, assuming $h_f = h_{fs}$, we similarly obtain

$$h_g = \frac{h - h_{fs}(1-x_c)}{x_c} \tag{2-2-25}$$

and

$$h_f = h_{fs}$$

Eq. (2–2–23) implies that h_f is less than h_{fs} at saturated equilibrium state close to the subcooled state, while Eq. (2–2–25) implies that h_g is greater than h_{gs} at saturated equilibrium state close to the superheated state.

Equilibrium specific enthalpies h_g and h_f thus obtained may be used to obtain gas and liquid densities. But, in order to obtain non-equilibrium gas and liquid densities in transient calculations, it is necessary to avoid the almost discontinuous changes of $\partial h_g / \partial h$ at $h = h_{gs}$ and $\partial h_f / \partial h$ at $h = h_{fs}$, which take place at $x_1 = 0$ and $x_1 = 1$, respectively.

Moreover, the equilibrium void fraction α_c defined by Eq. (2–2–19) behaves like a step function near $x_1 = 0$ at low pressure. This is the main reason for the water packing problem. In the next subsection, we intend to solve this problem by considering a non-equilibrium model.

2.2.3 Relaxation Equation for Void Fraction

In this subsection, we will derive the relaxation equation for void fraction, which is closely related to what is called the UT model or the non-equilibrium model. The assumptions and comments concerning this derivation are listed below:

(1) In this subsection, we will assume that mixture specific enthalpy h has already been obtained by solving Eq. (2–2–2), i.e., acounting for heat transferred from the wall and enthalpy transported by the flow. Therefore, these effects do not present themselves in the

following discussion, but only heat flow between the phases.

(2) Given any pair of p and h, we can uniquely define the (fictitious) equilibrium state with void fraction $\alpha_c(p, h)$ as described in the previous subsection. In the equilibrium state, vapour and liquid temperatures are equal to the saturation temperature $T_s(p)$ so that there is no heat flow between the phases.

(3) An actual (non-equilibrium) state can be defined by p, h and say, non-equilibrium void fraction α. In a non-equilibrium state, $T_g \neq T_f$ so that there will be heat flow between the phases.

(4) In view of comment (2), for each actual state with p, h and α, there corresponds an equilibrium state defined by p and h. An equilibrium state is usually fictitious, but assumed to actually exist if p and h are kept constant for a long time.

(5) Evaporation is assumed to take place (quasi-statically) with change of α_c regardless of equilibrium or non-equilibrium. In other words, evaporation in a non-equilibrium state is taking place as much as that in the corresponding equilibrium state. The deviation from the equilibrium state contributes not to evaporation, but heat flow between the phases leading to thermal-equilibrium.

(6) Consider a non-equilibrium state with constant p and constant h. Then, no evaporation occurs in the corresponding equilibrium state, and hence neither in the non-equilibrium state. But, non-equilibrium void fraction α can still change such that α asymptotically approaches to $\alpha_c(p, h)$ due to energy transfer (or heat flow) between the phases, if the mixture is left without external disturbances.

In the following, given p and h, we will examine how (α, T_g, T_f) can deviate from (α_c, T_s, T_s) and then derive the equation which governs the dynamic behavior of the actual void fraction α.

Let the incremental values with δ mean the deviation from the equilibrium value. Then, any quantity can be divided into two parts, e.g.,

$$\alpha = \alpha_c + \delta\alpha \qquad (2\text{–}2\text{–}27)$$

The interfacial heat flux

$$\Phi_{int} = h_{tr}^{int} (T_f - T_g) \qquad (2\text{–}2\text{–}28)$$

is an essentially non-equilibrium quantity since $T_f = T_g = T_s$ at equilibrium. We note that at non-equilibrium, neither the gas nor the liquid is at saturation. We assume that the interfacial heat flow, which is effective only at non-equilibrium, will be used not for phase change, but for temperature change of each phase, leading to an equilibrium state.

Energy conservation for the gas gives

$$\frac{\partial}{\partial t} \alpha \rho_g h_g + \frac{\partial}{\partial z} \alpha \rho_g h_g u_g = \frac{S_{int}\, \Phi_{int}}{V} \qquad (2\text{–}2\text{–}29)$$

where V is the total volume of the mixture. Mass conservation for the gas gives

$$\frac{\partial}{\partial t} \alpha \rho_g + \frac{\partial}{\partial z} \alpha \rho_g u_g = \Gamma \qquad (2\text{–}2\text{–}30)$$

where Γ may be expressed as

$$\Gamma = \Gamma_c + \delta\Gamma \quad . \qquad (2\text{–}2\text{–}31)$$

We assume that the gas production takes place only when the mixture is saturated and that the interfacial heat flow is used only to change the internal energy of the two phases, leading to the equilibrium state. Thus, we have,

$$\delta\Gamma = 0 \quad . \qquad (2\text{–}2\text{–}32)$$

If Γ_c is given by

$$\Gamma_c = \frac{\partial}{\partial t} \alpha_c \rho_{gs} + \frac{\partial}{\partial z} \alpha_c \rho_{gs} u_g \quad (2-2-33)$$

then Eq. (2–2–30) yields

$$\delta(\alpha \rho_g) = 0 \quad . \quad (2-2-35)$$

Substituting the equation of state for the gas

$$\rho_g = \frac{p}{RT_g} \quad (2-2-36)$$

into Eq. (2–2–35), we obtain

$$\frac{\delta \alpha}{\alpha} = \frac{\delta T_g}{T_g} \quad . \quad (2-2-37)$$

In terms of the non-equilibrium quantities, h in Eq. (2–2–18) can be expressed as

$$x h_g + (1-x) h_f = h \quad (2-2-39)$$

where

$$x = \frac{\alpha \rho_g}{\alpha \rho_g + (1-\alpha) \rho_f} \quad . \quad (2-2-40)$$

Neglecting $\delta \rho_f$ and using Eq. (2–2–35), we obtain

$$\delta x = \frac{\alpha \rho_g \rho_f}{\rho^2} \delta \alpha \quad . \quad (2-2-41)$$

Using Eq. (2–2–41) and $\delta h = 0$, we obtain from Eq. (2–2–39),

$$\left(\frac{h_{gf} \alpha \rho_f}{\rho} + C_{pg} T_g \right) \rho_g \delta \alpha + (1-\alpha) \rho_f C_{pf} \delta T_f = 0 \quad (2-2-42)$$

Now, in Eqs. (2–2–37) and (2–2–42), we set

$$\delta T_g = T_f - T_s$$

$$\delta T_g = T_g - T_s \quad (2-2-43)$$

$$\delta \alpha = \alpha - \alpha_c$$

to obtain

$$T_g - T_s = \frac{\alpha - \alpha_c}{\alpha} T_g \quad (2-2-44)$$

and

$$T_f - T_s = \frac{(h_{gf} \alpha \rho_f / \rho + C_{pg} T_g) \rho_g}{(1-\alpha) \rho_f C_{pf}} (\alpha_c - \alpha) \quad . \quad (2-2-45)$$

Eqs. (2–2–44) and (2–2–45) mean that (1) if one of the phases is saturated, so is the other, and (2) either $T_g > T_s > T_f$ or $T_g < T_s < T_f$ or $T_g = T_f = T_s$ is possible. These results are consistent with the assumptions made at the beginning.

Substituting Eqs. (2–2–44) and (2–2–45), into Eq. (2–2–33), we obtain

$$\Phi_{int} = h_{tr}^{int} \left[\frac{T_g}{\alpha} + \frac{h_{gf} \alpha \rho_f \rho_g / \rho + C_{pg} T_g \rho_g}{(1-\alpha) \rho_f C_{pf}} \right] (\alpha_c - \alpha) \quad (2-2-46)$$

Equation (2–2–29) with Eq. (2–2–46) describes void propagation with relaxation. In THYDE-P2, it will be further transformed to obtain the void relaxation equation without the propagation term. Substituting Eq. (2–2–46) into Eq. (2–2–29), assuming $T_g = T_f = T_s$ and $\rho_g h_g = \rho_{gs} h_{gs}$ and neglecting the second term of the left hand side, we obtain

$$\frac{d}{dt} \alpha = \frac{\alpha_c - \alpha}{\tau} \quad (2-2-47)$$

where the time constant is a function of void fraction, among other things, such that

$$\tau = \frac{\rho_{gs} h_{gs} A_\alpha}{h_{tr}^{int} T_s [1 + (C_{pg}\rho_{gs}/C_{pf}\rho_{fs} - 1)\alpha + (h_{gf}\rho_{fs}/T_g \rho C_{pf})\alpha^2]} \qquad (2\text{-}2\text{-}48)$$

with

$$A_\alpha = \frac{V\alpha(1-\alpha)}{S_{int}} \quad . \qquad (2\text{-}2\text{-}49)$$

Factor A_α can further be transformed for bubbly or dispersed flow such that it is independent of V and S_{int}. For bubbly flow, we note:

$$\frac{\alpha V}{S_{int}} = \frac{V_g}{S_{int}}$$

= (volume of single bubble)/(surface area of single bubble)

$$= \frac{d_g}{6} \quad .$$

A similar manipulation is possible for dispersed flow. Thus, we obtain;

$$A_\alpha = \frac{d_g}{6}(1-\alpha) \qquad ; \text{bubbly flow } (\alpha \ll 1) \qquad (2\text{-}2\text{-}50)$$

$$\frac{d_f}{6}\alpha \qquad ; \text{dispersed flow } (\alpha \sim 1)$$

where Taylor instability[45] gives

$$d_g = d_f = 2\left(\frac{\sigma}{g(\rho_f - \rho_g)}\right)^{1/2} \equiv d \quad .$$

In THYDE-P2, the interfacial heat transfer coefficient h_{tr}^{int} is chosen to be

$$h_{tr}^{int} = \frac{d\rho_g h_{gs}}{6T_s} \exp\left(\frac{p-b}{a}\right)\frac{\rho}{\rho_f} \qquad (2\text{-}2\text{-}51)$$

where

$[p]$ = ata

a = 15.4 ata

and

b = 30 ata .

Interpolating A_α smoothly between bubbly and dispersed flows, we obtain from Eq. (2–2–48),

$$\tau = \frac{1-\alpha-\alpha^2}{B\exp((p-b)/a)}$$

where

$$B = \frac{\rho}{\rho_f}[1 + (C_{pg}\rho_{gs}/C_{pf}\rho_{fs} - 1)\alpha + (h_{gf}\rho_{fs}/T_g\rho C_{pf})\alpha^2]$$

$$\sim (1-\alpha)^2 + \frac{h_{gf}}{T_s C_{pf}}\alpha^2 \quad .$$

In Eq. (2–2–51), the interfacial heat transfer coefficient h_{tr}^{int} is assumed (1) to have the same pressure dependence as of nucleate boiling, (2) to be large for bubbly flow and small for dispersed flow and (3) for τ given by Eq. (2–2–48) to be of order of 5 – 10 seconds at 5 ata. Factors exp $((p-b)/a)$, ρ/ρ_f and $d\rho_g h_{gs}/(6T_s)$ account for items (1), (2) and (3), respectively.

Eq. (2–2–47) will be referred to as the relaxation equation for the void fraction. We now let p and h vary, following the conservation equations for the mixture. We here note that the effect of change of h on the relaxation equation presents itself mainly through α_c. As h includes the contribution of external heat source (see Eq. (2–2–2)), so does α_c.

2.2.4 Normal Node Equations

We assume that a normal node has uniform cross section A, length L, height L_H, and external heat source q'''. It should be noted that height L_H is signed as shown in **Fig. 2–2–1**. Since we assume uniform cross section for a normal node, the symbol A in Eqs. (2–2–1) to (2–2–3) entirely drops.

In THYDE-P2, the number of the parallel channels, the flow area per channel A and the hydraulic diameter D are to be inputted. For a core flow associated with a fuel rod whose pitch and outer radius are l_p and r_R, respectively, A and D to be inputted may be given as follows.

$$A = l_p^2 - \pi r_R^2$$

and

$$D = \frac{2A}{\pi r_R}$$

In this report, the super- or sub-scripts A, E, av, new and old will be used to refer to point A, point E, node average point, time $t+\Delta t$ and time t, respectively. Symbols new and av. however, frequently will be dropped. For a variable $f(\rho, G, h)$, its node average f^{av} will be defined as

$$f^{av} = f(\rho^{av}, h^{av}, G^{av})$$

where

$$\rho^{av} = (\rho^A + \rho^E)/2$$

$$G^{av} = (G^A + G^E)/2$$

and h^{av} is given as the solution of Eq. (2–2–53).

Differencing Eqs. (2–2–1), (2–2–2) and (2–2–3), spatially between points A and E within a normal node and temporally between $t+\Delta t$ (new) and t (old), we obtain

$$f_{1n} = -L_n \frac{\rho_n - \rho_n^{old}}{\Delta t} + G_n^A - G_n^E = 0 \qquad (2\text{–}2\text{–}52)$$

$$f_{5n} = -L_n \frac{\rho_n h_n - \rho_n^{old} h_n^{old}}{\Delta t} + \Lambda_n^A - \Lambda_n^E + q_n''' L_n = 0 \qquad (2\text{–}2\text{–}53)$$

$$f_{4n} = -L_n \frac{G_n^A + G_n^E - G_n^{A\,old} - G_n^{E\,old}}{2\Delta t} + p_n^A - p_n^E + \Psi_n^A - \Psi_n^E - \frac{1}{2}\left(\kappa - \frac{fL}{D}|G|G\right)_n \frac{\Phi_n^2}{\rho_{fn}}$$
$$- \rho_n^{av} g (L_H - L_{head})_n = 0 \qquad (2\text{–}2\text{–}54)$$

In order to define specific enthalpies h_n^A and h_n^E for normal nodes and h_j^+ for normal junctions (see subsection 2.2.5), we define η_n^A and η_n^E for normal nodes such that

$$\frac{d}{dt}\eta_n^i = \frac{(S_i - \eta_n^i)}{\tau} \qquad (i = A \text{ or } E) \qquad (2\text{–}2\text{–}55)$$

where

$$S_i = 1 \qquad (G_n^i)^{old} < 0 \qquad (2\text{–}2\text{–}56)$$
$$\quad\; 0 \qquad (G_n^i)^{old} \geq 0.$$

Equation (2–2–55) describes the enthalpy mixing when a flow direction change takes place. The time constant τ may be obtained by physically considering the enthalpy mixing process, but it is set to be 0.05 sec in the present version of THYDE-P2.

Then, h_n^A and h_n^E can be defined such that

$h_n^A = h_{from}^+$ if the from-junction is volumeless and open (not break).

$= h_n^{old}$ if point A is closed.

$= h_{from}^+(1-\eta_n^A) + h_n\eta_n^A$ otherwise . (2–2–57)

and

$h_n^E = h_{to}^+$ if the to-junction is volumeless and open (not break).

$= h_n^{E\,old}$ if point E is closed.

$= h_{to}^+\eta_n^E + h_n(1-\eta_n^E)$ otherwise . (2–2–58)

If the to-junction is a boundary junction, then $h_{to}(t)$ in Eq. (2–2–58) should be given as a boundary condition. This is also the case with $h_{from}(t)$ in Eq. (2–2–57).

In Eq. (2–2–53), we note that

$$A = Gh + I$$

(see Eq. (2–2–11)). The relative enthalpy fluxes I_n^A and I_n^E must carefully be defined to ensure its continuity at junctions. First consider **Fig. 2–1–2**, in which normal nodes n and $n+1$ are connected by normal junction j. Let I_j^+ be the total relative enthalpy flux through junction j.

Then

$$I^+ = \begin{cases} A^+\tilde{I}^+ & C_{VH}^n + C_{VH}^{n+1} = 1 \text{ or } 2, \\ & (x_1)_n > 0, \quad (x_1)_{n+1} < 1 \\ -A^+\tilde{I}^+ & C_{VH}^n + C_{VH}^{n+1} = -1 \text{ or } -2, \\ & (x_1)_n < 1, \quad (x_1)_{n+1} > 0 \\ 0 & \text{otherwise} \end{cases}$$

where $\tilde{I}^+$ is the coordinate independent relative enthalpy flux and c_{VH} is defined to be

$c_{VH} = 1$ for $L_H > 0$

$= -1$ for $L_H < 0$

$= 0$ for $L_H = 0$.

Assuming continuity of total relative enthalpy flux,

$$I^+ = A_n(I_c^E)_n = A_{n+1}(I_c^A)_{n+1}$$

we obtain in general

$(I_c^E)_n = f_n^E \tilde{I}_{to}^+$ if the to-junction is normal (2–2–59)

and

$(I_c^A)_n = f_n^A \tilde{I}_{from}^+$ if the from-junction is normal (2–2–60)

where

$$f_n^E = \begin{cases} \gamma_n^E \xi_n^E & C_{VH}^n + C_{VH}^{n-1} = 1 \text{ or } 2, \\ & (x_1)_n > 0, \quad (x_1)_{n+1} < 1 \\ -\gamma_n^E \xi_n^E & C_{VH}^n + C_{VH}^{n+1} = -1 \text{ or } -2, \\ & (x_1)_n < 1, \quad (x_1)_{n+1} > 0 \end{cases}$$

$$0.0 \qquad \text{otherwise} \tag{2-2-61}$$

and

$$f_n^A = \begin{cases} \gamma_n^A \xi_n^A & C_{VH}^{n-1} + C_{VH}^n = 1 \text{ or } 2, \\ & (x_1)_{n-1} > 0,\ (x_1)_n < 1 \\ -\gamma_n^A \xi_n^A & C_{VH}^{n-1} + C_{VH}^n = -1 \text{ or } -2, \\ & (x_1)_{n-1} < 1,\ (x_1)_n > 0 \\ 0.0 & \text{otherwise} \end{cases} \tag{2-2-62}$$

Parameters ξ_n^A, ξ_n^E, ξ_n^A and γ_n^E will be defined in section 2.5. Equations (2–2–59) and (2–2–61) apply if the to-junction is normal, while Eqs. (2–2–60) and (2–2–62) apply if the from-junction is normal. Next, we consider the cases when the to-junction or from-junction is a mixing junction. If the to-junction is a mixing junction, we obtain

$$(I_c^E)_n = \begin{cases} \gamma_n^E \xi_n^E \tilde{I}_n & C_{VH}^n = 1,\ (x_1)_n > 0 \\ & (x_1)_{to}^+ < 1 \\ -\gamma_n^E \xi_n^E \tilde{I}_{to}^+ & C_{VH}^n = -1,\ (x_1)_{to}^+ > 0 \\ & (x_1)_n < 1 \\ 0 & \text{otherwise} \end{cases} \tag{2-2-63}$$

If the from-junction is a mixing junction, we obtain

$$(I_c^A)_n = \begin{cases} \gamma_n^A \xi_n^A \tilde{I}_{from}^+ & C_{VH}^n = 1,\ (x_1)_{from}^+ > 0 \\ & (x_1)_n < 1 \\ -\gamma_n^A \xi_n^A \tilde{I}_n & C_{VH}^n = -1,\ (x_1)_{from}^+ < 1 \\ & (x_1^+)_n > 0 \\ 0 & \text{otherwise} \end{cases} \tag{2-2-64}$$

Thus, we can obtain effective I^A or I^E such that

$$\frac{d}{dt} I^A = \frac{I_c^A - I^A}{\tau} \tag{2-2-65}$$

and

$$\frac{d}{dt} I^E = \frac{I_c^E - I^E}{\tau} \tag{2-2-66}$$

Here, we note that the time constants in Eqs. (2–2–65) and (2–2–66) must be identical for a given normal junction or for a given A or E point adjacent to a mixing junction so that the relative enthalpy flux has continuity. Physically Eqs. (2–2–65) and (2–2–66) describes the enthalpy transport due to relative velocity u_{rel} given by Eq. (2–2–14). Since the drift velocity u_{gj} given by Eq. (2–2–15) is related to the terminal velocity of a bubble, it is necessary to take into account the transition process in which the bubble tends to attain the terminal velocity. Time constant τ in Eqs. (2–2–65) and (2–2–66) can be obtained by considering how the transition process evolves. But, it is set to be 0.05 sec in the present version of THYDE-P2.

Next, we define the momentum coupling equation between a junction and a normal node. We assume that continuity of kinetic energy holds between point A of node n and its from-junction as well as between point E and the to-junction such that

$$p^{+}_{from}-\left(p^{A}_{n}+\frac{\Psi^{A}_{n}}{2}-\frac{\kappa^{-}_{from}}{2}\left(\frac{\Phi^{2}}{\rho_{f}}\right)^{A}_{n}\right)=0 \qquad (2\text{–}2\text{–}67)$$

and

$$\left(p^{E}_{n}-\frac{\Psi^{E}_{n}}{2}-\frac{\kappa^{+}_{to}}{2}\left(\frac{\Phi^{2}}{\rho_{f}}\right)^{E}_{n}\right)-p^{+}_{to}=0 \qquad . \qquad (2\text{–}2\text{–}68)$$

For turbulent flow, i.e., $(|G|D/\mu)^{-}_{from}>Re_{t}$, we have

$$\kappa^{+}_{from}=k^{A}_{n}G^{+}_{from}|G^{+}_{from}|=k^{A}_{n}\left(\frac{A_{n}}{A^{+}_{from}}\right)^{2}G^{A}_{n}|G^{A}_{n}|=\frac{k^{A}_{n}}{(\xi^{A}_{n}\gamma^{A}_{n})^{2}}G^{A}_{n}|G^{A}_{n}| \qquad .$$

Here we note that

$$(|G|D/\mu)^{+}_{from}=\sqrt{A^{A}_{n}/A^{-}_{from}}\;Re^{A}_{n}=Re^{A}_{n}/\sqrt{\gamma^{A}_{n}\xi^{A}_{n}}$$

where

$$\mu^{+}_{from}\sim\mu^{A}_{n} \qquad .$$

Thus, is general

$$k^{+}_{from}=\frac{1}{(\xi^{A}_{n})^{2}}\kappa^{A}_{n} \qquad (2\text{–}2\text{–}71)$$

and

$$k_{to}=\frac{1}{(\xi^{E}_{n})^{2}}\kappa^{E}_{n} \qquad (2\text{–}2\text{–}72)$$

where

$$\kappa^{i}_{n}=\begin{cases}\dfrac{k^{i}_{n}}{(\gamma^{i}_{n})^{2}}G^{i}_{n}|G^{i}_{n}| & Re^{i}_{n}/\sqrt{(\gamma\xi)^{i}_{n}}>Re_{t} \quad (i=A,\,E)\\[2ex] \dfrac{k^{i}_{n}}{(\gamma^{i}_{n})^{2}}\left(\dfrac{\mu}{D}\right)^{i}_{n}Re_{t}G^{i}_{n} & Re^{i}_{n}/\sqrt{(\gamma\xi)^{i}_{n}}\leqq Re_{t} \quad (i=A,\,E).\end{cases} \qquad (2\text{–}2\text{–}73)$$

Factors ξ^{A}_{n} and ξ^{E}_{n} show how much the valves placed at points A and E are open, respectively. Subscript opn refers to the case when the valve is opened completely, i.e., $\xi=1$.

Substituting Eqs. (2–2–71) and (2–2–72) into Eqs. (2–2–67) and (2–2–68), we obtain

$$f_{2n}=(\xi^{A}_{n})^{2}(p^{+}_{from}-p^{A}_{n}-\Psi^{A}_{n}/2)-\left(\frac{\kappa}{2}\right)^{A}_{n}\left(\frac{\Phi^{2}}{\rho_{f}}\right)^{A}_{n}=0 \qquad (2\text{–}2\text{–}74)$$

and

$$f_{3n}=(\xi^{E}_{n})^{2}(p^{E}_{n}-\Psi^{E}_{n}/2-p^{+}_{to})-\left(\frac{\kappa}{2}\right)^{E}_{n}\left(\frac{\Phi^{2}}{\rho_{f}}\right)^{E}_{n}=0 \qquad . \qquad (2\text{–}2\text{–}75)$$

When node n is a boundary node, see subsection 2.2.6.

Implications of Eqs. (2–2–74) and (2–2–75) can be seen with the help of Eq. (2–2–80) by applying them to two normal nodes in **Fig. 2–1–2**. From Eqs. (2–2–74) and (2–2–75), we obtain

$$p^{E}_{n}+\Psi^{E}_{n}/2-\frac{\kappa^{E}_{n}}{2(\xi^{E}_{n})^{2}}\left(\frac{\Phi^{2}}{\rho_{f}}\right)^{E}_{n}=p^{A}_{n+1}-\Psi^{A}_{n-1}/2+\frac{\kappa^{A}_{n+1}}{2(\xi^{A}_{n})^{2}}\left(\frac{\Phi^{2}}{\rho_{f}}\right)^{A}_{n+1} \qquad (2\text{–}2\text{–}76)$$

Neglecting B and I and assuming turbulent flow, we obtain

$$p^{E}_{n}+\frac{1}{2}\left(\frac{G^{2}}{\rho}\right)^{E}_{n}-\frac{k^{E}_{n}G^{E}_{n}|G^{E}_{n}|}{2(\xi^{E}_{n}\gamma^{E}_{n})^{2}}\left(\frac{\Phi^{2}}{\rho_{f}}\right)^{E}_{n}=p^{A}_{n+1}+\frac{1}{2}\left(\frac{G^{2}}{\rho}\right)^{A}_{n+1}+\frac{k^{A}_{n+1}G^{A}_{n+1}|G^{A}_{n+1}|}{2(\xi^{A}_{n+1}\gamma^{A}_{n+1})^{2}}\left(\frac{\Phi^{2}}{\rho_{f}}\right)^{A}_{n+1} \qquad .$$

Letting

$$\xi^{E}_{n}=\xi^{A}_{n+1}=\xi$$

$$\rho^{E}_{n}=\rho^{A}_{n+1}=\rho$$

and

$$\left(\frac{\Phi^2}{\rho_f}\right)_n^E = \left(\frac{\Phi^2}{\rho_f}\right)_{n+1}^A = \frac{\Phi^2}{\rho_f}$$

we obtain with the help of Eq. (2–2–80)

$$p_n^E - p_{n+1}^A = \frac{(G_n^E)^2}{2\rho}\left[1 - \left(\frac{A_n}{A_{n+1}}\right)^2\right] + \frac{G_n^E|G_n^E|}{2\xi^2}\left(\frac{\Phi^2}{\rho_f}\right)(k_n^E + k_{n+1}^A)\left(\frac{A_n}{A_{j,opn}^+}\right)^2$$

The first term on the right hand side is the reversible portion of the pressure change at the normal function, while the second term the irreversible portion. Thus Eqs. (2–2–71) and (2–2–72) implicitly contain the effect of area change on the pressure loss.

2.2.5 Junction Equations

We note that only a single normal node is involved in all the conservation equations discussed in the preceding subsection, i.e., Eqs. (2–2–52), (2–2–53), (2–2–54), (2–2–74) and (2–2–75). In this subsection, we will consider the conservation equations in which more than two normal nodes are involved. They are the conservation equations for mass and energy at a normal or mixing junction. We will not consider the equation for a boundary junction in this subsection, but in the next subsection.

For a mixing junction j, we have

$$f_{1j}^+ = \frac{(\rho_j^+ - \rho_j^{+old})}{\Delta t} - (\sum_{from} A_n G_n^E - \sum_{to} A_n G_n^A)/V_j^+ = 0 \qquad (2\text{–}2\text{–}78)$$

and

$$f_{2j}^+ = \frac{(\rho_j^- h_j^+ - \rho_j^{-old} h_j^{+old})}{\Delta t} - (\sum_{from} A_n \Lambda_n^E - \sum_{to} A_n \Lambda_n^A)/V_j^+ - q_j'''^+ = 0 \qquad (2\text{–}2\text{–}79)$$

where $\sum_{to}$ and $\sum_{from}$ are the summations over the to- and from-nodes of junction j, respectively.

If junction j is normal, Eqs. (2–2–78) and (2–2–79) reduce to

$$f_{1j}^+ = -A_{from} G_{from}^E + A_{to} G_{to}^A \qquad (2\text{–}2\text{–}80)$$

and

$$f_{2j}^+ = -h_{from}^{av}(1 - \eta_j^+) - h_{to}^{av}\eta_j^+ + h_j^+ \qquad (2\text{–}2\text{–}81)$$

respectively, where

$$\eta_j^+ = \eta_{from}^E = \eta_{to}^A \qquad (2\text{–}2\text{–}82)$$

2.2.6 Boundary Node Equations

Within the framework of our thermal-hydraulic network, what connects our network to its exterior is the boundary nodes, i.e., injection nodes, dead end nodes and break nodes. Special nodes are regarded as exterior and are connected to our network by the boundary junctions, which are also regarded as part of the exterior. In order words, within the framework of our network theory, the boundary conditions of our network must be specified by those equations of the boundary node which describe coupling of the variables with the adjacent boundary junction.

The boundary condition for enthalpy can be given by specifying h_{from} in Eq. (2–2–57) or h_{to} in Eq. (2–2–58). The other boundary condition can be given by specifying p_{to}^+ in Eq. (2–2–75). For example, in case of accumulator, h_{BC} and p_{to}^+ are given by Eqs. (2–4–69) and (2–4–70), respectively.

It is convenient to have another type of boundary condition instead of Eq. (2–2–75), that is,

$$G_n^E \quad G(p_n^E, h_n^E, t)=0 \qquad (2-2-83)$$

where $G(p, h, t)$ is a given function. We will call the former and the latter the p-source and G-source boundary conditions, respectively. The behavior of the pumped safety injection subsystems could be simulated by either the p- or G-source. Usually, however, the hydraulic boundary condition is the p-source boundary condition.

Next, we discuss the break boundary condition. Consider the to-node of the break junction. When the discharge flow is inertial, we consider in Eq. (2–2–75)

$$\frac{dp^+}{dt}=\frac{p_{ref}-p^+}{\tau} \qquad (2-2-84)$$

and

$$\xi_n^E=1$$

where it should be noted that parameter k_n^E in κ_n^E must be the loss coefficient "after the break". Time constant τ in Eq. (2–2–84) is an input of THYDE-P2.

If the network calculation with Eq. (2–2–84) results in

$$|G_n^E|>G_M(p_n^E, h_n^E)$$

then instead of Eq. (2–2–75), we use the critical flow condition

$$f_{3n}=|G_n^E|-G_M(p_n^E, h_n^E)=0$$

where G_M is given in subsection 2.5.3. Suppose that the break flow is in the region of critical flow. If the calculation with Eq. (2–2–86) turns out

$$|G_n^E|>G_N=C_{eff}\sqrt{2\rho(p-p_{ref})}$$

then, we return to Eq. (2–2–75) with Eq. (2–2–84). The equations for the from-node of the break can similarly be given.

2.3 Algorithm for Thermal-Hydraulic Network

2.3.1 Overall Strategy

In this section, we will develop the algorithm for a thermal-hydraulic network which can be represented in terms of the nodes and junctions defined and discussed in the preceding section. The special nodes will be treated separately and will be connected to our network by boundary junctions. An example of network is shown in **Fig. 2–3–1**.

In terms of the nodes and junctions discussed in the preceding section, we can represent hydraulic systems as networks. We note that in such a representation, any two neighboring normal nodes will be connected via a junction. In the following, some of the points which we should keep in mind when reticulating a coolant system are listed in order:

(a) A mixing junction has volume and is multiple-branched.

(b) For a double-ended break, we set a junction at the place where a break will be assumed to occur. Prior to the occurrence of the break, the junction will be regarded as a normal junction with which the steady state adjustment for the entire network will be performed. As soon as the break starts, however, the junction will then be regarded as exterior to our network. It should be noted that in case of the double-ended break even the topology of our network will change from that of its steady state.

(c) A split break may be simulated to occur at the end of a fictitious linkage node placed at the point where the break is assumed to take place.

(d) Whenever there are parallel channels, the entire flow area and the flow area per channel must be distinguished. If this were not taken into account, we would have pressure

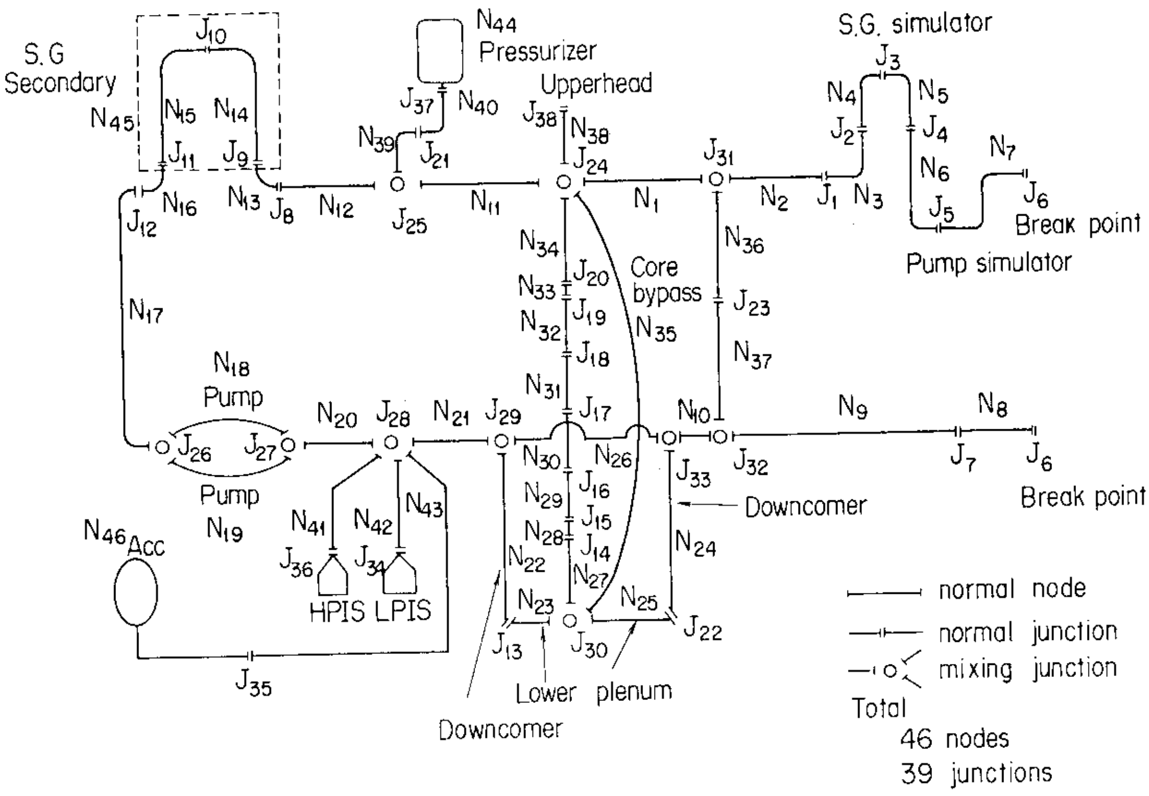

Fig. 2–3–1 Example of Thermal-Hydraulic Network (a).

and flow rate changes at the inlet and outlet of the parallel channels.

(e) In order to simulate the accumulators, the pressurizers, the SG secondary system and the discharge tanks, the THYDE-P2 users can use the options called special nodes which will be discussed in the next section. For the pressurizer, another option is available to represent it by a series of normal nodes.

(f) A flow between a boundary junction and a mixing junction which may be stagnant at the steady state will be referred to as a linkage flow. It will be represented by a series of normal nodes, called the linkage nodes, and normal junctions (see **Fig. 2–1–4**). In THYDE-P2, the flow to a double-ended break, however, will not be referred to as a linkage flow.

The computational procedure for use in THYDE-P2 is shown in **Fig. 2–3–2**. For the calculation of steady state, reference should be made to chapter 5. Looking over **Fig. 2–3–2**, we can see that the network and its exterior are coupled to each other with a time lag Δt. At step 1 in **Fig. 2–3–2**, the state of the exterior such as the pump head, the (old) heat input to the network, the degree of openings of the valves and the thermal-hydraulic condition at the boundary junctions must be specified. In this section, corresponding to step 2, we will present a new algorithm for a hydraulic network, which is an implicit scheme for the system described by the node-and-junction equations derived in the previous section. It is due to the entirely new node-and-junction representation of a hydraulic network that such an implicit integration technique can yield the algorithm which may well coincide with our physical intuition, as can be seen in the discussions that follow in this section. Step 3 is discussed in chapter 3. For step 4, reference should be made to section 6.3.

1. Obtain the new state of the boundary junctions, the new speeds of the pumps and the new openings of the valves.

2. Solve the simultaneous equation of order 5N+2J for p^{new}, G^{new} and h^{new} of all the normal nodes by means of the non-linear implicit method. Use old heat input to coolant flow.

3. Obtain new state of heat conductors under new coolant condition.

4. Check the time step width. If reduction of time step width is necessary, go back to step 1 and repeat the calculation all over again with the halved time step width. Otherwise, proceed to the calculation for the next time step.

Fig. 2–3–2 Overall Computational Procedure.

2.3.2 Vector Representation of Network Equations

By casting the equations discussed in section 2.2 into the vector forms, we can develop the solution procedure clearly, which is the second step in **Fig. 2–3–2**. In this section, only for the sake of clarity, we assume that the hydraulic network is composed of a single disjoint subnetwork. Looking over the discussions that follow, we can see that the solution in this section is quite general, independent of the thermal-hydraulic model as long as the Jacobian has the structure of the same kind.

For a hydraulic system we will define the unknown state vector of the system which is $(5N+2J)$-dimensional such that

$$\boldsymbol{x}=\begin{bmatrix} x_1 \\ x_2 \\ x_3 \\ \cdot \\ \cdot \\ \cdot \\ x_N \\ x_{N+1} \end{bmatrix} \qquad (2\text{–}3\text{–}1)$$

where

$$\boldsymbol{x}_n=\begin{bmatrix} x_{n1} \\ x_{n2} \\ x_{n3} \\ x_{n4} \\ x_{n5} \end{bmatrix}=\begin{bmatrix} G_n^A \\ p_n^A \\ G_n^E \\ p_n^E \\ h_n^{av} \end{bmatrix} \quad (1\leq n\leq N) \qquad (2\text{–}3\text{–}2)$$

and

$$\boldsymbol{x}_{N+1}=\begin{bmatrix} \boldsymbol{x}_1^+ \\ \boldsymbol{x}_2^+ \\ \boldsymbol{x}_3^+ \\ \boldsymbol{x}_4^+ \\ \cdot \\ \cdot \\ \boldsymbol{x}_J^+ \end{bmatrix}=\begin{bmatrix} p_1^+ \\ h_1^+ \\ p_2^+ \\ h_2^+ \\ \cdot \\ \cdot \\ p_J^+ \\ h_J^+ \end{bmatrix} \qquad (2\text{–}3\text{–}3)$$

so that x_n is 5 dimensional for $(1 \leqq n \leqq N)$ and $2J$ dimensional for $n = N+1$. In the above, J and N are the numbers of the junctions (excluding boundary junctions) and the nodes (including boundary nodes) respectively. We note that J includes the normal junction where a double-ended break may be assumed to occur. Vector x_n $(1 \leqq n \leqq N)$ is associated with node n, while vector x_{N+1} with the collection of the entire junctions except the boundary junctions. It should be noted here again that the states of the boundary junctions are not unknown, but are given as the boundary conditions. In order for the problem to be soluble, as many relationships as $5N+2J$ are needed.

There are 5 relationships associated with each normal node n, that is, (1) the mass equation within node n, f_{1n}, i.e., Eq. (2–2–52), (2) the equation of pressure linkage with the from-junction, f_{2n}, i.e., Eq. (2–2–74), (3) the equation of pressure linkage with the to-junction, f_{3n}, Eq. (2–2–75), (4) the momentum equation within node n, f_{4n}, i.e., Eq. (2–2–54), and (5) the energy equation within node n, f_{5n}, i.e., Eq. (2–2–53). We reproduce them in the following,

$$(f_1)_n = G_n^A - G_n^E - L_n \frac{\rho_n^{av} - \rho_n^{av\ old}}{\Delta t} = 0 \qquad (2\text{–}3\text{–}4)$$

$$(f_2)_n = (\xi_n^A)^2 \left(p_{from}^+ - p_n^A - \frac{\Psi_n^A}{2} \right) - \frac{\kappa_n^A}{2} \left(\frac{\Phi^2}{\rho_f} \right)_n^A = 0 \qquad (2\text{–}3\text{–}5)$$

$$(f_3)_n = (\xi_n^E)^2 \left(p_n^E + \frac{\Psi_n^E}{2} - p_{to}^- \right) - \frac{\kappa_n^E}{2} \left(\frac{\Phi^2}{\rho_f} \right)_n^E = 0 \qquad (2\text{–}3\text{–}6)$$

$$(f_4)_n = p_n^A - p_n^E - \Psi_n^A - \Psi_n^E - \frac{1}{2} \left(\kappa + \frac{fL}{D} |G| G \right)_n^{av} \left(\frac{\Phi^2}{\rho_f} \right)_n^{av} - \rho_n^{av} g (L_H - L_{head})_n$$
$$- L_n \frac{G_n^A + G_n^E - G_n^{A\,old} - G_n^{E\,old}}{2\Delta t} = 0 \qquad (2\text{–}3\text{–}7)$$

and

$$(f_5)_n = \frac{\Lambda_n^A - \Lambda_n^E}{L_n} + q_n''' - \frac{\rho_n^{av} h_n^{av} - \rho_n^{av,\,old} h^{av,\,old}}{\Delta t} = 0 \qquad (2\text{–}3\text{–}8)$$

Specific enthalpies h_n^A and h_n^E are given by Eqs. (2–2–57) and (2–2–58), respectively. Quantities κ, Ψ and Λ are defined by Eqs. (2–2–4), (2–2–7) and (2–2–8), respectively.

If node is a boundary node, them $(f_2)_n$ or $(f_3)_n$ is given as described in subsection 2.2.6.

There are two equations associated with each junction. For any normal junction j, we have Eqs. (2–2–80) and (2–2–81), i.e.,

$$(f_1^+)_j = -A_{from} G_{from}^E + A_{to} G_{to}^A = 0 \qquad (2\text{–}3\text{–}9)$$

and

$$(f_2^+)_j = h_j^+ - (1-\eta_j^-) h_{from}^{av} - \eta_j^+ h_{to}^{av} = 0 \qquad (2\text{–}3\text{–}10)$$

After a break occurs at junction j, it might no longer be regarded as a normal junction, but as a boundary junction. Therefore, the number of the unknowns as well as the structure of the system Jacobian would change after the break. In order to retain the same dimension and structure of the system Jacobian as before the break, even after the initiation of the break at junction j, we keep allocating the dummy unknown variables p_j^+ and p_j^+ and assume the following equations to hold

$$(f_1^+)_j = p_j^+ - p_j^{+old} \qquad (2\text{–}3\text{–}11)$$

and

$$(f_2^+)_j = h_j^+ - h_j^{+old} \qquad (2\text{–}3\text{–}12)$$

For a mixing junction j, we have Eqs. (2–2–78) and (2–2–79)

$$(f_1^+)_j = \sum_{to} A_k G_k^A - \sum_{from} A_l G_l^E + V_j^+(\rho_j^+ - \rho_j^{+old})/\Delta t = 0 \qquad (2\text{–}3\text{–}13)$$

and

$$(f_2^-)_j = \sum_{to} A_k \Lambda_k^A - \sum_{from} A_l \Lambda_l^E + V_j^+(\rho_j^+ h_j^+ - \rho_j^{+old} h_j^{+old})/\Delta t - q_j'''^+$$
$$= 0 \qquad . \qquad (2\text{–}3\text{–}14)$$

Eqs. (2–3–9) and (2–3–10) are the special case of Eqs. (2–3–13) and (2–3–14), respectively, when $V_j^+=0$ and there is no branching at junction j.

Thus, we have $5N+2J$ equations which can be cast into a function vector $\boldsymbol{f}$ such that

$$\boldsymbol{f} = \begin{bmatrix} \boldsymbol{f}_1 \\ \boldsymbol{f}_2 \\ \cdot \\ \cdot \\ \cdot \\ \boldsymbol{f}_N \\ \boldsymbol{f}_{N+1} \end{bmatrix} \qquad (2\text{–}3\text{–}15)$$

where

$$\boldsymbol{f}_n = \begin{bmatrix} \boldsymbol{f}_{1n} \\ \boldsymbol{f}_{2n} \\ \boldsymbol{f}_{3n} \\ \boldsymbol{f}_{4n} \\ \boldsymbol{f}_{5n} \end{bmatrix} \qquad (1 \leq n \leq N) \qquad (2\text{–}3\text{–}16)$$

and

$$\boldsymbol{f}_{N+1} = \begin{bmatrix} \boldsymbol{f}_1^+ \\ \boldsymbol{f}_2^+ \\ \cdot \\ \cdot \\ \cdot \\ \boldsymbol{f}_J^+ \end{bmatrix} = \begin{bmatrix} f_{11}^+ \\ f_{21}^+ \\ f_{12}^- \\ f_{22}^+ \\ \cdot \\ \cdot \\ \cdot \\ \cdot \\ \cdot \\ f_{1J}^- \\ f_{2J}^+ \end{bmatrix} \qquad . \qquad (2\text{–}3\text{–}17)$$

It should be noted that the function vector $\boldsymbol{f}_n$ associated with node n is 5 dimensional and is related to only one pair of junctions, i.e., the from- and to-junctions, but not directly to the other normal nodes. In other words, the nodes are decoupled to each other. Function vector $\boldsymbol{f}_{N+1}$ is the collection of the junction equations f_{1j}^+ and f_{2j+}.

We now have to solve the thermal-hydraulic network equation

$$\boldsymbol{f}(\boldsymbol{x}(t), t) = 0 \qquad . \qquad (2\text{–}3\text{–}18)$$

In order to solve the thermal-hydraulic network equation such as Eq. (2–3–18), it has been common to use what may be called the linear implicit method.(2),(3),(7),(18) Even if the space difference were correct, mass, momentum and energy would not conserve if the linear implicit method were used. In THYDE-P2, we use an iterative procedure that may be called the nonlinear implicit method to solve Eq. (2–3–18) with a strict convergence criterion. The linear implicit method is equivalent to performing no iteration in the nonlinear implicit method without paying no attention to convergence of any kind. In other words, it is equivalent to the nonlinear implicit method under a very weak convergence criterion so that no iteration is needed.

2.3.3 Method for Solution to Thermal-Hydraulic Network Equations

This subsection corresponds with step 2 in **Fig. 2–3–2**. Suppose that we have obtained the solution of Eq. (2–3–18) up to time t and now wish to solve it for new time $t+\Delta t$, i.e.,

$$\boldsymbol{f}(\boldsymbol{x}(t+\Delta t), t+\Delta t)=\boldsymbol{0} \qquad (2\text{–}3\text{–}19)$$

Step 1 in **Fig. 2–3–2** can be regarded as specifying the form of function vector $\boldsymbol{f}$ at time $t+\Delta t$. We now set the unknown state vector $\boldsymbol{x}^{new}=\boldsymbol{x}(t+\Delta t)$ to be

$$\boldsymbol{x}^{new}=\boldsymbol{x}_g+\Delta\boldsymbol{x} \qquad (2\text{–}3\text{–}20)$$

where x_g is an appropriate guess vector. Substituting Eq. (2–3–20) into Eq. (2–3–19), we obtain

$$\boldsymbol{f}(\boldsymbol{x}_g+\Delta\boldsymbol{x})=\boldsymbol{0} \qquad (2\text{–}3\text{–}21)$$

where the argument $t+\Delta t$ has been dropped. Expanding Eq. (2–3–21) around x_g and retaining only the terms up to the first order in $\Delta\boldsymbol{x}$, we obtain

$$\boldsymbol{f}(\boldsymbol{x}_g)+\boldsymbol{J}\Delta\boldsymbol{x}=\boldsymbol{0} \qquad (2\text{–}3\text{–}22)$$

where $\boldsymbol{J}$ is $(5N+2J)\times(5N+2J)$ Jacobian matrix such that

$$\boldsymbol{J}=\left.\frac{\partial\boldsymbol{f}}{\partial\boldsymbol{x}}\right|_{x=x_g}$$

By solving the linear equation Eq. (2–3–22), we could claim to have obtained the solution. But, it should be noted that the solution to Eq. (2–3–22) does not satisfy the conservation laws, i.e. Eq. (2–3–19). Instead, in THYDE-P2, we try to obtain the solution of Eq. (2–3–19) as rigorously as possible so that mass, energy and momentum do conserve.

The procedure to solve Eq. (2–3–19) or (2–3–21) is shown in **Fig. 2–3–3**, which is a nonlinear implicit method. Such a nonlinear implicit method is needed especially at low pressure where non-linearity of the flow equations predominates. The non-linear implicit method imperatively requires continuity of the various parameters involved in the flow equations, e.g., Eq. (2–2–18), which, in turn, makes the automatic time step width control possible. Reference should be made to section 7.3 for the TSWC (time step width control) with respect to the iteration number.

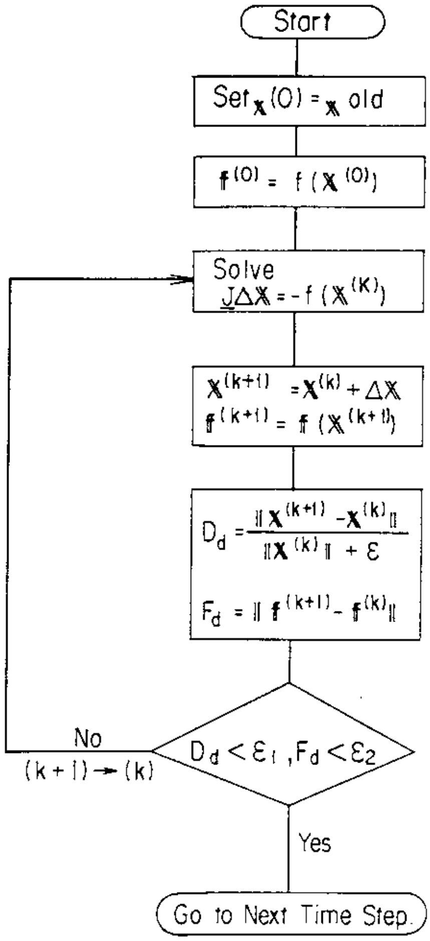

Fig. 2–3–3 Nonlinear Implicit Scheme for Thermal-Hydraulics.

The Jacobian matrix J has the following form

$$J=\begin{bmatrix} J_1 & 0 & 0 & \cdots & R_1 \\ 0 & J_2 & 0 & \cdots & R_2 \\ 0 & 0 & J_3 & \cdots & R_3 \\ 0 & 0 & 0 & \cdots & R_4 \\ \cdot & \cdot & \cdot & \cdots & \cdot \\ L_1 & L_2 & L_3 & \cdots & M \end{bmatrix} \qquad (2\text{–}3\text{–}23)$$

where J_n, R_n, L_n and M are (5×5), (5×2J), (2J×5) and (2J×2J) Jacobian matrices, respectively, such that

$$J_n=\frac{\partial f_n}{\partial x_n}$$

$$R_n=\frac{\partial f_n}{\partial x_{N+1}}$$

$$L_n=\frac{\partial f_{N+1}^{+}}{\partial x_n}$$

and

$$M=\frac{\partial f_{N+1}^{+}}{\partial x_{N+1}}$$

whose components are shown in Appendix A.2. We note that all the other elements of J vanish due to node-node decoupling.

With the help of Eq. (2–3–23), Eq. (2–3–22) can be decomposed to the following set of equations.

$$\boldsymbol{J}_n \Delta \boldsymbol{x}_n + \boldsymbol{R}_n \Delta \boldsymbol{x}_{N+1} = -\boldsymbol{f}_n \qquad (n=1,2,\ldots,N) \tag{2–3–24}$$

and

$$\sum_{n=1}^{N} \boldsymbol{L}_n \Delta \boldsymbol{x}_n + \boldsymbol{M} \Delta \boldsymbol{x}_{N+1} = -\boldsymbol{f}_{N+1} \quad . \tag{2–3–25}$$

From Eq. (2–3–24), we obtain

$$\Delta \boldsymbol{x}_n = -\boldsymbol{J}_n^{-1} \boldsymbol{R}_n \Delta \boldsymbol{x}_{N+1} - \boldsymbol{J}_n^{-1} \boldsymbol{f}_n \tag{2–3–26}$$

which is substituted into Eq. (2–3–25) to obtain

$$\boldsymbol{B} \Delta \boldsymbol{x}_{N+1} = \boldsymbol{F} \tag{2–3–27}$$

where $\boldsymbol{B}$ and $\boldsymbol{F}$ are (2J×2J) and (2J×1) matrices, respectively, such that

$$\boldsymbol{B} = \sum_{n=1}^{N} \boldsymbol{B}_n - \boldsymbol{M} = \sum_{n=1}^{N} \boldsymbol{L}_n \boldsymbol{J}_n^{-1} \boldsymbol{R}_n - \boldsymbol{M} \tag{2–3–28}$$

and

$$\boldsymbol{F} = \boldsymbol{f}_{N+1} - \sum_{n=1}^{N} \boldsymbol{L}_n \boldsymbol{J}_n^{-1} \boldsymbol{f}_n \quad . \tag{2–3–29}$$

Thus, the node-and-junction equation (2–3–22) has been reduced to the junction equation (2–3–27).

For a given branch, we number the junctions from upstream to downstream successively in the direction of the steady state flow. Then, for a given node, its from- and to-junctions are numbered consecutively so that the matrices $\boldsymbol{R}_n$ and $\boldsymbol{L}_n$ are made to have the following simple block structure whose non-zero elements correspond to the from- and to-junctions of node .

$$\boldsymbol{R}_n = [\,0 \quad 0 \quad \ldots \quad \boldsymbol{r}_n \quad \ldots \quad 0 \quad 0\,] \tag{2–3–30}$$

and

$$\boldsymbol{L}_n = \begin{bmatrix} 0 \\ 0 \\ \cdot \\ \cdot \\ \boldsymbol{l}_n \\ \cdot \\ \cdot \\ 0 \\ 0 \end{bmatrix} \tag{2–3–31}$$

where $\boldsymbol{r}_n$ and $\boldsymbol{l}_n$ are (5×4) and (4×5) matrices respectively such that

$$\boldsymbol{r}_n = (\partial \boldsymbol{f}_n^{+} / \partial \boldsymbol{x}_{from}^{+},\ \partial \boldsymbol{f}_{to}^{+} / \partial \boldsymbol{x}_{to}^{+}) \tag{2–3–32}$$

and

$$\boldsymbol{l}_n = \begin{bmatrix} \partial \boldsymbol{f}_{from}^{+} / \partial \boldsymbol{x}_n \\ \partial \boldsymbol{f}_{to}^{+} / \partial \boldsymbol{x}_n \end{bmatrix} \quad . \tag{2–3–33}$$

With the help of Eqs. (2–3–30) and (2–3–31), we obtain the elements of matrix $\boldsymbol{B}$ and matrix $\boldsymbol{F}$. First, we obtain

$$L_n J_n^{-1} f_n = \begin{bmatrix} 0 \\ 0 \\ \cdot \\ \cdot \\ l_n J_n^{-1} f_n \\ \cdot \\ \cdot \\ 0 \end{bmatrix} \tag{2-3-34}$$

where non-zero element $l_n J_n^{-1} f_n$

$$l_n J_n^{-1} f_n = \begin{bmatrix} \partial f^+_{from} / \partial x_n J_n^{-1} f_n \\ \partial f^+_{to} / \partial x_n J_n^{-1} f_n \end{bmatrix} \tag{2-3-35}$$

corresponds to the from- and to-junctions of node n . Let

$$F = \begin{bmatrix} F_1 \\ F_2 \\ \cdot \\ \cdot \\ F_{J-1} \\ F_J \end{bmatrix} \tag{2-3-36}$$

where $F_j (1 \leq j \leq J)$ is a 2 dimensional vector.

Substituting Eq. (2–3–34) with Eq. (2–3–35) into Eq. (2–3–29), we obtain

$$F_j = f_j^+ - \sum_{to-nodes} F_{j,\,to} - \sum_{from-nodes} F_{j,\,from} \tag{2-3-37}$$

where

$$F_{j,\,to} = \frac{\partial f_j^+}{\partial x_{to}} J_{to}^{-1} f_{to}$$

and

$$F_{j,\,from} = \frac{\partial f_j^+}{\partial x_{from}} J_{from}^{-1} f_{from}$$

The explicit forms of $F_{j,\,to}$ and $F_{j,\,from}$ are given in Appendix A.5.

With the help of Eqs. (2–3–30) and (2–3–31), we obtain

$$B_n = \begin{bmatrix} 0 & 0 & 0 & \dots & 0 & 0 \\ 0 & 0 & l_n J_n^{-1} r_n & \dots & 0 & 0 \\ 0 & 0 & 0 & \dots & 0 & 0 \\ 0 & 0 & 0 & \dots & 0 & 0 \end{bmatrix} \tag{2-3-38}$$

where non-zero element $l_n J_n^{-1} r_n$

$$l_n J_n^{-1} r_n = \begin{bmatrix} (b_{from,\,from})_n & (b_{from,\,to})_n \\ (b_{to,\,from})_n & (b_{to,\,to})_n \end{bmatrix} \tag{2-3-39}$$

corresponds to the from- and to-junctions of node n with

$$(b_{ij})_n = \frac{\partial f_i^+}{\partial x_n} J_n^{-1} \frac{\partial f_n}{\partial x_j^+} \quad (i, j = from \text{ or } to) \tag{2-3-40}$$

which is a (2×2) matrix (see Appendix A.3). The non-zero elements of B_n correspond, as shown in Eq. (2–3–39), to the to- and from-junctions of node n .

Matrix M can be expressed as

$$M=\begin{bmatrix} m_1 & 0 & \dots & 0 \\ 0 & m_2 & \dots & 0 \\ 0 & 0 & \dots & m_j \end{bmatrix} \tag{2-3-41}$$

where

$$m_j=\frac{\partial f_j^+}{\partial x_j^+} \tag{2-3-42}$$

which is given in Appendix A.4.

Then, we can regard (2J×2J) matrix $\boldsymbol{B}$ as a (J×J) matrix, the (i, j) component of which is given by

$$\begin{aligned} B_{ij} &= \sum_n (b_{ii})_n - m_i \qquad && i=j \\ &= (b_{ij})_{n_{ij}} && i \neq j \end{aligned} \tag{2-3-43}$$

where n_{ij} is the number of the node between junctions i and j and the summation for $i=j$ should be made over all from- and to-nodes of junction j .

Consider the hydraulic network shown in **Fig. 2–3–4** where N = 9 and J = 7. In this case, the (14×14) matrix $\boldsymbol{B}$ can be obtained as follows. First, we obtain matrices $\boldsymbol{B}_n$ (n = 1, 2, ... 7) given by Eq. (2–3–38):

$$B_1=\begin{bmatrix} (b_{11})_1 & 0 & 0 & (b_{14})_1 & 0 & 0 & 0 \\ 0 & 0 & 0 & 0 & 0 & 0 & 0 \\ (b_{41})_1 & 0 & 0 & 0 & 0 & 0 & 0 \\ 0 & 0 & 0 & (b_{44})_1 & 0 & 0 & 0 \\ 0 & 0 & 0 & 0 & 0 & 0 & 0 \\ 0 & 0 & 0 & 0 & 0 & 0 & 0 \\ 0 & 0 & 0 & 0 & 0 & 0 & 0 \end{bmatrix}$$

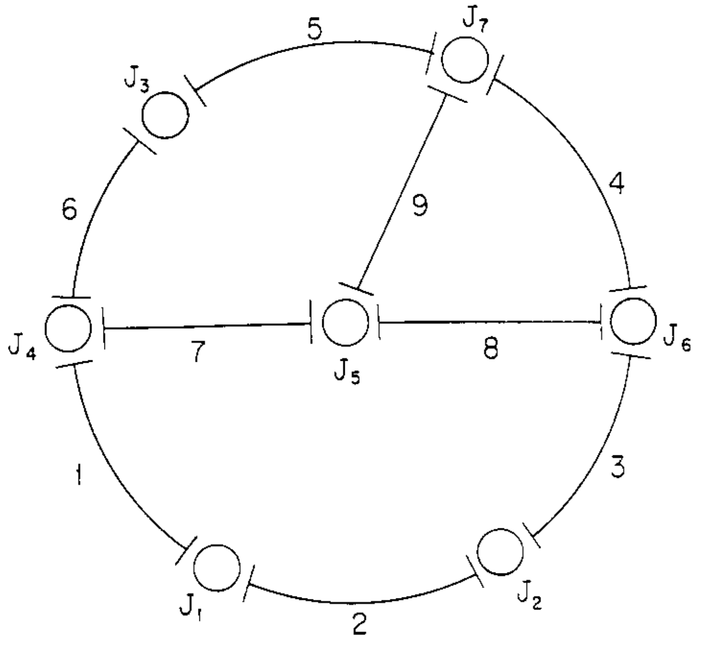

Fig. 2–3–4 Example of Thermal-Hydraulic Network (b).

$$\boldsymbol{B}_2=\begin{bmatrix} (\boldsymbol{b}_{11})_1 & (\boldsymbol{b}_{12})_2 & 0 & 0 & 0 & 0 & 0 \\ (\boldsymbol{b}_{21})_2 & (\boldsymbol{b}_{22})_2 & 0 & 0 & 0 & 0 & 0 \\ 0 & 0 & 0 & 0 & 0 & 0 & 0 \\ 0 & 0 & 0 & 0 & 0 & 0 & 0 \\ 0 & 0 & 0 & 0 & 0 & 0 & 0 \\ 0 & 0 & 0 & 0 & 0 & 0 & 0 \\ 0 & 0 & 0 & 0 & 0 & 0 & 0 \end{bmatrix}$$

$$\boldsymbol{B}_3=\begin{bmatrix} 0 & 0 & 0 & 0 & 0 & 0 & 0 \\ 0 & (\boldsymbol{b}_{22})_3 & 0 & 0 & 0 & (\boldsymbol{b}_{26})_3 & 0 \\ 0 & 0 & 0 & 0 & 0 & 0 & 0 \\ 0 & 0 & 0 & 0 & 0 & 0 & 0 \\ 0 & 0 & 0 & 0 & 0 & 0 & 0 \\ 0 & (\boldsymbol{b}_{62})_3 & 0 & 0 & 0 & (\boldsymbol{b}_{66})_3 & 0 \\ 0 & 0 & 0 & 0 & 0 & 0 & 0 \end{bmatrix}$$

$$\boldsymbol{B}_4=\begin{bmatrix} 0 & 0 & 0 & 0 & 0 & 0 & 0 \\ 0 & 0 & 0 & 0 & 0 & 0 & 0 \\ 0 & 0 & 0 & 0 & 0 & 0 & 0 \\ 0 & 0 & 0 & 0 & 0 & 0 & 0 \\ 0 & 0 & 0 & 0 & 0 & 0 & 0 \\ 0 & 0 & 0 & 0 & 0 & (\boldsymbol{b}_{66})_4 & (\boldsymbol{b}_{67})_4 \\ 0 & 0 & 0 & 0 & 0 & (\boldsymbol{b}_{76})_4 & (\boldsymbol{b}_{77})_4 \end{bmatrix}$$

$$\boldsymbol{B}_5=\begin{bmatrix} 0 & 0 & 0 & 0 & 0 & 0 & 0 \\ 0 & 0 & 0 & 0 & 0 & 0 & 0 \\ 0 & 0 & (\boldsymbol{b}_{33})_5 & 0 & 0 & 0 & (\boldsymbol{b}_{73})_5 \\ 0 & 0 & 0 & 0 & 0 & 0 & 0 \\ 0 & 0 & 0 & 0 & 0 & 0 & 0 \\ 0 & 0 & 0 & 0 & 0 & 0 & 0 \\ 0 & 0 & (\boldsymbol{b}_{37})_5 & 0 & 0 & 0 & (\boldsymbol{b}_{77})_5 \end{bmatrix}$$

$$\boldsymbol{B}_6=\begin{bmatrix} 0 & 0 & 0 & 0 & 0 & 0 & 0 \\ 0 & 0 & 0 & 0 & 0 & 0 & 0 \\ 0 & 0 & 0 & 0 & 0 & 0 & 0 \\ 0 & 0 & (\boldsymbol{b}_{33})_6 & (\boldsymbol{b}_{34})_6 & 0 & 0 & 0 \\ 0 & 0 & (\boldsymbol{b}_{43})_6 & (\boldsymbol{b}_{44})_6 & 0 & 0 & 0 \\ 0 & 0 & 0 & 0 & 0 & 0 & 0 \\ 0 & 0 & 0 & 0 & 0 & 0 & 0 \end{bmatrix}$$

$$\boldsymbol{B}_7=\begin{bmatrix} 0 & 0 & 0 & 0 & 0 & 0 & 0 \\ 0 & 0 & 0 & 0 & 0 & 0 & 0 \\ 0 & 0 & 0 & 0 & 0 & 0 & 0 \\ 0 & 0 & 0 & (\boldsymbol{b}_{44})_7 & (\boldsymbol{b}_{45})_7 & 0 & 0 \\ 0 & 0 & 0 & (\boldsymbol{b}_{54})_7 & (\boldsymbol{b}_{55})_7 & 0 & 0 \\ 0 & 0 & 0 & 0 & 0 & 0 & 0 \\ 0 & 0 & 0 & 0 & 0 & 0 & 0 \end{bmatrix}$$

$$B_8=\begin{bmatrix} 0&0&0&0&0&0&0\\ 0&0&0&0&0&0&0\\ 0&0&0&0&0&0&0\\ 0&0&0&0&0&0&0\\ 0&0&0&0&(b_{55})_8&(b_{56})_8&0\\ 0&0&0&0&(b_{65})_8&(b_{66})_8&0\\ 0&0&0&0&0&0&0 \end{bmatrix}$$

and

$$B_9=\begin{bmatrix} 0&0&0&0&0&0&0\\ 0&0&0&0&0&0&0\\ 0&0&0&0&0&0&0\\ 0&0&0&0&0&0&0\\ 0&0&0&0&(b_{55})_9&0&(b_{57})_9\\ 0&0&0&0&0&0&0\\ 0&0&0&0&(b_{75})_9&0&(b_{77})_9 \end{bmatrix}$$

Thus, we obtain matrix B defined by Eq. (2–3–43) as

$$B=\begin{bmatrix} B_{11}&(b_{12})_2&0&(b_{14})_1&0&0&0\\ (b_{21})_2&B_{22}&0&0&0&(b_{26})_3&0\\ 0&0&B_{33}&(b_{34})_6&0&0&(b_{37})_5\\ (b_{41})_1&0&(b_{43})_6&B_{44}&(b_{45})_7&0&0\\ 0&0&0&(b_{54})_7&B_{55}&(b_{56})_8&(b_{57})_9\\ 0&(b_{62})_3&0&0&(b_{65})_8&B_{66}&(b_{67})_4\\ 0&0&(b_{73})_5&0&(b_{75})_9&(b_{76})_4&B_{77} \end{bmatrix}$$

where

$$B_{11}=(b_{11})_1+(b_{11})_2-m_1$$

$$B_{22}=(b_{22})_2+(b_{22})_3-m_2$$

$$B_{33}=(b_{33})_5+(b_{33})_6-m_3$$

$$B_{44}=(b_{44})_1+(b_{44})_6+(b_{44})_7-m_4$$

$$B_{55}=(b_{55})_7+(b_{55})_8+(b_{55})_9-m_5$$

$$B_{66}=(b_{66})_3+(b_{66})_4+(b_{66})_8-m_6$$

and

$$B_{77}=(b_{77})_4+(b_{77})_5+(b_{77})_9-m_7.$$

Junction equation (2–3–27) can further be reduced to what may be called the mixing junction equation. To this end, we use the following numbering convention for junctions. Let q be the number of branches in the network with at least one normal junction. Then partitioning the normal junctions branch-wise into q groups and collecting the mixing junctions as one group (group $q+1$), we have $q+1$ junction groups. Let $l_k(1\leq k\leq q+1)$ be the size of junction group k .

Then we can cast Eq. (2–3–27) to the following form.

$$\boldsymbol{B}=\begin{bmatrix} \boldsymbol{B}_{d_1} & 0 & \cdots & \cdot & \boldsymbol{B}_{R_1} \\ 0 & \boldsymbol{B}_{d_2} & \cdots & \cdot & \boldsymbol{B}_{R_2} \\ 0 & 0 & \cdots & \boldsymbol{B}_{d_g} & \boldsymbol{B}_{R_g} \\ \boldsymbol{B}_{L_1} & \boldsymbol{B}_{L_2} & \cdots & \boldsymbol{B}_{l_g} & \boldsymbol{B}_{d_{g+1}} \end{bmatrix} \tag{2-3-44}$$

$$\Delta \boldsymbol{x}_{N+1}=\begin{bmatrix} \Delta\tilde{\boldsymbol{x}}_1 \\ \Delta\tilde{\boldsymbol{x}}_2 \\ \cdot \\ \cdot \\ \Delta\tilde{\boldsymbol{x}}_{q+1} \end{bmatrix} \tag{2-3-45}$$

and

$$\boldsymbol{F}=\begin{bmatrix} \tilde{\boldsymbol{F}}_1 \\ \tilde{\boldsymbol{F}}_2 \\ \cdot \\ \cdot \\ \tilde{\boldsymbol{F}}_{q+1} \end{bmatrix} \tag{2-3-46}$$

where the tilde refers to a junction group.

The matrices $\boldsymbol{B}_{R_k}$ and $\boldsymbol{B}_{L_k}$, which are $2l_k \times 2l_{q+1}$ and $2l_{q+1} \times 2l_k$ respectively, show how junction groups k and $q+1$ are coupled to each other such that

$$\boldsymbol{B}_{R_k}=\begin{bmatrix} \cdot & (\boldsymbol{b}_{k_a^+,k_f})_{k_a} & \cdot & \cdots & \cdot & \cdot \\ \cdot & \cdot & \cdot & \cdots & \cdot & \cdot \\ \cdot & \cdot & \cdot & \cdots & \cdot & \cdot \\ \cdot & \cdot & \cdot & \cdots & (\boldsymbol{b}_{k_e^+,k_t})_{k_e} & \cdot \end{bmatrix} \begin{matrix} (1) \\ \\ \\ (l_k) \end{matrix} \tag{2-3-47}$$

$$\qquad\qquad (k_f) \qquad\qquad\qquad (k_t)$$

and

$$\boldsymbol{B}_{L_k}=\begin{bmatrix} \cdot & \cdots & \cdot & \cdot \\ (\boldsymbol{b}_{k_f,k_a^+})_{k_a} & \cdots & \cdot & \cdot \\ \cdot & \cdots & \cdot & \cdot \\ \cdot & \cdots & \cdot & \cdot \\ \cdot & \cdots & \cdot & (\boldsymbol{b}_{k_t,k_e^+})_{k_e} \\ \cdot & \cdots & \cdot & \cdot \end{bmatrix} \begin{matrix} \\ (k_f) \\ \\ \\ (k_t) \\ \\ \end{matrix} \tag{2-3-48}$$

$$(1) \qquad\qquad\qquad (l_k)$$

where k_a, k_e, k_a^+, k_e^+, k_f and k_t are the most upstream node, the most downstream node, the from-junction and the to-junction for junction group $k(1 \leq k \leq q)$, respectively. Eq. (2–3–47) shows that the non-zero 2X2 elements of matrix $\boldsymbol{B}_{R_k}$ are $(1, k_f)$ and (l_k, k_t), while Eq. (2–3–48) shows that the non-zero 2X2 elements of matrix $\boldsymbol{B}_{L_k}$ are $(k_f, 1)$ and (k_t, l_k). These mean that, for a given junction group $k(1 \leq k \leq q)$, the most upstream junction in group k is linked to from-mixing junction k_f, while the most downstream junction to to-mixing junction k_t.

Substituting Eqs. (2–3–44), (2–3–45) and (2–3–46) into Eq. (2–3–27), we obtain

$$\boldsymbol{B}_{d_k}\Delta\tilde{\boldsymbol{x}}_k+\boldsymbol{B}_{d_{q+1}}\Delta\tilde{\boldsymbol{x}}_{q+1}=\tilde{\boldsymbol{F}}_k \qquad (1 \leq k \leq q) \tag{2-3-49}$$

and

$$\sum_{k=1}^{q}\boldsymbol{B}_{L_k}\Delta\tilde{\boldsymbol{x}}_k+\boldsymbol{B}_{d_{q+1}}\Delta\tilde{\boldsymbol{x}}_{q+1}=\tilde{\boldsymbol{F}}_{q+1} \quad . \tag{2-3-50}$$

We obtain from Eq. (2–3–49),

$$\Delta\tilde{\boldsymbol{x}}_k = -\boldsymbol{B}_{d_k}^{-1}\boldsymbol{B}_{R_k}\Delta\tilde{\boldsymbol{x}}_{q+1} - \boldsymbol{B}_{d_k}^{-1}\tilde{\boldsymbol{F}}_k \quad (1 \leq k \leq q) \tag{2–3–51}$$

which is substituted into Eq. (2–3–36) to obtain

$$\boldsymbol{C}\Delta\tilde{\boldsymbol{x}}_{q+1} = \boldsymbol{G} \tag{2–3–52}$$

where

$$\boldsymbol{C} = \boldsymbol{B}_{g_{q+1}} - \sum_{k=1}^{q} \boldsymbol{B}_{L_k}(\boldsymbol{B}_{d_k})^{-1}\boldsymbol{B}_{R_k} \tag{2–3–53}$$

and

$$\boldsymbol{G} = \tilde{\boldsymbol{F}}_{q+1} - \sum_{k=1}^{q} \boldsymbol{B}_{L_k}(\boldsymbol{B}_{d_k})^{-1}\tilde{\boldsymbol{F}}_k \quad . \tag{2–3–54}$$

We call Eq. (2–3–52) the mixing junction equation which is a simultaneous equation of order $2l_{q+1}$, i.e., twice as many as the number of mixing junctions.

In case of **Fig. 2–3–4**, noting that

$q = 2$

$l_1 = 1 \ (j = 3)$

$l_2 = 2 \ (j = 1 \text{ and } 2)$

and

$l_3 = 4 \ (j = 4, 5, 6, 7)$

we obtain matrices $\boldsymbol{B}_{L_k}$ and $\boldsymbol{B}_{R_k}$ ($k = 1$ and 2) and $\boldsymbol{B}_{d_k}$ ($k = 1, 2, 3$) as follows:

$$\boldsymbol{B}_{L_1} = \begin{bmatrix} (\boldsymbol{b}_{41})_1 & 0 \\ 0 & 0 \\ 0 & (\boldsymbol{b}_{62})_3 \\ 0 & 0 \end{bmatrix}$$

$$\boldsymbol{B}_{L_2} = \begin{bmatrix} (\boldsymbol{b}_{43})_6 \\ 0 \\ 0 \\ (\boldsymbol{b}_{37})_5 \end{bmatrix}$$

$$\boldsymbol{B}_{R_1} = \begin{bmatrix} (\boldsymbol{b}_{14})_1 & 0 & 0 & 0 \\ 0 & 0 & (\boldsymbol{b}_{26})_3 & 0 \end{bmatrix}$$

$$\boldsymbol{B}_{R_2} = \begin{bmatrix} (\boldsymbol{b}_{34})_6 & 0 & 0 & (\boldsymbol{b}_{73})_5 \end{bmatrix}$$

$$\boldsymbol{B}_{d_1} = \begin{bmatrix} (\boldsymbol{b}_{11})_1 + (\boldsymbol{b}_{11})_2 & (\boldsymbol{b}_{12})_2 \\ (\boldsymbol{b}_{21})_2 & (\boldsymbol{b}_{22})_2 + (\boldsymbol{b}_{22})_3 \end{bmatrix}$$

$$\boldsymbol{B}_{d_2} = (\boldsymbol{b}_{33})_5 + (\boldsymbol{b}_{33})_6$$

and

$$\boldsymbol{B}_{d_3} = \begin{bmatrix} (\boldsymbol{B}_{d_3})_{11} & (\boldsymbol{b}_{45})_7 & & \\ (\boldsymbol{b}_{54})_7 & (\boldsymbol{B}_{d_3})_{22} & (\boldsymbol{b}_{56})_8 & (\boldsymbol{b}_{57})_9 \\ 0 & (\boldsymbol{b}_{65})_8 & (\boldsymbol{B}_{d_3})_{33} & (\boldsymbol{b}_{67})_4 \\ 0 & (\boldsymbol{b}_{75})_9 & (\boldsymbol{b}_{76})_4 & (\boldsymbol{B}_{d_3})_{44} \end{bmatrix}$$

where

$$(\boldsymbol{B}_{d_3})_{11} = (\boldsymbol{b}_{44})_1 + (\boldsymbol{b}_{44})_6 + (\boldsymbol{b}_{44})_7$$

$$(\boldsymbol{B}_{d_3})_{22} = (\boldsymbol{b}_{55})_7 + (\boldsymbol{b}_{55})_8 + (\boldsymbol{b}_{55})_9$$

$$(\boldsymbol{B}_{d_3})_{33} = (\boldsymbol{b}_{66})_3 + (\boldsymbol{b}_{66})_4 + (\boldsymbol{b}_{66})_8$$

and

$$(\boldsymbol{B}_{d_3})_{33} = (\boldsymbol{b}_{77})_4 + (\boldsymbol{b}_{77})_5 + (\boldsymbol{b}_{77})_9 \quad .$$

By tracing back the discussions, we can obtain $\Delta \boldsymbol{x}$ in Eq. (2–3–22). First of all, we solve Eq. (2–3–52) to obtain the mixing junction vector $\Delta \boldsymbol{x}_{q+1}$. Secondly, substituting $\Delta \boldsymbol{x}_{q+1}$ into Eq. (2–3–51), we obtain branch vectors $\Delta \boldsymbol{x}_k$ ($k = 1, 2, \ldots, q$). Thus, we have obtained junction vector $\Delta \boldsymbol{x}_{N+1}$ corresponding to Eq. (2–3–45). Thirdly, substituting $\Delta \boldsymbol{x}_{N+1}$ into Eq. (2–3–26), we obtain normal node vector $\Delta \boldsymbol{x}_n$ ($n = 1, 2, \ldots, N$). Thus, we have obtained the state vector of the system $\Delta \boldsymbol{x}$. This procedure will be repeated following the scheme in **Fig. 2–3–3** until the solution converges.

2.4 Special Nodes and Pump

In this chapter, we talk about the special nodes as classified in **Table 2–1**, for which THYDE-P2 has simplified models. We also discuss the pump model for use in THYDE-P2. It is possible in principle to simulate pressurizer and SG secondary system by means of the method described in section 2.3. But, in THYDE-P2, simulation of SG secondary system is done by the simplified model to be described in this section. In the next version, however, detailed simulation of secondary system will be made. The discussions in this section correspond to a part of step 1 of **Fig. 2–3–2**. We note that the special nodes are excluded from the implicit scheme discussed in the preceding section. They are linked to our hydraulic network via the boundary nodes (see subsection 2.2.6).

2.4.1 Tank Model

For the pressurizer and the secondary coolant system in the steam generator, we modified the model in Ref. (19) to contrive a model whose configuration is schematically depicted in **Fig. 2–4–1** or **2–4–2**. We call it the Tank model. Assuming that the tank is at uniform pressure, we have

$$V_T = V_I + V_{II} \tag{2–4–1}$$

$$\frac{dU_I}{dt} = E_I - p\frac{dV_I}{dt} / Je \tag{2–4–2}$$

$$\frac{dU_{II}}{dt} = E_{II} - p\frac{dV_{II}}{dt} / Je \tag{2–4–3}$$

$$\frac{dM_I}{dt} = Y_I \tag{2–4–4}$$

and

$$\frac{dM_{II}}{dt} = Y_{II} \tag{2–4–5}$$

Eqs. (2–4–2) and (2–4–3) are the energy equations, whereas Eqs. (2–4–4) and (2–4–5) are the mass equations. E and Y are the energy and mass inputs to the respective regions. The respective forms for Y_I, Y_{II}, E_I and E_{II} will be given later for the pressurizer and the SG secondary systems separately.

Depending on the thermodynamic states of region I and II, we consider three cases (IST = 1, 2 and 3)

Case 1. (IST = 1)

Case 1 occurs when region I is saturated mixture and region II is subcooled. In this case,

$$V_T = V_I + V_{II} = v_{gs} M_{Ig} + v_{fs} M_{If} + v_{II} M_{II} \tag{2-4-6}$$

$$M_I = M_{Ig} + M_{If} \tag{2-4-7}$$

$$U_I = M_{Ig} h_{gs} + M_{If} h_{fs} - \frac{pV_I}{J_e} \tag{2-4-8}$$

and

$$U_{II} = M_{II} h_{II} - \frac{pV_{II}}{J_e} \quad . \tag{2-4-9}$$

Differentiating Eqs. (2-4-6) and (2-4-7) with respect to time, we obtain,

$$\frac{dM_{Ig}}{dt} + \frac{M_{If}}{dt} \tag{2-4-10}$$

and

$$O = \left(v'_{gs} M_{Ig} + v'_{fs} M_{If} + M_{II} \frac{\partial v_{II}}{\partial p} \right) \frac{dp}{dt} + v_{gs} \frac{dM_I}{dt} + v_{fs} \frac{dM_{If}}{dt} + v_{II} \frac{dM_{II}}{dt}$$
$$+ M_{II} \frac{\partial v_{II}}{\partial h_{II}} \frac{dh_{II}}{dt} \quad . \tag{2-4-11}$$

Substituting Eqs. (2-4-8) and (2-4-9) into Eqs. (2-4-2) and (2-4-3), we obtain,

$$\frac{dM_{Ig}}{dt} h_{gs} + \frac{dM_{If}}{dt} h_{fs} + \left(M_{Ig} h_{gs} + M_{If} h_{fs} - \frac{V_I}{J_e} \right) \frac{dp}{dt} = E_I \tag{2-4-12}$$

and

$$\frac{dM_{II}}{dt} h_{II} + M_{II} \frac{dh_{II}}{dt} - \frac{V_{II}}{J_e} \frac{dp}{dt} = E_{II} \quad . \tag{2-4-13}$$

Solving Eqs. (2-4-10) and (2-4-12) for $\frac{dM_{Ig}}{dt}$ and $\frac{dM_{If}}{dt}$, we obtain

$$\frac{dM_{Ig}}{dt} = \left[E_I - (M_{Ig} h_{gs} + M_{If} h_{fs} - V_I / J_e) \frac{dp}{dt} - h_{fs} \frac{dM_I}{dt} \right] / h_{fg} \tag{2-4-14}$$

and

$$\frac{dM_{If}}{dt} = \left[-E_I + (M_{Ig} h_{gs} + M_{If} h_{fs} - V_I / J_e) \frac{dp}{dt} + h_{gs} \frac{dM_I}{dt} \right] / h_{fg} \quad . \tag{2-4-15}$$

Substituting Eqs. (2-4-14), (2-4-15) and (2-4-13) into Eq. (2-4-11), we obtain

$$\frac{dp}{dt} = -\left[\left(v_{fs} - h_{fs} \frac{v_{fg}}{h_{fg}} \right) \frac{dM_I}{dt} + \left(v_{II} - h_{II} \frac{\partial v_{II}}{\partial h_{II}} \right) \frac{dM_{II}}{dt} + E_{II} \frac{\partial v_{II}}{\partial h_{II}} + E_I \frac{v_{fg}}{h_{fg}} \Big/ \left[\frac{1}{J_e} \left(\frac{v_{fg}}{h_{fg}} V_I + \frac{\partial v_{II}}{\partial h_{II}} V_{II} \right) \right. \right.$$
$$\left. - \frac{v_{fg}}{h_{fg}} (M_{Ig} h'_{GS} + M_{If} h'_{fs}) + v'_{gs} M_{Ig} + v'_{fs} M_{If} + \frac{\partial v_{II}}{\partial p} M_{II} \right] \quad . \tag{2-4-16}$$

Substituting Eqs. (2-4-4) to (2-4-5) into Eq. (2-4-16), we can finally obtain the governing equation for the pressure.

Case 2. (IST = 2)

Case 2 occurs when region I is superheated and region II is subcooled. In this case, we have

$$V_T = V_I + V_{II} = M_I v_I + M_{II} v_{II} \tag{2-4-17}$$

$$U_I = M_I h_I - \frac{pV_I}{J_e} \tag{2-4-18}$$

and

$$U_{II}=M_{II}h_{II}-\frac{pV_{II}}{J_e} \tag{2-4-19}$$

Substituting Eqs. (2–4–18) and (2–4–19) into Eqs. (2–4–2) and (2–4–3), we obtain

$$\frac{dh_I}{dt}=\left[-\frac{dM_I}{dt}h_I+E_I+\frac{dp}{dt}V_I/J_e\right]/M_I \tag{2-4-20}$$

$$\frac{dh_{II}}{dt}=\left[-\frac{dM_{II}}{dt}h_{II}+E_{II}+\frac{dp}{dt}V_{II}/J_e\right]/M_{II} \quad . \tag{2-4-21}$$

Differentiating Eq. (2–4–17) with respect to time, we have

$$O=\frac{dM_I}{dt}v_I+\frac{dM_{II}}{dt}v_{II}+\left(M_{II}\frac{\partial v_{II}}{\partial p}+M_I\frac{\partial v_I}{\partial p}\right)\frac{dp}{dt}+M_I\frac{\partial v_I}{\partial h}\frac{dh_I}{dt}+M_{II}\frac{\partial v_{II}}{\partial h}\frac{dh_{II}}{dt} . \tag{2-4-22}$$

Substituting Eqs. (2–4–24) and (2–4–25) into Eq. (2–4–26), we obtain,

$$p=-\left[\frac{dM_I}{dt}\left(v_I-h_I\frac{\partial v_I}{\partial h}\right)+\frac{dM_{II}}{dt}\left(v_{II}-h_{II}\frac{\partial v_{II}}{\partial h}\right)+E_I\frac{\partial v_{II}}{\partial h}+E_{II}\frac{\partial v_{II}}{\partial h}\right.$$

$$/\left[M_I\frac{\partial v_I}{\partial p}+M_{II}\frac{\partial v_{II}}{\partial p}+\frac{1}{J_e}\left(V_I\frac{\partial v_I}{\partial h}+V_{II}\frac{\partial v_{II}}{\partial h}\right)\right] \quad . \tag{2-4-23}$$

Case 3. (IST = 3)

Case 3 occurs when region I is superheated steam and region II is saturated. In this case, we have,

$$V_T=V_I+V_{II}=M_Iv_I+M_{IIf}v_{fs}+M_{IIg}v_{gs} \tag{2-4-24}$$

$$M_{II}=M_{IIg}+M_{IIf} \tag{2-4-25}$$

$$U_I=h_IM_I-\frac{pV_I}{J_e} \tag{2-4-26}$$

and

$$U_{II}=h_{gs}M_{IIg}+h_{fs}M_{IIf}-\frac{pV_{II}}{J_e} \quad . \tag{2-4-27}$$

Substituting Eq. (2–4–26) into Eq. (2–4–2), we obtain

$$\frac{dh_I}{dt}=\left[E_I+\frac{dp}{dt}V_I/J_e-h_I\frac{dM_I}{dt}\right]/M_I \quad . \tag{2-4-28}$$

Substituting Eq. (2–4–27) into Eq. (2–4–5), we obtain

$$h_{gs}\frac{dM_{IIg}}{dt}+h_{fs}\frac{dM_{IIf}}{dt}+\left(h'_{gs}M_{IIg}+h'_{fs}M_{IIf}-\frac{V_{II}}{J_e}\right)\frac{dp}{dt}=E_{II} \quad . \tag{2-4-29}$$

On the other hand, we have from Eq. (2–4–25),

$$\frac{dM_{IIg}}{dt}+\frac{dM_{IIf}}{dt}=\frac{dM_{II}}{dt} \quad . \tag{2-4-30}$$

Solving Eqs. (2–4–29) and (2–4–30) for M_{IIg} and M_{IIf}, we obtain

$$\frac{dM_{IIg}}{dt}=\left[E_{II}-(h'_{gs}M_{IIg}+h'_{fs}M_{IIf}-V_{II}/J_e)\frac{dp}{dt}-h_{fs}\frac{dM_{II}}{dt}\right]/h_{fs} \tag{2-4-31}$$

and

$$\frac{dM_{IIf}}{dt}=\left[-E_{II}+(h'_{gs}M_{IIg}+h'_{fs}M_{IIf}-V_{II}/J_e)\frac{dp}{dt}+h_{gfs}\frac{dM_{II}}{dt}\right]/h_{fg} \tag{2-4-32}$$

Differentiating Eq. (2–4–24) with respect to time and substituting Eqs. (2–4–28), (2–4–31) and (2–4–32) into the resulting equation, we obtain

$$\frac{dp}{dt}=-\left[E_{II}\frac{v_{fg}}{h_{fg}}+\frac{dM_{II}}{dt}\left(\frac{h_{gs}v_{fs}-v_{gs}h_{fs}}{h_{fg}}\right)+E_I\frac{\partial v_I}{\partial h_I}+\frac{dM_I}{dt}\left(v_I-h_I\frac{\partial v_I}{\partial h_I}\right)\right]$$

$$/\left[-\frac{v_{fg}}{h_{fs}}\left(h'_{gs}M_{IIg}+h'_{fs}M_{IIf}-\frac{V_{II}}{J_e}\right)+M_{Ig}v'_{gs}+M_{IIf}v'_{fs}+M_Iv'_I+\frac{V_I}{J_e}\frac{\partial v_I}{\partial h_I}\right]$$

(2–4–34)

Case 4. (IST = 4)

Case 4 occurs as soon as region II becomes saturated due to decompression starting from Case 1. We note that case 4 is a non-equilibrium state.

We set

$$V_i = v_{gs} M_{ig} + v_{fs} M_{if} \qquad (i = I \text{ and } II) \qquad (2\text{–}4\text{–}35)$$

$$M_i = M_{ig} + M_{if} \qquad (i = I \text{ and } II) \qquad (2\text{–}4\text{–}36)$$

$$U_i = M_{ig} h_{gs} + M_{if} h_{fs} - \frac{pV_i}{J_e} \qquad (i = I \text{ and } II) \quad . \qquad (2\text{–}4\text{–}37)$$

Differentiating Eqs. (2–4–1) and (2–4–36), we obtain

$$O = [v'_{gs}(M_{Ig} + M_{IIg}) + v'_{fs}(M_{If} + M_{IIf} + M_{cs})] \frac{dp}{dt} + v_{gs}\left(\frac{dM_{Ig}}{dt} + \frac{dM_{IIg}}{dt}\right) + v_{fs}\left(\frac{dM_{IF}}{dt} + \frac{dM_{IIf}}{dt} + \frac{dM_{cs}}{dt}\right) \qquad (2\text{–}4\text{–}38)$$

$$\frac{dM_i}{dt} = \frac{dM_{ig}}{dt} + \frac{dM_{if}}{dt} \qquad (i = I \text{ and } II) \qquad (2\text{–}4\text{–}39)$$

Substituting Eq. (2–4–37) into Eqs. (2–4–2) and (2–4–3), we obtain,

$$\frac{dM_{ig}}{dt} h_{gs} + \frac{dM_{if}}{dt} h_{fs} + \left(M_{ig} h'_{gs} + M_{if} h'_{fs} - \frac{V_i}{J_e}\right)\frac{dp}{dt} = E_i \; (i = I \text{ and } II) \qquad (2\text{–}4\text{–}40)$$

From, Eqs. (2–4–39) and (2–4–40), we obtain

$$\frac{dM_{ig}}{dt} = \left[E_i - (M_{ig} h'_{gs} + M_{if} h'_{fs} - V_i / J_e)\frac{dp}{dt} - h_{fs}\frac{dM_i}{dt}\right] / h_{fg} \qquad (2\text{–}4\text{–}41)$$

and

$$\frac{dM_{if}}{dt} = \left[-E_i + (M_{ig} h'_{gs} + M_{if} h'_{fs} - V_i / J_e)\frac{dp}{dt} + h_{gs}\frac{dM_i}{dt}\right] / h_{fg} \quad . \qquad (2\text{–}4\text{–}42)$$

where i = I and II. Substituting Eqs. (2–4–41) and (2–4–42) into Eqs. (2–4–38) we obtain,

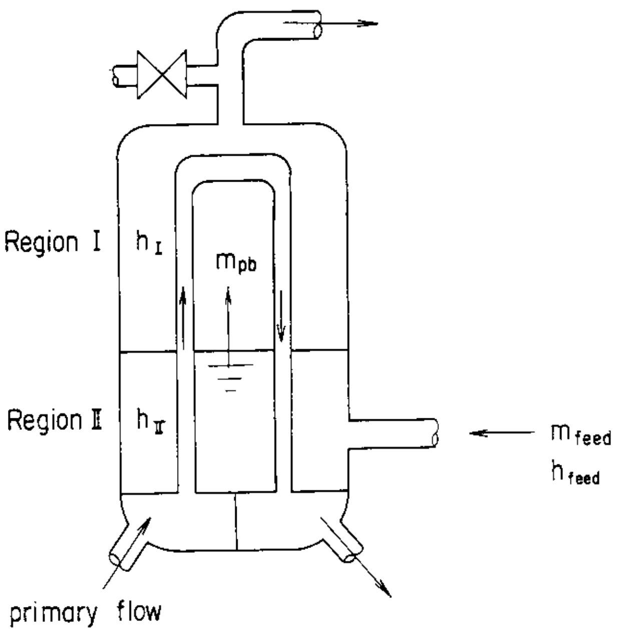

Fig. 2–4–1 Schematic Figure of SG 2ndry System Tank Model.

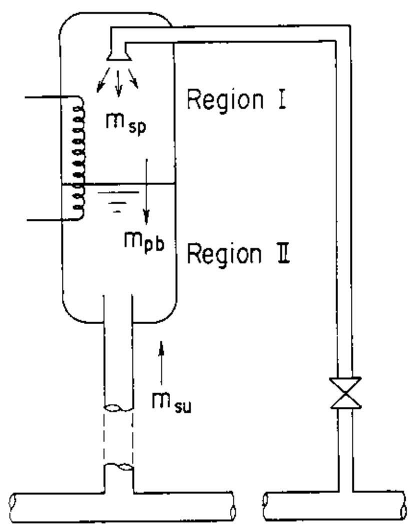

Fig. 2–4–2 Schematic Figure of Pressurizer Tank Model.

$$\frac{dp}{dt}=\left[Ev_{fg}/h_{fg}+\frac{dM}{dt}(v_{fs}h_{gs}-v_{gs}h_{fs})/h_{fs}+v_{fs}\frac{dM_{cs}}{dt}\right]/\{v_{fg}/h_{fg}(M_g h'_{gs}$$

$$+M_f h'_{fs}-V/J_e)-v'_{gs}M_g-v'_{fs}M_f\} \qquad (2-4-43)$$

where

$M_g=M_{Ig}+M_{IIg}$

$M_f=M_{If}+M_{IIf} \qquad (\neq M_{If}+M_{IIf}+M_{cs})$

$M=M_I+M_{II} \qquad (\neq M_I+M_{II}+M_{cs})$

$E=E_I+E_{II}$

$V=V_I+V_{II} \qquad (\neq V_T)$.

We should note that Eq. (2–4–43) can be obtained from Eq. (2–4–16) by neglecting all the quantities with subscript II and then entirely dropping subscript I from the remaining quantities.

2.4.1.1 SG 2ndry System

The schemtic figure of SG 2ndry system tank model is show in **Fig. 2–4–1**. In this model, (1) condensate region is not assumed, (2) heat transfer between regions I and II is assumed only due to m_{pb} with h_{fs} and (3) mass flow rate m_{pb} between regions I and II satisfies

$m_{pb}=m_{feed}$

whose initial value is an input. Mass flow rate $m_{feed}(t)$ is assumed to reduce upon closure of the isolation valve controlled in the code by subroutine TRIP.

2.4.1.2 Pressurizer

The pressurizer may be simulated by the Tank Model under the following assumptions.

(i) If region I is saturated two-phase or superheated steam, water through the spray line is assumed immediately to become saturated by obtaining heat from region I and to reach region II.

(ii) Presence of condensates is neglected so that there is no heat and mass transfer due to falling condensates, i.e.,

$m_{cs}=0$

and

$m_d=0$.

(iii) Heat and mass transfer with bubble rise is neglected so that

$m_{pd}=0$.

Thus, we obtain

$$y_I=-m_{re} \qquad (2-4-44)$$

$$y_{II}=m_{su}+m_{sp} \qquad (2-4-45)$$

$$E_I=-m_{sp}(h_{fs}-h_{sp})-m_{re}h_I+Q_I \qquad (2-4-46)$$

and

$$E_{II}=m_{sp}h_{fs}+m_{su}h_{su}+Q_{II} \qquad (2-4-47)$$

with

$$h_{su} = \begin{cases} h_I & m_{su} < 0 \\ h_{loop} & m_{su} \geqq 0 \end{cases} \quad . \tag{2-4-48}$$

The spray flow may be simulated by

$$m_{sp} = A_{sp} G_{sp} \tag{2-4-49}$$

with

$$G_{sp} = a_1 (p_P - p'_L)^2 + a_2 (p_P - p'_L)$$

where a_1 and a_2 are constants and p_L and p_P stand for pressure in the cold leg and the pressurizer, respectively. The back pressure of the relief flow m_{re} is the pressure of the discharge tank, which is not simulated in the present version of THYDE-P2.

If the saturated mixture in region II will become exhausted, we may have discontinuity in enthalpy of the flow out of the pressurizer. To ensure a smooth transition of enthalpy in this situation, we consider a fictitious length ℓ such that

$$h_{su} = \begin{cases} h_{II} & H_{pipe} + l < H_{II} \\ \beta h_{II} + (1-\beta) h_{II} & H_{pipe} < H_{II} < H_{pipe} + l \\ h_I & H_{II} < H_{pipe} \end{cases} \tag{2-4-50}$$

where

$$l = \text{(an input constant)} \times H_{pipe}$$

$$\beta = \frac{(H - H_{pipe})}{l}$$

and $H_{pipe} (\geqq 0)$ is the height of the stand pipe in the pressurizer tank.

2.4.2 Pump

It should be noted that both the head and torque of a pump are proportional to density. In THYDE-P2, L_{head} is defined without density (see Eq. (2–2–54)), whereas T, T_h and T_r are defined with density.

The equation of angular momentum of the impeller-flywheel assembly is given by[20]

$$\frac{da}{dt} = \lambda \{ \tau_e(t) - b(t) - k_1 a|a| - k_2 \, singn(a) |a|^{1/2} \} \tag{2-4-51}$$

where

$$a = \frac{\Omega(t)}{\Omega_r}$$

$$b = \frac{T_h(t)}{T_r}$$

$$\tau_e = \frac{T_e(t)}{T_r}$$

$$\lambda = \frac{30 T_r}{(\pi I_m \Omega_r)}$$

and k_1 and k_2 are constants and subscript r refers to the rated values not to be confused with the initial or steady state values. Eq. (2–4–51) is integrated with time to find the pump speed. Evaluation of the hydraulic torque $b(t)$ in Eq. (2–4–51) and the pump head L_{head} in Eq. (2–2–54) is performed by using the single phase homologous pump curves[21] (see **Figs. 2–4–3** and **2–4–4**) with modifications for two-phase mixture or cavitation as follows.

First we discuss how to obtain the hydraulic pump head L_{head} and torque T_h for non-

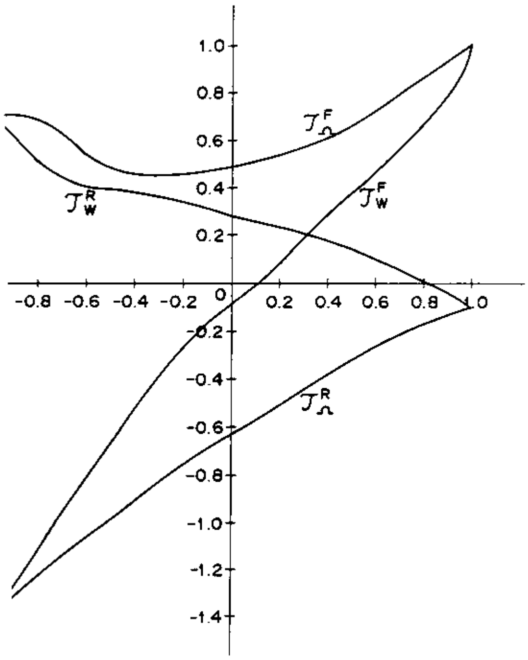

Fig. 2–4–3 Example of Homologous Torque Curves.

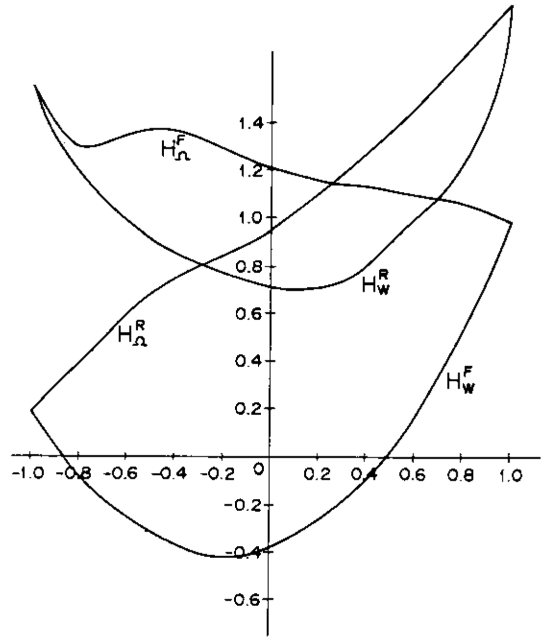

Fig. 2–4–4 Example of Homologous Head Curves.

cavitating subcooled water flow when the flow rate and the pump speed are given. We set

$$p_{head}=\frac{L_{head}}{L_{head,\,r}} \qquad (2\text{–}4\text{–}52)$$

and

$$w=\frac{W}{W_r} \quad . \qquad (2\text{–}4\text{–}53)$$

The head-discharge curve may be represented by two plots H_Ω^F and H_Ω^R of h_{head}/a^2 versus w/a which is valid for all speeds in the forward and reverse directions, respectively, i.e.,

$$p'_{head}=a^2H_\Omega^F(w/a) \qquad (a\geqq 0) \qquad (2\text{–}4\text{–}54)$$

and

$$p'_{head}=a^2H_\Omega^R(w/a) \qquad (a<0) \qquad (2\text{–}4\text{–}55)$$

where the prime means the non-cavitating subcooled case to be modified later with the corrections for cavitation or saturated two-phase mixture. The similar homologous relations apply for the hydraulic torque:

$$b'=a^2T_\Omega^F(w/a) \qquad (a\geqq 0) \qquad (2\text{–}4\text{–}56)$$

and

$$b'=a^2T_\Omega^R(w/a) \qquad (a\leqq 0) \quad . \qquad (2\text{–}4\text{–}57)$$

For small a , the above relationships may become unsatisfactory so that the second set of homologous relations is utilized, although the two sets of relationships may be equivalent in principle. The THYDE-P2 code selects the applicable set of homologous relations according to the relative magnitudes of w and a : If $w < a$, then the relationships (2–4–54) through (2–4–57) are selected. Otherwise, if $w\geqq 0$, then

$$p'_{head}=w^2H_w^F(a/w) \qquad (2\text{–}4\text{–}58)$$

and

$$b' = w^2 T_w^F (a/w) \tag{2-4-59}$$

and if $w < 0$, then

$$p'_{head} = w^2 H_w^R (a/w) \tag{2-4-60}$$

and

$$b' = w^2 T_w^R (a/w) \quad . \tag{2-4-61}$$

In the THYDE-P2 code, the correction of the above homologous relationships due to cavitation or two-phase mixture is performed as follows. The cavitation is assumed to occur if the quality at the impeller eye x_{eye} as defined below is calculated to be positive. First we define the pressure and specific enthalpy at the impeller eye as

$$p_{eye} = \begin{cases} p^E_{n_p-1} - NPSH_R \rho^E_{n_p-1} g & \text{(normal)} \\ p^A_{n_p+1} & \text{(reverse)} \end{cases} \tag{2-4-62}$$

and

$$h_{eye} = \begin{cases} h^E_{n_p-1} & \text{(normal)} \\ h^A_{n_p+1} & \text{(reverse)} \end{cases} \tag{2-4-63}$$

where the required net positive suction head $NPSH_R$ is assumed to be given by a function of a and w . Then the quality and density at the eye are given by

$$x_{eye} = \begin{cases} 1 & h_{eye} \geqq h_{gs}(p_{eye}) \\ 0 & h_{eye} \leqq h_{fs}(p_{eye}) \\ \dfrac{h_{eye} - h_{fs}(p_{eye})}{h_{fg}(p_{eye})}, & h_{fs}(p_{eye}) < h_{eye} < h_{gs}(p_{eye}) \end{cases} \tag{2-4-64}$$

and

$$\rho_{eye} = \frac{\rho_{gs}(p_{eye}) \rho_{fs}(p_{eye})}{\rho_{gs}(p_{eye})(1 - X_{eye}) + \rho_{fs}(p_{eye}) X_{eye}} \quad . \tag{2-4-65}$$

We assume that the pump torque and head under cavitation can be expressed as

$$T_h = \frac{\rho_{eye}}{\rho_r} T'_h - M_t (T'_h - T_h)$$

and

$$L_{head} = L'_{head} - M_h (L'_{head} - L_{head})$$

where M_t and M_h are the torque and head multipliers as functions of void fraction. Thus we have

$$b = \frac{p_{eye}}{\rho_r} b' - M_t \left(\frac{T'_h - T_h}{T_r} \right) \tag{2-4-66}$$

and

$$p_{head} = p'_{head} - M_h \left(\frac{L'_{head} - L_{head}}{L_{head,r}} \right) \tag{2-4-67}$$

where $(T'_h - T_h)/T_r$ and $(L'_{head} - L_{head})/L_{head,r}$ are input functions of pump speed. It should be noted that the factor ρ_{eye}/ρ_r in Eq. (2-4-66) can be traced back to the definition of torque in THYDE-P2. Therefore, care must be taken for the inputs $(T'_h - T_h)/T_r$ and $(L'_{head} - L_{head})/L_{head,r}$.

Prior to pump trip, we assume that a remains to be a_c (the initial steady state value).

2.4.3 Accumulator

The accumulator (AC) system is one of the safety injection subsystems. It consists of a large volume reservoir of borated water maintained under gas pressure. A check valve in the accumulator piping isolates the accumulator water from the primary coolant flow during normal operation. In the event of a depressurization accident, the water from the accumulator discharges to the primary loop whenever the system pressure falls below the pressure of the accumulator. The operation of the accumulator is completely passive in that no separate control device is required to enable it to function.

The schematic figure of an accumulator is presented in **Fig. 2–4–5**. The governing equations for the accumulator are obtained assuming the ideal gas for nitrogen as

$$dh_{H_2O} = -\frac{r p_{N_2}(0) V_{N_2}^{r}(0)}{\rho_{N_2} V_{N_2}^{1+r} J_e} dV_{N_2} + \frac{h_{ACD} - h_{H_2O}}{V_{H_2O}} dV_{H_2O} C \qquad (2\text{–}4\text{–}68)$$

where

$C = 0$ outflow

$= 1$ inflow

and

$r = 1.4$

In THYDE-P2, the duct that extends from the AC bottom to the cold leg is divided into two parts as shown in **Fig. 2–4–5**. Region 2 should be represented by a number of linkage nodes as a linkage duct. Region 1, however, is included in the AC model. Specific enthalpy in the accumulator duct is obtained by

$$\frac{dh_{ACD}}{dt} = \frac{h_{ACD}^{c} - h_{ACD}}{\tau} \qquad (2\text{–}4\text{–}69)$$

where

$h_{ACD}^{c} = h_{H_2O}$ outflow

$= h^{-}$ inflow

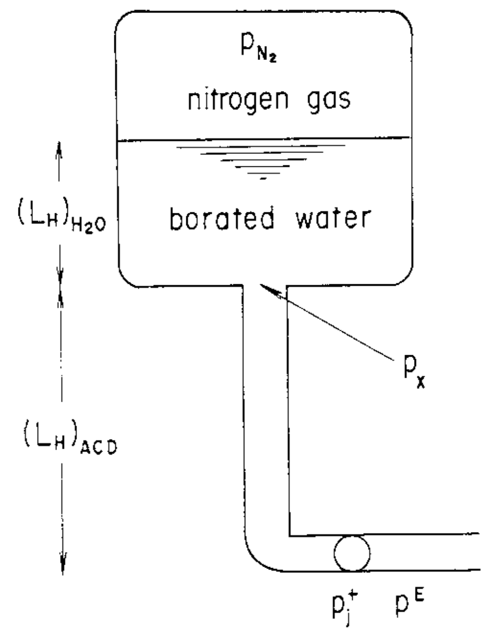

Fig. 2–4–5 Schematic Figure of Accumulator.

and

$$\tau = \frac{(\rho V)_{ACD}}{A_{ACD} G^E} \quad (\leq 10^{10}) \quad .$$

The injection junction pressure is given by

$$p^+ = p_x + g(\rho L_H)_{ACD} \qquad (2-4-70)$$

where

$$p_x = p_{N_2} + g(\rho L_H)_{H_2O} \qquad (2-4-71)$$

Water density in Eq. (2–4–71) ρ_{H_2O} is defined by h_{H_2O} and $(p_{N2}+p_x^{old})/2$, while ρ_{ACD} by h_{ACD} and $(p_x+p^{+old})/2$.

2.4.4 Discharge Tank

In the present version of THYDE-P2, no special model for the container is provided except the input discharge tank pressure.

2.5 Loss Coefficient, Valve and Critical Flow

2.5.1 Loss Coefficient

Loss coefficients at node average points k^{av} are inputs for initially stagnant nodes, while they will be obtained by the steady state adjustment for initially non-stagnant nodes. On the other hand, junction loss coefficients k^A and k^E are inputted or calculated in the code.

In order to explain the option to calculate junction loss coefficients, we consider a normal junction and its from- and to-nodes. Then,

$A^E_{from} < A^A_{to}$

$$(k^f_A)_{to} = (k^r_A)_{to} = 0$$

$$(k^f_E)_{from} = (1 - A^E_{from}/A^A_{to})^2$$

$$(k^r_E)_{from} = 0.45(1 - A^E_{from}/A^A_{to})$$

$A^E_{from} > A^A_{to}$

$$(k^f_E)_{from} = (k^r_E)_{from} = 0$$

$$(k^r_A)_{to} = (1 - A^A_{to}/A^E_{from})^2$$

$$(k^f_A)_{to} = 0.45(1 - A^A_{to}/A^E_{from}).$$

The loss coefficients at a break may change after break so that they can be imputted separately.

2.5.2 Junction Area

For each normal node n, we define the from-junction area A^+_{from} and the to-junction area A^+_{to} such that

$$A^+_{from} = (A^+_{from})_{opn} \xi^A_n \qquad (2-5-1)$$

and

$$A^+_{to} = (A^+_{to})_{opn} \xi^E_n \qquad (2-5-2)$$

where $(A^+_{from})_{opn}$ and $(A^+_{to})_{opn}$ are obtained as follows.

If junction j is normal,

$$A^{+}_{jopn} = min(A^{E}_{from}, A^{A}_{to}, A^{+}_{input}) \quad \text{for} \quad A^{+}_{input} \neq 0$$

$$= min(A^{E}_{from}, A^{A}_{to}) \quad \text{for} \quad A^{+}_{input} = 0.$$

If junction j is a mixing junction and node n is a to-node of it,

$$A^{+}_{jopn} = A^{A}_{n} \quad .$$

If junction j is a mixing junction and node n is a from-node of it,

$$A^{-}_{jopn} = A^{E}_{n} \quad .$$

If junction j is a boundary junction,

$$A^{+}_{jopn} = A^{E}_{from} \quad \text{for} \quad A^{+}_{input} = 0$$

$$= min(A^{E}_{from}, A^{+}_{input}) \quad \text{for} \quad A^{+}_{input} \neq 0.$$

The parameter $\xi(t)$ represents how the valve placed at the junction behaves temporally. We define

$$r^{A}_{n} = \frac{(A^{+}_{from})_{opn}}{A_n} \tag{2–5–3}$$

and

$$r^{E}_{n} = \frac{(A^{+}_{to})_{opn}}{A_n} \tag{2–5–4}$$

so that Eqs. (2–5–1) and (2–5–2) reduce to

$$A^{+}_{from} = r^{A}_{n} \xi^{A}_{n} A_n$$

and

$$A^{+}_{to} = r^{E}_{n} \xi^{E}_{n} A_n$$

which have already been used in Eqs. (2–2–63), (2–2–64), (2–2–74) and (2–2–75).

2.5.3 Valve

The valve behavior can be simulated by

$$\frac{d\xi}{dt} = \frac{\xi_c - \xi}{\tau} \tag{2–5–5}$$

where

$\xi_c = 1$ when it is completely open.

$= 0$ when it is completely closed.

The time constant τ and the logic to determine ξ_c depend on the type of the valve.

In addition to the valves specified by the inputs, there are pseudo valves presumed in the code which include:

(1) dead end valve ; always closed
(2) open valves at ordinary nomal nodes ; always open
(except at nodes with actual valves)
(3) valve to imperatively cut off accumulator ; closes when residual water is less than 5%.

All valves including the pseudo valves can be placed only on the E point of a normal node. Thus

$$\xi^{A}_{n} = \begin{cases} \xi^{E}_{nf} & \text{if the from-junction of node } n \text{ is normal.} \\ 1 & \text{if the from-junction of node } n \text{ is a mixing junction.} \end{cases}$$

2.5.4 Critical Flows

Given the specific enthalpy h and the pressure at the discharge point p, the critical flow G_M can be given by the following set of equations.

a) If the coolant is subcooled, the critical flow is given by

$$G_M = c_1 \sqrt{2\rho(p, h)(p - C_2 p_s)} \qquad (2-5-6)$$

where

$$p_s = h_{fs}^{-1}(h)$$

$$\rho = \begin{cases} \rho_{fs}(p) & x \geqq 0 \\ \rho_f(p, h) & x < 0 \end{cases}$$

and c_1 is a function of enthalpy h such that

$$c_1 = C_d G_M(p_s, h) / \sqrt{2\rho_{fs}(h)(1 - C_2 p_s)} \quad .$$

b) If $0.02 < x < 1$, then

$$G_M = C_c C_D g_M(p, h) \qquad (2-5-7)$$

where $g_m(p, h)$ is given by Moody Table(17).

c) If > 1, then

$$G_M = D_1 \sqrt{r(2/(r+1))^{((r+1)/(r-1))} \rho_g(p, h) p} \qquad (2-5-8)$$

where

$$D_1(p) = C_c C_D g_M(p, h_{gs}(p))) / \sqrt{r(2/(r+1))^{((r+1)/(r-1))} \rho_{gs}(p) p} \ .$$

In the above, C_c is the factor to ensure continuity of G_M at $X = 0.02$.

3. Heat Transfer

In this chapter, we will discuss heat transfer aspects of THYDE-P2. In section 3.1, various heat sources in a fuel rod including metal-water reaction are discussed. In section 3.2, given heat transfer coefficient, we will give the method to calculate heat transfer rate to coolant. In section 3.4, rod-to-rod radiative heat transfer is discussed, using a model made of a 3×3 rod cluster. In section 3.5, the heat transfer and critical heat flux correlations are cited.

3.1 Heat Generation inside Fuel

Heat sources inside fuel, i.e., Ξ in Eq. (3–3–1) are (i) fission power, (ii) decay heat of fission products, (iii) decay heat of actinides and (iv) metal-water reaction heat. In the following, we will discuss them, separately. Items (i), (ii), and (iii) are not accounted for in the non-nuclear calculation option.

3.1.1 Fission Power

The nuclear reactor kinetics equation in the THYDE-P2 code is based on point kinetics model with 6 groups of delayed neutron precursors.

$$\frac{dn}{dt}=\frac{\beta}{l}(\Gamma_{tot}-1)n+\sum_{i=1}^{6}\lambda_i C_i \qquad (3-1-1)$$

$$\frac{dC_i}{dt}=-\lambda_i C_i+\frac{\beta_i}{l}n \qquad (i=1,2,\ldots\ldots 6) \qquad (3-1-2)$$

where

$$\beta=\sum_{i=1}^{6}\beta_i$$

and

$$n(0)=1 \quad .$$

The reactivity insertion $\Gamma(t)$ in Eq. (3–1–1) is calculated as the sum of three reactivity components, i.e.,

$$\Gamma_{tot}(t)=\Gamma_{ex}(t)+\sum_i \Gamma_{Fi}+\sum_i \Gamma_{ci} \qquad (3-1-3)$$

where the first term $\Gamma_{ex}(t)$ represents the external reactivity contributions such as control rod insertion, whereas the second and third terms the feedback effects due to fuel temperature change and void fraction change, respectively, such that

$$\Gamma_{Fi}=r_{Ti}(T_{Fi}(t)-T_{Fi}(0))$$

and

$$\Gamma_{ci}=r_{\alpha i}(\alpha_i(t)-\alpha_i(0)) \quad .$$

3.1.2 Fission Products Decay Heat

The decay heat due to FP (fission products) except actinides is calculated as follows[7].

$$R_{FP}=\varepsilon\sum_{i=1}^{11}x_i \qquad (3-1-4)$$

where

$$\frac{d}{dt}x_i=\lambda_i(nE_i-x_i) \qquad (1\leq i\leq 11) \qquad (3-1-5)$$

$$\varepsilon=\begin{cases}1.0 \text{ for BE calculation}\\ 1.2 \text{ for EM calculation}\end{cases} \qquad (3-1-6)$$

and

$$x_i(0)=E_i \qquad (1\leq i\leq 11) \quad .$$

For the BE and EM calculations, see chap 5. Parameters E_i and λ_i are given in Ref. (7).

3.1.3 Actinides Decay Heat

The heat contribution from actinides decay is calculated as follows. We consider only ^{239}U and ^{239}Np.

$$^{238}_{92}U(n,r)^{239}_{92}U \xrightarrow{\beta^-} {}^{239}_{93}Np \xrightarrow{\beta^-} {}^{239}_{94}Pu$$

Then

$$\frac{d}{dt}N_{29}=-\lambda_{29}N_{29}+C_c\Sigma_a\varphi(0)n(t) \qquad (3-1-7)$$

and

$$\frac{d}{dt}N_{39}=-\lambda_{39}N_{39}+\lambda_{29}N_{29} \qquad (3-1-8)$$

where

$$\lambda_{29}=4.91\times10^{-4}\ \text{sec}^{-1}$$

and

$$\lambda_{39}=3.41\times10^{-4}\ \text{sec}^{-1} \quad .$$

If the chain is at steady state, then

$$N_i(0)=C_c\Sigma_a\varphi(0)/\lambda_i \qquad (i=29 \text{ and } 39)$$

Relative power R_{ACT} produced by actinides decay is given by

$$R_{ACT}=\frac{(y\lambda N)_{29}+(y\lambda N)_{39}}{Y\Sigma_f\varphi(0)} \qquad (3-1-9)$$

where

Y = 207.3 MeV/fission

y_{29}= 0.456 MeV/decay

and

y_{39}= 0.434 MeV/decay .

If we set

$$N_i=C_c\Sigma_a\frac{\varphi(0)x_i}{\lambda_i} \qquad (i=29,\ 39)$$

then Eq. (3–1–9) will be transformed to

$$R_{ACT}=C_c\frac{\Sigma_a}{\Sigma_f}\ \frac{(yx)_{29}+(yx)_{39}}{Y} \qquad (3-1-10)$$

where

$$\frac{d}{dt}x_{29}=\lambda_{29}(n-x_{29}) \qquad (3-1-11)$$

and

$$\frac{d}{dt}x_{39}=\lambda_{39}(x_{29}-x_{39}) \qquad (3-1-12)$$

with the initial condition

$$x_i(0)=1 \qquad (i=29 \text{ and } 39)$$

3.1.4 Metal-Water Reaction

Heat generation in the cladding due to metal-water reaction is calculated based on the equation of Baker and Just[26] with no limitations for steam availability as required by Ref. (1). When burst is calculated to occur, the Zircaloy cladding is assumed to react on the inside as well as outside for a length of the burst node. The equation of Baker and Just is

$$\frac{d\Theta}{dt}=K_1\frac{e^{-K_2/(T+273)}}{\Theta} \qquad (3-1-13)$$

where

$$K_1=0.775\times10^{-4} \quad \text{m}^2/\text{sec}$$

and

$$K_2=2.29\times10^{-4} \quad {}^\circ K$$

In the THYDE-P2 code, it is assumed that the heat generation is uniformly distributed in the clad node where the boundary of the reacted zircaloy is present. The volumetric heat source of the node with thickness Δr is given by

$$\Xi_{MW}=\rho_{zr}\Delta h_{reac}\frac{d\Theta}{dt}/\Delta r \qquad (3-1-14)$$

where

$$\rho_{zr}=6.568\times10^{-3}$$

Following assumption (b) in subsection 4.1.2, oxide thinning resulting from clad burst will be taken into consideration in Eq. (3-1-13).

3.2 Heat Transfer to Coolant

A distinction is made for two kinds of heat transfer coefficients, i.e., the one which is the coefficient of heat transfer to the coolant and the other which is the heat transfer coefficient for the calculation of the wall surface temperature. The difference arises when rod-to-rod radiation becomes effective, for example, after clad burst. In section 3.3, heat conduction is discussed.

3.2.1 Heat Transfer to Core Flow

3.2.1.1 Before burst (Elevation without burst)

In the following discussion, we will drop the subscript indicating the core node in question. The heat source to the core coolant q''' in Eq. (2-3-8) is given by

$$q'''=\frac{2\pi r_R\Phi_R}{A} \qquad (3-2-1)$$

with

$$\Phi_R=h^c_{tr}(T_R-T_b) \qquad (3-2-2)$$

where h^c_{tr} is the coefficient of heat transfer to the coolant which is not to be confused with h^{cs}_{tr} , i.e., the heat transfer coefficient for the calculation of the clad surface temperature (see section 3.5). The heat transfer coefficient h_{tr}^{c} is given by

$$h_{tr}^{c}=h_{w-c}+h_{cvn} \qquad (3-2-3)$$

The readers can refer to subsections 3.5.1 and 3.5.3 for the conventional heat transfer coefficient h_{cvn}, and the rod-to-coolant radiative heat transfer coefficient h_{w-c}, respectively.

3.2.1.2 After burst (Elevation with burst)

The core will be divided into several regions, each of which will be regarded as a collection of respective average coolant channels. The average coolant channel is associated with the average fuel rod or plate. Suppose that an average fuel was calculated to burst at a certain elevation. Then, it will be interpreted that bursts have occurred at that elevation with a certain pattern in the entire region. With the calculated occurrence of burst, the two fuel rod calculation will be started for the region to include rod-to-rod radiative heat transfer on the basis of the 3 X 3 rod matrix to be described in section 3.4.

Among the parameters in Eqs. (3–2–1) and (3–2–2), not only the heat transfer coefficient, but also the wetted perimeter and the cross-sectional flow area will be influenced. The former will be explained in section 3.4, while the latter two in the following.

Averaging the latter two over the 3 X 3 matrix, the heat input from the burst axial node of the matrix to the average core flow is obtained as follows:

First we obtain the change in the wetted perimeter. If the center rod is burst, then the wetted perimeter in the matrix changes from

$$l_w=8\pi r_R$$

to

$$l_w^*=\pi r_R^*\left(8-M_b-\frac{N_b}{2}\right)+\pi r_R\left(M_b+\frac{N_b}{2}\right) \qquad (3-2-4a)$$

And if the center rod is not burst, then the wetted perimeter changes to

$$l_w^*=\pi r_R^*\left(6-M_n-\frac{N_n}{2}\right)+\pi r_R\left(2+M_n+\frac{N_n}{2}\right) \qquad (3-2-4b)$$

Thus the heat input from the axial matrix node with clad burst to the average core flow is given by

$$q'''=\frac{w_1(2\pi r_R)\Phi_R+w_2(2\pi r_R^*)\Phi_R^*}{A_9^*} \qquad (3-2-5)$$

with

$$w_1+w_2=4$$

$$w_1=\begin{cases} M_b/2+N_b/4 & \text{if center rod is burst} \\ 1+M_b/2+N_b/4 & \text{if center rod is non-burst}\end{cases}$$

$$\Phi_R^*=h_{tr}^{cs*}(T_R^b-T_b)=(h_{tr}^{c*}+h_b)(T_R^b-T_b)$$

and

$$\Phi_R=h_{tr}^{cs}(T_R^n-T_b)=(h_{tr}^{c}+h_n)(T_R^n-T_b)$$

where h_{tr}^{cs} is defined in Eqs. (3–5–3) and (3–5–4). The flow area A_9^* in Eq. (3–2–5) is given by Eq. (4–1–20) or (4–1–22). The heat transfer coefficient h_{tr}^{c} is given by Eq. (3–2–3), and h_{tr}^{c*} is the coefficient of heat transfer to coolant for the burst node. For the meaning of N_b and M_b or N_n and M_n, reference should be made to section 3.4.

3.2.2 Heat Transfer between SG Primary and Secondary Coolants

In the THYDE-P2 code, the SG primary coolant flow is represented by a series of normal nodes, while the secondary coolant system is represented by the Tank model (see subsection 2.3.1). In addition, we divide the U-tube wall into as many nodes as the primary coolant nodes and label them with the same index as that of the corresponding primary coolant nodes.

It should be noted that Q_I and Q_{II} of the Tank model are, by definition, heat inputs minus heat leak (see subsection 2.3.1). In Eqs. (3–2–11) and (3–2–12), however, heat leak from the SG secondary system will be ignored in the present version of THYDE-P2.

The heat input to the primary node n, q_n''' is

$$q_n''' = \frac{l_{wn}}{A_n} \Phi_n \qquad (3\text{–}2\text{–}6)$$

where l_{wn} is the wetted perimeter of a SG primary coolant node n, which is not to be confused with the outer wetted perimeter of the U-tube wall node n.

The heat flux Φ_n into the primary coolant node is given by

$$\Phi_n = \lambda_n^I (T_{SGn}^I - T_{bn}) \qquad (3\text{–}2\text{–}7)$$

if node belongs to region I. And otherwise

$$\Phi_n = \lambda_n^{II} (T_{SGn}^{II} - T_{bn}) \qquad (3\text{–}2\text{–}8)$$

In Eqs. (3–2–7) and (3–2–8), λ_n^I and λ_n^{II} are given by

$$\frac{1}{\lambda_n^I} = \frac{1}{h_{trn}^c} + \frac{\delta_{wn}}{k_{wn}} + \frac{1}{h_{trSGI}^c} \qquad (3\text{–}2\text{–}9)$$

and

$$\frac{1}{\gamma_n^{II}} = \frac{1}{h_{trn}^c} + \frac{\delta_{wn}}{k_{wn}} + \frac{1}{h_{trSGII}^c} \qquad (3\text{–}2\text{–}10)$$

If node n contains the interface of regions I and II (see **Fig. 3–2–1**), the heat flux Φ_n is given as follows (subscript n is deleted)

$$\Phi = \frac{(L_I \Phi_I + L_{II} \Phi_{II})}{L} = \frac{\{L_I \lambda_I (T_{SG}^I - T_b) + L_{II} \lambda^{II} (T_{SG}^{II} - T_b)\}}{L} \qquad (3\text{–}2\text{–}11)$$

where λ^I and λ^{II} are given by Eqs. (3–2–9) and (3–2–10), respectively.

Then the heat sources in the Tank model for the SG secondary coolant is

$$Q_I = -n_{SG} L_{WSG} \sum_I \Phi_n L_n \qquad (3\text{–}2\text{–}12)$$

and

$$Q_{II} = -n_{SG} L_{WSG} \sum_{II} \Phi_n L_n \qquad (3\text{–}2\text{–}13)$$

It should be noted that Q_I and Q_{II} of the Tank model are, by definition, heat input minus heat leak. In Eqs. (3–2–12) and (3–2–13), however, heat leak was ignored. Moreover, we have the following relationships between the U-tube wall temperatures and the coolant bulk temperatures.

$$T_{wn} = \frac{\Phi_n}{h_{trn}^c} + T_{bn} \qquad (3\text{–}2\text{–}14)$$

and

$$T_{SG.wn} = \frac{-\Phi_n}{h_{tr.SGI}^c} + T_{SG}^I \quad \text{if node } n \text{ belongs to region I} \qquad (3\text{–}2\text{–}15)$$

$$\frac{-\Phi_n}{h_{tr.SGII}^c} + T_{SG}^{II} \quad \text{otherwise.}$$

If node has the interface of regions I and II, then we have the two secondary wall temperatures for this node.

Readers may refer to subsection 7.2.3 for the steady state calculation of the U-tube wall temperatures.

3.2.3 Pressurizer Heater in Tank Model

Three types of heaters are accounted for[19] by THYDE-P2. Heater (i = 1 and 2) is turned on at pressure p_{on} and off at p_{off}. Heater 3 is turned on at water temperature T_{on} and off at T_{off}. The heat transferred from the heaters to coolant may be discribed by

$$\tau_I \frac{d}{dt} Q_I = \sum_{i=1}^{3} E_i (1-e_i) - Q_I - E_{lossI}(t) \qquad (3-2-16)$$

and

$$\tau_{II} \frac{d}{dt} Q_{II} = \sum_{i=1}^{3} E_i e_i - Q_{II} - E_{lossII}(t) \qquad (3-2-17)$$

where the heat production rate by the heaters E_i (i = 1, 2 and 3) and the heat losses from the pressurizer E_{lossI} and E_{lossII} may be represented by

$$E_i(T) = S_{wi}(t) G_i(t) \qquad (i = 1, 2 \text{ and } 3) \qquad (3-2-18)$$

$$S_{wi}(t) = 1 \qquad \text{heater on}$$
$$= 0 \qquad \text{heater off}$$

$$E_{lossI}(T) = E_{lossI}(0) + E_{lossII}(0) \frac{z_w(t) - z_w(0)}{H_p - z_w(0)}$$

and

$$E_{lossI}(t) + E_{lossII}(t) = \sum_{i=1}^{3} E_i(0) \ .$$

It should be noted that Eqs. (3–2–16), (3–2–17) and (3–2–20) give Eq. (2–3–46) at a steady state. In the above, the quantity e_i is defined to be

$$e_i = \frac{z_w - b_i}{L_i} \qquad (i = 1, 2, 3)$$

where L_i and b_i are defined **Fig. 3–2–2.**

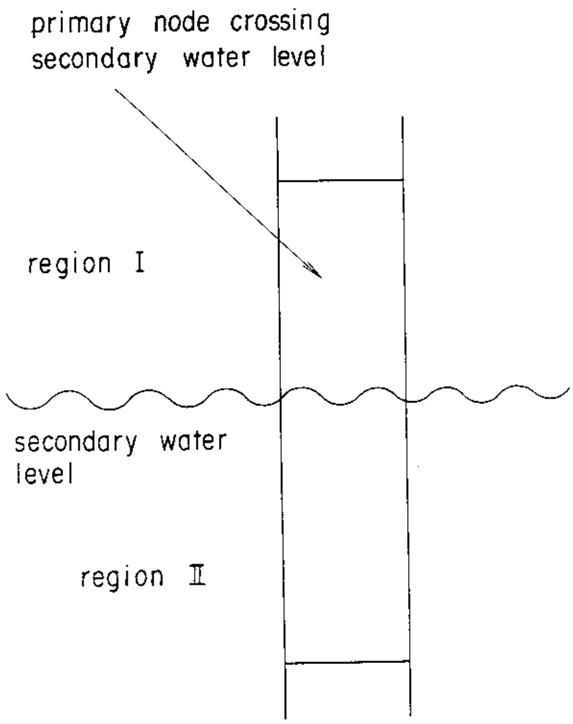

Fig. 3–2–1 Primary Node with Secondary Water Level.

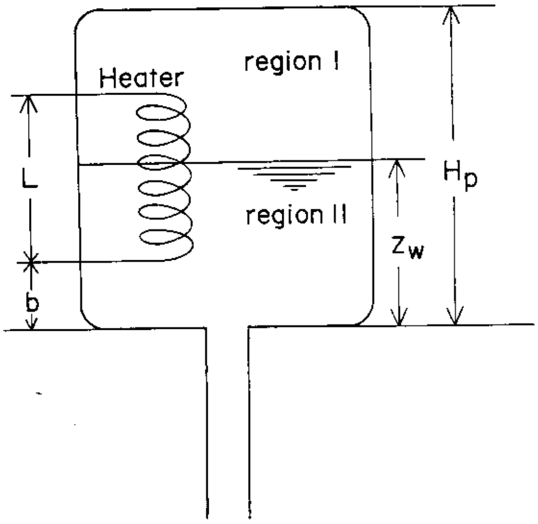

Fig. 3–2–2 Pressurizer Heaters in Tank Model.

3.3 Heat Conduction

3.3.1 Heat Conductor Configuration

Heat conduction in heat conductors is assumed one-dimensional, i.e., perpendicular to the coolant flow so that heat transfer between adjacent two conductors are not taken into consideration.

Depending on the type of boundary condition at the left (or inner) and right (or outer) surfaces of the conductor, there are 7 cases as shown in **Fig. 3–3–1**. Each case can further be subdivided depending on whether the conductor is cylindrical or rectangular.

3.3.2 Temperature Distribution

The heat conduction in a heat conductor is given by

$$\rho C_p \frac{\partial T}{\partial t} = \frac{1}{r^\alpha} \frac{\partial}{\partial r} \left(k r^\alpha \frac{\partial T}{\partial t} \right) + \Xi \qquad (3\text{–}3\text{–}1)$$

where

$\alpha = 0$ for cartesian coordinate system

$= 1$ for cylindrical coordinate system.

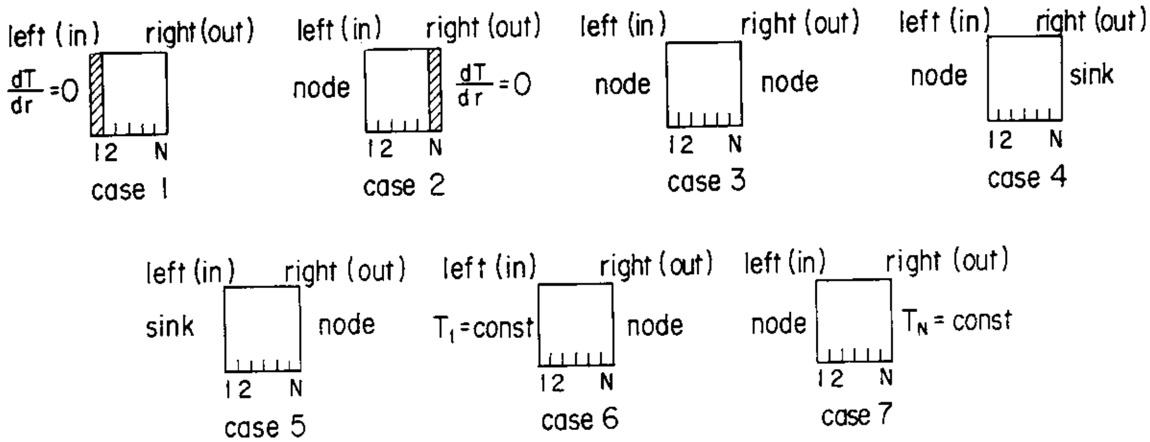

Fig. 3–3–1 Heat Conductor Configurations.

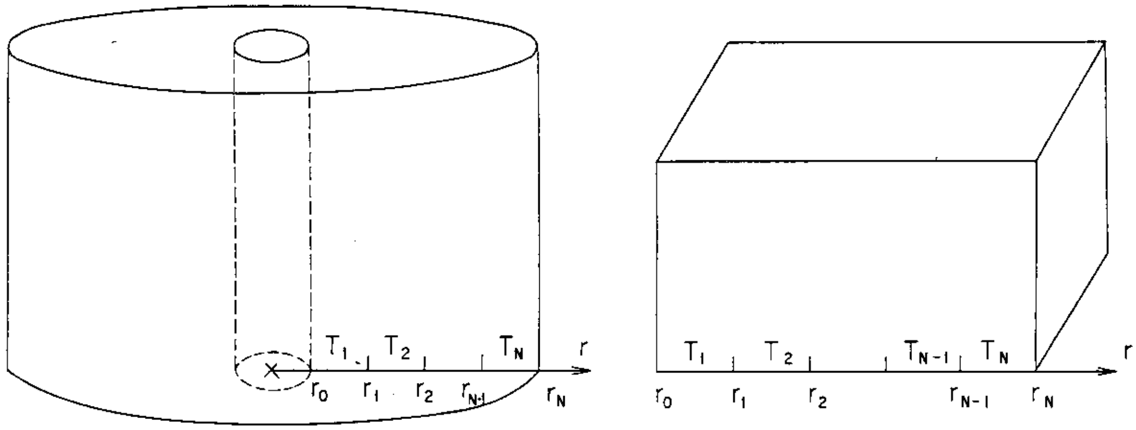

Fig. 3–3–2 Noding of Heat Conductor.

We define the noding convention in the heat conductor as shown in **Fig. 3–3–2**. For a solid cylinder, we let $r_0=0$.

For rod type fuel, the heat production rate $\Xi(r, t)$ may be represented by

$$\Xi=\frac{2}{r_F}\Phi_F(z, 0)\Pi(t), \quad 0<r<r_F \tag{3–3–2}$$

$$=\Xi_{MW} \quad , \quad r_{cl}^{IN}<r<r_R \tag{3–3–3}$$

where heat production is assumed uniform in the fuel pellet and Ξ_{MW} is assumed to vanish in the clad nodes in which the boundary of the reacted zirconium is not present (see Eq. 3–1–14). The temporal behavior of the heat generation in nuclear fuel $\Pi(t)$ is given by

$$\Pi=\frac{[n+\varepsilon R_{FP}+R_{ACT}]}{(1+\varepsilon R_{FP}(0)+R_{ACT}(0))} \tag{3–3–4}$$

where the condition $\Pi(0)=1.0$ is satisfied. Factor ε is given by Eq. (3–1–6).

Integrating Eq. (3–3–1) from $r=r_{i-1}$ to $r=r_i$ and differencing it with respect to time to obtain

$$\frac{T_i^{new}-T_i^{old}}{\Delta t}=G_i \tag{3–3–5}$$

with

$1\leqq i\leqq N$ for IC = 1, 2, 3, 4 and 5

$2\leqq i\leqq N$ for IC = 6

and

$1\leqq i\leqq N-1$ for IC = 7

where

$$G_i=\frac{\delta_i T_{i+1}-(\delta_i+\delta_{i-1})T_i+\delta_{i-1}T_{i-1}}{\gamma_i S_i^c}+(\Xi/\gamma)_i$$

$$\delta_i=\left(\frac{2S_i^s}{\Delta z_i}\right)\frac{k_{i+1}(r_i-r_{i-1})+k_i(r_{i+1}-r_i)}{(r_{i+1}-r_{i-1})^2}$$

and

$$\gamma_i=(\rho c_p)_i \quad (1\leqq i\leqq N-1) \quad .$$

For δ_i, δ_N, T_0 and T_{N+1}, we have

$$\delta_0 = 0 \qquad \text{for IC} = 1$$

$$= \frac{S_0^s h_{tr}}{\Delta z_i} \qquad \text{for IC} = 2, 3, 4, 7$$

$$= \frac{S_0^s h_{rad}((T_0^{old}+273)^3-(T_1^{old}+273)^3)}{\Delta z_i (T_0^{old}-T_1^{old})} \qquad \text{for IC} = 5$$

not defined for IC = 6

$$\delta_N = \frac{S_N^s h_{tr}}{\Delta z_i} \qquad \text{for IC} = 1, 3, 5, 6$$

$$= 0 \qquad \text{for IC} = 2$$

$$= \frac{S_N^s h_{rad}((T_{N+1}^{old}+273)^3-(T_N^{old}+273)^3)}{\Delta z_i (T_{N+1}^{old}-T_N^{old})} \qquad \text{for IC} = 4$$

not defined for IC = 7

$$T_0 = T_b \qquad \text{for IC} = 2, 3, 4, 7$$

$$= T_{sink} \qquad \text{for IC} = 5$$

not defined for IC = 1 and 6

and

$$T_{N+1} = T_b \qquad \text{for IC} = 1, 3, 5, 6$$

$$= T_{sink} \qquad \text{for IC} = 4$$

not defined for IC = 2 and 7.

We now solve Eq. (3–3–5) by the Crank-Nicolson method, i.e.,

$$\frac{T_i^{new}-T_i^{old}}{\Delta t} = \theta G_i^{new} + (1-\theta) G_i^{old} \qquad (0 < \theta \leq 1) \tag{3–3–6}$$

which can be transformed to be

$$(-A_i T_{i+1} + B_i T_i - C_i T_{i-1})^{new} = D_i \tag{3–3–7}$$

where

$$A_i = \frac{\Delta t \theta \delta_i}{\gamma_i S_i^c}$$

$$B_i = 1 + \frac{\Delta t \theta (\delta_i + \delta_{i-1})}{\gamma_i S_i^c}$$

$$C_i = \frac{\Delta t \theta (\delta_i + \delta_{i-1})}{\gamma_i S_i^c}$$

$$D_i = T_i^{old} + \Delta t \left((1-\theta) G_i^{old} + \theta \left(\frac{\Xi}{\gamma}\right)_i^{new}\right)$$

$$D_N = T_N^{old} + \Delta t \left((1-\theta) G_i^{old} + \theta \left(\frac{\Xi}{\gamma}\right)_N^{new}\right) + A_N T_b \qquad \text{for IC} = 3$$

$$D_N = T_N^{old} + \Delta t \left((1-\theta) G_i^{old} + \theta \left(\frac{\Xi}{\gamma}\right)_N^{new}\right) + A_N T_{sink} \qquad \text{for IC} = 4$$

$$D_{N-1} = T_{N-1}^{old} + \Delta t \left((1-\theta) G_{N-1}^{old} + \theta \left(\frac{\Xi}{\gamma}\right)_{N-1}^{new}\right) + A_{N-1} T_{wall} \qquad \text{for IC} = 7$$

$$D_1 = T_1^{old} + \Delta t\left((1-\theta)G_1^{old} + \theta\left(\frac{\Xi}{\gamma}\right)_1^{new}\right) + C_1 T_{sink} \qquad \text{for IC} = 5$$

and

$$D_2 = T_2^{old} + \Delta t\left((1-\theta)G_2^{old} + \theta\left(\frac{\Xi}{\gamma}\right)_2^{new}\right) + C_2 T_{wall} \qquad \text{for IC} = 6.$$

In the linear implicit scheme, the coefficient A_i, B_i, C_i and D_i in Eq. (3–3–7) are the old values so that it becomes a tri-diagonal matrix equation to which Thomas algorithm can be applied.

3.3.3 Gap Conductivity [27],[28]

Special treatment is needed for fuel rod with a gap. We assume the following relationship to hold

$$\Phi_{CL}^{in}(r_F + r_{gap}) = \Phi_F^{out} r_F \qquad (3-3-8)$$

which means that the total heat flux at the clad inner surface coincides with that at the pellet outer surface. In THYDE-P2, the gap conductivity h_{gap}^t is defined in terms of Φ_{CL}^{in} such that

$$\Phi_{CL}^{in} = h_{gap}^t\ (T_F^{out} - T_{CL}^{in}) \quad .$$

Then, Eq. (3–3–8) gives

$$\Phi_F^{out} = \frac{r_F - r_{gap}}{r_F} h_{gap}^t\ (T_F^{out} - T_{CL}^{in}) \quad .$$

Heat flux through the gap is composed of two components, (1) heat conduction and (2) radiation. We first discuss heat conduction. If $r_{gap} > 0$, then

$$h_{gap} = \frac{\lambda_{gap}}{r_{gap} + 4.39\times10^{-6}} \qquad (3-3-13)$$

and if $r_{gap} = 0$, then

$$h_{gap} = 1.16\times10^{-6} p_{gc} + \frac{\lambda_{gap}}{4.39\times10^{-6}} \qquad (3-3-14)$$

where p_{gc} is the contact pressure between fuel pellet and cladding.

The conductivity of the gas mixture λ_{gap} in Eqs. (3–3–13) and (3–3–14) is calculated from a formula based on work of Brokaw[29].

$$\lambda_{gap} = \sum_{i=1}^{n_{gap}} \lambda_i \Big/ \left(1 + \sum_{i=1,\, j\neq i}^{n} \Psi_{ij} y_j / y_i\right) \qquad (3-3-15)$$

where

$$\Psi_{ij} = \frac{\Phi_{ij}[1 + (\lambda_i/\lambda_i)^{1/2}(M_i/M_j)^{1/4}]^2}{2^{1.5}(1 - M_i/M_j)^{1/2}} \qquad (3-3-16)$$

$$\Phi_{ij} = 1 + 2.41\frac{(M_i - M_j)(M_i - 0.142M_j)}{(M_i + M_j)^2} \qquad (3-3-17)$$

and : n_{gap} = number of component gases in the mixture
M = molecular weight of a component gas
Y = molecular fraction of the gas
λ = the thermal conductivity of the pure gas.

The following expressions are used for the thermal conductivities of He, Xe, Kr, air, N_2 and H_2:

If r_{gap} is less than the mean free path of the Helium molecule, then

$$\lambda_{He} = \lambda_{He}^o f_1 (p_{gap}, T_{gap}) \qquad (3-3-18)$$

and otherwise

$$\lambda_{He} = \lambda_{He}^o \qquad (3-3-19)$$

where

$$\lambda^o_{He}=5.43\times10^{-7}[1.8(T_{gap}+276)]^{0.668} \quad (3-3-20)$$

The others are[5]

$$\lambda_{Xe}=5.75\times10^{-9}[1.8(T_{gap}+273)]^{0.872} \quad (3-3-21)$$

$$\lambda_{Kr}=6.56\times10^{-9}[1.8(T_{gap}+273)]^{0.923} \quad (3-3-22)$$

$$\lambda_{Air}=3.03\times10^{-8}[1.8(T_{gap}+273)]^{0.846} \quad (3-3-23)$$

$$\lambda_{N_2}=3.03\times10^{-8}[1.8(T_{gap}+273)]^{0.846} \quad (3-3-24)$$

$$\lambda_{H_2}=2.41\times10^{-7}[1.8(T_{gap}+273)]^{0.821} \quad (3-3-25)$$

and

$$\lambda_{H_2O}=f_2(p_{gap},\ T_{gap}) \quad (3-3-26)$$

In the above, f_1 and f_2 are input functions of p_{gap} and T_{gap}.
The gap conductivity due to thermal radiation is given by[30] h_{rad}

$$=\frac{1.369\times10^{-11}[(T_F^{out}+273)^4-(T_{CL}^{in}+273)^4]}{(2r_F+r_{gap})/2r_F[1/\varepsilon_F+r_F/(r_F+r_{gap})(1/\varepsilon_{cl}-1)](T_{CL}^{out}-T_{CL}^{in})} \quad (3-3-27)$$

Thus the total gap conductivity h^t_{gao} is given by

$$h^t_{gap}=h_{gap}+h_{rad} \quad (3-3-28)$$

In summary, the parameters influencing the gap conductivity are;

temperatures of the surrounding surfaces
gas temperature
gas composition
gas pressure (p_{gap})

and

gas width (r_{gap})

The temperatures of the surrounding surfaces can be calculated by the method discussed in subsection 3.3.2 while the gas temperature is set equal to the arithmetic average of the pellet surface temperature and the clad inner surface temperature (see Eq. (4–2–10)). The temperature of the upper and lower plenums are given by

$$T_{upl}=T_b^{top}+C_T \quad (3-3-29)$$

and

$$T_{lpl}=T_b^{bottom}+C \quad (3-3-30)$$

where T_b^{top} and T_b^{bottom} are the bulk temperatures at the top and bottom nodes of the core channel flow, respectively, and C_T and C_B are constants. The gap gas composition is an input to the THYDE-P2 code and is assumed to remain constant throughout the transient except that, if burst is calculated to occur, the gas composition in the burst node is assumed to be steam. For the calculation of the gap width r_{gap} and the mixture gas pressure p_{gap}, the readers can refer to section 4.2.

Thus, we have the following set of equations:

$$T_{gap}=\frac{T_F^{out}+T_{CL}^{in}}{2} \quad (3-3-31)$$

$p_{gap}=p_{gap}(T_{gap},\ r_{gap})$ from Eq. (4–2–9) (3–3–32)

$r_{gap}=r_{gap}(p_{gap},$ temp distribution$)$ from Eq. (4–2–3) (3–3–33)

$$\lambda_{gap}=\lambda_{gap}(p_{gap},\ T_{gap}) \qquad \text{from Eq. (3–3–15)} \qquad (3–3–34)$$

$$h_{gap}=h_{gap}(\lambda_{gap},\ r_{gap}) \qquad \text{from Eq. (3–3–13)} \qquad (3–3–35)$$

and

$$h_{rad}=h_{rad}(T_F^{out},\ T_{CL}^{in},\ r_{gap}) \qquad \text{from Eq. (3–3–27).} \qquad (3–3–36)$$

Suppose that the temperature distribution in fuel is known. Then, we can obtain p_{gap} and r_{gap} by solving Eqs. (3–3–32) and (3–3–33) simultaneously. Next, λ_{gap} and then h_{gap} and h_{rad} can be obtained from Eqs. (3–3–34), (3–3–35) and (3–3–36), respectively.

3.4 Rod-to-Rod Radiative Heat Transfer

In this section, we will obtain the radiative heat transfer coefficients for the burst and non-burst rods, h_n and h_b, which are to be used for Eqs. (3–5–3) and (3–5–4) to give Φ_R and Φ_R^* in Eq. (3–2–5). To this end, we will consider a 3 X 3 rod matrix[5] as shown in **Fig. 3–4–1**, in which some of the rods are burst.

In THYDE-P2, rod-to-rod radiative heat transfer will be accounted for in the following way only after clad burst. The core will be divided into several regions, each of which will be regarded as a collection of respective average coolant channels. The average coolant channel is associated with the average fuel rod or plate. Suppose that an average fuel was calculated to burst at a certain elevation. Then, it will be interpreted that bursts have occurred at that elevation with a certain pattern in the entire region. With the calculated occurrence of burst, the two fuel rod calculation will be started for the region to include rod-to-rod radiative heat transfer on the basis of the 3 X 3 rod matrix.

The burst pattern must be specified by inputs, by choosing it from **Figs. 3–4–2** or **3–4–3**. We also assume that the matrices with the prescribed burst pattern is isolated from each other with respect to rod-to-rod radiation.

The conceivable rods burst patterns are shown in **Figs. 3–4–2** and **3–4–3**, where the definitions of M_n, N_n, M_b and M_b are shown in Nomenclature. The diagonal rod refers to rod 2, 4, 6 and 8, and the off-diagonal rod to rod 3, 5, 7 and 9. Let n_b be the number of burst rods in the matrix. Then we have a relationship

$$M_n+M_n=8-n_b$$

if the center rod is non-burst, and

$$M_b+N_b=9-n_b$$

if the center rod is burst.

According to Hottel[30], the radiative heat flux from the center rod may be given by

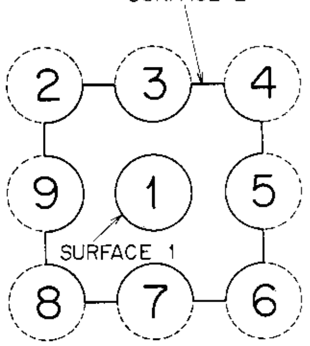

Fig. 3–4–1
3 X 3 Rod Cluster Model.

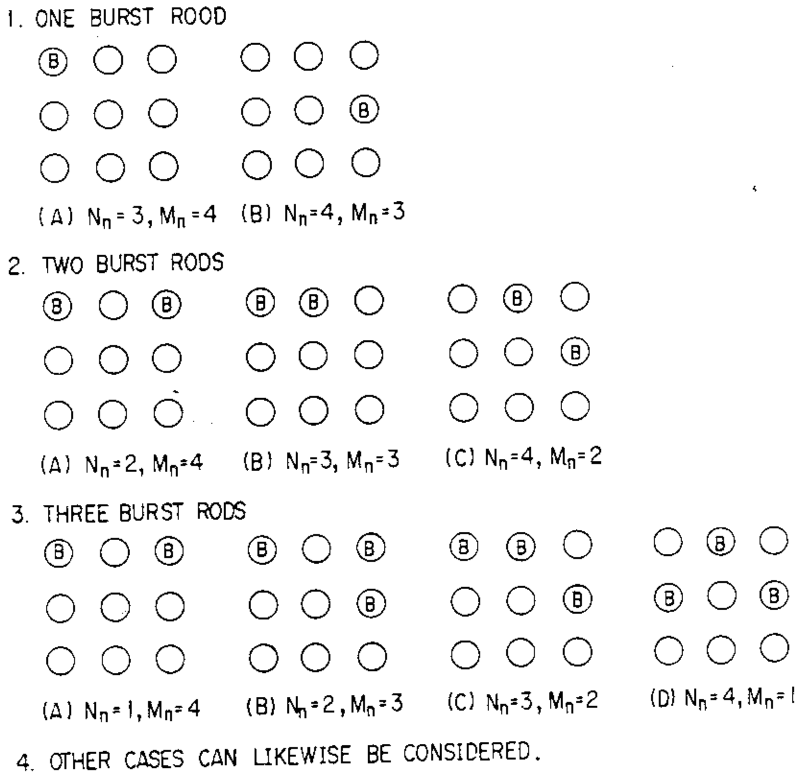

Fig. 3–4–2 Burst Patterns (Non-burst center rod).

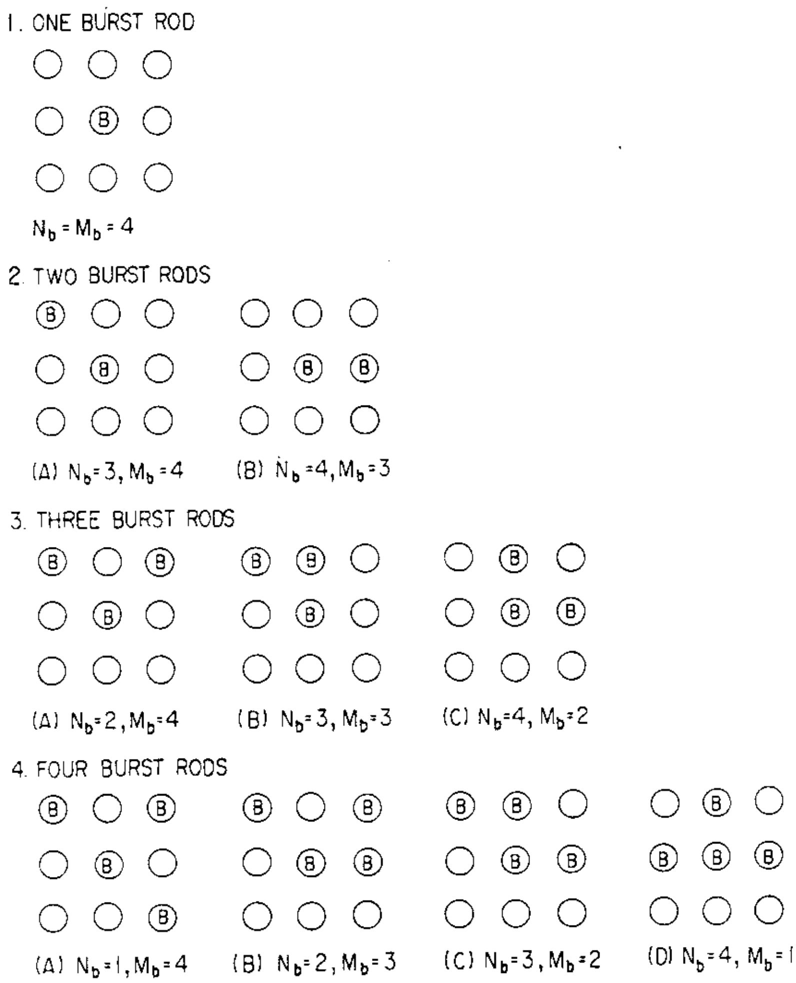

Fig. 3–4–3 Burst Patterns (Burst center rod).

$$q_{rad,i}=F_{12}\sigma[(T_R^i+273)^4-(T_2+273)^4] \quad (i=n \text{ or } b) \tag{3-4-1}$$

where

$$F_{12}=\frac{1}{\bar{F}_{12}+(1/\varepsilon_1-1)+A_1/A_2(1/\varepsilon_2-1)}$$

$\bar{F}_{12}$ = modified geometrical factor

A_1 = area of surface 1

A_2 = area of surface 2

T_2 = average temperature of surface 2

ε_1 = emissivity of surface 1

and

ε_2 = average emissivity of surface 1

Since surface 1 does not see itself, but only surface 2, we can set

$$\bar{F}_{12}=1$$

whence

$$F_{12}=\frac{1}{1/\varepsilon_1-A_1/A_2(1/\varepsilon_2-1)} \tag{3-4-2}$$

The emissivity ε_1 is that of zircaloy ε_{zr}, i.e.,

$$\varepsilon_1=\varepsilon_{zr}(T_R^i) \quad (i=n \text{ or } b)$$

as a function of temperature.

The ratio A_1/A_2 can be obtained in terms of the radii of the burst and non-burst rod

$$d_n=2r_R$$

and

$$d_b=2r_R^*$$

as

$$\frac{A_1}{A_2}=\frac{d_i}{3d_b+((M_i+M_i)/\pi-N_i/4-M_i/4)(d_b-d_n)+8/\pi(l_p-d_b)} \quad (i=n \text{ or } b)$$

In calculating the average values over surface 2, T_2 and ε_2, we will neglect the values at the coolant portion of surface 2 and obtain them, for example, as averages weighed by area, i.e.,

$$\varepsilon_2=\frac{3d_b\varepsilon_{zr}(T_R^b)-(N_i/4+M_i/2)[d_b\varepsilon_{zr}(T_R^b)-d_n(T_R^n)]}{3d_b-(d_b-d_m)(N_i/4-M_i/2)} \tag{3-4-4}$$

and

$$T_2=\frac{3d_bT_R^b-(N_i/4+M_i/2)[d_bT_R^b-d_nT_R^n]}{3d_b-(d_b-d_m)(N_i/4-M_i/2)} \tag{3-4-5}$$

Thus the rod-to-rod radiative heat transfer coefficient to be used for the calculation of clad surface temperature (see section 3.5) is given by

$$h_i=\frac{q_{rad,i}}{T_R^i-T_2} \quad (i=n \text{ or } b) \tag{3-4-6}$$

The outer rod diameter of the burst rod $d_b=2r_R^*$ can be obtained from Eq. (4-1-5).

3.5 Heat Transfer and CHF Correlations

First of all, it is important to make the following distinction between two kinds of heat transfer coefficients, h_{ir}^c and h_{ir}^{cs}. The heat transfer coefficient h_{ir}^c will be used in Eq. (3-2-2) to obtain heat transfer from the wall to the coolant, whereas the heat transfer coefficient h_{ir}^{cs} will be used in Eq. (3-3-12) to obtain the wall surface temperature. These two heat transfer coefficients are identical if rod-to-rod radiation is absent.

The heat transfer coefficient from the wall to the coolant h^c_{tr} is composed of two components, the one the convective or boiling or condensation heat transfer coefficient and the other the wall-to-coolant radiative heat transfer coefficient. We will refer to the former as h_{cvn} and the latter as h_{w-c}. Thus, the coefficient of heat transfer from the fuel rod to the core flow can be represented by Eq. (3–2–3), which we reproduce here again,

$$h^c_{tr} = h_{w-c} + h_{cvn} \qquad (3\text{–}5\text{–}1)$$

The heat transfer coefficient h^{cs}_{tr} to obtain the wall surface temperature is given as follows:

Before burst;

$$h^{cs}_{tr} = h^c_{tr} \qquad (3\text{–}5\text{–}2)$$

After burst;

$$h^{cs}_{tr} = h^c_{tr} + h_b \quad \text{(burst rod)} \qquad (3\text{–}5\text{–}3)$$

$$h^{cs}_{tr} = h^c_{tr} + h_n \quad \text{(non-burst rod).} \qquad (3\text{–}5\text{–}4)$$

The radiative heat transfer coefficients h_b and h_n are given by Eq. (3–4–6).

In the following subsections 3.5.1 to 3.5.3, we will show the heat transfer correlations used in THYDE-P2.

Table 3–1 Heat Transfer Coefficients

mode	Condition	Correlation
10	$T_b,\ T_w < T_s$ Re > 2,000	Dittus-Boelter
11	$T_b,\ T_w < T_s$ Re < 2,000	
20/21	$T_b < T_s < T_w$	Interpolation between modes 10/11 and 31
20/22	$T_b < T_s < T_w$	Interpolation between modes 10/11 and 32
31	$T_b = T_s$ $T_s < T_w$ $\Phi < \Phi_{CHF}$	Jens-Lottes
32	$T_b = T_s$ $T_s < T_w$ $\Phi < \Phi_{CHF}$	Thom
41–45	$T_b = T_s$ $T_s < T_w$ $\Phi > \Phi_{CHF}$	Post-CHF correlations (see **Table 3–2**)
60	$T_b = T_s$ $T_s > T_w$	Condensation
51	$T_b > T_s$ Re < 3,000	Laminar steam flow cooling
52	$T_b > T_s$ 3,000 < Re < 5,000	Interpolation between modes 51 and 53
53	$T_b > T_s$ 5,000 < Re	McEligot

Table 3–2 Post-CHF Heat Transfer Coefficients

Modes 41–45 for post-CHF shown in **Table 3–2** all satisfy the following conditions : $T_b=T_s$ $T_s<T_w$ and $\Phi>\Phi_{CHF}$.

mode	Condition		Correlation	
41	$x>0.5$ $p>30$ ata	$G>G_t$	Groeneveld	
42	$x>0.5$ $p<30$ ata	$G>G_t$	Dougall and Rohsenow	
43	$x<0.5$	$G>G_t$	Interpolation between h_{tr}^{41} or h_{tr}^{42} (x=0.5) and h_{tr}^{CHF} (x=0)	
44		$G<G_t$	Berenson Modified Bromley Bromley-Pomeranz	IHTROP(2) = 1 IHTROP(2) = 2 IHTROP(2) = 3

3.5.1 Heat Transfer Coefficients

(a) Subcooled Forced Convection

The Dittus-Boelter equation(31) is used to determine h_{tr} for subcooled forced convection.

$$h_{tr}=0.023\frac{\lambda_f}{D}\left(\frac{|G|D}{\mu_f}\right)^{0.8}P_{rf}^{0.4} \tag{3-5-5}$$

(b) Nucleate Boiling

The Jens-Lottes equation(32) is used to determine the heat flux at the cladding surface and the heat transfer coefficient is determined by:

$$h_{tr}=\frac{(T_w-T_s)^4(e^{p/0.33\times10^{-5}}/6.37)^4}{(T_w-T_b)} \tag{3-5-6}$$

(c) Subcooled Boiling under Natural and Forced Convection

When coolant is subcooled, but the wall temperature is higher than the saturation temperature, then an intermediate process is assumed to take place. Let

h_{tr}^1= subcooled heat transfer coefficient (mode 10 or 11)

and

h_{tr}^2= saturated heat transfer coefficient (mode 31/32).

Then, we consider in the following way as shown in **Fig. 3–4–4**.

If $h_{tr}^2>h_{tr}^1$, then

$$h_{tr}=h_{tr}^1$$

Otherwise

$$h_{tr}=\beta h_{tr}^1+(1-\beta)h_{tr}^{2*}. \tag{3-5-7}$$

with

$$h_{tr}^{2*}=\alpha h_{tr}^2+(1-\alpha)h_{tr}^1$$

where

$$\alpha=exp\left[\frac{(T_b-T_s)}{(T_s+273)}\right]$$

$$\beta=exp\left[\frac{(T_{w0}-T_w)}{T_{w0}}\right]$$

T_{w0}; the solution to $h_{tr}^2=h_{tr}^1$

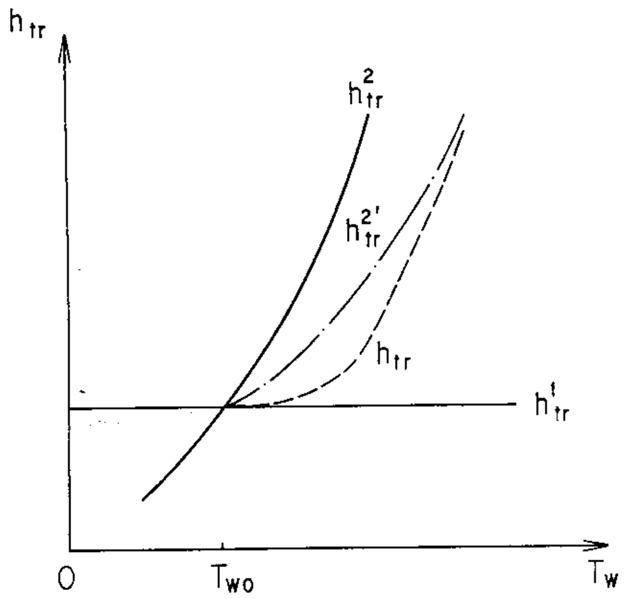

Fig. 3-4-4 Interpolation between Modes 10/11 and 31/32.

and

$$\gamma \sim 100$$

(d) Stable Film Boiling

The stable film boiling heat transfer correlation by Groeneveld(34) is used to calculate heat transfer after DNB.

$$h_{tr}=0.052\frac{\lambda_g}{D}\left[\frac{|G|D}{\mu_g}\left(x+\frac{\rho_g}{\rho_f}(1-x)\right)\right]^{0.688} Pr_{fw}^{1.26}Y^{-1.06} \qquad (3\text{-}5\text{-}8)$$

where

$$Y=max[0.1,\ 1-0.1(\rho_g/\rho_f-1)^{0.4}(1-x)^{0.4}]$$

Pr_{gw} = Pr of superheated steam whose temperature is equal to the cladding surface temperature.

(e) Steam Cooling

The following correlations are used during the period of steam cooling. For laminar flow (Re < 3000)(5)

$$h_{tr}=C_1\frac{\lambda_g}{D}\left(\frac{T_b+273}{T_w+273}\right)^{C_2} \qquad (3\text{-}5\text{-}9)$$

where C_1 and C_2 are constants and for turbulent flow (Re < 5000)(35)

$$h_{tr}=0.02\left(\frac{\lambda_g}{D}\right)Re_g^{0.5}Pr^{0.4}\left(\frac{T_b+276}{T_w+276}\right)^{0.5} \qquad (3\text{-}5\text{-}10)$$

(f) Condensation

When bulk temperature of saturated fluid is greater than wall temperature, condensation may occur. Hence the following heat transfer correlation(36) is used for condensation.

$$h_{tr}=0.009856\left(\frac{\lambda_f^2\rho_f^2 g}{\mu_f^2}\right)\left(\frac{4\Gamma_c}{\mu_f}\right)^{0.4} \qquad (3\text{-}5\text{-}11)$$

where

$$\Gamma_c=\frac{\Phi\Delta z}{h_{fg}}$$

(g) Natural Convection

For single phase flow, the following natural convection heat transfer correlation is

Table 3–3 CHF Correlations

Condition	Option	Correlation
$G>G_t$	(1)	Biasi
	(2)	GE
	(3)	RELAP
$G<G_t$	(1)	Interpolation between $\varphi_{CHF}(G-G_t)$ for $G>G_t$ and $9x10^4\ Btu/ft^2/hr$
	(2)	Modified Zuber
	(3)	Zuber

available.[37]

$$h_{tr}=0.47\frac{\lambda}{D}(GrPr_f)^{1/4} \qquad (GrPr_f<2.54\times10^2) \qquad (3-5-12)$$

$$=0.10\frac{\lambda}{D}(GrPr_f)^{0.33} \qquad (GrPr_f>32.54\times10^3)$$

where

$$Gr=D^3\rho_f^2 g|T_w-T_b|\left(\frac{\sigma}{g(\rho_f-\rho_g)}\right)^{1/2}/\mu_f^2 \quad .$$

3.5.2 CHF Correlations

$G>G_t$

(1) Biasi[46]

(2) GE[33]

$$\varphi_{CHF}=7.54\times10^2(0.84-x) \qquad |G|<0.678\times10^3$$

$$\varphi_{CHF}=7.54\times10^2(0.80-x) \qquad 0.678\times10^3<|G|<1.02\times10^3 \qquad (3-5-13)$$

(3) RELAP[7]

$G<G_t$

(1) Interpolation between $\Phi_{CHF}(G-G_t)$ for $G>G_t$ and 90,000 $Btu/ft^2/hr$

(2) Modified Zuber[47]

(3) Zuber[47]

3.5.3 Rod-to-Coolant Radiative Heat Transfer Coefficient

The following additional heat transfer coefficient due to thermal radiation should be added in each mode of the previous subsection before clad burst (see Eq. (3–5–1)).

$$h_{tr}=\eta_\alpha\frac{(T_w+273)^4-(T_b+273)^4}{T_w-T_b} \qquad (3-5-14)$$

where η_α is a function of α to be determined experimentally, e.g.[5],

$$\eta_\alpha=\frac{1-0.6\alpha}{1.25-0.15\alpha}$$

3.5.4 Pool Quenching Model

Suppose that a heat conductor with volume V, length Δz is placed in the coolant, which is at saturated pool condition and that the conductor surface is at post-CHF.

First, we heuristically derive a necessary condition for pool quenching. Integrating Eq. (3–3–1) over the material regions in the conductor, we obtain

$$\frac{d}{dt}\sum_i(\rho c_p TV)_i=\sum_i(\Xi V)_i-l_w\Delta z\varphi. \qquad (3-5-15)$$

where subscript i stands for a material region. Dividing this equation by V, we obtain

$$\frac{d}{dt}<\rho c_p T>=<\Xi>-\frac{l_w\Delta z\varphi}{V}$$
$$=\frac{l_w\Delta Z}{V}(\varphi^*-\varphi) \qquad (3-5-16)$$

where

$$\varphi^*=\frac{V}{l_w\Delta z}<\Xi>$$

and the bracket means averaging over fuel.

In order for the temperature not only at the surface, but also in its interior to be quenched, Eq. (3–5–16) requires[49] that

$$\varphi^*<\varphi \qquad (3-5-17)$$

at saturated post-CHF condition.

In THYDE-P2, we use the modified form of Eq. (3–5–17) such that

$$\varphi^*<c\varphi \qquad (3-5-18)$$

where

$$c=1.5$$

Factor c obviously depends upon the correlation of heat transfer coefficient for pool film boiling.

Suppose that quenching criterion (3–5–18) is satisfied. Then, the quenching heat flux will be assumed to be

$$\varphi_q=h_q(T_w-T_b) \qquad (3-5-19)$$

where

$$h_q=2.0 \quad kcal/sec/m^2$$

Thus, if condition (3–5–18) is satisfied under saturated post-CHF pool condition, quenching is assumed to take place with the heat flux given by Eq. (3–5–19).

4. Mechanical Behavior of Clad and Fuel

Mechanical behavior of the clad and the fuel influences gap width, gap pressure, flow area, rod-to-rod radiation and oxide thinning. Among them, the last three are assumed in THYDE-P2 to be effective only after clad burst.

The geometrical dimensions of a fuel rod at the initial operating condition must be determined by calculating, for example, the deformations due to pressure and temperature changes from the room to the operating condition. Indeed, there are computer codes, which are specialized in the problem. The problem is outside the scope of this work so that all the geometric dimensions of a fuel rod at the initial operating condition are assumed to be given as inputs.

Throughout this report, we will neglect the axial deformation of clad and fuel.

4.1 Clad Deformation

Prior to burst, the clad expands due to the thermal- and pressure-induced elastic strains and the plastic hoop strain. In THYDE-P2, as long as clad burst does not occur, only their effect on the gap width is taken into consideration. If the clad continues to strain plastically, it will eventually burst. When the burst is predicted, we, for the first time, take into account the contribution of clad deformation to flow area reduction, rod-to-rod radiation and oxide thinning.

Before we discuss clad deformation, we will present the expressions Eqs. (4–1–1) and (4–1–5) for the clad inner and outer radii, r_{cl}^{in} and r_R, respectively.

First, we express the clad inner radius r_{CL}^{in} as

$$r_{CL}^{in}=r_{CL}^{ino}(1+S_p-S_t+S_{in}) \qquad (4-1-1)$$

where S_p, S_t and S_{in} are the strains of the clad inner radius due to pressure change, temperature change and hoop stress, respectively. S_p[4] and S_t are given by

$$S_p=\frac{[\{1+\mu_p+e^2(1-2\mu_p)\}(p_{gap}-p_{gap}^0)-(2-\mu_p)(p_{flow}-p_{flow}^0)]}{[E_y(1-e^2)]} \qquad (4-1-2)$$

$$S_t=\alpha_{CL}(T_{CL}^{in})(T_{CL}^{in}-T_{CL}^{ino}) \qquad (4-1-3)$$

$$e=\left[\frac{r_{CL}^{ino}}{r_R^0}\right] \qquad (4-1-4)$$

As stated above, S_p and S_t are so small that they need be accounted for only in the calculation of gap with.

Next, neglecting the elastic strains, we express the clad outer radius r_R as

$$r_R=r_R^0(1+S_{out}) \qquad (4-1-5)$$

which will not be used until Eq. (4–1–15).

We now try to express S_{in} in Eq. (4–1–1) and S_{out} in Eq. (4–1–5) in terms of S and e, where S is the hoop strain S at the initial radius, $(r_{CL}^{ino}+r_R^0)/2$. Assuming constant cross-sectional area under plastic or burst hoop strain, we obtain,

$$r_m\theta=r_m^0\theta^0 \qquad (4-1-6)$$

where r_m is the radius which was initially equal to

$$(r_R^0+r_{CL}^{ino})/2$$

and θ is the clad thickness and superscript 0 referrs to the corresponding initial value. Since

$$r_m = r_m^0 (1 - S) \qquad (4-1-7)$$

Eq. (4–1–6) gives

$$\theta = \frac{\theta^\circ}{(1+S)} \qquad (4-1-8)$$

Then the plastic or burst radial strains at the inner and outer surfaces, S_{in} and S_{out} can be given in terms of S and e as

$$S_{in} = \left[r_m - \frac{\theta}{2} - \left(r_m^o - \frac{\theta^\circ}{2} \right) \right] / r_{CL}^{ino} = \frac{S}{2e} \left(1 - e + \frac{1+e}{1+S} \right) \qquad (4-1-9)$$

and

$$S_{out} = \left[r_m + \frac{\theta}{2} - \left(r_m^o + \frac{\theta^\circ}{2} \right) \right] / r_R^o = \frac{S}{2} \left(1 + e - \frac{1+e}{1+S} \right) \qquad (4-1-10)$$

Therefore, once the hoop strain S is given, we can obtain S_{in} and S_{out} from Eqs. (4–1–9) and (4–1–10), respectively. The plastic and burst hoop strains S in Eqs. (4–1–9) and (4–1–10) are discussed in subsections 4.1.1 and 4.1.3, respectively.

4.1.1 Clad Deformation prior to Burst

Hardy[41] performed a series of tests in which rods with constant internal pressure were ramped to a series of temperatures at various ramp rates. Analyzing his data, the following form of equation for plastic hoop strain S may be obtained.

$$\frac{dS}{dt} = f_1 \left(S, \sigma_h, T_{CL}, \frac{dT_{CL}}{dt} \right) \qquad (4-1-11)$$

where

$$\sigma_h = \frac{r_m}{r_c} (p_{gap} - p_{flow}) \qquad (4-1-12)$$

and f_1 is an input function.

Substituting the solution S of Eq. (4–1–11) into Eqs. (4–1–9) and (4–1–10), we obtain S_{in} and S_{out}. Then substituting S_{in} and S_{out} into Eqs. (4–1–4) and (4–1–5), we obtain r_{CL}^{in} and r_R.

4.1.2 Clad Burst

Clad is assumed to burst if the hoop strain S calculated by Eq. (4–1–11) reaches a certain value (an input) or if the clad temperature reaches the burst temperature. The burst temperature is calculated from a correlation of σ_h versus cladding temperature with the following form from various sources, notably ORNL[42]

$$T_{burst} = f_2(\sigma_h)$$

where f_2 is an input function.

If burst is predicted, the following assumptions are used to calculate the rupture rod conditions:

(a) The rod internal pressure is reduced in one time step to that in the corresponding coolant node and is set equal to it for the remainder of the calculation.

(b) The metal-water reaction is continued on the surface with the oxide layer being thinned in accordance with the calculated swelling.

(c) The local hoop strain and the flow blockage after burst are calculated according to the method described in the next section. The axial length of the swollen zone is that of the burst node.

(d) The metal-water reaction is started on the inside of the burst clad node. The reaction inside the cladding is assumed not to be steam limited, i.e., the gas composition of the burst node is set to be steam for the rest of the calculation.

4.1.3 Local Hoop Strain and Flow Blockage after Burst

It is assumed that at the time of clad burst the localized diametral swelling occurs very rapidly and changes the hydraulic diameter of the corresponding core flow node discontinuously. The diametral swelling is calculated from a correlation of the form,

$$S=f_3(\sigma_h) \qquad (4-1-14)$$

where f_3 is an input function of σ_h which is the hoop stress at the time of burst. Substituting S obtained from Eq. (4–1–14) into Eqs. (4–1–1) and (4–1–5), we obtain

$$r_R^*=r_R^0(1+S_{out}(S)) \qquad (4-1-15)$$

and

$$r_{CL}^{in*}=r_{CL}^{in0}(1+S_{in}(S)) \qquad (4-1-16)$$

where elastic strain has been ignored.

The outer radius after burst r_R^*, however, is limited such that

$$r_R^*<r_{R_{max}}$$

and hence

$$r_R^*(1+S_{out}(S))<r_{R_{max}} \qquad (4-1-17)$$

where $r_{R_{max}}$ is an input. Hence, S to be obtained from Eq. (4–1–14) also is limited; i.e., from Eq. (4–1–17) we obtain

$$S_{max}=a+\sqrt{a^2+4b}/2 \qquad (4-1-18)$$

where

$$a=(2/+\sqrt{R}))\left(\frac{r_{R_{max}}}{r_R^0}-1-e\right)$$

and

$$b=\frac{2}{1+e}\left(\frac{r_{Rmax}}{r_R^0}-1\right).$$

In the THYDE-P2 code, the flow area after burst A^* is not simply set equal to $l_p^2-\pi r_R^{*2}$, but is obtained in the following way by utilizing the 3×3 rod matrix model introduced in section 2.4.

If the center rod is burst, then the flow area in the 3×3 matrix changes from

$$A_q=4(l_p^2-\pi r_R^2) \qquad (4-1-19)$$

to

$$A_q^*=4l_p^2-\left(\frac{M_b}{2}+\frac{N_b}{4}\right)\pi r_R^2-\left(4-\frac{M_b}{2}-\frac{N_b}{2}\right)\pi r_R^{*2} \qquad (4-1-20)$$

Thus the flow blockage is given by

$$BL=100\left(1-\frac{A_q^*}{A_q}\right)=\frac{(4-M_b/2-N_b/4)\pi(r_R^{*2}-r_R^2)}{4(l_p^2-\pi r_R^2)}\times 100 \qquad (4-1-21)$$

If the center rod is not burst, then the flow area at the burst elevation of the matrix changes to

$$A_q^*=4l_p^2-\pi r_R^2\left(\frac{M_n}{2}-\frac{N_n}{4}+1\right)-\pi r_R^{*2}\left(3-\frac{M_n}{2}-\frac{N_n}{4}\right) \qquad (4-1-22)$$

so that the flow blockage in this case is given by

$$BL=\frac{(3-M_n/2-N_n/4)\pi(r_R^{*2}-r_R^2)}{4(l_p^2-\pi r_R^2)} \qquad (4-1-23)$$

Since we consider two elevations with clad burst in the 3×3 rod bundle, we have two values for BL. We choose the larger of the two as the effective values for BL. We also assume that BL is bounded from below so that $BL>BLM$ (an input value; see BB24).

When clad burst occurs, it is assumed that the flow area of the corresponding flow node change from A to

$$A^*=0.25A_g^* \qquad (4-1-24)$$

which, in turn, changes the hydraulic diameter and the Reynolds number of the burst node to

$$D^*=2\frac{A^*}{(\pi r_R^*)} \qquad (4-1-25)$$

and

$$R_e=|G|\frac{D^*}{\mu} \qquad (4-1-26)$$

It should be noted in view of the discussions in subsection 2.1.5, that the effect of sudden contraction and expansion of the flow area brought about by clad burst are automatically incorporated in the formulation.

4.2 Mechanical Behavior of Fuel and Gap

Among the various factors influencing the gap conductivity, it has not yet been shown how to calculate the gap width and gap gas pressure. To obtain these, we have to investigate the deformation of the bounding surfaces i.e., the clad inner surface and the fuel pellet surface. Deformation of clad inner surface has already been discussed in section 4.1.

4.2.1 Gap Width

Radial thermal expansion of the pellet is calculated by

$$r_F=r_F^o+\Delta r_F \qquad (4-2-1)$$

where the increment due to temperature rise Δr_F is given by

$$\Delta r_F=\sum_{n=0}^{N_f-1}(r_{n+1}^o-r_n^o)\alpha_F(T_{n+1})(T_{n+1}-T_{n+1}^o) \qquad (4-2-2)$$

Using Eqs. (4–1–1) and (4–2–2), the gap width is given for each axial node by

$$r_{gap}=r_{gap}^0+\Delta r_{CL}^{in}-\Delta r_F$$

Thus the gap width is given for each axial node by

$$r_{gap}=r_{gap}^o+r_{CL}^{ino}[\alpha_{CL}(T_{CL}^{in})(T_{CL}^{in}-T_{CL}^{ino})+S_{in}(S)+S_p]-\sum_{n=0}^{N_f-1}(r_{n+1}^o-r_n^o)\alpha_F(T_{n+1})(T_{n+1}-T_{n+1}^o) \qquad (4-2-3)$$

where S_p and $S_{in}(S)$ are given by Eqs. (4–1–2) and (4–1–9), respectively. The hoop strain S, in turn, is given by Eqs. (4–1–11) and (4–1–14) before and after burst, respectively.

4.2.2 Gap Gas Pressure

The gas volume inside a fuel rod may be composed of the following volumes in addition to the clad-pellet gap: (1) plenum volume (2) crack and dish volume (3) open porosity volume and (4) chip and roughness volume.

We neglect the open porosity volume and the chip and roghness volume. We note there is a difference between the fuel envelope volume and the net fuel volume, which now is the crack and dish volume.

Then the pellet envelope volume in an axial node is given by

$$V_{en}(t)=\pi r_F^2(t)\Delta z \qquad (4-2-4)$$

The initial net fuel pellet volume is given by

$$V_{FO}=V_{en}^o-V_{cd}^o=\pi(r_F^o)^2\Delta z-V_{cd}^o \qquad (4-2-5)$$

where the initial dish and crack volume is an input to the THYDE-P2 code. Utilizing the initial net fuel volume obtained by Eq. (4–2–5), we can obtain the thermally expanded net pellet volume at any time during the transient as

$$V_F(t)=V_{Fo}[1+3\alpha_F(<T_F>)(<T_F>-<T_F^o>)] \qquad (4-2-6)$$

With the help of Eqs. (4–2–4) and (4–2–6), the crack and dish volume at any time during the transient can be obtained as

$$V_{CD}(t)=V_{en}(t)-V_F(t)=\pi r_F^2(t)\Delta z-V_{Fo}[1-3\alpha_F(<T_F>)(<T_F>-<T_F^o>)] \qquad (4-2-7)$$

where the fuel pellet radius is given by Eq. (4–2–1).

The gap gas volume of the axial node is given by

$$V_{gap}(t)=\pi\Delta z[r_{CL}^{in}(t)^2-r_F^2]=\pi\Delta z[2r_F(t)+r_{gap}(t)]\,r_{gap}(t) \qquad (4-2-8)$$

where the fuel pellet radius r_F and the gap width r_{gap} are given by Eqs. (4–2–1) and (4–2–3), respectively.

The upper and lower plenum volumes are assumed to remain constant throughout the transient.

Thus the gas pressure inside a fuel rod is given by

$$p_{gap}=R_gN/[V_{upl}/T_{upl}+V_{lpl}/T_{lpl}+\sum_j(V_{gap\,j}/T_{gap\,j}+V_{cd\,j}/T_{cd\,j})] \qquad (4-2-9)$$

where the summation extends over all the axial nodes of a fuel rod. The plenum temperatures T_{upl} and T_{lpl} are given by Eqs. (3–3–29) and (3–3–30), respectively, in subsection 3.3.3, while the temperatures T_{gap} is given by

$$T_{gap}=\frac{T_F^{out}+T_{CL}^{in}}{2} \qquad (4-2-10)$$

for each axial node. The crack and dish temperature may be set equal to the volume-averaged temperature of the fuel, but then the steady state adjustment will become unnecessarily complicated. Since T_{cd} appears only in Eq. (4–2–9), we set the crack and dish temperature T_{cd} be equal to the arithmetic average of the fuel center and fuel surface temperatures.

5. Steady State Adjustment

When we wish to solve an initial value problem, it is desirable to start the calculation with an initial state which is consistent with the equations describing the transient in that the initial state is an exact solution to the transient equations without external disturbances. Thus, when we wish to solve an initial value problem described by a set of equations, we first must obtain the steady state solution of the equations with their time derivatives vanishing. The steady state solution thus obtained must agree with the actual steady state, and moreover, the characteristics of the steady state solution must agree with those of the actual steady state. We will call the procedure to set up the initial state the steady state adjustment.

From a different point of view, the steady state adjustment can be regarded as verification of the design of the system in question. In other words, any transient model should contain steady state analysis capability.

5.1 Heat Conductors

First of all, we note that some of the equations do not have a steady state, e.g., Eq. (3–1–7) for metal-water reaction of Zircaloy cladding and Eq. (4–1–11) for plastic hoop strain of Zircaloy cladding. Since $d\Theta/dt$ and dS/dt are very small at steady state, however, they are neglected in the steady state adjustment.

Since THYDE-P2 is intended to analyze transient phenomena, we will, if possible, try to keep unnecessary complications from being involved in the steady state calculation.

For example, the calculation of hot geometrical dimensions of a fuel element at the initial operating condition is outside the scope of this work, since it is a complicated steady state problem itself, involving various calculations such as the deformations due to pressure and temperature changes from room to operating condition. But, in THYDE-P2, all the hot geometrical dimensions of a fuel rod are assumed to be given as inputs and we consider only the deviations from the hot dimensions, e.g., Eqs. (4–1–2), (4–1–3) and (4–2–3).

Moreover, we note if we defined the crack and dish temperature T_{cd} in Eq. (4–2–9) to be the volume-averaged temperature of the fuel, then the steady state adjustment would become unnecessarily complicated. Since T_{cd} appears only in Eq. (4–2–9), we have simply defined T_{cd} to be the arithmetic average of the fuel center temperature and the fuel surface temperature.

The steady state temperature distribution in a heat conductor can be obtained in exactly the same manner as the transient distribution discussed in subsection 3.3.2.

For fuel with gap, we have relationships Eqs. (3–3–31) to (3–3–36) so that the gap conductance h_{gap} can be obtained according to the procedure shown in **Fig. 5–1–1**. We note that the hot dimensions such as r_{gap} are inputs.

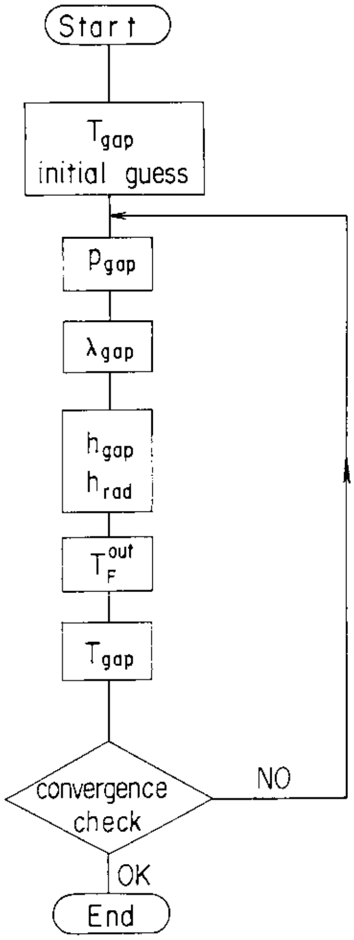

Fig. 5–1–1 Procedure to Obtain h_{gap} and h_{rad} at Steady State.

5.2 Special Nodes and Pump

In the following, we may drop the subscript "o" referring to a steady state whenever confusions can be avoided.

5.2.1 Accumulator

If the accumulator junction is closed so that it is isolated from the network, then the steady state is obtained as follows. Since $p_{N_2}(0)$ and $h_{H_2O}(0)$ are inputs, AC bottom pressure p_x can be obtained by iteratively solving Eq. (2–4–71). Next, similarly AC junction pressure p^- can be obtained by iteratively solving Eq. (2–4–70), where $h_{ACD}(0)$ is an input (see BB16).

If AC junction is open so that AC is connected with the main network, then the steady state is obtained by assuming that p^+ and h^+ at AC junction have already been obtained by the main network adjustment. First, we solve Eq. (2–4–70) iteratively to obtain p_x. Next, we solve Eq. (2–4–71) iteratively for $p_{N_2}(0)$.

5.2.2 Pressurizer Tank Model

If we select the tank model to describe the pressurizer, then its steady state will be given as follows. Since we assume that the steady state of the loop has already been decided, we know the pressure p^+ and the enthalpy h^+ at the injection junction. Moreover, α_l and H_{ll} are given as inputs.

Setting

$$Q_I = Q_I$$

and

$$m_{re} = m_{pb} = m_{su} = m_{sp} = 0$$

we have

$$p = p^{+} - (head)$$

$$h_{II} = (h^{+} + h_{fs}(p))/2$$

$$h_{su} = h_{II}$$

$$V_I = V_T - H_{II} A_T$$

$$M_{If} = (1 - \alpha_1) V_I \rho_{fs}$$

$$M_{Ig} = \alpha_I V_I \rho_{gs}$$

$$M_I = M_{Ig} + M_{If}$$

and

$$M_{II} = A_T H_{II} \rho_f (p,\ h_{II})$$

5.2.3 SG 2ndry System Tank Model

The input data for SG are (1) the dimensions, (2) the water level, (3) the specific enthalpy of feed water, (4) the flow rate of feed water, (5) coefficient β , (6) the void fraction in region I, (7) the internal pressure and (8) the heat fluxes across the tube wall. Since data (1), (3), (4) and (7) are given as measured values, the rest may be changed so that realistic steady state will be materialized. It is the nodes crossing the water level whose steady state is difficult to obtain. The reason is that such a node has a constraint

$$f = r - \frac{(T_{WS} - T_{WP})^{II}}{(T_{WS} - T_{WP})^{I}}$$

where $r = \Phi^0_{II} / \Phi^0_I$ (see **Fig. 3–2–1**).

It is data (2) and (8) among the input data (2), (5), (6) and (8) that most influence convergence of SG secondary system. Therefore, by changing data (2) and (8), a steady state can hopefully be obtained.

5.2.4 Pump

Since initial pump speed $\Omega(0)$ is an input, we have

$$a(0) = \frac{\Omega(0)}{\Omega_r} .$$

Assuming that initial volumetric flow rate $W(0)$ has already been known by step 2 in subsection 5.3.2, we have

$$w(0) = \frac{W(0)}{W_r} .$$

Given $a(0)$ and $w(0)$, the homologous law gives normalized pump head and torque $p_{head}(0)$ and $b(0)$, which in turn give the initial head and torque;

$$L_{head}(0) = L_{head,r} \cdot p_{head}(0)$$

and

(1) Obtain heat fluxes from conductors to coolant. They are initial guess values except for fuel conductors. (Subroutine STHINT)

(2) Obtain node quantities such as T_b. (Subroutines STFLOW, STENT and STPRHO)

(3) Obtain temperature distributions inside heat conductors. For conductors attached to stagnant nodes, set temperatures to be equal to T_b. (Subroutines STSLGP and STSLAB)

(4) Renew heat fluxes based on T_b and T_w except for fuel conductors. (Subroutine STSLAB)

(5) Check convergence of T_b (Subroutine STPYCK) and repeat steps (2) to (4) until T_b converges. (Subroutine STEADY)

(6) After convergence, adjust input pressures (BB10) to obtain realistic loss coefficients.

Fig. 5–3–1 Overall Procedure to Obtain Steady State Thermal-Hydraulic Network.

(1) Energy balance in primary loop

(2) Determination of G of all loop nodes

(3) Determination of specific enthalpies $\tilde{h}_i^A$, $\tilde{h}_i^E$ for each chain and $h_j^\dagger$ for each mixing junction

(4) Determination of h_n^A and h_n^E of all normal nodes

(5) Determination of ρ_n^A, ρ_n^E, p_n^E and $p_j^\dagger$ for non-stagnant nodes

(6) Determination of ρ_n^A, ρ_n^E, p_n^A and p_n^E of stagnant nodes

(7) Determination of κ_n of non-stagnant nodes

Fig. 5–3–2 Procedure to Obtain Node Quantities.

$$T_e(0)=T_r\tau_e(0)$$

where $\tau_e(0)$ is given by Eq. (2–4–51) as

$$\tau_e(0)=b(0)^2-k_2a(0)^{1/2}\ .$$

5.3 Thermal-Hydraulic Network

Main inputs to THYDE-P2 in conjunction with thermal-hydraulics are Φ_n and p_n^A for all nodes and G_n^A and h_n^A for a certain node and the ratios r of the outflow rates at each mixing junction. The present adjustment does not require such a tedious step as would otherwise be needed to calculate the steady state flow rates of all the nodes in the system.

In the following, the tilde and dagger are used to refer to chains and junctions, respectively.

5.3.1 Overall Procedure

The overall procedure to obtain steady state of the thermal-hydraulic network is shown in **Fig. 5–3–1**, where step 2 is explained in the next subsection, while step 6 in subsection

5.3.3.

5.3.2 Node Quantities

This subsection corresponds with step 2 in **Fig. 5–3–1**, which can further be subdivided as shown in **Fig. 5–3–2**. Let q^* be the number of the branches in the network. We note $q \leqq q^*$ where q stands for the number of the branches with at least one normal junction. In the following, each step of **Fig. 5–3–2** will be explained in order.

(1) Energy balance adjustment in the system

This is accomplished by uniformly changing heat fluxes across the U-tube walls of the steam generator.

(2) Determination of mass velocity G of all normal nodes

We have a simple linear simultaneous equation for mass flow rates $\tilde{m}_i$ of order $l_{q+1}-1$ in terms of γ which represents mass balance at each mixing junction. We note that l_{q+1} is the number of the mixing junctions (see subsection 2.3.3). It should be noted that since G_n^A for a certain node IVOL is given as an input, the mass flow rate $\tilde{m}_i$ of the corresponding chain has already been specified. The linear simultaneous equation can iteratively be solved for $\tilde{m}_i$ and hence for $G_n^A = G_n^A = \tilde{m}_i / A_n$ at all the nodes in each chain i. In order to obtain fast convergence of the iteration, it is important to choose a suitable node number for IVOL (an input, see subsection 7.4.10).

(3) Determination of specific enthalpies at inlet and outlet of each chain and at mixing junctions

Let us use superscripts A and E for a chain as well. Then we obtain

$$\tilde{h}_i^E = \tilde{h}_i^A + (\sum_{**-1} q_n''' L_n A_n) / \tilde{m}_i \qquad (1 \leqq i \leqq q^*)$$

(** −1: all nodes in chain i)

$$\tilde{h}_j^+ \sum_{**-2} \tilde{m}_i = \sum_{**-3} \tilde{m}_i h_i^E \qquad (1 \leqq j \leqq l_{q+1})$$

(** −2: all chain flows out of mixing junction j)

(** − 3: all chain flows into mixing junction j)

$h_i^A = h_j^+$ for all chain flows out of mixing junction j.

There are q^* equations of the last type in the above so that we have $2q^* + l_{q+1}$ equations whereas there are the same number of unknowns, i.e., h_i^A and h_i^E for i = 1, 2, ..., q^* and h_j^+ for j = 1, 2, ..., l_{q-1}.

(4) Determination of h_n^A and h_n^E of all the normal nodes

Suppose that the nodes in a chain are labelled successively from upstream to downstream. Let us determine h_n^A and h_n^E of all the nodes in the chain. For any node n in the chain, we have

$$h_n^E = h_n^A + L_n A_n q_n'''$$

where if node n in the most upstream of the chain, then h_n^A is given by the specific enthalpy of the from-mixing junction which has already been determined. We can likewise apply the above equation to the next downstream node with Eq. (2–1–21), i.e.,

$$h_n^A = h_{n-1}^E$$

Thus, we can determine h_n^A and h_n^E successively for all the nodes in any chain.

(5) Determination of densities ρ_n^A and ρ_n^E and pressures p_n^E and p_j^- for non-stagnant nodes

(a) First, we obtain

$$\rho_n^{+A} = \rho(p_n^A, h_n^A)$$

(b) Next, we determine junction pressures as

$$p_j^+ = \frac{1}{j_{out}} \sum \left(p_n^A + \frac{G_n^{A^2}}{2\rho_n^A} \right)$$

where the summation is over all the node whose from-junction coincides with junction j and j_{out} means the number of these nodes.

(c) Obtain density of mixing junctions such that

$$\rho_j^+ = \rho(p_j^+, h_j^+) .$$

(d) Modify some of p_n^A given as inputs.

For nodes whose from-junction is a mixing junction, the inputs p_n^A should be considered tentative and now be replaced by the solutions of the following equations for those nodes,

$$\rho_n^A + \frac{G_n^{A^2}}{2\rho(p_n^A, h_n^A)} + \frac{k_n^A}{2\rho(p_n^A, h_n^A)} = p_{from}^+ .$$

(e) Solve the following equations to obtain p_n^E for all the normal nodes,

$$p_n^E + \frac{G_n^{E^2}}{2\rho(p_n^E, h_n^E)} - \frac{k_n^E}{2\rho(p_n^E, h_n^E)} = p_{to}^- .$$

(6) Determination of ρ_n^A, ρ_n^E, p_n^A and p_n^E for stagnant nodes

(7) Determination of k_n for non-stagnant nodes

Obtain loss coefficients k_n such that

$$k_n = \frac{2\rho_n}{G_n^{A^2}} \left(p_n^A - p_n^E + \frac{G_n^{A^2}}{\rho_n^A} - \frac{G_n^{E^2}}{\rho_n^E} - \rho_n g L_{Hn} \right) - \frac{f_n}{D_n} L_n > 0 .$$

5.3.3 Adjustment of Loss Coefficient

Based on the input values such as pressure p_A of each node and mass flux G_A and specific enthalpy h_A of node IVOL (see BB09) at the steady state, as described in the previous two sections, THYDE-P2 obtains G_A, G_E, h_A, h_E and k throughout the network by solving the steady state equation. Often, however, the loss coefficient k turns out to be unrealistic or negative. In the following, a recipie for steady state adjustment to yield realistic loss coefficients will be shown. This is step (6) in **Fig. 5–3–1**.

We make use of the relationship which exists between the loss coefficient and the neighboring pressures, depending on node-node coupling or node-mixing junction coupling (see **Figs. 5–3–3** and **5–3–4**, respectively). In the following, we assume turbulent flow, neglect the momentum flux B due to u_{rel} and set

$$\frac{\Phi^2}{\rho_f} = \frac{1}{\rho} .$$

5.3.3.1 Node-Node Coupling

We assume

$$k_n^A = 0 .$$

Then, equation f_3 for node n and f_2 for node n' gives when $k_{n'} = 0$

$$p_n^E + \frac{1}{2}(1 + k_n^E) \frac{G_n^2}{\rho_n^E} = p_{n'}^{A'} + \frac{G_{n'}^2}{2\rho_{n'}^A} \qquad (5–3–1)$$

and f_4 for node n gives

$$p_n^A + \frac{G_n^2}{\rho_n^A} - p_n^E - \frac{G_n^2}{\rho_n^E} - \frac{1}{2}\left(k_n + \frac{f_n L_n}{D_n} \right) \frac{G_n^2}{\rho_n} - \rho_n g L_{Hn} = 0 . \qquad (5–3–2)$$

Eliminating p_n^E from Eqs. (5–3–1) and (5–3–2) and solving the resulting equation for k_n, we obtain

$$k_n=\frac{2\rho_n}{G_n^2}\left\{p_n^A-p_n^{A'}+G_n^2\left[\frac{1}{p_n^A}-\frac{1}{2\rho_n^E}(k_n^E+1)\right]-\rho_n g L_{Hn}-\frac{G_{n'}^2}{2\rho_{n'}^A}\right\}-\frac{f_n L_n}{D_n} \quad (5\text{-}3\text{-}3)$$

5.3.3.2 Node-Mixing Junction Coupling

Suppose that junction friction factor k_j at E-point of node n has been inputted (see **Fig. 5–3–4**). Then equation f_3 for node n gives for turbulent flow

$$p_n^E+\frac{1}{2}(1-k_n^E)\frac{G_n^2}{\rho_n^E}=p_j^+ \quad . \quad (5\text{-}3\text{-}4)$$

Eliminating p_n^E from Eqs. (5–3–2) and (5–3–4) and solving the resulting equation for k_n, we obtain

$$k_n=\frac{2\rho_n}{G_n^2}\left\{p_n^A-p_j^+ + G_n^2\left[\frac{1}{\rho_n^A}-\frac{1}{2\rho_n^E}(1+k_n^E)\right]-\rho_n g L_{Hn}\right\}-\frac{f_n L_n}{D_n} \quad . \quad (5\text{-}3\text{-}5)$$

We note that mixing junction pressure p_j^+ is given by

$$p_j^+=\frac{1}{n_{out}}\sum_{i=1}^{n_{out}}\left(p_i^A+\frac{G_i^2}{2\rho_i^A}\right)$$

5.3.3.3 Determination of p_n^A

We transform Eqs. (5–3–3) and (5–3–5) as follows, respectively,

$$p_n^A=p_n^A+x_1 k_n+x_2 \quad (5\text{-}3\text{-}6)$$

and

$$p_j^+=p_n^A+x_1 k_n+x_2$$

where it should be noted that x_1 and x_2 are insensitive to p or k. Therefore, the values k_1 and k_2 of each node will be printed out as a guide to select new pressure distribution to yield realistic loss coefficients.

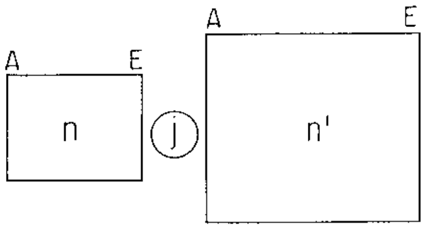

Fig. 5–3–3 Node-Node Coupling.

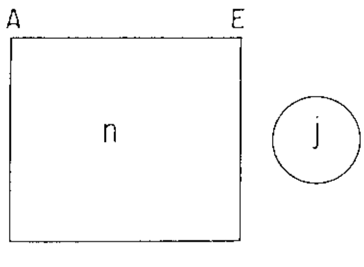

Fig. 5–3–4 Node-Mixing Junction Coupling.

6. Program Control

In this chapter, we will briefly present the main program controls of the THYDE-P2 code.

6.1 Null Transient Calculation

The system simulated by THYDE-P2 is a very complicated non-linear system whose exact solution is in general impossible to obtain. But, there is one exception for which we know the exact solution, i.e., the null transient problem. In the null transient problem, as time goes by, the solution must not deviate from the initial steady state obtained by the procedure described in chapter 5. In the course of the THYDE-P2 development, the null transient calculation capability has been confirmed with NPERT = 1 in BB01 (see subsection 7.4.2) whenever a new modification was made to the code.

In the null transient calculation, the metal-water reaction is not accounted for, since it does not have a steady state.

6.2 EM and BE Calculations

For calculation of a PWR LB-LOCA, a special option is provided in the THYDE-P2 code, i.e., EM (evaluation model) calculation based on the conservative assumptions. The ordinary calculation not based on these assumptions is called the BE (best estimate) option as opposed to the EM option. The BE option includes all the up-to-date knowledge or realistic assumptions so that it can be applied to all the transients including LB-LOCA.

The EM option is composed from;

(1) the special noding, for example, a single downcomer (see **Fig. 6–2–1**),
(2) the FLECHT correlation so that the core is assumed to be 12 ft long,
(3) factor 1.2 for FP decay,
(4) a series of closings and openings of the fictitious valves V_1, V_2 and V_3 after blowdown (see **Fig. 6–2–1**),
(5) a special form of equation f_2 for the downcomer node,
(6) no return to nucleate boiling during blowdown,
(7) hypothetical heating of subcooled and saturated nodes from end of bypass to beginning of lower plenum injection, and
(8) saturated enthalpy for ECC water after end of blowdown.

In the EM calculation, the scenario of the transient (see **Table 6–1**) must be specified in advance by means of the input data in BB06 in subsection 7.4.7 and the input data for valves V_1, V_2 and V_3 (BB29 in subsection 7.4.30) in addition to the corresponding valve trip data (BB04 in subsection 7.4.5). The time of end of bypass T_{EOBP} should be determined by the plotter output or the major edit of a tentative run with a very large input value for it. The time of bottom of core recovery T_{EOBP} should likewise be obtained. We note that lower plenum injection is assumed to start as soon as the hypothetical heatup of subcooled and saturated nodes (see BB06 in subsection 7.4.7) ends.

On the other hand, in the BE calculation, the program determines the scenario by itself in response to the "scenario" of the boundary conditions and the external disturbances.

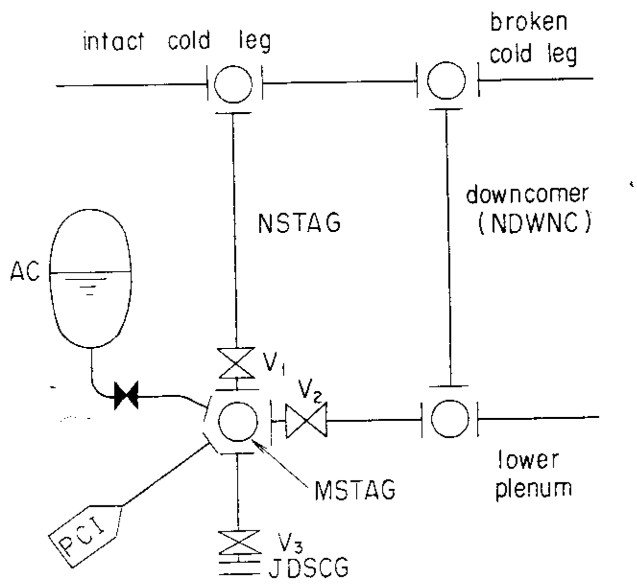

Fig. 6–2–1 PWR LB–LOCA EM Noding.

Table 6–1 PWR LB–LOCA EM Calculation Scheme

Time			T_{EOBP}	T_{LPINJ}	T_{BOCREC}
phase		blowdown	fictitious heatup of subcooled and saturated nodes	refill	reflood
ECC injection mode		cold leg injection	discharging out of system	lower planum injection	
fictitious	V_1	open	closed	closed	
valve	V_2	closed	closed	open	
operations	V_3	closed	open	closed	
core heat transfer		no return to nucleate boiling	adiabatic heatup ($h_{tr} = 0$)		(1) $h_{tr} = 50+950\ (1-x)$ for quenched and quenching nodes (2) FLECHT correlation for other nodes

The EM assumptions may conform to Ref. (1). Therefore, if this code should be used as part of a PWR licencing application, the calculation may be performed using the EM option. Judgment of the overall adequacy of each engineered ECCS feature may be made in the light of the criteria stated in Ref. (1), which, for example, requires that the calculated maximum fuel cladding temperature shall not exceed 1,200°C.

6.3 Time Step Width Control

The THYDE-P2 TSWC (time step width control) has been made possible by the efforts to ensure continuity of all the parameters in the conservation equations required for the THYDE-P2 nonlinear implicit method.

TSWC with respect to the number of the iterations in the thermal-hydraulic network calculation is performed according to the scheme shown in **Table 6–2**.

If a steam table error takes place, the calculation will be done all over again with the halved time step width.

For TSWC with respect to the rates of change of the following variables, the two TSWC options are available (see next two subsections).

(a) the normal node variables p, G, h and E ,

(b) the SG secondary pressure,

(c) the accumulator variables M_{H_2O}, h_{H_2O}, V_{N_2} and,

(d) all center and surface temperatures of heat conductors.

TSWC for the reactor power is not explicitly performed, since it is effectively done by means of the heat conductor temperatures.

6.3.1 2-and-1/2 TSWC

This TSWC is based on the relative increments of the above-mentioned variables. At each time step, the value

$$\frac{|x^{new} - x^{old}|}{(|x^{old}| - e_3)} \qquad (e_3 \text{ : an input})$$

will be calculated. Let the maximum of these values be REL. If REL is greater than e_1 (an input value), the time step width will be halved and the calculation is to be done over again. If REL is less than $e_1 e_2$ (e_2 ; an input value), then the calculation proceeds to the next time step which has twice as large a width as the last. If REL is in between e_1 and $e_1 e_2$, then the next time step calculation is to be done with the same time step width as the last.

The parameters e_1 , e_2 and e_3 are given in **Table 6–3** or to be inputted by BB03 (see subsection 7.4.4).

6.3.2 Table-Controlled TSWC

In this option, the time step width control for the rate of change of the above-mentioned variables (a) to (d) will be done as shown in **Fig. 6–3–1**, on the basis of $dx/dt/x$ versus Δt table to be inputted by input data block BB03 (see subsection 7.4.4). In this method, the time step width control may be more efficient, if the TSWC table is appropriately given. The best table to be used will be dependent on the kind ot transients to be analyzed so that it will be very difficult to obtain the table with a wide range of applicability. The table can easily be changed by giving input data subblock SB0301, whose default is shown in **Table 6–4**.

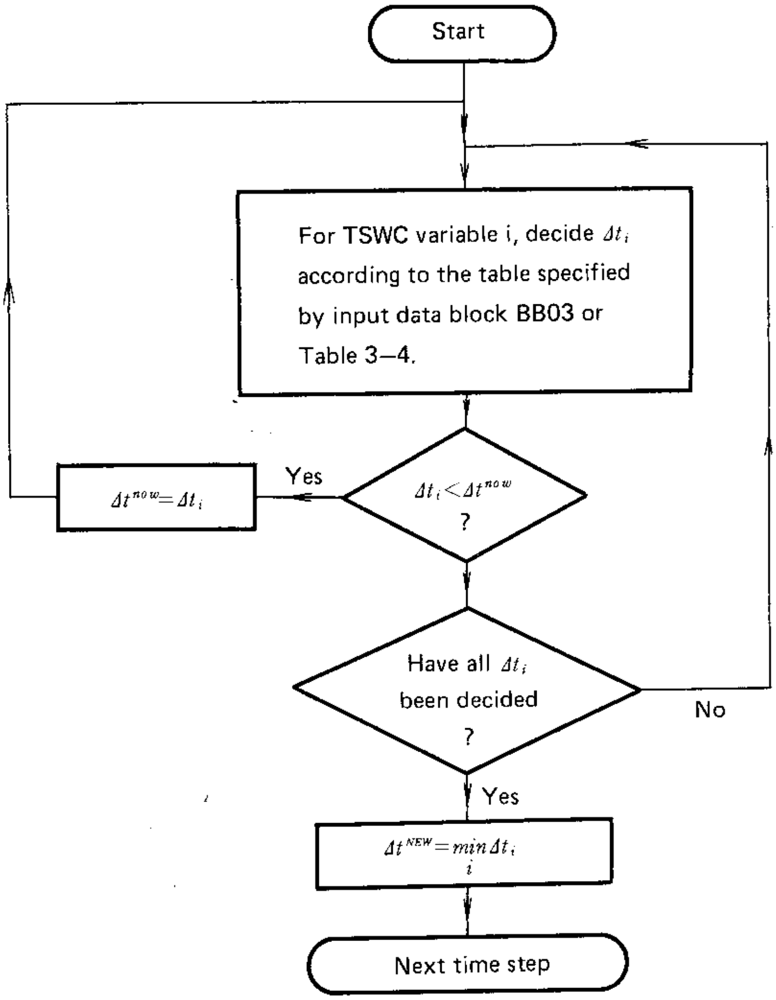

Δt^{now} : present TSW (time step width)
The initial Δt^{now} is Δt^{OLD} decided at the previous time step

Δt^{NEW} : TSW to be used for next time step

Fig. 6–3–1 Table-Controlled TSWC.

Table 6–2 TSWC w.r.t Thermal-Hydraulic Iteration

Condition	TSWC
$N > N_1$	Recalculate with $0.5\Delta t$.
$N_1 > N > N_2$	Go to next time step with $0.5\Delta t$.
$N_2 > N > N_3$	Go to next time step with Δt.
$N_3 > N$	Go to next time step with $2\Delta t$.

If ITSTYP < 0 is inputted, then the default values (N_1, N_2, N_3) = (20, 13, 9) will be used. Otherwise, (N_1, N_2, N_3) must be given as the inputs (see subsection 7.4.4).

Table 6–3 2-and-1/2 TSWC Parameters

Variables	e_1	e_2	e_3
p	0.1*	0.2	0.001
G	0.2*	0.2*	100.*
h	0.1*	0.2	0.001
T	0.01*	0.2	0.001
SG	0.1*	0.2	0.001
AC	0.05*	0.2	0.001
E	0.1*	0.2	0.001

The parameters shown above are those for use in ITSTYP = −1. For ITSTYP = 1, the data with * must be given as the inputs (see subsection 7.4.4).

Table 6–4 Default for Table-Controlled TSWC Parameters

Δt (ms)	$dp/dt/p$	$dG/dt/G$	$dh/dt/h$	$dE/dt/E$	$dX/dt/X$
128.	0.1<	2.0<	0.4<	1.0<	1.0<
64.	0.2	4.0	0.8	2.	2.
32.	0.4	8.0	1.6	4.	4.
16.	0.8	16.	3.2	8.	8.
8.	1.6	32.	6.4	16.	16.
4.	3.2	64.	12.8	32.	32.
2.	6.4	128.	25.6	64.	64.
1.	12.8	256.	51.2	128.	128.
0.5	25.6	512.	102.4	256.	256.
0.25	51.2	1024.	>102.4	512.	512.
0.125	>51.2	>1024.		>512.	>512.

X stands for the variables other than node variables p, G, h and E.

7. Input Requirements

In the following, the requirements for noding, data deck organization, input data cards and problem restart are presented.

7.1 Noding for Thermal-Hydraulic Network

When we intend to use THYDE-P2, first of all we have to reticulate the coolant system by means of nodes and junctions according to the THYDE-P2 network model. It is required that the network has at least one mixing junction and that a normal node without heat source must be placed both at the top and bottom ends of the core. After so reticulating the plant, we have to number the nodes and junctions separately, strictly in numeric order in accordance with the following rules:

(a) Normal nodes (except linkage nodes) should be numbered in numeric order chain-wise from one mixing junction to another according to the direction of the steady state chain flow.

(b) Then linkage nodes should be numbered in numeric order chainwise from the corresponding mixing junction.

(c) Special nodes should be numbered after all the normal and linkage nodes.

(d) Among junctions, normal (and guillotion break) junctions should be numbered first in numeric order chain-wise from upstream to downstream. Then the mixing junctions should be numbered according to the direction of the steady state flow. After them, the injection junctions and finally the dead end junctions should be numbered.

(e) For PWR EM calculation, special noding is required (see section 6.2).

(f) A pump should be represented by a single node.

(g) The loss coefficients to be inputted are those for reverse flow at initially flowing nodes, those at initially stagnant nodes and those at break point after break. All the others are calculated by the steady state adjustment.

(h) A plural number of core channels can be simulated. But, the axial noding of the channels must be identical.

An example of thermal-hydraulic noding is shown in **Fig. 10–1–1**. In the figure, junctions 1–28, 29–37 and 38–43 are normal junctions, mixing junctions and boundary junctions, respectively. Nodes 1–36 are normal nodes, 37–46 are linkage nodes, node 49 is the pressurizer, nodes 50 and 51 are the accumulators and nodes 47 and 48 are the SG secondary systems. In **Fig. 7–1–1**, we note that the tank model is used for the pressurizer and that there are 24 heat conductors (see next section).

7.2 Numbering and Noding for Heat Conductors

An example of heat conductors numbering is shown in **Fig. 7–2–1**. Depending on the type of boundary condition at the left (or inner) and right (or outer) surfaces of the conductor, there are 7 cases as shown in **Fig. 7–2–2**. We define the noding convention in the heat conductor as shown in **Fig. 7–2–3**. For a solid cylinder, we let $r_0=0$.

In the following, the requirements for numbering and noding of heat conductors are

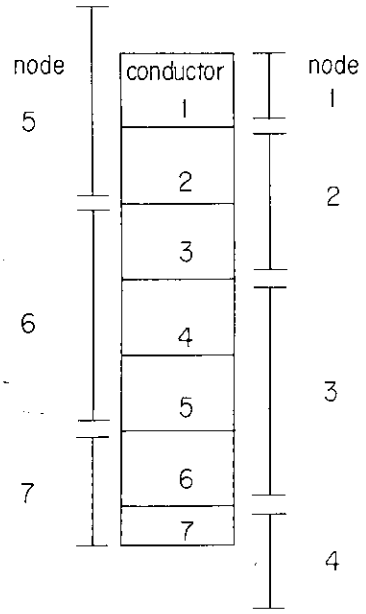

Fig. 7–2–1 Example of Heat Conductors Numbering.

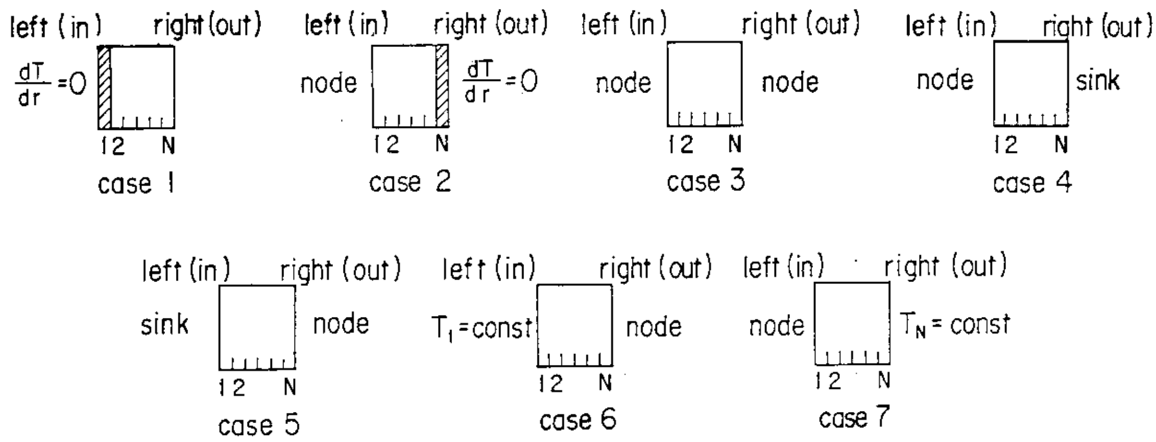

Fig. 7–2–2 Heat Conductor Configurations.

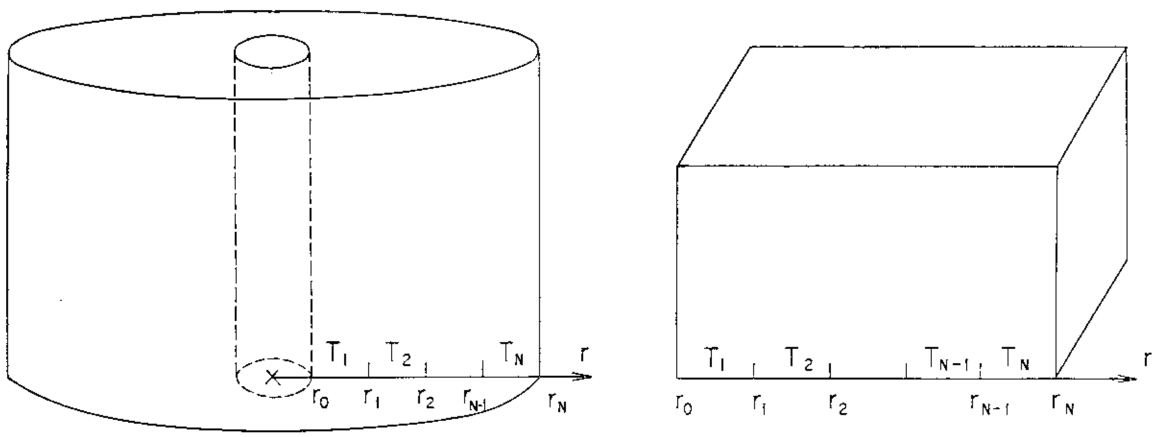

Fig. 7–2–3 Noding of Heat Conductor.

listed in order.

(a) At least, one heat conductor is required.

(b) First, fuel conductors with gap and then fuel conductors without gap and finally other conductors should be numbered.

(c) Heat conductors must be either rectangular or cylindrical. Fuel with gap must be cylindrical.

(d) The first inputted fuel is regarded as the average fuel rod or plate with IDROD = 1.

(e) Since, in the present version, the tank model is used for the SG secondary system, the primary nodes corresponding to the U-tube must not be equipped with heat conductors.

(f) More than one heat conductor can be associated with one normal coolant node. It is not allowed that one surface of a conductor is associated with plural coolant nodes.

(g) For a given fuel rod or plate, numbering of heat conductors must be in numeric order.

(h) For a given core coolant channel, it is possible to define more than one kind of fuel.

(i) A heat conductor is radially composed of one or several regions, each of which has the same λ (heat conductivity), the same c_p (specific heat under constant pressure), the same ρ (density) and the same heat production rate. Each region is made from one or several meshes. Numbering of meshes in a region should be made from left to right for a rectangular conductor and from inside to outside for a cylindrical conductor.

(j) Numbering of meshes must be made not region-wise, but conductor-wise.

(k) For a given fuel rod or plate, the most upstream and most downstream conductors must be without heat sources.

7.3 Data Deck Organization

A THYDE-P2 data deck, ending with the terminator BEND card, could contain more than one problem, each of which consists of a title card, data cards and the subterminator card. The terminator is a card whose first 4 columns are punched as BEND, while the subterminator is the identification card for dummy data block 99. A listing of the data cards is printed at the beginning and end of each THYDE-P2 job.

A block identification card is placed for the top of each data block and is punched in the first 4 columns as BBXX, where XX indicates the data block number. If the block XX has more than one sub-block, a sub-block identification card must be placed at the top of each data sub-block and will be punched in the first 6 columns as SBXXYY where YY indicates the sub-block number starting with 01

7.4 Data Card Summary

In the following description of the data cards, the data block number is given along with a descriptive title of the data block and the number of the sub-blocks. Then, the order of the data (1, 2, ...), the format (I, R, A or table), the variable name and the input data description are given where applicable. The formats of the field, i.e., integer, real (floating), alphanumeric and table is indicated by I, R, A, and T, respectively. Table data for an independent variable should be given as follows. First, the number of points must be given. Then as many sets of the independent and dependent variables as the number of points must be inputted.

A card whose first column is "/" is regarded as a comment card which must not be placed before the title card. Some limitations exist in placing a comment card in BB05, BB06 and BB00. Reading input cards is performed soley by the free-format input routine REAG[51].

7.4.1 Problem Title (No block numbers)

1–A ITITLE Problem title

The problem title must be punched in columns 1 to 72 on an IMB card.

7.4.2 Problem Control Data BB01

TSWC stands for time step width control.

```
1-I  LDMP     Restart file control
              0 = no restart file used
              N = restart at restart number N using the file
                  on FORTRAN Unit 3.
2-I  NEDI     Number of minor edit variables desired
              (0≦ NEDI≦ 9)
3-I  NTC      Number of time step width controls
              (1≦ NTC ≦ 20)
4-I  NTRP     Number of trip controls
              (1≦ NTRP ≦ 20)
5-I  IOUT     Output option for edited input
              0 = no output
              1 =    output
6-I  NPERT    Null transient flag
              0 = normal transient
              1 = null transient
7-I  ICLASS   T.? in JCL card
              (1≦ ICLASS ≦ 8)
8-I  LSEC     CPU time (sec) to end calculation
              ( 0 = no limitation )
9-I  IDPSTP   Time step to end calculation
              ( 0 = no limitation )
10-R DMPTM    Physical time to end calculation (sec)
              ( 0.0 = no limitation )
11-I NOCK     Number of nodes to which TSWC for G is not applied
              (1≦ NOCK ≦ 50)
12-I ND1      Number of nodes free from TSWC for G
     ND2
     .                  .
     .                  .
     NDNOCK
```

7.4.3 Minor Edit Variable Data BB02

Data block BB02 is required if NEDI is greater than zero. This data block specifies the variables to be edited in the minor edits. NEDI specifications must be inputted. Each specification consists of an alphanumeric entry and an integer entry as shown below, in which

XXX ~ XXX' ; are the variable symbols to be edited, and

YY ~ YY' ; are the position indexes.

```
    1 – A4        XXX–YY
      .              .
      .              .
 NEDI – A4        XXX'–YY'
```

The symbols of available minor edit variables are shown below. In the present version, however, minor edit is not possible for fuel variables. See Appendix C for the convention of the position index, since the same position index convention is used for both minor edit and plotter output.

Symbol	Variable (with reference to normal node)
PRA	Pressure as point A
PRE	Pressure as point E
GLA	Mass velocity at point A
GLE	Mass velocity at point E
HLA	Specific enthalpy at point A
HLE	Specific enthalpy at point E
RHA	Density at point A
RHE	Density at point E
XLA	Quality at point A
XLE	Quality at point E
ALA	Void fraction at point A
ALE	Void fraction at point E
QQQ	Power density
TMP	Temperature

Symbol	Variable (With reference to injection)
JMI	Injection flow rate

Symbol	Variable (with reference to pump)
HDP	Pump head
AAA	Relative pump speed
BBB	Relative pump torque
WWW	Relative volumetric flow rate
PEY	Pump eye pressure
XEY	Pump eye quality
HEY	Pump eye specific enthalpy

Symbol	Variable (with reference to accumulator)
PAC	Nitrogen pressure
GAJ	Mass flow rate
HAC	Water specific enthalpy
VAG	Nitrogen volume
VAL	Water volume
XAC	Phase index

Symbol	Variable (with reference to SG secondary system)
PSG	Pressure
MUG	Feed water flow
MRG	Relief flow
MSG	Spray line flow
IVG	Phase index
HS1	Specific enthalpy of region I
HS2	Specific enthalpy of region II
MG1	Mass of region I
MG2	Mass of region II
HT1	Heat transfer coefficient of primary side
HT2	Heat transfer coefficient of secondary side

Symbol	Variable (with reference to pressurizer tank model)
PPP	Pressure
GPR	Surge flow rate
MRP	Relief flow rate
MSP	Spray line flow
ISV	Phase index
HP1	Specific enthalpy of ragion I
HP2	Specific enthalpy of region II
MS1	Mass of region I
MS2	Mass of region II

Symbol	Variable (with reference to fuel)
QCR	Relative power
PG1	Gap pressure of rod 1
PG2	Gap pressure of rod 2
HC1	Heat transfer coefficient of rod 1
HC2	Heat transfer coefficient of rod 2
HG1	Gap conductivity of rod 1
HG2	Gap conductivity of rod 2
LI1	Thickness of zircaloy reacted at the clad inner surface of rod 1
LI2	Thickness of zircaloy reacted at the clad inner surface of rod 2
LO1	Thickness of zircaloy reacted at the clad outer surface of rod 1
LO2	Thickness of zircaloy reacted at the clad outer surface of rod 2
QM1	Metal-water heat production rate of rod 1
QM2	Metal-water heat production rate of rod 2
TS1	Fuel rod surface temperature of rod 1
TS2	Fuel rod surface temperature of rod 2
TC1	Fuel rod center temperature of rod 1
TC2	Fuel rod center temperature of rod 2

7.4.4 Time Step Width Control (TSWC) Data BB03

Number of subblocks = 1 + NTC

The time step width control is made according to the method described in section 6.3

The following data form the first subblock SB0301, which includes the option-dependent data. Data 2 to 4 are the parameters to be used for TSWC with regard to the thermal-hydraulic network iteration.

1-I	ITSTYP	1 = 2-and-1/2 TSWC (Data 2 to 13 must be inputted. Data 14 to 18 are not needed.)
		-1 = 2-and-1/2 TSWC (Use the default values, i.e., Table 3-3 and (N_1, N_2, N_3) =(20,13,9). Data 2 to 18 are not needed.)
		2 = table-controlled TSWC (Data 2 to 4 and data 14 to 18 must be inputted with data 15 to 18 repeated ITBLN times. Data 5 to 13 are not needed.)
		-2 = table-controlled TSWC (Use the default values i.e., Table 3-4 and (N_1, N_2, N_3) =(20,13,9). Data 2 to 18 are not needed.)
2-I	N_1	(see Table 6-2.)
3-I	N_2	
4-I	N_3	

5-R	P-E_1	e_1 for node pressure p
6-R	H-E_1	e_1 for node enthalpy h
7-R	T-E_1	e_1 for heat conductor temperature T
8-R	SG-E_1	e_1 for SG 2ndry pressure
9-R	AC-E_1	e_1 for AC variables
10-R	E-E_1	e_1 for node energy E
11-R	G-E_1	e_1 for node mass flux G
12-R	G-E_2	e_2 for node mass flux G
13-R	G-E_3	e_3 for node mass flux G
14-I	ITBLN	Number of variables whose TSWC are to be changed from the default method.
15-I	ICOMP	ID of variable x for which the input specified table-controlled TSWC is to be applied 1 = node pressure 2 = node mass flux 3 = node enthalpy 4 = heat conductor temperature 5 = SG 2ndry pressure 6 = AC variables 7 = node energy
16-I	NTBN	Number of points in TSWC table for x
17-R	$\Delta T(1)$ . . ΔT(NTBN)	Value of Δt . . .
18-R	$\Delta X(1)$ . . ΔX(NTBN)	Value of $\Delta x/\Delta t/x$ . . .

In ITSTYP = 2 or −2, the time step width Δt will be chosen such that

$$\Delta t=\Delta T(i+1) \quad \text{if} \quad \Delta X(i)<x<\Delta X(i+1).$$

The following must be repeated NTC times as subblock SB0302, SB0303, ..., SB030 (NTC+1).

1-I	NMIN	Number of DTMAX's per minor edit (1≦ NMIN≦ 1000) Note: Minor edit frequency is the same for output to plotter file FT50F001.
2-I	NMAJ	Number of minor edits per major edit (1≦ NMAJ≦ 1000)
3-I	NDMP	Number of major edits per restart file edit (1≦ NDMP≦ 100)
4-I	NCHK	Dummy data
5-R	DTMAX	Maximum time step width (sec)
6-R	DTMIN	Minimum time step width (sec) : If time step width becomes less than DTMIN, then calculation stops.
7-R	TLAST	End of control by this subblock (sec)

7.4.5 Trip Control Data BB04

Number of subblocks = NTRP

1-I	IDTRP	Action to be taken (|IDTRP|≦NTRP) ± 1 = end of problem ± 2 = pump trip ± 3 = reactor scram ± 4 = valve on/off ± 5 = SG feed water stop ± 6 = pressurizer heater off If IDTRP is positive, the corresponding trip is made in action. Otherwise, it is made out of action. For IDTRP=4,-4, the trip is as follows.

	IDTRP = 4	IDTRP = –4
initially closed valve	open	close
initially open valve	close	open

2-I IZ Location where action is to be taken.
(0≦ IZ≦ NVOL)
(1) Node number for IDTRP = ± 2 and ± 5)
(2) Valve number NVLV (see BB29) for IDTRP = ± 4
(3) Heater number (see BB14) for IDTRP = ± 6
(4) 0 for IDTRIP = ±1 *and* ±3

3-I IDSIG Signal being compared to trigger the action
± 1 = time
± 2 = pressure(only for SG,PZR and valves)
± 3 = temperature (only for SG and PZR)
If IDSIG is positive, the trip is actuated when the signal becomes greater than the value of SETPT. If IDSIG is negative, the trip is actuated when the signal becomes less than the value of SETPT.

4-I IX Node number where signal IDSIG belongs (0≦ IX≦ NVOL). IX must be set equal to 0 when IDSIG = ± 1.

5-R SETPT Setpoint for signal IDSIG, i.e., time (sec) for IDSIG =± 1, pressure (ata) for IDSIG = ± 2 and temperature (° C) for IDSIG = ± 3.

6-R DELAY Delay time for initiation of action after reaching setpoint (sec)

If more than one trip control are inputted for the same IZ, then off-actions override on-actions. For each |IVLV| = 2 (see BB29), IDTRP = 4 and –4 should be inputted in this order.

7.4.6 Delay Constant Data BB05

(Not required when NOPTD = 2 or 4 (see BB07))

1-I NTAUD Number of nodes whose delay constant is to be changed (0≦ NTAUD≦ 50)

2-R DTAUD Default value

In the following, first 10 ITAUD's and corresponding 10 TAUD's shoud be inputted. Then, next 10 ITAUD's and corresponding 10 TAUD's should be inputted, and so on.

3-I ITAUD1 Number of node whose dealy constant is set to be a value not equal to DTAUD.
ITAUD2
.

4-R TAUD1 Delay constant to be set for node ITAUD1
TAUD2 Delay constant to be set for node ITAUD2
.
.

5-I NTAUDJ Number of junction whose delay constant is to be changed (0≦ NTAUDJ≦ 50)

6-R DTAUDJ Default value for TAUDJ

In the following, first 10 ITAUDJ's and corresponding 10 TAUDJ's shoud be inputted. Then, next 10 ITAUDJ's and corresponding 10 TAUDJ's should be inputted, and so on.

7-I ITAUDJ1 Number of junction whose delay constant is set to be a value not equal to DTAUDJ.
ITAUDJ2
.
.

8-R TAUDJ1 Delay constant to be set for node ITAUDJ1
TAUDJ2 Delay constant to be set for node ITAUDJ2
.
.

7.4.7 PWR LB-LOCA EM Option Data BB06

(Not required for IEM = 1 (see BB07).)

(Refer to section 6.2 for the detail of this data block.)

1-I MSTAG
2-I NSTAG (See Fig.6-2-1)
3-I JDSG
4-I JCOLD
5-I NDWNC Downcomer node number
6-R RCOLD Height of downcomer top mixing junction (m)
7-R TEOBP EOBP time (sec)
8-R TBOCREC BOCREC time (sec)
9-R TQDELT Hypothetical heating time (sec)
(TEOBP + TQDELT = TLPINJ)
10-I NQ Number of nodes for which hypothetical heating is assumed

In the following, first, 10 NQNODE's and corresponding 10 QNODE's shoud be inputted. Then, next 10 NQNODE's and corresponding 10 QNODE's should be inputted, and so on.

11-I ND_1 Number of node for which hypothetical heating is assumed
ND_2
.
.
ND_{NQ}
12-I Q_1 Hypothetical heating for node ND_1 (kcal/sec)
Q_2 Hypothetical heating for node ND_2 (kcal/sec)
.
.
Q_{NDNQ} Hypothetical heating for node ND_{NQ} (kcal/sec)

7.4.8 Problem Option Card BB07

1-I NMODEL Calculation model ID
0 = standard calculation
1 = core calculation
At present, only NMODEL = 0 is available.
2-I IEM BE/EM option flag
0 = EM calculation for PWR LB-LOCA
1 = otherwise (BE calculation)
3-I NOPTF Fuel heating mode flag
0 = nuclear heating (reactor kinetics and decay heat)
1 = non-nuclear heating (table input)

4-I NOPTD Relaxation model index
1 = relaxation of void fraction , τ input (BB05)
2 = relaxation of void fraction , τ calculation
3 = relaxation of density , τ input (BB05)
4 = relaxation of density , τ calculation

5-I ICHFOP(1) CHF correlation index for flow condition
1 = Biasi's correlation
2 = GE correlation
3 = RELAP type correlation (combination of B&W2, Barnett and modified Barnett)

6-I ICHFOP(2) CHF correlation index for pool condition
1 = Interpolation by G between CHF of ICHFOP(1) at $G=G_{min}$ (=271.2 $kg/m^2/s$) and 66.9 kcal/m^2/sec.
2 = Modified Zuber's correlation
3 = Zuber's correlation

7-I IHTROP(1) Index for heat transfer correlation for nuclear boiling
1 = Jens - Lottes
2 = Thom

8-I IHTROP(2) Index for heat transfer correlation for film boiling at pool condition
1 = Berenson
2 = Bromley and Pomerantz
3 = Modified Bromley

7.4.9 Problem Dimensions Data BB08

1-I NVOL Number of normal and special nodes
(1≦ NVOL≦ 100)

2-I NJUNC Number of junctions including boundary junctions
(1≦ NJUNC≦ 100)

3-I NMIX Number of mixing junctions
(1≦ NMIX≦ 20)

4-I NPINJ Number of hydraulic sources (pumped injections)
(1≦ NPINJ≦ 10)
Dead-end breaks are not included in hydraulic sources.

5-I NPUMP Number of pumps
(1≦ NPUMP≦ 4)

6-I NACCUM Number of accumulators
(1≦ NACCUM≦ 4)

7-I NPRS Number of pressurizer tank models used
(0≦ NPRS≦ 1)

8-I NSG Number of SG 2ndry tank model used
(0≦ NSG ≦ 4)

9-I NSGT Maximum number of primary nodes per SG unit
(0≦ NSG ≦ 10)

10-I KROD Number of fuel types
(1≦ KROD ≦ 10)

11-I NCTOT Total number of fuel slabs ($\sum_{i=1}^{KROD} N_i$ where N_i is number of slabs in type i fuel)
(1≦ NCTOT ≦ 50)

12-I NCORE Number of axial coolant nodes per core channel
(3≦ NCORE ≦ 50)

13-I NSLB Number of heat conductors
(1≦ NSLB ≦ 100)

14-I NRGN Maximum number of material regions in conductors
(1≦ NRGN ≦ 6)

15-I NMESH Maximum number of radial meshes in conductors
(3< NMESH ≦ 50)

16-I NVLV Number of valves
(1≦ NVLV ≦ 30)

7.4.10 Data for Steady State Adjustment of Loop Hydraulics BB09

1-I	IVOL	number of the node from which steady state calculation starts
2-R	G_A	G at point A of node IVOL (Kg/m^2/sec)
3-R	h_A	h at point A of node IVOL (kcal/kg).

7.4.11 Normal or Linkage Node Data BB10

Number of subblocks = NLOOP

1-I	NOV	Node number (1≦ NOV≦ NLOOP)
2-I	ITYP	Node type 1 = duct 2 = core 3 = core bypass 4 = downcomer 5 = lower plenum 6 = upper head 7 = SG primary duct 8 = pump 9 = orifice 10 = SG secondary flow 11 = pressurizer 12 = accumulator 13 = linkage duct Note: In the present version, ITYP = 9,10 and 12 are not allowed.
3-I	FJN	From-junction number (1≦ IW1≦ NJUNC)
4-I	TJN	To-junction number (1≦ IW2≦ NJUNC)
5-I	INU	Number of parallel nodes (1≦ INU)
6-R	p^A or k	Initial pressure (ata) for non-stagnant node or loss coefficient for stagnant node(input negative value)
7-R	A	Cross section at average point (m)
8-R	A^A	Cross section at point A (m) = A if zero is inputted
9-R	A^E	Cross section at point E (m) = A if zero is inputted
10-R	D	Hydraulic Diameter (m) $=(4A/\pi)^{1/2}$ if zero is inputted
11-R	L	Node length (m)
12-R	L_H	Node height with reference to point A (m) $(-L \leq L_H \leq L)$
13-R	k_A^f	Junction loss coefficient at point A for forward flow
14-R	k_A^r	Junction loss coefficient at point A for reverse flow
15-R	k_E^f	Junction loss coefficient at point E for forward flow
16-R	k_E^r	Junction loss coefficient at point E for reverse flow

For a core flow associated with a fuel rod, for example, whose pitch and outer radius are l_p and r_R, respectively, A and D to be inputted may be given as follows.

$$A=l_p^2-\pi r_R^2$$

and

$$D=\frac{2A}{\pi r_R}$$

If one wants to set k_f for forward flow (or k_r for reverse flow) at junction j, then one can input k_f (or k_r) either for k_A^f (or k_A^r) of the to-node or for k_E^f (or k_E^r) of the from-node, respectively. Moreover, the built-in formula can be used to obtain the junction loss coefficient for a normal junction, if −1.0 is inputted for either A or E point adjacent to the junction. No built-in formula, however, is available for the junction loss coefficients around a mixing junction. (see subsection 2.5.1).

7.4.12 Junction Data BB11

Number of subblocks = NJUNC

1-I	JNO	Junction number (1≦ JNO≦ NJUNC)
2-I	JTP	Junction type 1 = normal junction 2 = upper plenum 3 = downcomer top 4 = other mixing junction 5 = injection junction (accumulator) 6 = injection junction (pressurizer) 7 = injection junction (pumped injection) 8 = dead end junction
3-R	V^+ or A^+	Junction volume for mixing junction (m^3) Junction Area for volumeless junction (m^3) Note: If A^+ = 0.0 is inputted for a volumeless junction, the minimum of A_{from}^A and A_{to}^E will be set. Otherwise, the minimum of the three will be set. Refer to section 2.5.2.
4-R	PJO	Pressure of initially stagnant junction (ata) If junction JNO is not stagnant, input 0.0. If junction JNO belongs to a stagnant branch with a closed valve, input 0.0.
5-R	HJO	Specific enthalpy of initially stagnant junction (kcal/kg) If junction JNO is not stagnant, input 0.0. If 0.0 is inputted for stagnant junction, HJO will be set to be the specific enthalpy of the from-mixing junction.

7.4.13 Mixing Junction Data BB12

Number of subblocks = NMIX

Data (3, 4, 5, 6) must correspond to data (7, 8, 9, 10), respectively.

Data 7 to 10 are the ratios of mass flow rates in (kg/s).

1-I	JNO	Junction number (1≦ JNO≦ NJUNC)
2-I	NOUT	Number of outgoing flows at steady state (1≦ NOUT≦ 4)
3-I	NVOUT1	To-node number (1) (0≦ NVOUT1≦ NVOL)
4-I	NVOUT2	To-node number (2) (0≦ NVOUT2≦ NVOL)
5-I	NVOUT3	To-node number (3) (0≦ NVOUT3≦ NVOL)
6-I	NVOUT4	To-node number (4) (0≦ NVOUT4≦ NVOL)
7-R	ROUT1	Fraction of outgoing flow (1) at steady state (0≦ ROUT1≦ 1.0)
8-R	ROUT2	Fraction of outgoing flow (2) at steady state (0≦ ROUT2≦ 1.0)
9-R	ROUT3	Fraction of outgoing flow (3) at steady state (0≦ ROUT3≦ 1.0)
10-R	ROUT4	Fraction of outgoing flow (4) at steady state (0≦ OMAS4≦ 1.0)

7.4.14 Hydraulic Source Data BB13

Number of subblocks = NPINJ

Dead end breaks are not included in hydraulic sources.

1-I	NOPINJ	Number of hydraulic source (1≦ NOPINJ≦ NPINJ)
2-I	IJ	Number of boundary junction (1≦ IJ≦ NJUNC)
3-I	IFPT	Injection table option flag 1 = (t-m) table 2 = (p-m) table 3 = (t-p) table 4 = (G-p) table
4-R	h^{inj}	Specific enthalpy of injected water (kcal/kg)
5-I	NPI	Number of points in injection table
6-T		NPI pairs of (t-m) or (p-m) or (t-p) or (G-p) for injection t = time (sec) after opening of valve to be actuated by TRIP p = pressure (ata) m = flow rate (kg/sec)

7.4.15 Pump Data BB14

Number of subblocks = NPUMP

If ID = 0 is inputted, data 4 to 12 can be arbitrary.

1-I	INO	Node number (1≦ INO≦ NLOOP)
2-I	ITAP	Number of table group to be used (see BB15) (1≦ ITAP≦ NPTB) (see NPTB in BB11)
3-I	ID	Trip index 0 = locking of rotor 1 = pump coastdown
4-R	Ω_r	Rated pump speed (rpm)
5-R	W_r	Rated volumetric flow rate (m^3/sec)
6-R	T_r	Rated torque (kgm^2/sec^2/rad)
7-R	L_{headr}	Rated head (m)
8-R	ρ_{fr}	Rated density (kg/m^3)
9-R	$\Omega(0)$	Initial pump speed (rpm)
10-R	I_m	Moment of inertia (kgm^2/rad^2)
11-R	k_1	Coefficient of angular momentum equation ($0 \leqq k_1$) (See Eq.(2-4-51) in Ref(2).)
12-R	k_2	Coefficient of angular momentum equation ($0 \leqq k_2$) (See Eq.(2-4-51).)
13-R	$\tau = \tau_a$ $= \tau_t$ =0.01	(decay constant for pump speed) when ID = 0 (decay constant for electric torque) when ID = 1 (default)

7.4.16 Pump Characteristic Curves Data BB15

Number of subblocks ≦ NPUMP

0-I	NPTB	Table group number (1≦ NPTB≦ NPUMP)

The following 19 table inputs should be inputted according to THYDE-P2 table input specification. In the data from 9 to 16, $\Delta\tau$ and ΔH mean $\tau_{2_\varphi} - \tau_{1_\varphi}$ and $H_{2_\varphi} - H_{1_\varphi}$, respectively, with 1_φ = single phase and 2_φ = two phase.

```
1     (Head-discharge curve for positive speed)
1a-I        IP1    Number of points
1b-T               IP1 pairs of (w/a, H)
2     (Head-discharge curve for negative speed)
2a-I        IP2    Number of points
2b-T               IP2 pairs of (w/a, H)
3     (Head-speed curve for positive flow)
3a-I        IP3    Number of points
3b-T               IP3 pairs of (a/w, H)
4     (Head-speed curve for negative flow)
4a-I        IP4    Number of points
4b-T               IP4 pairs of (a/w, H)
5     (Torque-discharge curve for positive speed)
5a-I        IP5    Number of points
5b-T               IP5 pairs of (w/a, T)
6     (Torque-discharge curve for negative speed)
6a-I        IP6    Number of points
6b-T               IP6 pairs of (w/a, T)
7     (Torque-speed curve for positive flow)
7a-I        IP7    Number of points
7b-T               IP7 pairs of (a/w, T)
8     (Torque-speed cuver for negative flow)
8a-I        IP8    Number of points
8b-T               IP8 pairs of (a/w, T)
9     (ΔH-discharge curve for positive speed)
9a-I        IP9    Number of points
9b-T               IP9 pairs of (w/a, ΔH)
10    (ΔH-discharge curve for negative speed)
10a-I       IP10   Number of points
10b-T              IP10 pairs of (w/a, ΔH)
11    (ΔH-speed curve for positive flow)
11a-I       IP11   Number of points
11b-T              IP11 pairs of (a/w, ΔH)
12    (ΔH-speed curve for negative flow)
12a-I       IP12   Number of points
12b-T              IP12 pairs of (a/w, ΔH)
13    (Δτ-discharge curve for positive speed)
13a-I       IP13   Number of points
13b-T              IP13 pairs of (w/a, Δτ)
14    (Δτ-discharge curve for negative speed)
14a-I       IP14   Number of points
14b-T              IP14 pairs of (w/a, Δτ)
15    (Δτ-speed curve for positive flow)
15a-I       IP15   Number of points
15b-T              IP15 pairs of (a/w, Δτ)
16    (Δτ-speed curve for negative flow)
16a-I       IP16   Number of points
16b-T              IP16 pairs of (a/w, Δτ)
17    (Head multiplier)
17a-I       IP17   Number of points
17b-T              IP17 pairs of (α, M_H)
18    (Torque multiplier)
18a-I       IP18   Number of points
18b-T              Ip18 pairs of (α, M_T)
19    (NPSH table )
19a-I       IP191 Number of points for a
19b-I       IP192 Number of points for w
19c-T                    (Give as follows.)
```

$$
\begin{bmatrix}
 & a_1 & \cdot & a_{IP191} \\
w_1 & NPSH(w_1, a_1) & \cdot & NPSH(w_1, a_{IP191}) \\
w_2 & NPSH(w_2, a_1) & \cdot & NPSH(w_2, a_{IP191}) \\
\cdot & \cdot & \cdot & \cdot \\
\cdot & & \cdot & \cdot \\
w_{IP192} & NPSH(w_{IP192}, a_1) & \cdot & NSPH(w_{IP192}, a_{IP191})
\end{bmatrix}
$$

7.4.17 Accumulator Data BB16

Number of subblocks = NACCUM

In the following, AC duct means the duct from accumulator to check valve or to AC injection junction.

1-I	NOV	Node number (NLOOP+1≤ NOV≤ NVOL)
2-I	IJUNC	Injection junction number (1≤ IJUNC≤ NJUNC)
3-R	$V_{H_2O}(0)$	Initial water volume (m^3)
4-R	$V_{N_2}(0)$	Nitrogen gas volume (m^3)
5-R	$h_{H_2O}(0)$	Initial specific enthalpy of water (kcal/kg)
6-R	$P_{N_2}(0)$	Initial pressure (ata) Note; effective for initially isolated accumulator not effective for initially linked accumulator
7-R	$(L_H)_{H_2O}(0)$	Initial water level (m)
8-R	$h_{ACD}(0)$	Initial enthalpy of coolant in AC duct (kcal/kg)
9-R	V_{ACD}	AC Duct volume (m^3)
10-R	$(L_H)_{ACD}$	Height of AC duct (m)

7.4.18 Break Point Data BB17

In case of guillotine break, the data 3 to 5 are associated with the to-node of the break junction, while the data 6 to 8 with the other. In case of dead-end break, the former must be set to be zeros.

1-I	IBJ	Break junction number (1≤ NBREAK≤ NJUNC)
2-R	TBRK	Break time (sec) (0 < TBRK)
3-R	C_2	See Eq. (2-5-6). (downstream of break)
4-R	C_D	Discharge coefficient for critical flow (downstream of break)
5-R	C_{eff}	Discharge coefficient for inertial flow (downstream of break)
6-R	C_2	(Same as above, upstream of break)
7-R	C_D	(Same as above, upstream of break)
8-R	C_{eff}	(Same as above, upstream of break)
9-R	k_U^D	Loss coefficient at break (upstream of break, discharge)
10-R	k_U^S	Loss coefficient at break (upstream of break, suction)
11-R	k_D^D	Loss coefficient at break (downstream of break, discharge)
12-R	k_D^S	Loss coefficient at break (downstream of break, suction)
13-R	UTAUB	Break time constant at upstream side of break (sec)
14-R	DTAUB	Break time constant at downstream side of break (sec)
15-I	IP	Number of points for container pressure
16-T		IP pairs of (t, p) for container pressure t ; time (sec) after start of calculation p ; pressure (ata)

7.4.19 Pressurizer Data BB18

In the present version, the relief line and the relief valve are not implemented for the tank model so that data 11 to 13 are dummy. THYDE-P2, however, can simulate a pressurizer without this data block by means of normal nodes and heat conductors. At least one of the heaters must be partly or entirely under the water level. At least one of the heaters must be initially on.

1-I	NOV	Node number (1≦ NOV≦ NVOL)
2-I	IJ	Injection junction number (1≦ IJ≦ NJUNC)
3-I	NSP	Node number whose pressure P_{NSP} actuates spray when $P_{NSP}<P_{ZR}$. (1≦ NSP≦ NVOL)
4-R	A_T	Pressurizer cross section (m^2)
5-R	H_T	Pressurizer height (m)
6-R	$Z_W(0)$	Initial water level (m) (initial region II height) ($0 \leq Z_{WO} \leq H_T$)
7-R	$\alpha_I(0)$	Initial void fraction of region I.
8-R	l_{in}	Stand pipe length (m) ($l_{in}>0$)
9-R	V_D	Warm duct volume (m^3)
10-R	$h_{II}(0)$	Initial specific enthalpy of region II.(kcal/kg)
11-R	p_{set}	Relief valve setpoint (ata)
12-R	A_{re}	Relief line cross section (m^2)
13-R	A_{SP}	Spray line cross section (m^2)
14-R	a_1	See Eq.(2-4-49).
15-R	a_2	See Eq.(2-4-49).
16-R	L_1	Length of heater 1 (m)
17-R	L_2	Length of heater 2 (m)
18-R	L_3	Length of heater 3 (m)
19-R	b_1	
20-R	b_2	See Fig. 3-2-1.
21-R	b_3	
22-R	τ_{sub}	Heater time constant when coolant is subcooled. (sec)
23-R	τ_{sat}	Heater time constant when coolant is saturated. (sec)
24-R	τ_{sup}	Heater time constant when coolant is superheated steam. (sec)
25-I	IP	Number of points for heater power table
26-T		IP sets of $(t, G_1, G_2, G_3)$for heater powers t ; time (sec) G_i; relative power of heater i (i=1,2,3)

7.4.20 SG 2ndry System Data BB19

Number of subblocks = NSG

1-I	NOV	Node number (NLOOP+1≦NOV≦NVOL)
2-I	NTUBE	Number of U-tubes (1≦NTUBE≦20000)
3-I	NSGS	Number of inlet node of primary flow
4-I	NSGE	Number of outlet node of primary flow
5-I	NSGN	Number of SG primary nodes
6-I	NREF	Number of relief valves in turbine steam supply flow
7-R	A_T	SG vessel cross-section (m^2)
8-R	H_T	SG vessel height (m)
9-R	A_{s-l}	Cross-section of turbine steam supply flow (m^3)
10-R	τ_{is}	Time constant of isolation valve of the secondary flow.(see IDTRP =± 5 in BB04)
11-R	A_U	Cross-sectional flow area per U-tube (m^2)
12-R	R_{SGin}	U-tube inner radius (m) ($=D_{eff}/2$)
13-R	l_{TSG}	Wetted perimeter of SG vessel (m)
14-R	$Z_W(0)$	Initial region II level (m)
15-R	$h_{SU}(0)$	Initial specific enthalpy of feedwater(kg/kcal)
16-R	$M_{SU}(0)$	Initial feedwater flow rate (kg/sec)
17-R	β	Coefficient to decide the initial specific enthalpy of region II such taht $h_{II}=\beta h_{fs}+(1-\beta)h_{su}$ ($0.0 \leq \beta \leq 1.0$)
18-R	$\alpha_I(0)$	Initial void fraction in region I ($0.0 \leq \alpha_{I0} \leq 1.0$)

19-R $p(0)$ Initial pressure (ata)
20-R r_2 Recirculation fraction
($0.0 \leq r_2 \leq 1.0$)
21-R h_{DOWN} Downcomer height (m)

22-R $\Phi_{SG}(1, 0)$ Initial heat flux of node NSGS
: (negative, kcal/m^2/sec)
:
$\Phi_{SG}(NSGN, 0)$ Initial heat flux of node NSGE
(negative, kcal/m^2/sec)
23-R (Repeat the following set NREF times)

A_{re} Relief line cross-section (m^2)
p_{set} Relief valve setpoint (ata)
C_2 See Eq. (2-5-6).
C_D Discharge coefficient for critical flow (-)
C_m Discharge coefficient for inertial flow (-)

24-I IP Number of time points in SG secondary flow table
25-T IP sets of t, R_{msu}, R_{hsu}, R_G for secondary flow
R_{msu} : Relative flow rate(-)
R_{hsu} : Relative specific enthalpy(-)
R_G : dummy

7.4.21 Core Control Data BB20

Number of subblocks = KROD

Fuel rods or fuel plates should be inputted first. Fuel rods with gap should be inputted earlier than fuel rods without gap. First inputted fuel is regarded as the average rod or plate. Data 9 and 10 are needed only for the first subblock SB2001.

1-I IDROD Rod type identification number
($1 \leq IDROD \leq KROD$)
2-I NROD Number of fuel rods
($1 \leq NROD \leq 50{,}000$)
3-I NBOT Number of most upstream core node
($1 \leq NCL \leq NLOOP$)
4-I NTOP Number of most downstream core node
($NBOT \leq NCH \leq NLOOP$)
5-I NSLBOT Number of most upstream conductor
($1 \leq NCL \leq NSLB$)
6-I NSLTOP Number of most downstream conductor
($NSLBOT \leq NCH \leq NSLB$)
7-I IGAP GAP option
0 = fuel without gap
1 = fuel with gap
Note: For IGAP = 1, fuel must be cylindrical.
8-I IQMW Metal-water reaction option
0 = without reaction
1 = with reaction
9-I NR Number of radial meshes for IGAP=1
($1 \leq NR \leq NMESH$)
10-I NF Number of radial meshes in pellet for IGAP=1
($1 \leq NF < NR$)

7.4.22 Nuclear Heating Data BB21

1-R l Neutron lifetime (sec)
2-R (λ_1, β_1) λ_j = Decay constant of delayed
: neutron precursor of i-th group (1/sec)
:
(λ_6, β_6) β_j = Delayed nuetron

		fraction of i-th group (-) (1/sec)
3-R	C_c	Conversion ratio (-)
4-R	Σ_a/Σ_f	See Eq. (3-1-10).
5-I	IP1	Number of points in void coefficient table
6-T		IP1 sets of (α, γ_α) α : void fraction γ_α: void coefficient ($)
7-I	IP2	Number of points in fuel temperature coefficient table
8-T		IP2 sets of (T, γ_T) T : fuel temperature (°C) γ_T: fuel temperature coefficient ($/°C)
9-I	IP3	Number of points in external reactivity table
10-T		IP3 sets of (t, R_{ex}) t ; time (sec) R_{ex} ; external reactivity ($)

7.4.23 Metal-Water Reaction Data BB22

(to be inputted only when IQMW = 1)

Number of subblocks = number of rod type subgroups, each of which has the same values for the following data (≦KROD)

1-I	NN	Number of IDROD's
2-I		$IDROD_1$ $IDROD_2$ ⋮ $IDROD_{NN}$
3-R	Δh_{reac}	Heat of metal-water reaction (kcal/kg)
4-R	k_1	Coefficient of Eq. (3-1-13) (m^2/sec)
5-R	k_2	Coefficient of Eq. (3-1-13) (°K)
6-R		$(l^{out}, l^{in})_1$ ⋮ from upstream to downstream $(l^{out}, l^{in})_{NCORE}$ l^{out} ; initial thickness of zircaloy reacted at outer surface (m) l^{in} ; initial thickness of zircaloy reacted at inner surface (m)

7.4.24 Fuel Gap Data BB23

Number of subblocks = number of rod type subgroups, each of which has the same values for the following data (≦KROD)

1-I	NN	Number of IDROD's
2-I		$IDROD_1$ $IDROD_2$ ⋮ $IDROD_{NN}$
3-R	N	Mols of gas in pin
4-R	p_{gc}	Contact pressure (ata)
5-R	$r_{gap}(0)$	Initial gap width (m)
6-R	V_{pe}	Plenum gas volume (m^3)
7-R	V_{opr}	Open porosity volume (m^3)
8-R	V_{cr}	Chip and roughness volume (m^3)
9-R	$V_{cd}(0)$	Initial clad and dish volume (m^3)
10-R	C_T	Constant in Eq. (3-3-29) (°C)
11-R	ε_{NF}	Fuel pellet emissivity (-)
12-R	ε_{cl}	Fuel clad emissivity (-)
13-R	FRASM	Mean free path (m)

14-R	η_{He}	Mol fraction of H_e (-)
15-R	η_{Xe}	Mol fraction of X_e (-)
16-R	η_{Kr}	Mol Fraction of K_r (-)
17-R	η_{air}	Mol fraction of air (-)
18-R	η_{N2}	Mol fraction of N_2 (-)
19-R	η_{H2}	Mol fraction of H_2 (-)
20-R	η_{H2O}	Mol fraction of H_2O (-)

7.4.25 Clad Burst Description Data BB24

Number of subblocks = number of rod type subgroups, each of which has the same values for the following data (≤KROD)

1-I	NN	Number of IDROD's
2-I		$IDROD_1$
		$IDROD_2$
		:
		$IDROD_{NN}$
3-I	N_j	Number of non-burst digonal rods in 3 x 3 matrix
4-I	M_j	Number of non-burst off-diagonal rods in 3 x 3 matrix
5-I	A	
6-R	B	
7-R	C	Coefficient of Eq.(4-1-11)
8-R	D	
9-R	E	
10-R	A_0	
11-R	A_1	
12-R	A_2	Coefficients of Eq.(4-1-14)
13-R	A_3	
14-R	A_4	
15-R	A	Coefficients of Eq.(4-1-13)
16-R	B	
17-R	S_{burst}	Threshold strain for burst (-) ($0.0<S_{burst}<1.0$)
18-R	BLM	Minimum blockage ratio (-) due to rod burst

7.4.26 Heat Conductor Control Data BB25

1-I	NMAT	Total number of heat conductor material tables to be inputted (UO_2 and Zircaloy tables are contained in the code so that they need not be inputted.)
2-I	NRPW	Total number of heat conductor relative power tables

7.4.27 Heat Conductor Data BB26

Group the heat conductors so that each group has the same input values for data 3 to 16. For each group, NSB1 is the first conductor number, while NSB2 the last.

1-I	NSB1	Conductor number ($1 \leq NSB1 \leq NSLB$)
2-I	NSB2	Conductor number (NSB2=0 or $NSB1 \leq NSB2 \leq NSLB$)
3-I		Geometric type 1 = rectangular 2 = cylindrical
4-I		Conductor category 0 = ordinary 1 = fuel 2 = SG
5-I		Number of conductors
6-I	NRG	Number of regions
7-R		Inner radius or width (m)
8-R		Outer radius or thickness (m)

9-R		Sink temperature or wall temperature (°C) Effective when N_L = -1, -2 or N_R = -1, -2. Otherwise, arbitrary.
10-R		Emissivity Effective when N_L = -1 or N_R = -1. Otherwise, arbitrary.

Input region-wise NRG sets for data 11 to 16.
(Regions numbering should be started from inside/left).

11-I	IDRGN	Region number
12-I	IM	Material number >0 : Material number (see BB27) -1 = UO_2 (Use bulit-in table) -2 = Zircaloy (Use bulit-in table)
13-I		Number of meshes
14-I		Number of relative power table >0 : Relative power table number (see BB28) -1 = Nuclear power (Eq.(3-3-4)) 0 = without power input
15-R		Region thickness (m)
16-R		Initial power density (kcal/sec/m^3)

Input (NSB2-NSB1+1) sets for data 17 to 19.

17-I	N_L	Coolant node number at inner or left side of conductor 0 = adiabatic at inner or left side of conductor -1 = radiative at inner or left side of conductor -2 = constant temperature at inner or left side of conduct
18-I	N_R	Coolant node number at outer or right side of conductor 0 = adiabatic at outer or right side of conductor -1 = radiative at outer or right side of conductor -2 = constant temperature at outer or right side of conduc
19-R		Conductor length parallel to flow (m)

7.4.28 Heat Conductor Material Property Tables BB27

Number of subblocks = NMAT

1-I	MAT	Material ID number
2-A		Material name (in less than 72 characters)
3-I	IP1	Number of points
4-T		IP1 sets of (T, ρ) T : temperature (°C) ρ : density (kg/m^3)
5-I	IP2	Number of points
6-T		IP2 sets of (T, C_p) T : temperature (°C) C_p : specific heat (kcal/kg/°C)
7-I	IP3	Number of points
8-T		IP3 sets of (T, λ) T : temperature (°C) λ : heat conductivity (kcal/m/sec/°C)

7.4.29 Heat Conductor Power Tables BB28

Number of subblocks = NRPW

1-I		ID number of relative power table
2-I	IP	Number of points
3-T		IP sets of (t, P_{wr}) t : time (sec) P_{wr} : relative power (-)

7.4.30 Valve Data BB29

Number of subblocks = NVLV

```
1-I   NVLV    Valve number
2-I   IVLV    Valve type
               2 = mannual valve, initially open
              -2 = mannual valve, initially closed
               3 = check valve, to open for forward flow
              -3 = check valve, initially closed, to open
                   for reverse flow
3-I   NDV     Number of node where valve is located
4-R   TAUOPN  Time constant in opening
              = 0.1 when zero is inputted  (sec)
5-R   TAUCLS  Time constant in closing
              = 1.0 when zero is inputted  (sec)
```

A boundary node with a hydraulic source must have an initially closed mannual valve. A valve can be placed only at E point of a normal or linkage node. For IVLV = ±4, only trip-on (IDTRP = 4) is acceptable, except for the relief valve placed at junction JDSCG in the EM calculation. Valve on/off is controlled by BB04. No trip input is required for check valve.

7.4.31 Dump Control Data BB00

These data should be placed after the BEND card.

```
1-I   NCLL    Dumping index of flow network iteration
               0 = no dumping
              -1 = start dumping at time step NCSTEP
2-I   NCSTEP  Time step number when dumping of network iteration starts
3-I   NXDMP   Numer of groups of array dumping
```

7.5 Input for Restarting

An old restart data file to be used must be mounted on FORTRAN Unit 3 and a blank on Unit 2. A new plotter file will be generated on Unit 50. There are two methods to control creation of restart file, i.e., by specifying (1) one of ICLASS, LSEC, IDPSTP and DMPTM in BB01 or (2) NDMP in BB03. THYDE-P2 is used with the following input definitions.

Problem Control Data BB01

LDMP = a positive integer

NTRP ; must be equal to be the value at the previous run.

The others can be changed.

Minor Edit Variable Data BB02

The quantities being edited on the new run need not have any relation to those of the original run. The same rules apply as for the original problem.

Time Step Width Control Sequence Data BB03

TLAST ; must be greater than the time at which the present run starts. The same rules as for the original problem apply to the rest of the variables.

Trip Control Data BB04

Data block BB04 must not be changed only with the following exception. For the sub-block corresponding to IDTRP = 1, the value for SETPT must be greater than that of the previous run.

Delay Constant Data BB05

Data Block BB05 can be changed.

EM Option Data BB06

This data block is not required for a BE calculation.

The other data need not be inputted except the dump control data block BB00 and the BEND card.

8. Execution of THYDE-P2 Job

The following data sets are required to perform a THYDE-P2 calculation. The relationship among these data sets are shown in **Fig. 8–2–1**.

input data sets

- FT01F001 : steam table
- FT03F001 : restart data
- FT12F001 : input data

output data sets

- FT02F001 : data for next restart
- FT06F001 : data for ordinary FORTRAN output
- FT08F001 : data for compiled output
- FT09F001 : data for debugging output
- FT10F001 : data for restart at the latest major edit in case of abnormal ending
- FT20F001 : data for output of input data
- FT50F001 : data for plotter

When a THYDE-P2 calculation is started from an initial state, all the data described in section 7.4 are required with LDMP = 0 in BB01 (see subsection 7.4.2) and with a dummy data set FT03F001. When a THYDE-P2 calculation is restarted from a restart dump point in a previous run, all the data in section 7.4 is not required. Input data requirements for restart are described in section 7.5.

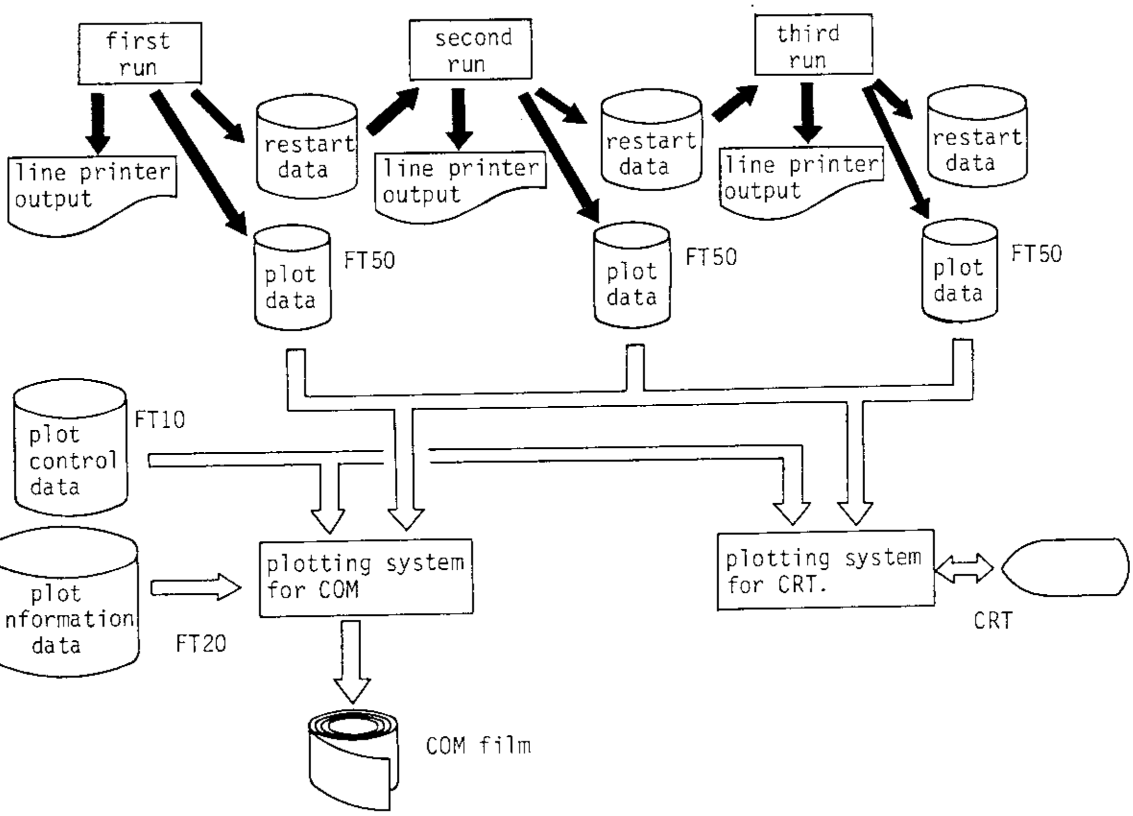

Fig. 8–1–1 Data Flow of THYDE–P2 Runs.

Restart dump frequency can be controlled by NDMP in BB03 (see subsection 7.4.4). In addition, a restart dump is also made, when ICLASS or IDPSTP or DMPTM in problem control data block BB01 (see subsection 7.4.2) is specified. The restart dump is made on FORTRAN Unit 2 in case of normal ending. To back up the cases when the run stops abnormally, the restart data at the latest major edit is storted in FORTRAN Unit 10 with LDMP = 1.

Control cards for execution is computer system dependent so that they will not be discussed in detail. **Tables 8–1** to **8–3** show examples of control cards.

Table 8–1 Control Cards for Compile of Source WRK.FORT77, Linkage and Execution Starting form a Steady State

```
// JCLG    JOB
//         EXEC  JCLG
//SYSIN    DD    DATA,DLM='**'
//            JUSER CARD
 T.5C.3W.4I.5 SRP
 OPTP PASSWORD=xxxxx
//FORT     EXEC FORT77VP,SO='J2937.WRK',A='NOSOURCE,ELM(*)',
//         B='NOPRINT',OBJS='300,10'
//SYSINC   DD DSN=J2937.V4L8INC.FORT77,DISP=SHR
//LKEDIT   EXEC LKEDIT,LM='J2937.V04L08'
//EXEC SYSA
//EXEC GOA
//FT06F001 DD SYSOUT=*,DCB=(RECFM=FBA,LRECL=137,BLSIZE=274)
//SYSPRINT DD SYSOUT=*
//SYSIN    DD DUMMY
//*           *** STEAM TALBE DATA ***
// EXPAND  DISKTO,DDN=FT01F001,DSN='J3149.ALMST4',Q='.DATA'
//FT03F001 DD DUMMY
//*           *** PRINT OUT DATASET***
//FT08F001 DD SYSOUT=*,DCB=(RECFM=FBA,LRECL=144,BLKSIZE=3168)
//FT09F001 DD DUMMY
//FT10F001 DD DUMMY
//*           *** INPUT DATA ***
// EXPAND  DISKTO,DDN=FT12F001,DSN='J2937.RUNDATA',Q='.DATA(TEST)'
//*           *** INPUT DATA PRINT OUT DATASET ***
//FT20F001 DD SYSOUT=*,DCB=(RECFM=FBA,LRECL=144,BLKSIZE=3168)
//*           *** RESTART DUMP DATA ***
// EXPAND  DISKTO,DDN=FT02F001,DSN='J2937.F01',Q='.DATA'
//*           *** PLOTTER OUT PUT DATASET ***
// EXPAND  DISKTO,DDN=FT50F001,DSN='J2937.PL01',Q='.DATA'
**
//
```

Table 8–2 Control Cards for Execution Starting for a Steady State by Load Module SV04L08

```
//JCLG    JOB
//        EXEC    JCLG
//SYSIN   DD      DATA,DLM='***'
//        JUSER   CARD
  T.5C.3W.4I.5 SRP
  OPTP PASSWORD=XXXX,CLASS=0
//     EXEC SYSA
//LMGOA  EXEC LMGOA,LM='J2937.V04L08'
//*
//FT06F001 DD SYSOUT=*,DCB=(RECFM=FBA,LRECL=137,BLSIZE=274)
//SYSPRINT DD SYSOUT=*
//SYSIN    DD DUMMY
//*           *** STEAM TABLE DATA ***
// EXPAND  DISKTO,DDN=FT01F001.DSN='J3149.ALMST4',Q='.DATA'
```

```
//FT03F001 DD DUMMY
//*              *** PRINT OUT DATASET ***
//FT08F001 DD SYSOUT=*,DCB=(RECFM=FBA,LRECL=137,BLKSIZE=274)
//FT09F001 DD DUMMY
//FT10F001 DD DUMMY
//*              *** INPUT DATA ***
// EXPAND  DISKTO,DDN=FT12F001,DSN='J2937.RUNDATA',Q='.DATA(TEST)'
//*              *** INPUT DATA PRINT OUT DATASET ***
//FT20F001 DD SYSOUT=*,DCB=(RECFM=FBA,LRECL=144,BLKSIZE=3168)
//*              *** RESTART DUMP DATASET ***
// EXPAND  DISKTO,DDN=FT02F001,DSN='J2936.F01',Q='.DATA'
//*              *** PLOTTER OUT PUT DATASET ***
// EXPAND  DISKTO,DDN=FT50F001,DSN='J2937.PL01',Q='.DATA'
**
//
```

Table 8–3 Control Cards for Restarted Execution by Load Module V04L08 (Required memory is about 2.4 M bytes)

```
//JCLG.    JOB
//         EXEC  JCLG
//SYSIN   DD     DATA,DLM='***'
//         JUSER CARD
T.5C.3W.4I.5 SRP
OPTP PASSWORD=XXXXX
// EXEC SYSA
//LMGOA EXEC LMGOA,LM='J2937.V04L08'
//FT06F001 DD SYSOUT=*,DCB=(RECFM=FBA,LRECL=137,BLSIZE=274)
//SYSPRINT DD SYSOUT=*
//SYSIN     DD DUMMY
//*              *** STEAM TABLE DATA ***
// EXPAND  DISKTO,DDN=FT01F001,DSN='J3149.ALMST4',Q='.DATA'
//*              *** RESTART DATASET ***
// EXPAND  DISKTO,DDN=FT03F001,DSN='J2937.F01',Q='.DATA'
//*              *** PRINT OUT DATASET ***
//FT08F001 DD SYSOUT=I,DCB=(RECFM=FBA,LRECL=144,BLKSIZE=3168)
//FT09F001 DD DUMMY
//FT10F001 DD DUMMY
//*              *** INPUT DATA ***
// EXPAND  DISKTO,DDN=FT12F001,DSN='J2937.RUNDATA',Q='.DATA(RTEST)'
//*              *** INPUT DATA PRINT OUT DATASET ***
//FT20F001 DD SYSOUT=I,DCB=(RECFM=FBA,LRECL=144,BLKSIZE=3168)
//*              *** RESTART DUMP DATASET ***
// EXPAND  DISKTO,DDN=FT02F001,DSN='J2936.F02',Q='.DATA'
//*              *** PLOTTER OUTPUT DATASET ***
// EXPAND  DISKTO,DDN=FT50F001,DSN='J2936.PL02',Q='.DATA'
**
//
```

9. Output Specifications

9.1 Output Listing

The format of the output listing of THYDE-P2 is shown in **Fig. 9–1–1**. **Fig. 9–1–2** shows an example of error message. **Fig. 9–1–3** shows the message which will be printed out when need for time step width control occurs. When the module where this need occurred is TRPGH, the number AYYY indicated by * in **Fig. 9–1–3** has the following meaning.

A = 3 TSWC due to pressure change at node YYY

4 TSWC due to mass flux change at node YYY

5 TSWC due to low pressure (≦ 1 atm) (refer to TRPG for YYY)

9.2 THYDE-P2 Plotting System

The THYDE-P2 plotting system can show on a cathod-ray tube the results of THYDE-P2 by compiling the data sets generated in a series of THYDE-P2 jobs. The data for the THYDE-P2 plotting system are stored in a data set defined by FT50F001 with the same frequency as for minor edit controlled by NMIN in BB03 (see subsection 7.4.4) during execution of a THYDE-P2 job. **Fig. 9–2–1** shows relationship between execution of THYDE-P2 jobs and generation of plot data.

Fig. 9–2–2 shows relationship between the plotting system and the required input data sets. In the following, each of the data sets will be explained.

first job		restarted job	
	JCL		JCL
FT06F001	system messages	FT06F001	system messages
FT08F001	(1) output of editted input data (2) output of steady state calculation (3) output of transient calculation	FT08F001	(1) output of editted input data (2) output of transient calculation
FT20F001	output of input data	FT20F001	output of input data

Fig. 9–1–1 Format of Output Listing.

****ERROR	0	3 2000	TRSGC	AT	2	1.000D–4	RETURN CODE ERROR
****ERROR	1	3 3355	SGHTRC	AT	2	1.000D–4	ABNORMAL RETURN AT (CALL PHASE)
	numbers set in THYDE–P program		name of module where error occured		time step	time step width	error description

Fig. 9–1–2 Error Message.

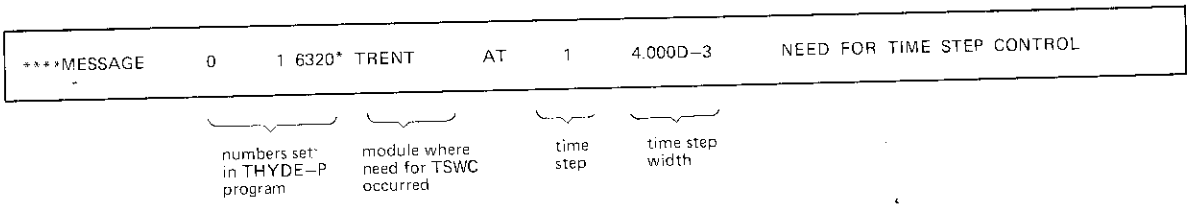

Fig. 9–1–3 Message of Time Step Width Control.

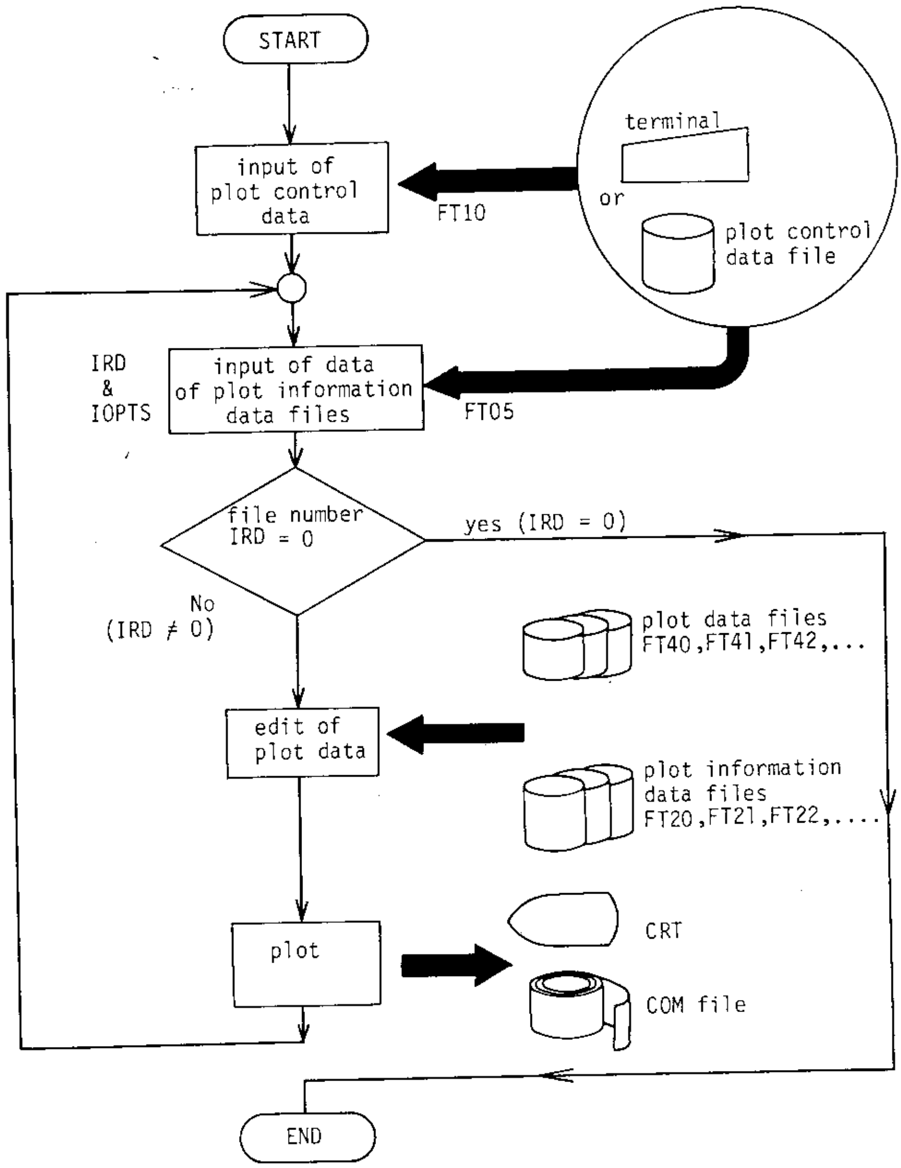

Fig. 9–2–1 Relationship between THYDE–P2 Execution and Plot Data.

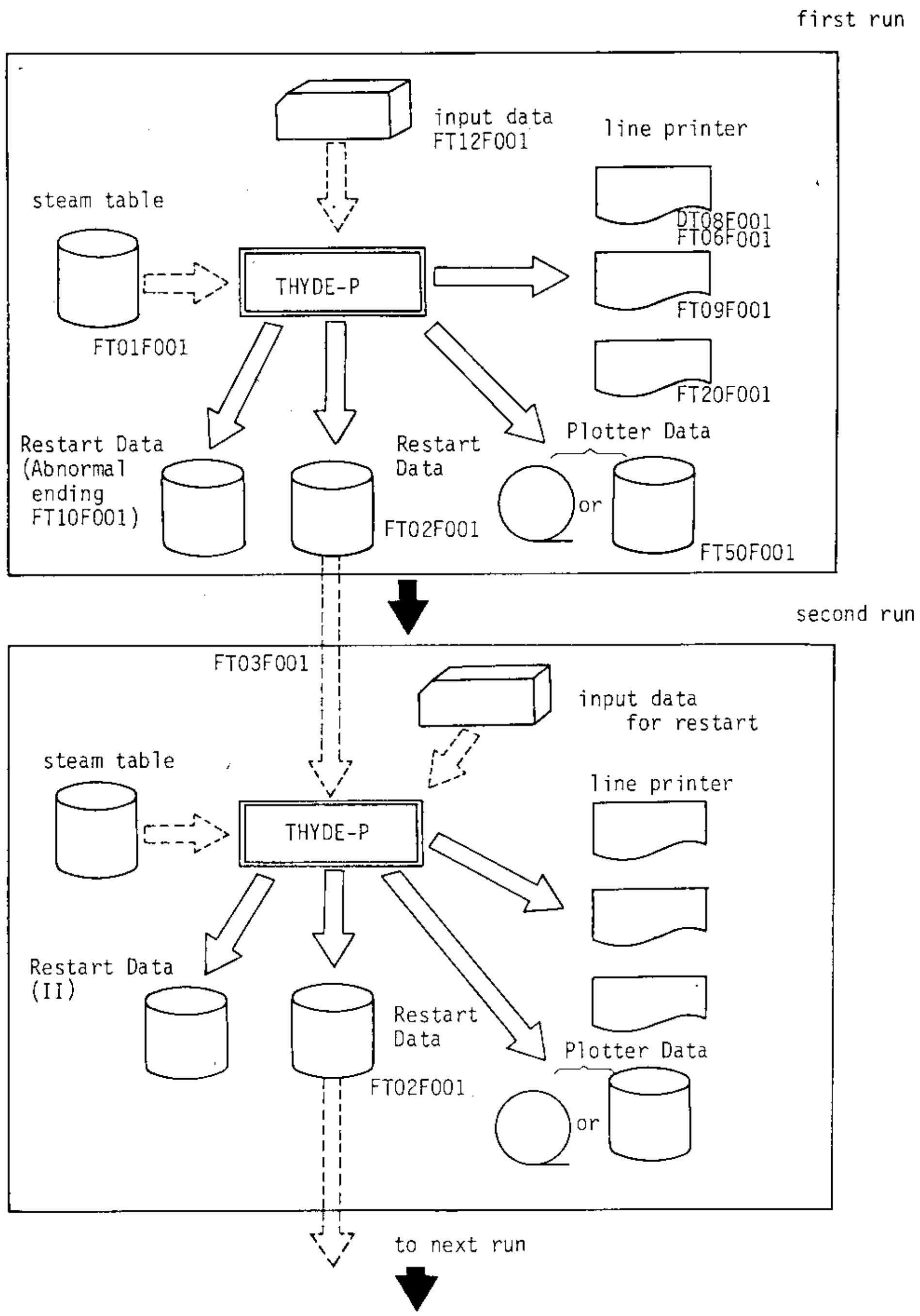

Fig. 9–2–2 Flow Chart of Plotting System (Sample Problem).

9.2.1 Plot Control Data (to be inputted by FORTRAN Unit 10)

1-A	KTITLE	Title to be printed on top of each figure
2-(A, I)	(FEND, IXTIN)	
	FEND	Number of plot data sets (1≤ FEND)
	IXTIN	Flag for editting plot data sets 0 = When time spans of two data sets overlap, the data set for the earlier period overrides the other. 1 = For each data set, the data in the period specified by additional

		inputs as indicated next are used.
2a-(R,R)	(TIM1, TIM2)	Not required for IXTIN=0. FEND pairs should be inputted. For each data set, the data in the period (TIM1, TIM2) are used.
3-(R,R)	(TIMES,TIMEE)	
	TIMES	The smallest time of the abscissa(sec)
	TIMEE	The largest time of the abscissa (sec)
4-I	IFLAG5	Flag for setting origin and scale Not required for COM film outputting. 0 = use default values (see Appendix C) origin of abscissa = 0 for TYPE = 1 origin of ordinate = 0 for TYPE = 1 scale = 0.8 1 = origin of abscissa, origin of ordinate and scale should be inputted in order.

9.2.2 Data of Plot Information Data Sets (to be inputted by FORTRAN Unit 5)

1-(I, I)	(IRD, IOPTS)	
	IRD	Number of file unit which contains plot information data (20≦ IRD)
	IOPTS	Flag to classify plot information file 0 = use index to select the valuables to be plotted. 1 = mannual setting

9.2.3 Plot Information Data (to be inputted by FORTRAN Unit 20, 21, 22 etc.)

The data show what is to be plotted among the variables contained in the plot data sets. In the following, only the case when IOPTS = 0 will be described. In this case, only the same kinds of variables can be plotted. **Table 9–1** and **9–2** show examples of plot information data.

1-I	IPLNO	Number of curves to be plotted in the figure (1≦*IPLNO*≦ 20)
2-I	IAXTY	1 = give the minimum and maximum values of the oridnate. 0 = use default values for each variable. (see Appendix C)
2a - (R, R)	(YM1,YM2)	Give when IAXTY = 1. YM1 : Maximum value YM2 : Minimum value
3 - A	Title	Title of figure
4 - A	ITAX	Give within a single line IPLNO variables to be plotted with a blank between each pair. The variables must be represented by the symbols with an index as shown in Appendix C.

9.2.4 Output to Cathod Ray Tube (T4014 or T4006)

Graphic display output of THYDE-P2 results can be made by source file TXPLOT. FORT. In the following, the method to use command procedure TXPLOT (see **Table 9–3**) will be described.

Before TXPLOT is actuated, plot data sets FT40F001, FT41F001, ... and plot information data sets FT20F001, FT21F001, ... have to be allocated. When TXPLOT is actuated, FT05F001, and F10F001 are automatically allocated to the graphic display terminal. The former is to be used to give the data of the plot information data sets, while the latter the plot control data.

Table 9–1 Example of Plot Information Data (a)

```
0005  4  0
0010  PRESSURE BESIDE INJECTION-1
0020  PRE-37 PRA-37 PRA-22 PRE-21
0030  4  0
0040  FLOW BESIDE INJECTION-1
0050  GLE-37 GLA-37 GLA-22 GLE-21
0060  4  0
0070  ENTHALPY BESIDE INJECTION-1
0080  HLE-37 HLA-37 HLA-22 HLE-21
0090  4  0
0100  QUALITY BESIDE INJECTION-1
0110  XLE-37 ELA-37 XLA-22 XLE-21
0120  0  0
```

Numbers 4 and 0 in line 5 show that IPLNO and IAXTY are 4 and 0, respectively. Numbers 0 and 0 in line 120 indicate END of DATA.

Table 9–2 Example of Plot Information Data (b)

```
00010  2  0
00020  SG PRESSURE
00030  PSG-01  PSG-02
00040  2  0
00050  SG FEED WATER FLOW
00060  MUG-01  MUG-02
00070  3  0
00080  HTR AT SG-1 2NDARY SIDE
00090  HT2-11 HT-2-12 HT2-13
00100  3  0
00110  HTR AT SG-1 PRIMARY SIDE
00120  HT1-11 HT1-12 HT1-13
00130  3  1
00131  5.0E4
00140  HEAT FLOW FROM SG-1
00150  QQQ-05 QQQ-06 QQQ-07
00160  0  0
```

Number 1 in line 130 shows that the maximum and minimum values of the ordinate are to be given. Line 131 shows that they are 5×10^4 and -5×10^4, respectively.

Table 9–3 Command Procedure TXPLOT

```
00010  PROC 0
00020  CONTROL NOMSG FLUSH
00030  WRITE **** ENTER THYDEP PLOTTING SYSTEM (& SYSDATE & SYSTIME) ****
00040  DELETE TEMP.OBJ
00050  FREE F(FT10F001)
00060  FREE F(FT06F001)
00070  FREE F(FT05F001)
00080  FREE AT(TY)
00220  LIB 'SYS9.PTS.LOAD'
00230  ATTR TY BLKSIZE(144) RECFM(UA)
00370  FREE AT(F10)
00380  ATTR F10 BLKSIZE(80) LRECL(80) RECFM(F)
00390  ALLOC DA(*) F(FT10F001) USING(F10)
00400  ALLOC DA(*) F(FT85F001)
00410  ALLOC DA(*) F(FT06F001) USING(TY)
```

```
ALLOC DA(*) F(FT05F001)
ALLOC DA(TEMP.OBJ) F(SYSLIN) NEW
FORTHE TXPLOT.FORT TERM NOPRINT OBJ(TEMP.OBJ) ELM(*) BYNAME
WRITE **** END OF FORTRAN COND CODE=&LASTCC ****
WRITE **** ENTER LOADGO PROCESS ****
LOADGO (TEMP.OBJ) LIB('SYS9.PTS.LOAD') FORTLIB NOLIBDD SIZE(512K)
DELETE TEMP.OBJ
FREE F(FT10F001)
 WRITE **** END OF PLOTTING SYSTEM (& SYSDATE & SYSTIME) ****
 EXIT
```

In this command procedure, FT05F001, FT06F001 and FT10 are allocated for the terminal.

10. Sample Problem : PWR LB-LOCA

We will present the THYDE-P2 result calculated for LB-LOCA of a typical 4-loop 1,000 MWe PWR. The main assumptions for the calculation include;

(1) BE calculation
(2) a double-ended guillotine break at the cold leg
(3) through calculation to the end of reflooding
(4) two (hot and average) channel representation for the core with a single cross flow
(5) discharge coefficient 0.6
(6) locked rotor of the centrifugal pumps
(7) ECC water enthalpy of 35 kcal/kg
(8) the same heat transfer correlations in reflooding as in blowdown, and
(9) the time constant in the relaxation equation for void fraction was calculated according to the method described in subsection 2.2.3.

As shown in **Fig. 10–1–1**, the primary system is represented by the two loops, the one for the intact 3 loops and the other for the broken loop. The primary system except the pressurizer and the accumulators is nodalized into 46 nodes and 43 junctions with 2 hydraulic sources, 24 heat conductors and 5 valves. For the pressurizer and the SG secondary systems, the tank model is applied.

Note that the expressions like "at *T* sec" in this chapter mean "at *T* sec after the initiation of LOCA". The transient is assumed to start at 0.002 sec when the guillotine break takes place in the cold leg. The main pumps are assumed to be locked at 0.1 sec. The SG feedwaters are assumed to stop at 0.4 sec. The pumped injections (PIs) are assumed to start at 20.01 sec.

The calculation was made until 70 sec when all the fuel nodes had been completely quenched. It is interesting to note that the present calculation yielded practically the same tendency as LOFT L2-3[53]. It is also interesting to compare these results with the THYDE-P1 EM result[48].

The CPU time required for the calculation with a FACOM VP100 computer was about 13 minutes 45 seconds. The required core memory was 2,436 KB.

10.1 Description of Input Data

The input data used in the present calculation are listed in Appendices D.1 and D.2. The one shown in Appendix D.1 is for the first calculation starting from the initial steady state and the other shown in Appendix D.2 for restarting from a restarting dump point of the previous run. In this section, we will give only the main input data for use in the present calculation.

10.1.1 Nodalization

The nodalization scheme in the present calculation is shown in **Fig. 10–1–1**. The geometrical data of nodes are shown in **Table 10–1**.

Broken loop	Nodes	1 to 12
Intact loop	Nodes	13 to 22
Downcomer	Node	23

Lower plenum	Node	24
Average core channel	Nodes	25 to 29
Hot core channel	Nodes	30 to 34
(Nodes 25, 29, 30 and 34 are non-heated.)		
Core crossflow	Node	35
Upper plenum	Node	36
Upper head	Node	37
Pressurizer surge line	Nodes	38 to 42
PI duct	Nodes	43 and 45
Accumulator duct	Nodes	44 and 46
Pressurizer	Node	49
S.G. secondary systems	Nodes	47 and 48
Accumulator	Nodes	50 and 51

10.1.2 Initial Thermal-Hydraulic State

The data for steady state adjustment for the primary system are

$(G_A, h_A) = (9{,}000 \text{ kg/m}^2/\text{s}, \ 360 \text{ kcal/kg})$ for node 1.

The branching ratios at the mixing junctions are shown in BB12 in Appendix D.1. The loss coefficients shown in **Table 10–2** are determined according to the method described in section 5.3.3.

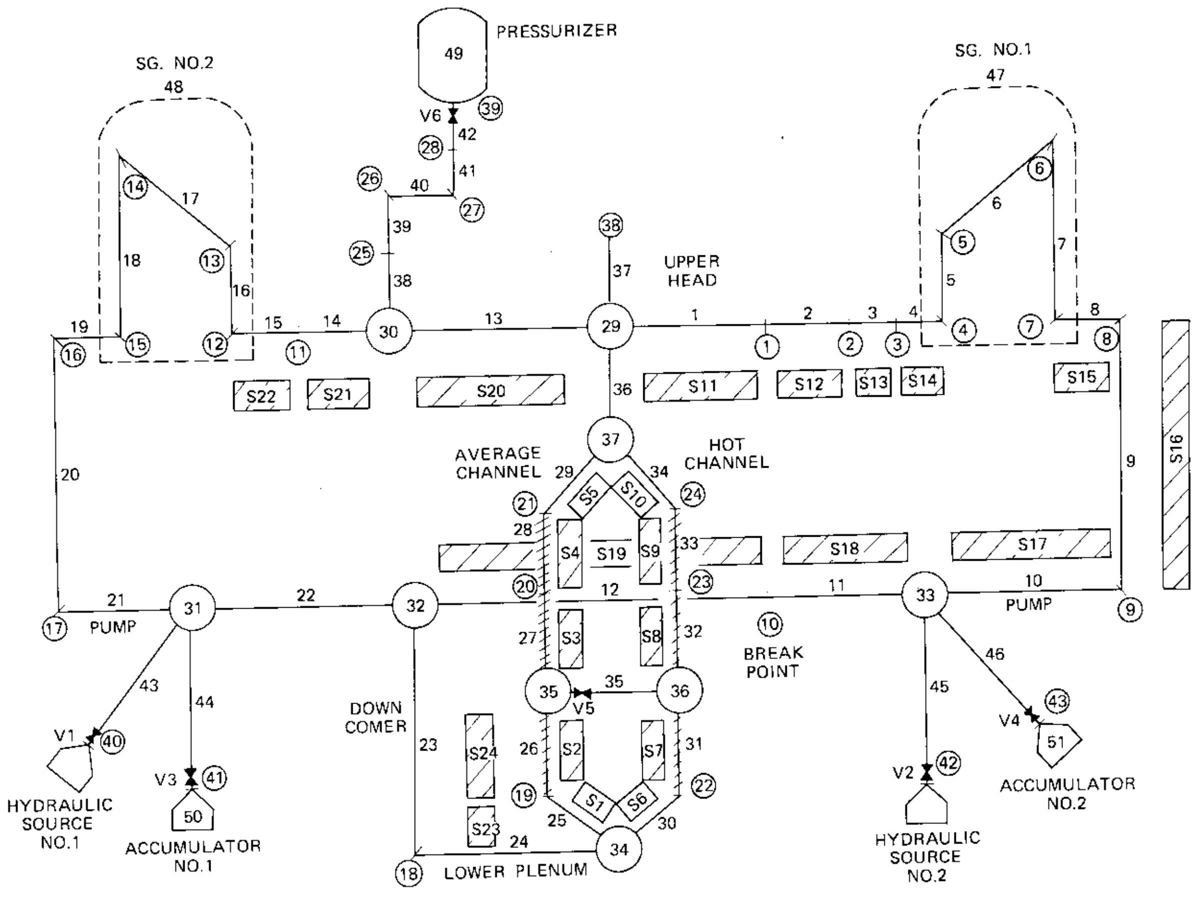

Fig. 10–1–1 Nodalization of 1,000 MWe PWR (Sample Problem).

Table 10–1 Geometrical Data of Nodes

Node No.	Description	Flow area A (m^2)	Node length L (m)	Node volume V (m^3)
1	Broken loop hot leg	0.43	5.2	2.235
2	Broken loop hot leg	0.69	1.0	0.694
3	Broken loop hot leg	1.00	1.5	1.5
4	SG inlet plenum	1.31	2.0	2.61
5	SG U-tube	3.14×10^{-4}	5.0	1.57×10^{-3}
6	SG U-tube	3.14×10^{-4}	6.8	2.14×10^{-3}
7	SG U-tube	3.14×10^{-4}	11.8	3.71×10^{-3}
8	SG outlet plenum	1.31	1.6	2.09
9	Broken loop crossover leg	0.50	12.9	6.48
10	Pump	0.38	6.6	2.54
11	Broken loop cold leg	0.38	1.5	0.58
12	Broken loop cold leg	0.38	3.0	1.15
13	Intact loop hot leg	0.43	2.0	0.86
14	Intact loop hot leg	0.43	3.2	1.38
15	SG inlet plenum	1.31	4.5	5.88
16	SG U-tube	3.14×10^{-4}	5.0	1.57×10^{-3}
17	SG U-tube	3.14×10^{-4}	6.8	2.14×10^{-3}
18	SG U-tube	3.14×10^{-4}	11.8	3.71×10^{-3}
19	SG outlet plenum	1.31	1.6	2.09
20	Intact loop crossover leg	0.5	12.9	6.48
21	Pump	0.38	6.6	2.54
22	Intact loop cold leg	0.38	4.5	1.73
23	Downcomer	2.75	8.0	21.97
24	Lower plenum	4.83	5.0	24.15
25	Core (average channel)	1.11×10^{-4}	0.3	3.34×10^{-5}
26	Core (average channel)	1.11×10^{-4}	1.0	1.11×10^{-4}
27	Core (average channel)	1.11×10^{-4}	1.0	1.11×10^{-4}
28	Core (average channel)	1.11×10^{-4}	1.0	1.11×10^{-4}
29	Core (average channel)	1.11×10^{-4}	0.3	3.34×10^{-5}
30	Core (hot channel)	1.11×10^{-4}	0.3	3.34×10^{-5}
31	Core (hot channel)	1.11×10^{-4}	1.0	1.11×10^{-4}
32	Core (hot channel)	1.11×10^{-4}	1.0	1.11×10^{-4}
33	Core (hot channel)	1.11×10^{-4}	1.0	1.11×10^{-4}
34	Core (hot channel)	1.11×10^{-4}	0.3	3.34×10^{-5}
35	Core cross flow	9.08×10^{-4}	0.1	9.08×10^{-5}
36	Upper plenum	9.40	1.3	12.22
37	Upper head	8.85	2.0	17.70
38	Pressurizer surge line	0.20	6.0	1.18
39	Pressurizer surge line	0.20	6.0	1.18
40	Pressurizer surge line	0.20	6.0	1.18
41	Pressurizer surge line	0.20	6.0	1.18
42	Pressurizer surge line	0.20	6.0	1.18
43	PI duct	0.071	0.1	7.1×10^{-3}
44	Accumulator duct	0.039	0.42	1.6×10^{-2}
45	PI duct	0.071	0.1	7.1×10^{-3}
46	Accumulator duct	0.039	0.42	1.6×10^{-2}

Table 10–2 Loss Coefficients of Nodes

Node No.	k	k_A^f	k_A^r	k_E^f	k_E^r
1	0.152	0.0	0.0	0.146	0.171
2	0.080	0.0	0.0	0.095	0.139
3	0.084	0.0	0.0	0.054	0.105
4	0.076	0.0	0.0	0.0	0.0
5	1.57	0.099	0.048	0.0	0.0
6	2.53	0.0	0.0	0.0	0.0
7	0.33	0.0	0.0	0.048	0.099
8	0.42	0.0	0.0	0.0	0.0
9	3.41	0.277	0.379	0.0	0.0
10	0.32	0.105	0.055	0.0	100.
11	0.37	0.0	0.0	0.0	0.0
12	1.12	0.0	0.0	0.0	0.0
13	0.024	0.0	0.0	0.0	0.0
14	0.367	0.0	0.0	0.0	0.0
15	0.069	0.0	0.0	0.0	0.0
16	1.57	0.099	0.048	0.0	0.0
17	2.53	0.0	0.0	0.0	0.0
18	0.332	0.0	0.0	0.048	0.099
19	0.42	0.0	0.0	0.0	0.0
20	3.41	0.277	0.379	0.0	0.0
21	0.32	0.105	0.055	0.0	100.
22	1.49	0.0	0.0	0.0	0.0
23	5.82	0.0	0.0	0.0	0.0
24	4.63	0.0	0.0	0.0	0.0
25	1.09	0.0	0.0	0.0	0.0
26	1.11	0.0	0.0	0.0	0.0
27	0.996	0.0	0.0	0.0	0.0
28	0.437	0.0	0.0	0.0	0.0
29	3.61	0.0	0.0	0.0	0.0
30	1.09	0.0	0.0	0.0	0.0
31	1.09	0.0	0.0	0.0	0.0
32	0.95	0.0	0.0	0.0	0.0
33	0.39	0.0	0.0	0.0	0.0
34	3.52	0.0	0.0	0.0	0.0
35	8.73	5.0	5.0	5.0	5.0
36	2.94	0.0	0.0	0.0	0.0
37	5.0	10.	10.0	0.0	0.0
38	5.0	1.0	1.0	0.0	0.0
39	5.0	0.0	0.0	0.0	0.0
40	5.0	0.0	0.0	0.0	0.0
41	5.0	0.0	0.0	0.0	0.0
42	5.0	0.0	0.0	0.0	0.0
43	10.0	1.	0.0	0.0	0.0
44	10.0	1.	0.0	0.0	0.0
45	10.0	1.	0.0	0.0	0.0
46	10.0	1.	0.0	0.0	0.0

10.1.3 Break Data

The double-end guillotine break was assumed to occur at junction 10 at 0.002 sec after the calculation started.

10.1.4 SG 2ndry System Data

The initial heat fluxes through the U-tube were determined by the steady state adjustment at shown in **Table 10–3**.

The feed water was assumed to be cut off at 0.4 sec. The other data are as follows:

U-tube pitch	3.0×10^{-2} m
Number of U-tube of one unit	3,248
Initial secondary system pressure	62 atm
Initial specific enthalpy of feed water	222 kcal/kg
Initial mass flow rate of feed water	474.5 kg/sec
Initial subcooled water level	4.0 m
Initial void fraction of saturated region	0.95

Table 10–3 Initial Heat Flux of SGs

Node No.	Heat flux ($kcal/m^2/sec$)
5 and 16	77.52
6 and 17	50.55
7 and 18	25.28

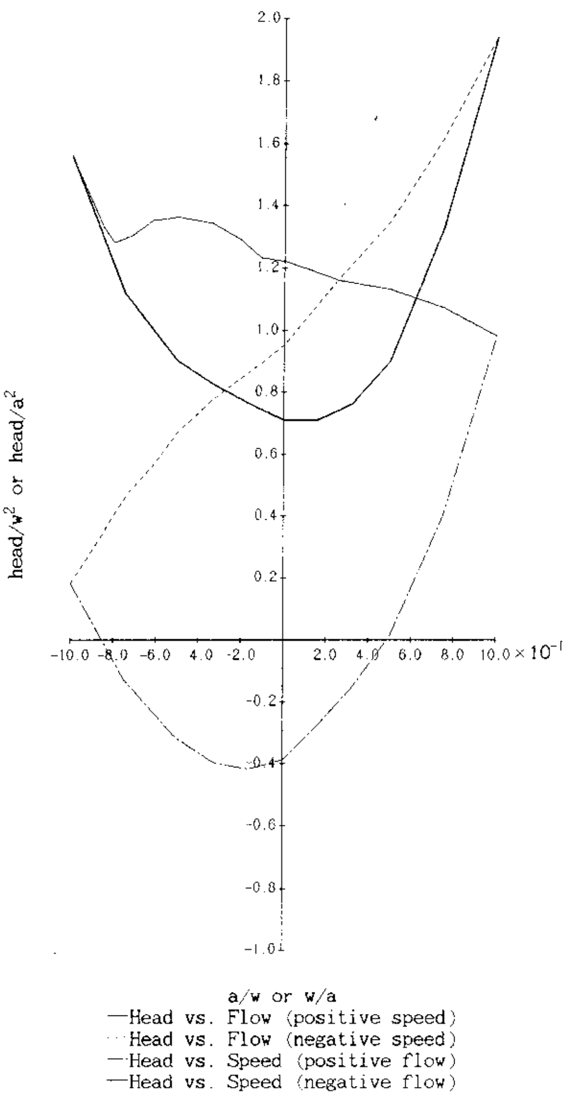

Fig. 10–1–2 Single-phase Homologous Head Curves (Sample Problem).

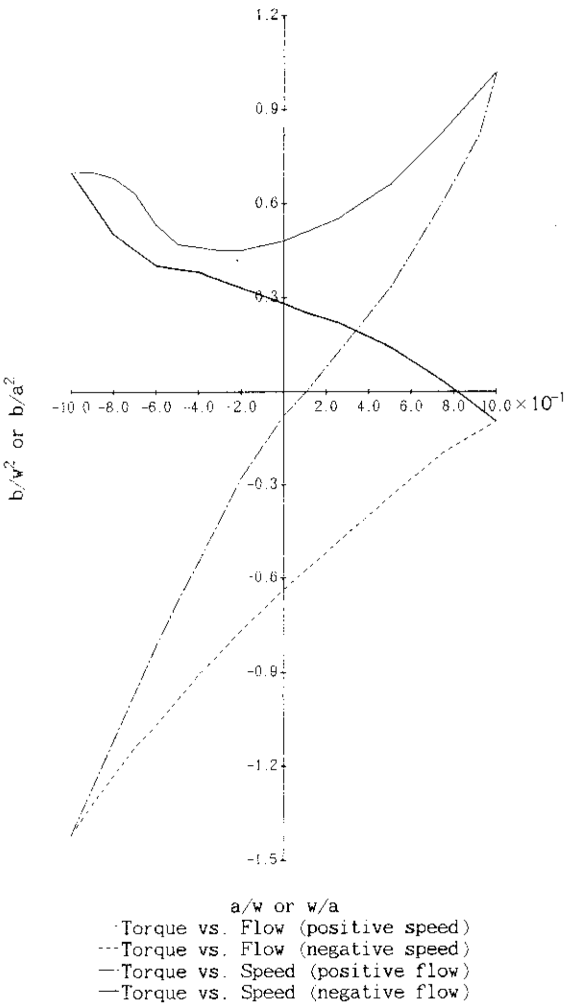

Fig. 10–1–3 Single-phase Homologous Torque Curves (Sample Problem).

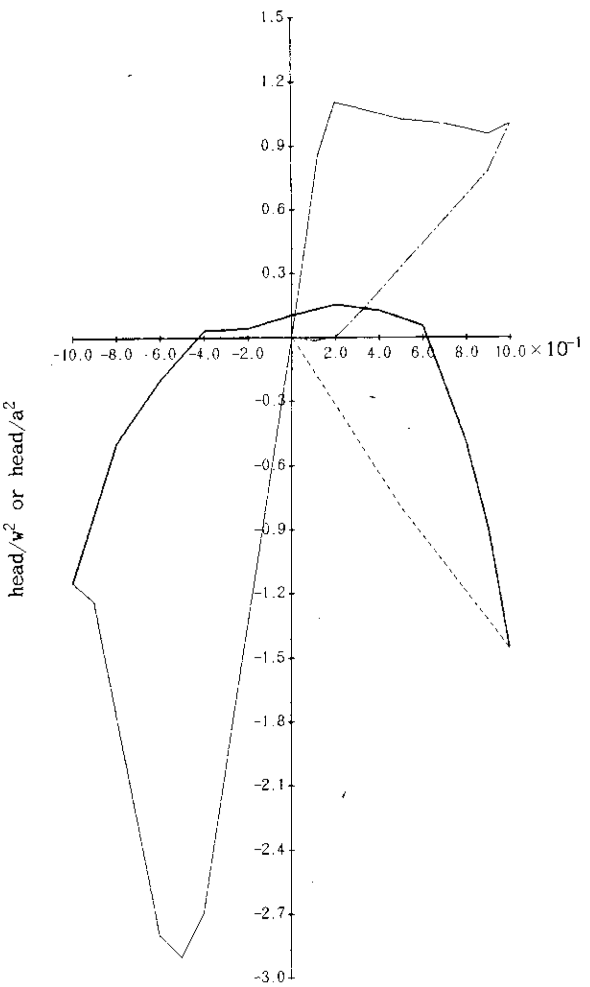

Fig. 10–1–4 Head Difference Homologous Curves (Sample Problem).

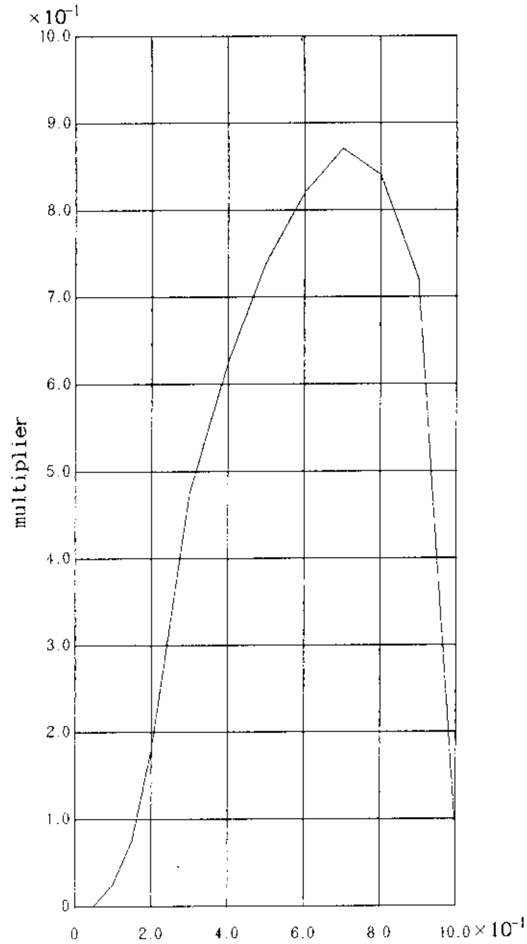

Fig. 10–1–5 Head Multiplier Curve (Sample Problem).

10.1.5 Pump Data

The data of the single-phase head and torque homologous curves are shown in **Figs. 10–1–2** and **10–1–3**, respectively. And the head difference homologous curves are shown in **Fig. 10–1–4**. The head and torque multipliers as functions of void fraction are shown in **Fig. 10–1–5**.

The other pump data are as follows:

Rated speed	1,185	(rpm)
Initial speed	1,150	(rpm)
Rated flow	5.583	(m^3/sec)
Rated torque	43,250	(J/rad)
Rated head	10.50	(m)
Rated density	749.0	(kg/m^3)
Moment of inertia	3,460	(kgm^2/rad^2)

10.1.6 Core Data

The core was divided radially into two regions, i.e. one collection of "average" channels and the other of "hot" channels. The radial peaking factor of the hot one was assumed to be 1.30.

Table 10–4 Initial Heat Flux in Core

	average channel region		hot channel region	
	node no.	heat flux (kcal/m^2/sec)	node no.	heat flux (kcal/m^2/sec)
initial heat flux	25	non-heated	30	non-heated
	26	156.0	31	221.7
	27	234.0	32	385.1
	28	234.0	33	221.7
	29	non-heated	34	non-heated
number of rods	39,800		200	

The other core data are:

Reactor thermal power	3,479 MWt
Fuel length	3.66 m
Plenum gas volume	1.235×10^{-5} m^3
Clad outer diameter	1.0732×10^{-2} m
Clad thickness	6.187×10^{-4} m
Pellet diameter	9.3146×10^{-3} m
Fuel rod pitch	1.42×10^{-2} m

where the last four values are those at a full power operating condition.

10.1.7 Pressurizer Data

The pressurizer data are:

Cross sectional area	3.58 m^2
Height	15.56 m
Stand pipe length	0.1 m
Initial subcooled water level	9.0 m
Initial void fraction of saturated region	0.99

The stand pipe is the part of the pressurizer surge line which is sticking out into the pressurizer tank.

10.1.8 ECCS Data

The accumulator data are:

Initial water volume/unit	23.2 m^3
Initial nitrogen volume/unit	10.0 m^3
Specific enthalpy of water	35.0 kcal/kg
Initial pressure	44 atm

The pumped injection data are:

Specific enthalpy of water	35.0 kcal/kg
Mass flow rate of PI–1 and –2	700 kg/sec

10.1.9 Heat Conductor Data

The heat slab data are shown in **Table 10–5**.

Table 10–5 Geometrical Data of Heat Conductors

inner node	outer node	No. of slabs	shape	No. of region	length of slabs	inner radius (width)*	outer radius (thickness)*
1	0	1	Rect.	1	5.2	0.37	0.37
2	0	1	Cyl.	1	1.0	0.47	0.57
3	−1	1	Rect.	1	1.5	0.565	0.565
4	−1	1	Cyl.	1	2.0	0.645	0.775
8	−2	1	Rect.	1	1.6	0.645	0.645
9	−2	1	Cyl.	1	1.29	0.4	0.48
0	10	1	Rect.	1	6.6	0.35	0.35
0	11	1	Cyl.	1	1.5	0.35	0.43
−1	12	1	Rect.	1	3.0	0.35	0.35
−1	13	1	Cyl.	1	2.0	0.37	0.45
−2	14	1	Rect.	1	3.2	0.37	0.37
−2	15	1	Cyl.	1	4.5	0.645	0.775
25	23	1	Rect.	1	0.3	0.119	0.119
26	23	1	Cyl.	1	1.0	1.19	1.29

(   )* is for rectangular shape.
Node No. = 0 ; adiabatic boundary
Node No. = −1 ; radiative boundary
Node No. = −2 ; constant temperature boundary

Table 10–6 Chronology of Events

Time (sec)	Events
0.002	Break took place and pumps were tripped off, and reactor scrammed.
0.1	Rotors of main pumps were locked.
0.15	Voiding started at center of hot channel.
0.30	Voiding started at center of average channel.
0.4	SG feed water was tripped off.
0.68	Voiding started at intact loop hot leg.
1.69	Voiding started at lower plenum.
2.9	Voiding started at downcomer.
7.7	ACC injection started in broken loop.
15.5	Pressurizer emptied.
17.4	ACC injection started in intact loop.
20.8	ECC water filled up cold leg.
20.01	Pumped injections were tripped on.
31.0	End of blowdown.
36.4	Subcooled water started to penetrate downcomer (EOBP).
39.6	Subcooled water started to penetrate lower plenum.
47.1	Core bottom became subcooled (BOCREC).
56.7	Center of average rod quenched.
58.9	Acc injection ended in broken loop.
64.5	Upper plenum inlet was reflooded.
65.2	Center of hot rod quenched.
65.3	Acc injection ended in intact loop.

10.1.10 Container Pressure

No particular model for the container was provided except the temporal behavior of the container pressure which was a function of time, i.e.;

Time (sec)	0.0	7.5	15.0	30.0	1000.0
Pressure (atm)	1.0	2.7	4.0	4.0	4.0

10.1.11 Maximum Time Step Width Used in the Present Calculation

The maximum time step width allowed in the present calculation was given by the inputs as follows;

$$\Delta t_{max} = 0.001 \text{ sec} \quad \text{for} \quad t < 0.004 \text{ sec}$$

$$= 0.064 \text{ sec} \quad \text{for} \quad 0.004 < t$$

10.2 Calculated Results and Discussions

The chronology of events is summarized in **Table 7–6**. The detailed discussions about the events will be made in the following subsections.

10.2.1 Nuclear Power

As shown in **Fig. 10–1–6**, the nuclear power suddenly dropped to the level of the decay heat due to the scram. It is important to note that the decay heat level is sufficiently low so that the calculation can give the clad surface rewetting from 10 sec to 30 sec during the blowdown and the fuel quenching at the end of reflooding (see Figures in subsection 10.2.9).

10.2.2 Pressure

The calculated pressure transients are shown in **Figs. 10–1–7** and **10–1–8**. The system pressure shown in **Fig. 10–1–7** decreased very quickly from 1.61×10^7 Pa. (initial pressure) to 1.27×10^7 Pa. in 0.63 sec. Then, choking at the break points as well as in the pressurizer surge line and voiding at the core made the gradient smaller. By 5 sec both break flows became saturated (see next subsection), making the gradient even less. At 31.0 sec, the system pressure is almost equal to that of the containment (about 4×10^5 Pa.) (the end of blowdown).

The pressures in the primary system showed a very similar behavior except those of the pump-side break point and the pressurizer. The pressurizer pressure (see **Fig. 10–1–7**) showed a rather gradual transient because of choking in the surge line, until 15.5 sec, when the water level in the pressurizer reached the minimum level so that steam outsurge started. The pump-side break pressure (see **Fig. 10–1–8**) was substantially smaller during the blowdown, because the large break flow caused a large pressure drop across the pump.

It seems that choking in the pressurizer line as well as at the break has a large impact on the behavior of the system pressure.

10.2.3 Break Flow

The break flow rates and their qualities are shown in **Figs. 10–1–9** to **10–1–11**. Note that as the negative flow means discharging at the core side of the break, so does the positive flow at the pump side.

At the core side of the break, the discharge flow was large until 4 sec, because it was a single phase flow. And after that, the two-phase critical flow made the gradient less. The quality was large because of decompression boiling until 20 sec when it suddenly decreased due to the effect of the ACC(accumulator)-1 injection, which had begun at 17.4 sec. Moreover, the ACC-1 injection stopped the decreasing tendency of the break flow. The PI-1, which was started at 25.01 sec, helped the break flow to clear the threshold of zero quality and to become subcooled at 31 sec. As refill evolved, rapid condensation took place in the downcomer and the lower plenum, resulting in the big inflow and thereby the increase of the quality at the break. The inflow is determined by the boundary condition at the break (see section 2.2.6), i.e. pressure $p_B(t)$ and specific enthalpy $h_B(t)$ at the break. In the present calculation, p_B is given as shown in data block BB17 in Appendix D, while h_B is assumed equal to that of two-phase mixture with mass quality 0.1 at the container pressure. The thermal-hydraulic conditions of the inflow are determined solely by p_B and h_B. It is assumed that air is not contained in the inflow.

At the pump side of the break, a similar behavior was observed, but no subcooled critical flow was calculated to occur. The decompression was so rapid that voiding at the pump side break began at 1.5 sec. The quality began to decrease when the ACC-2 injection started at 7.7 sec. The PI-2, which was started at 25.01 sec, helped the break flow to clear the threshold of zero quality and to become subcooled at 30 sec.

10.2.4 Core Flow

As shown in **Figs. 10–1–12** and **10–1–13**, the core flow in the hot channel and in the average channel showed quite a similar behavior. That is, at first, just after the rupture, a reverse flow occurred and continued until 40 sec. At 47.1 sec, the coolant at the core bottom became subcooled (BOCREC) and the reflooding started. The negative core flow partly supplied the core-side break flow.

10.2.5 Intact Loop Flow

As shown in **Fig. 10–1–14**, the hot leg inlet flow had almost the same tendency as the core and downcomer flows. The pump outlet flow and its quality are shown in **Figs. 10–1–15** and **10–1–16**, respectively. The condensation in the pump due to the ACC-1 injection gave rise to the sudden decrease of the pump outlet quality at 33 sec and the negative pump outlet flow from 34 to 46 sec. The cold leg outlet flow is shown in **Fig. 10–1–17**. The difference between **Figs. 10–1–15** and **10–1–17** can be accounted for by the ACC-1 injection.

10.2.6 Broken Loop Flow

The mass flux and quality of the pump outlet flow are shown in **Figs. 10–1–18** and **10–1–19**, respectively. The sudden decrease of pump outlet quality at 44 sec were caused by the ACC-2 injection. The difference between the pump outlet flow and the pump-side break flow (see **Fig. 10–1–9**) results from the ACC-2 injection.

As shown in **Fig. 10–1–20**, the hot leg inlet flow was forward practically at any time. Its behavior, however, could be much influenced by the size of mixing junction 29. At junction 29, the flow coming from the intact loop hot leg is branching off in the two directions, i.e., to the core and to the broken loop hot leg. The negative core flow eventually goes to the core-side break point after merging the flow from the intact loop cold leg flow. The transient branching ratio could be very dependent on the size of mixing junction 29. Therefore, it could be a topic of the sensitivity study.

10.2.7 ECC Behavior

The ACC behaviors are shown in **Figs. 10–1–21** and **10–1–22**. The ACC injections started at 7.7 and 17.4 sec and ended at 58.9 and 65.3 sec in the broken and intact loops, respectively, when the pressure of the boundary junction became under 40 atm. The PIs started at 25.01 sec at both loops by the trip conditions. ACC water stopped voiding at the cold leg and increased the break flow rate, and the PI water touched off coolant subcooling in both broken and intact loops.

10.2.8 Downcomer

Downcomer mass flux and quality are shown in **Figs. 10–1–23** and **10–1–24**, respectively. Due to the reverse flow in the downcomer and the core, the downcomer quality was large and even exceeded one untill the refill started at 36.4 sec. The condensation in the downcomer and the lower plenum with ECC water ingress was so large that its influence can be seen in almost all the Figures. After the end of condensation at 38.8 sec, the downcomer flow became subcooled and positive. And subcooled water kept on moving toward the core. This can be seen by looking over the figures for the core. For example, **Fig. 10–1–31** clearly shows that the reflooding started at 47.1 sec.

10.2.9 Fuel Temperature and HTC (heat transfer coefficient in Core)

The fuel center and clad surface temperatures are shown in **Figs. 10–1–25** to **10–1–30**. The coolant qualities in the core are shown in **Figs. 10–1–31** to **10–1–34**. The heat transfer coefficients at the clad surface in the hot channel are shown in **Figs. 10–1–35** to **10–1–37**. It should be noted that the calculated clad surface temperatures show the tendencies very similar to those of LOFT L2-3[52].

Looking over the calculated fuel temperatures shown in **Figs. 10–1–25** to **10–1–30**, we observe as follows. The temperature at the center of the fuel suddenly fell due to the scram. The cladding surface temperature rose quickly just after the rupture, because the decrease of the flow rate and the flashing at the core caused DNB (departure of nucleate boiling). After 30 sec, the core flow became stagnant and again DNB took place, followed by superheated steam cooling. Then, ECC water began to come into effect and the precursory cooling took place, evetually leading to quenching.

Figures 10–1–32 to **10–1–34** show the qualities at the outlet of the hot channel nodes 31, 32 and 33, respectively. Owing to the negative flow, the quality of node 31 is rather large from 10 to 20 sec as compared to those of nodes 32 and 33. As a result, the predicted heat transfer coefficient was not large enough to lead to rewetting at node 31. This can be seen by comparing the calculated heat transfer coefficients shown in **Figs. 10–1–35** to **10–1–37**. The situation is the same for node 26 in the average channel.

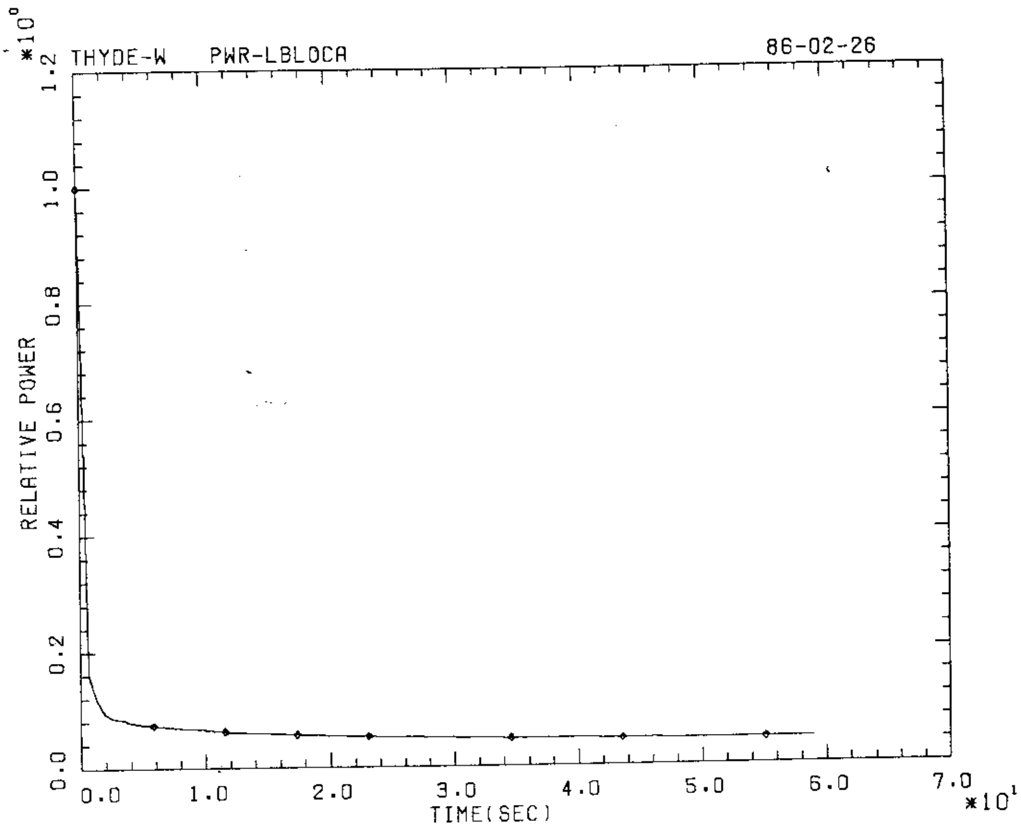

Fig. 10–1–6 Nuclear Power (Sample Problem).

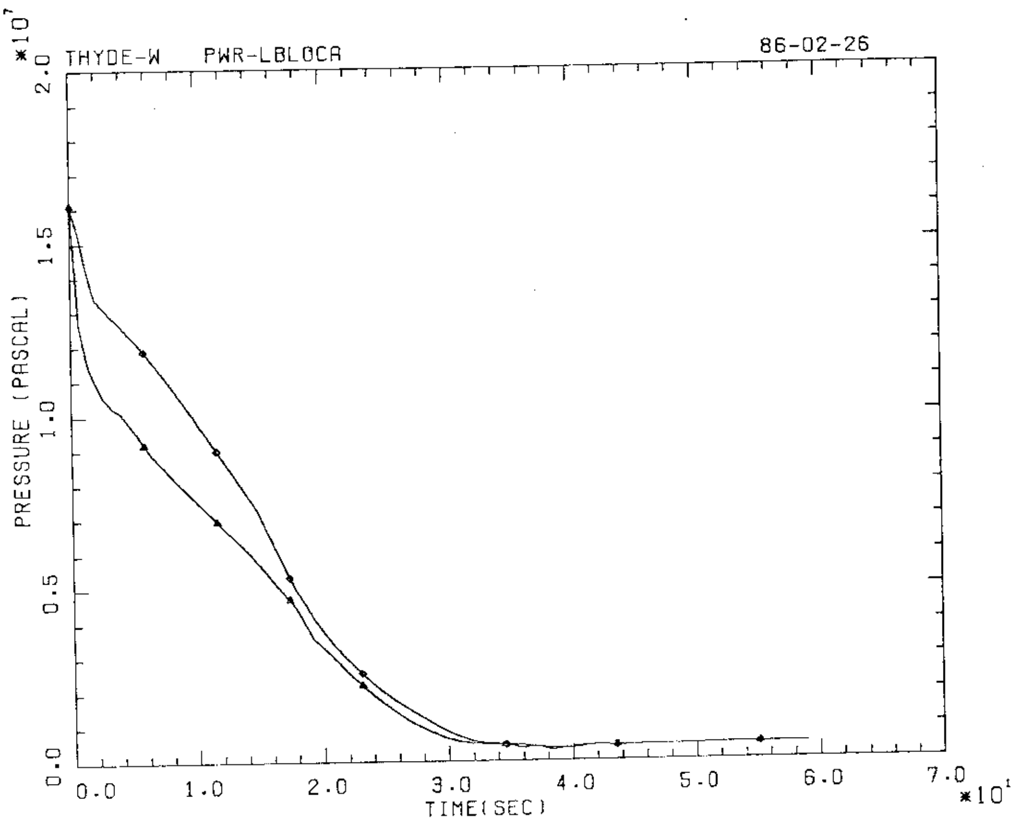

Fig. 10–1–7 Pressurizer and System Pressures (Sample Problem).

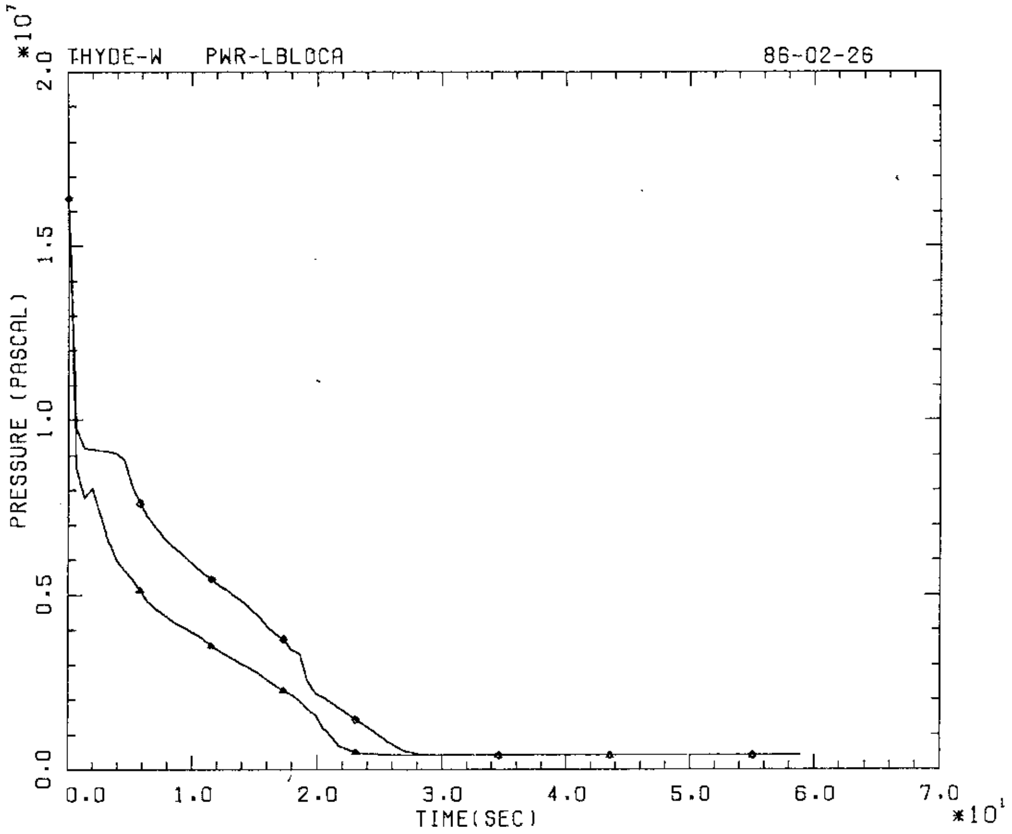

Fig. 10–1–8 Break Point Pressures (Sample Problem).

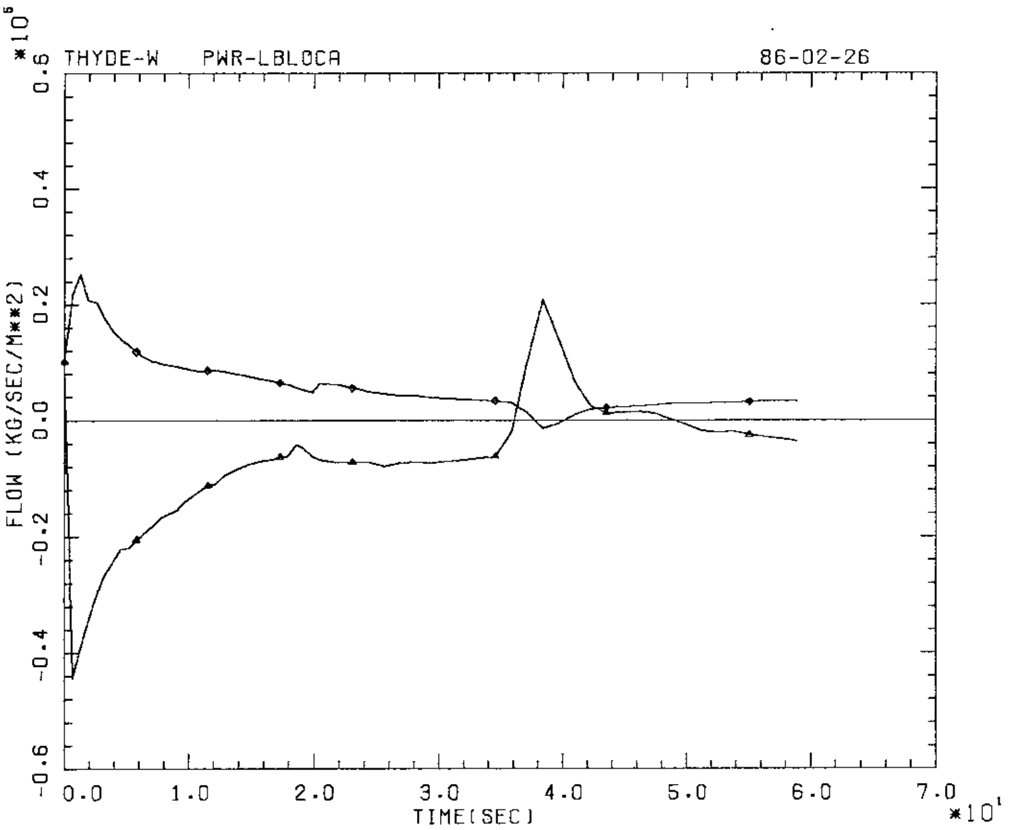

Fig. 10–1–9 Break Flows (Sample Problem).

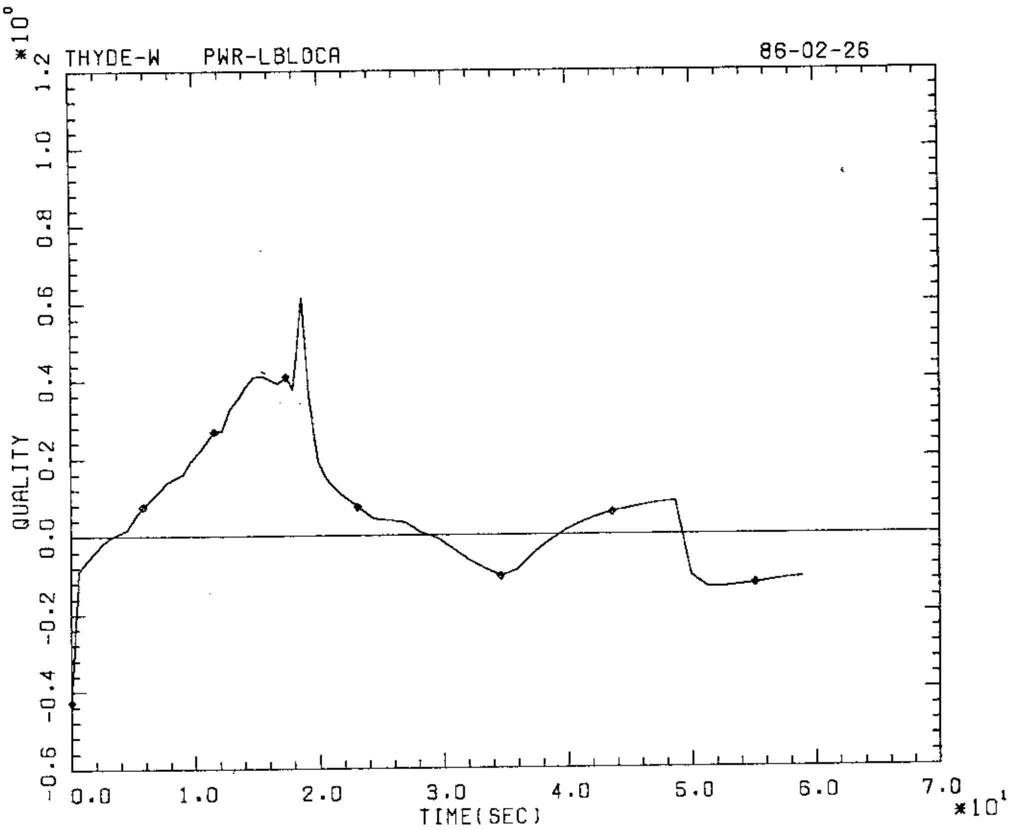

Fig. 10–1–10 Break Point Quality (Core Side) (Sample Problem).

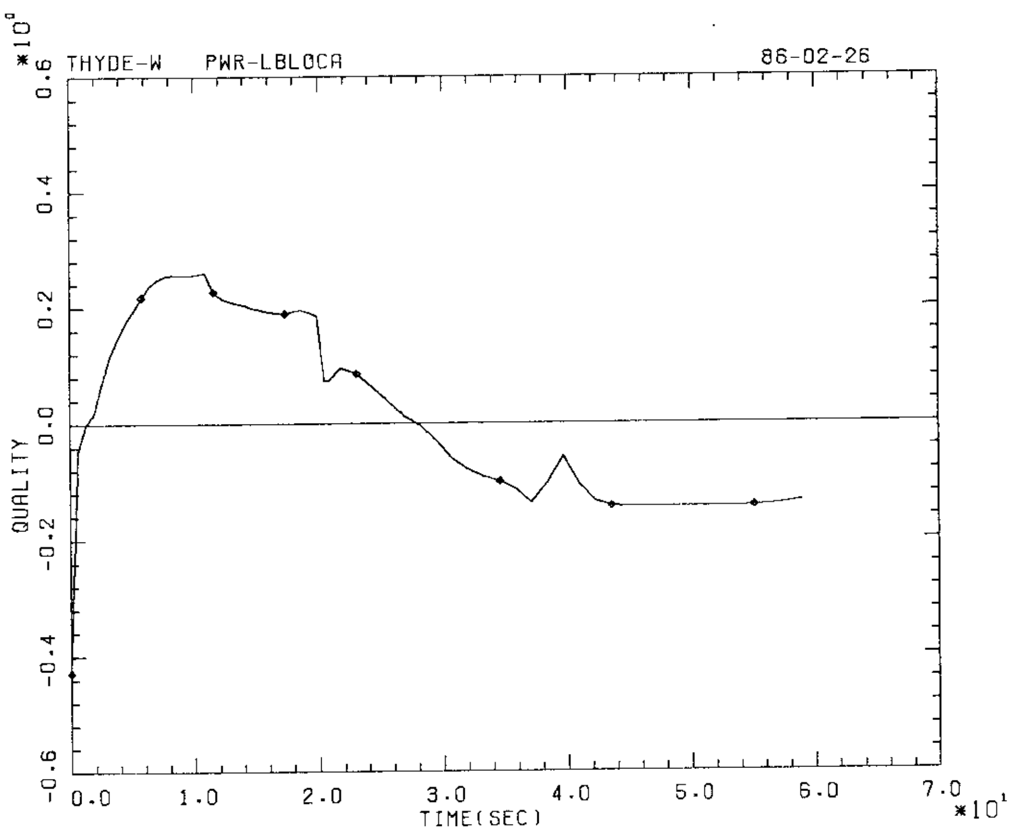

Fig. 10–1–11 Break Point Quality (Pump Side) (Sample Problem).

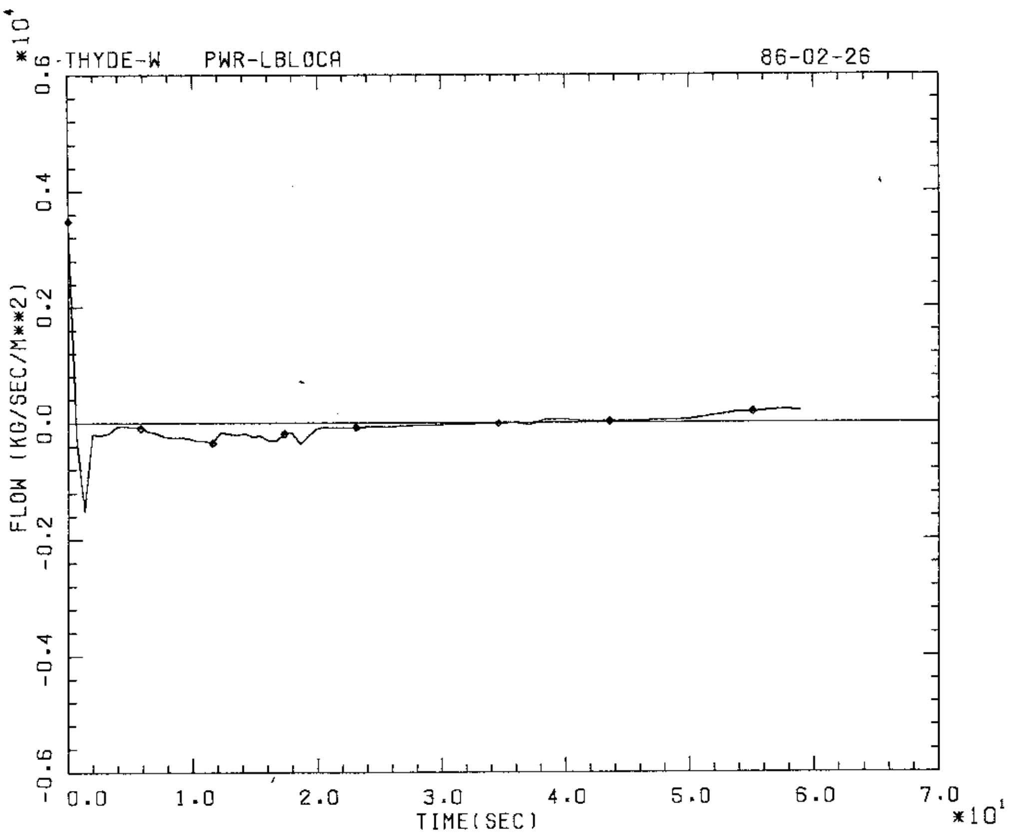

Fig. 10–1–12 Core Inlet Flow (Average Channel) (Sample Problem).

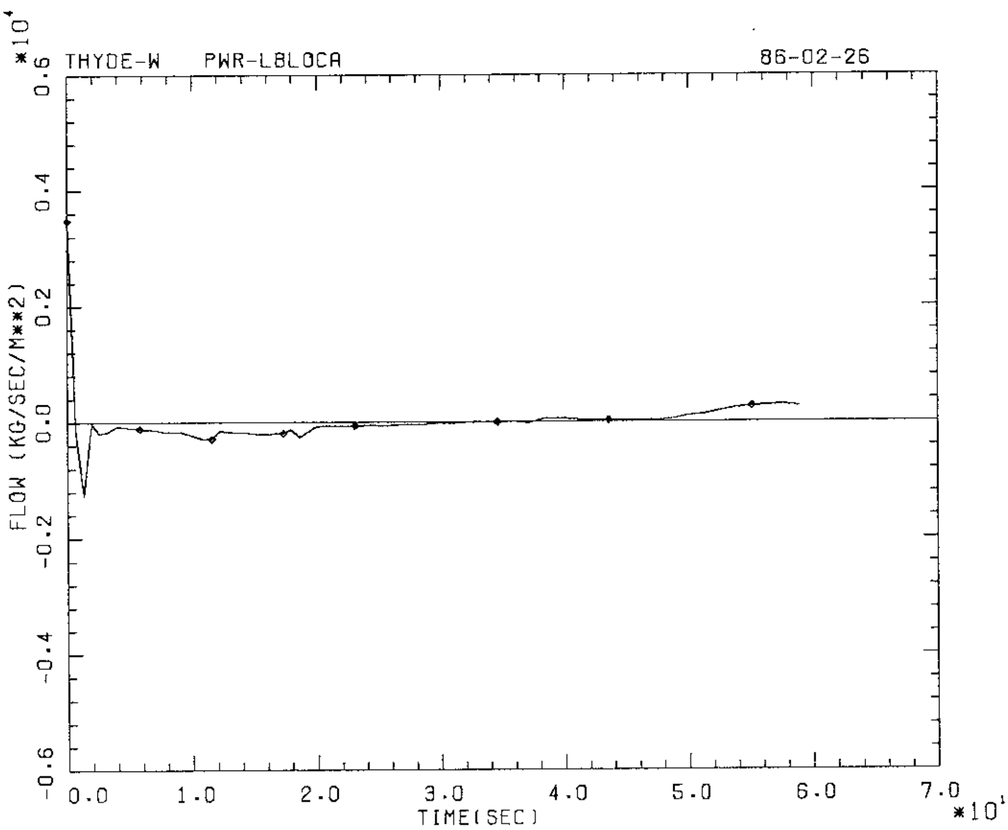

Fig. 10–1–13 Core Inlet Flow (Hot Channel) (Sample Problem).

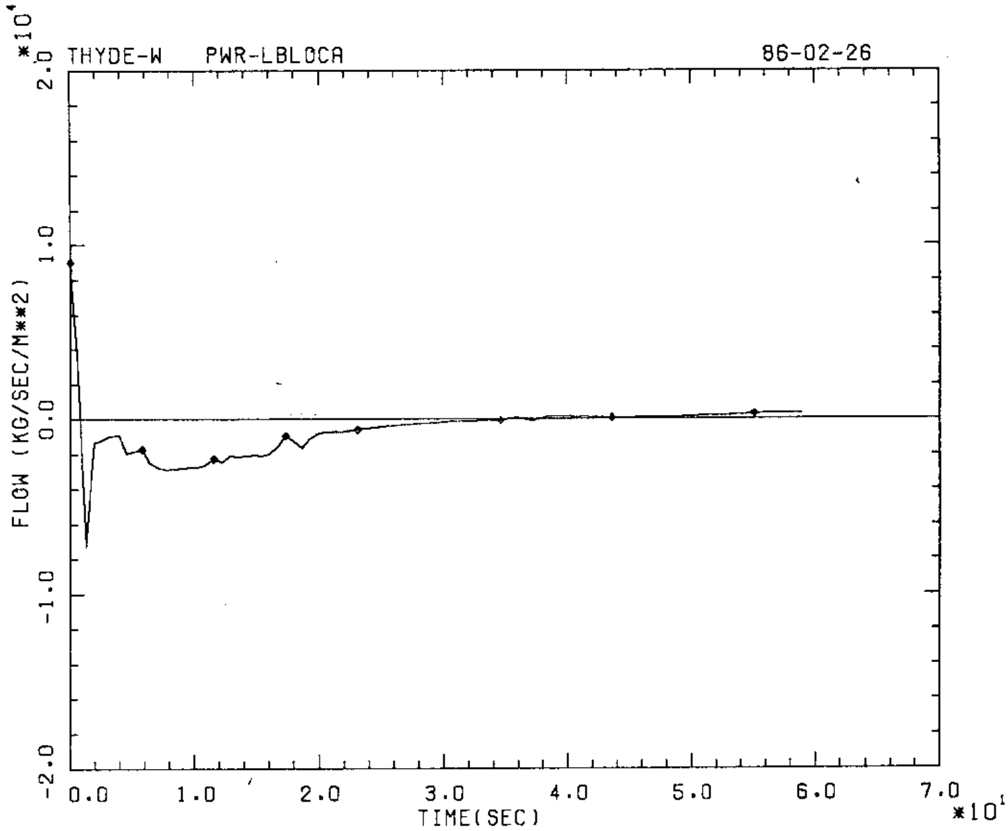

Fig. 10–1–14 Hot Leg Flow (Intact Loop) (Sample Problem).

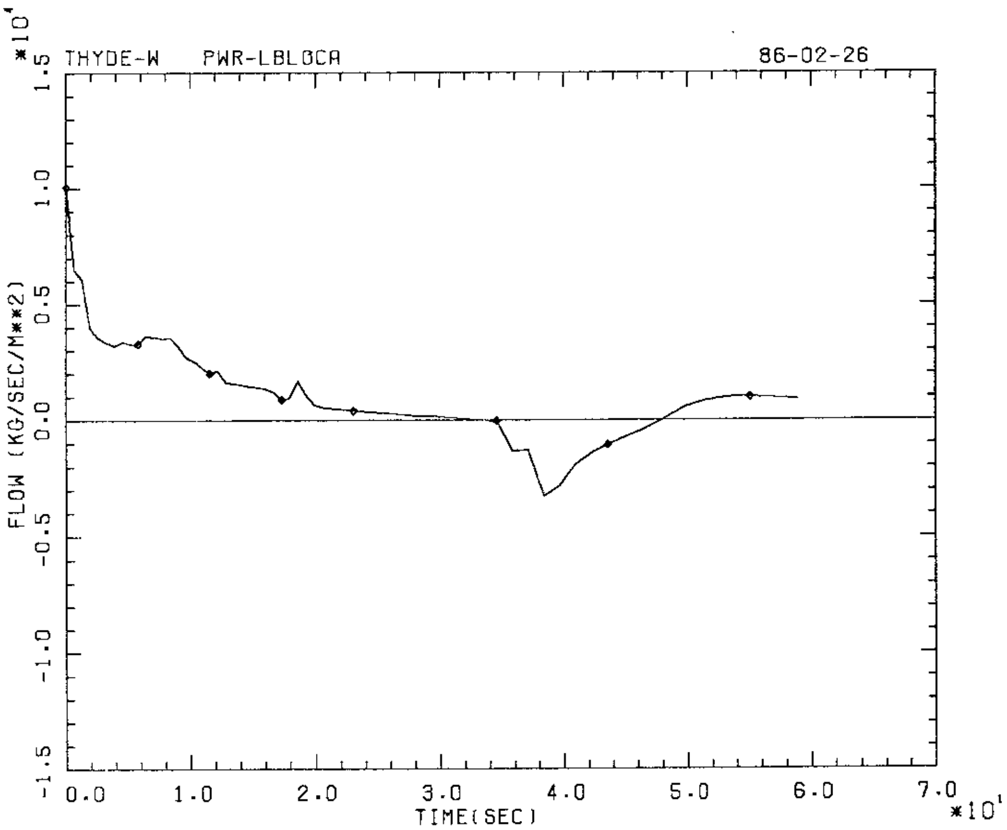

Fig. 10–1–15 Pump Outlet Flow (Intact Loop) (Sample Problem).

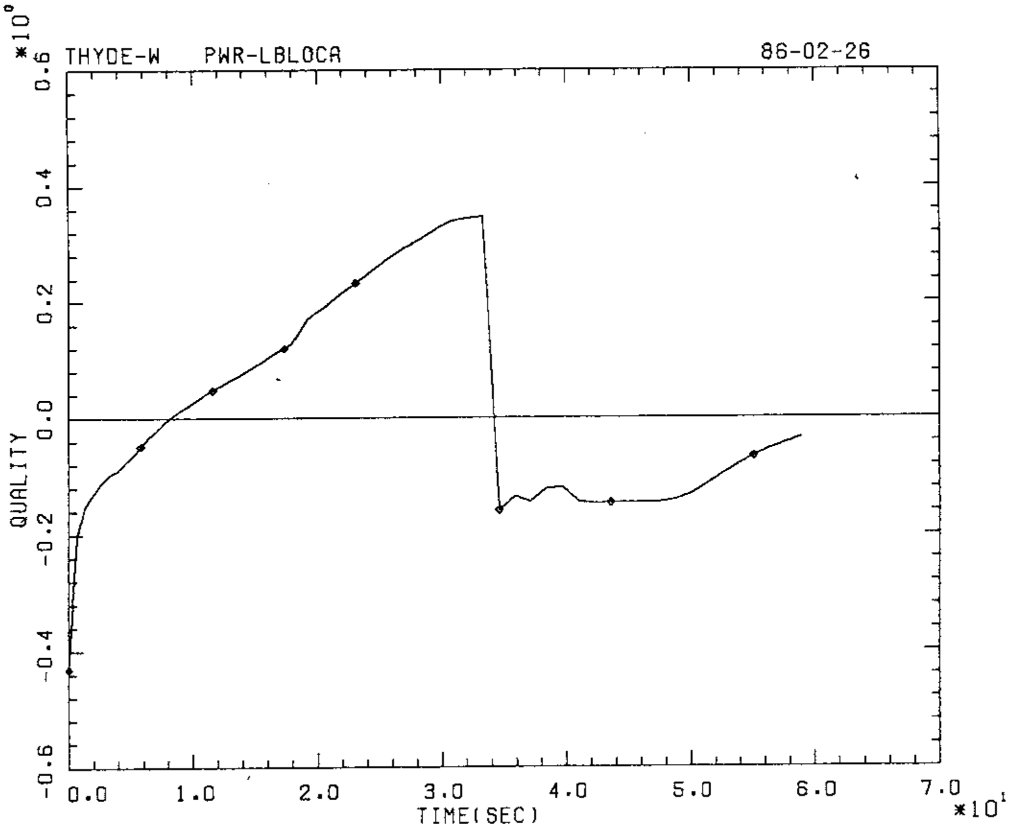

Fig. 10–1–16 Pump Outlet Quality (Intact Loop) (Sample Problem).

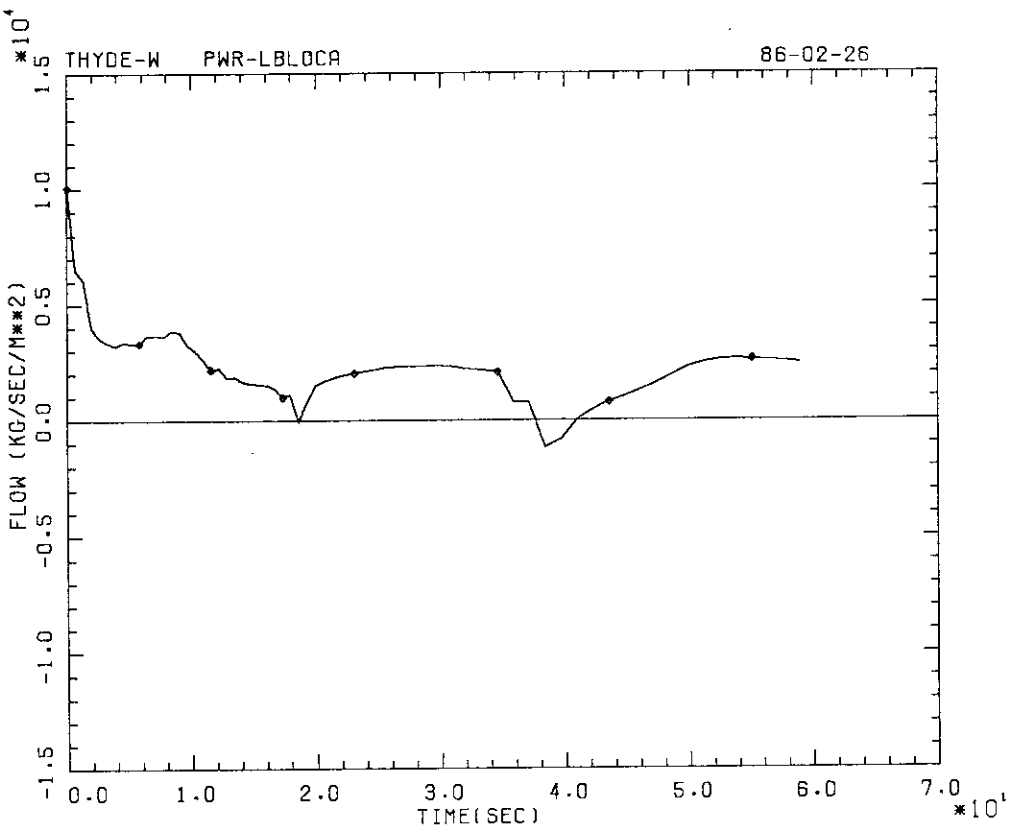

Fig. 10–1–17 Cold Leg Flow (Intact Loop) (Sample Problem).

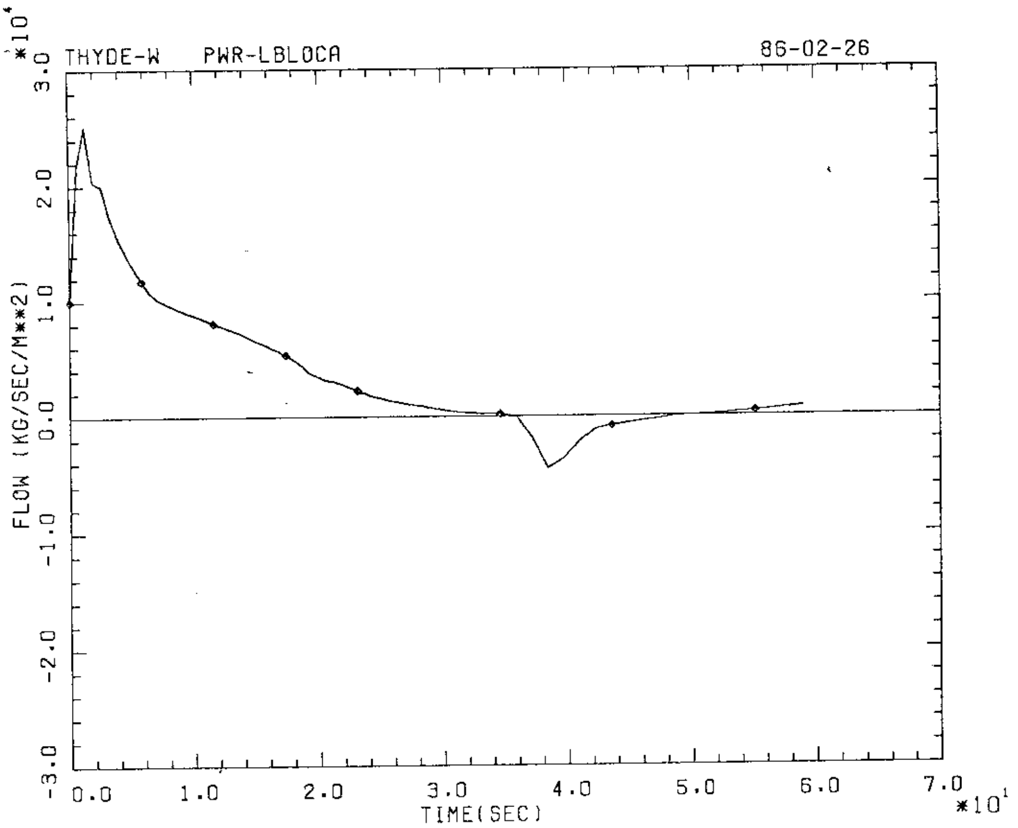

Fig. 10–1–18 Pump Outlet Flow (Broken Loop) (Sample Problem).

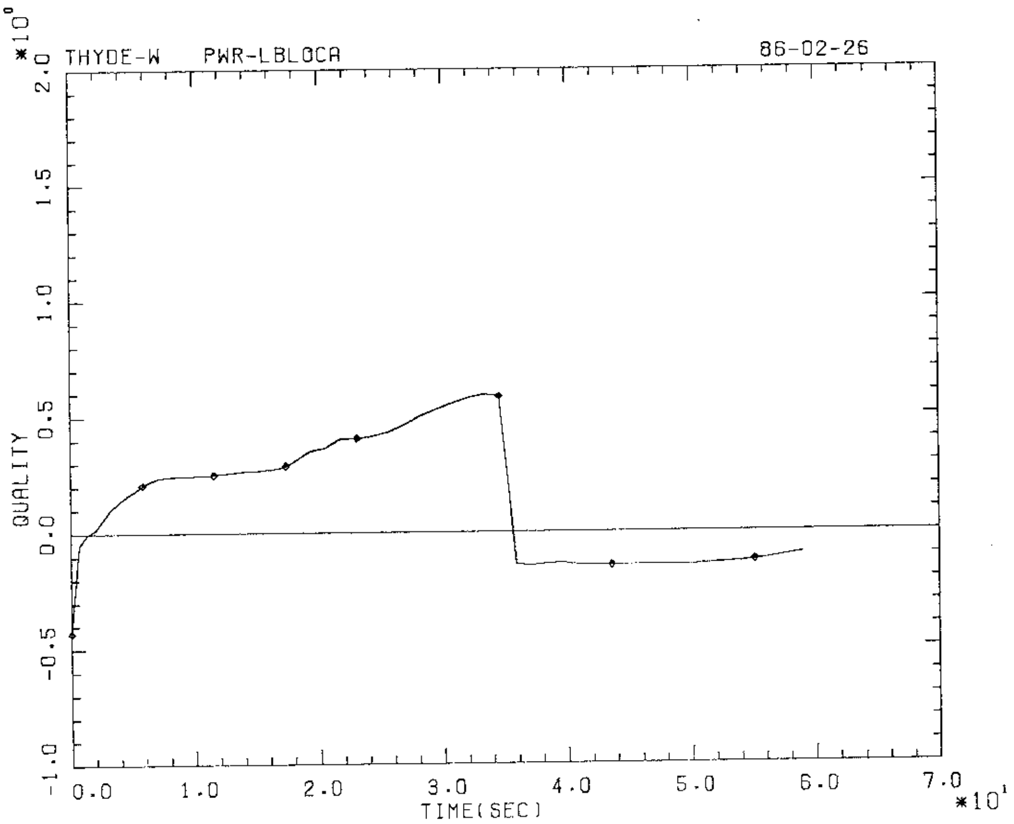

Fig. 10–1–19 Pump Outlet Quality (Broken Loop) (Sample Problem).

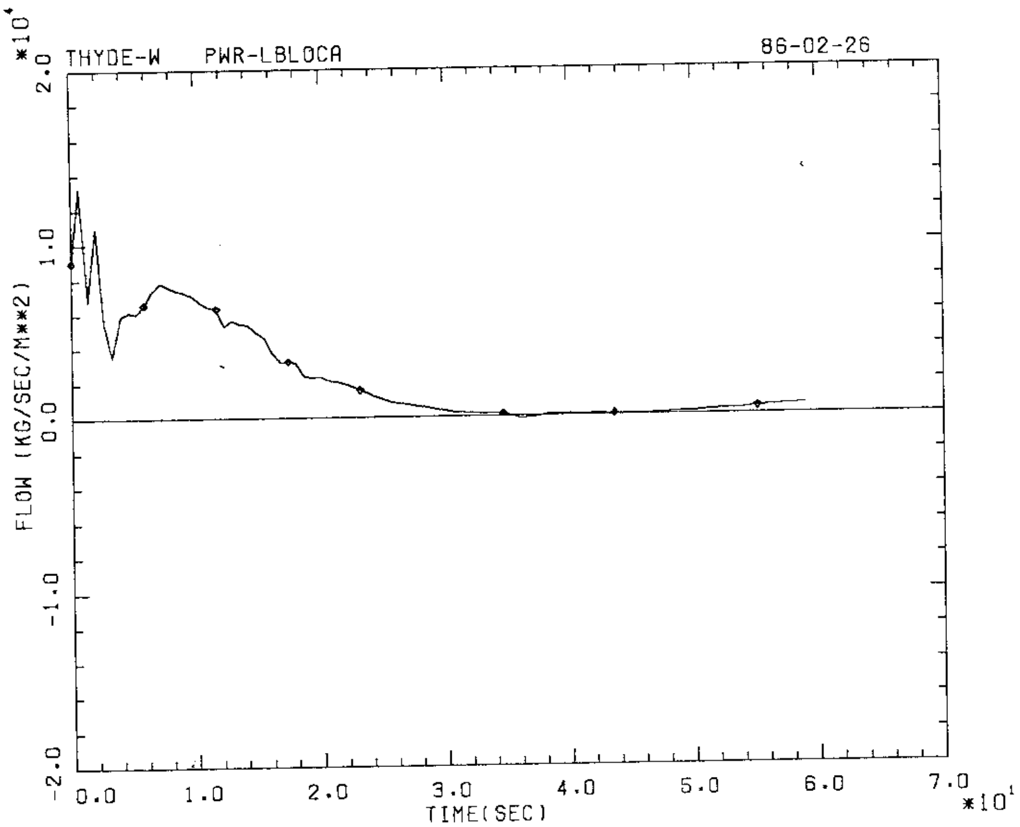

Fig. 10–1–20 Hot Leg Flow (Broken Loop) (Sample Problem).

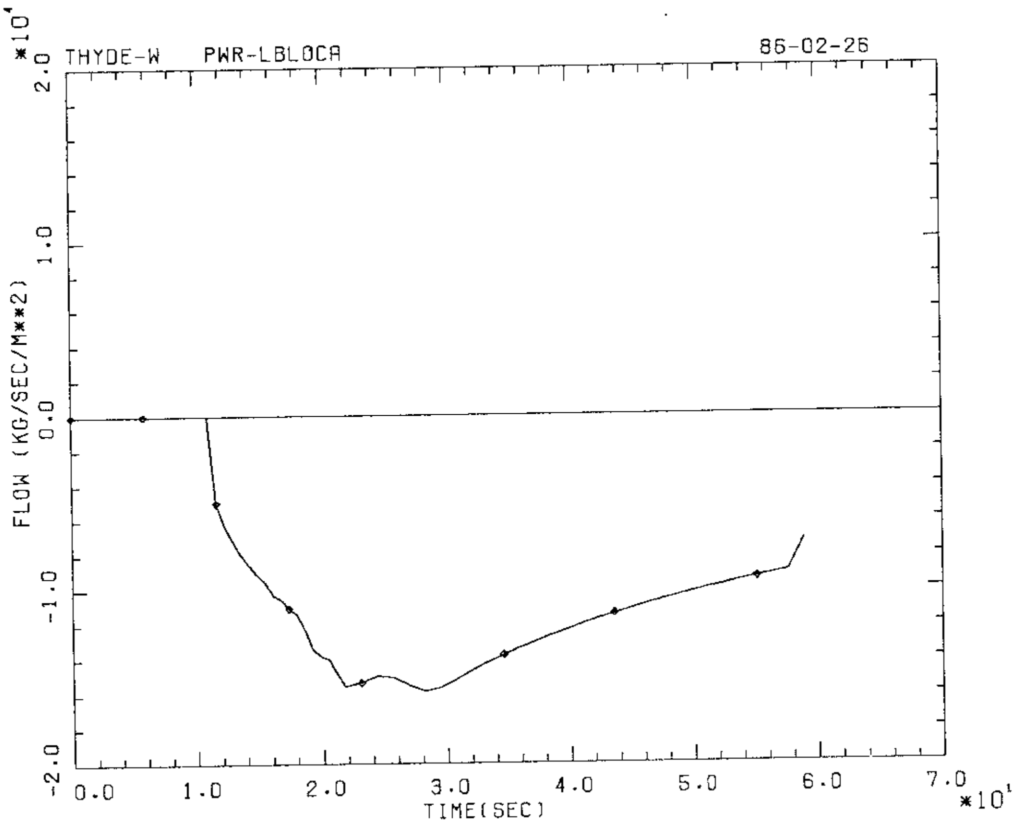

Fig. 10–1–21 ACC–2 Injection Flow (Sample Problem).

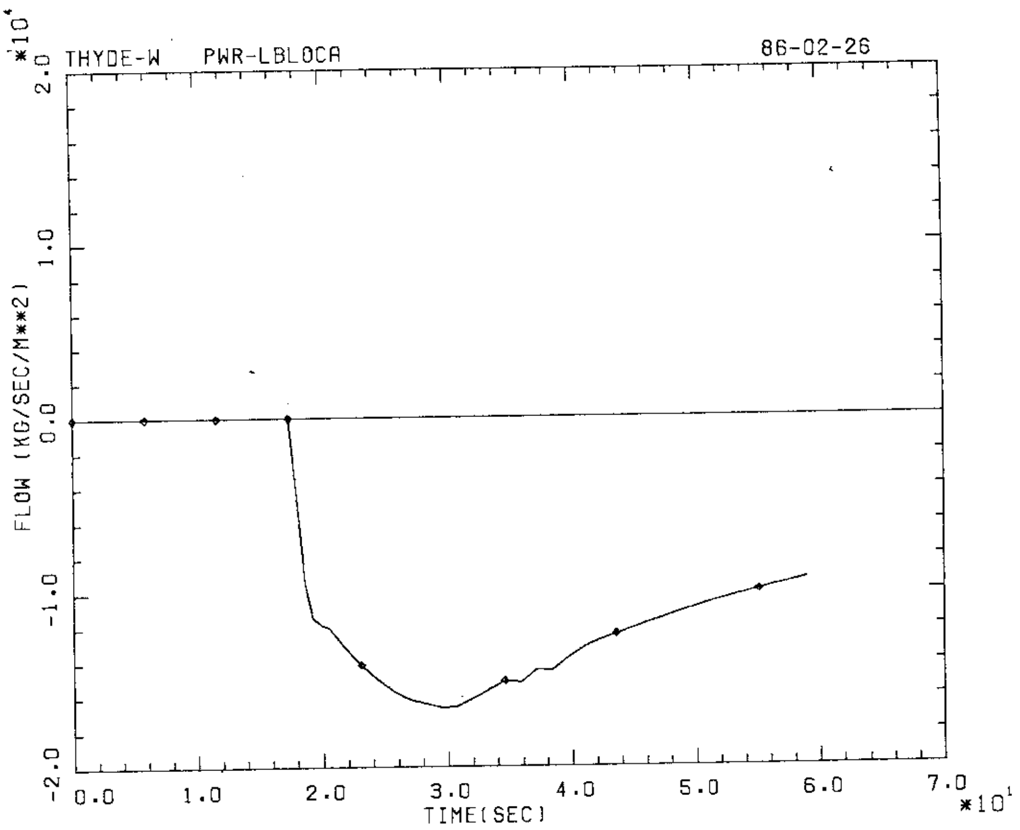

Fig. 10–1–22 ACC–1 Injection Flow (Sample Problem).

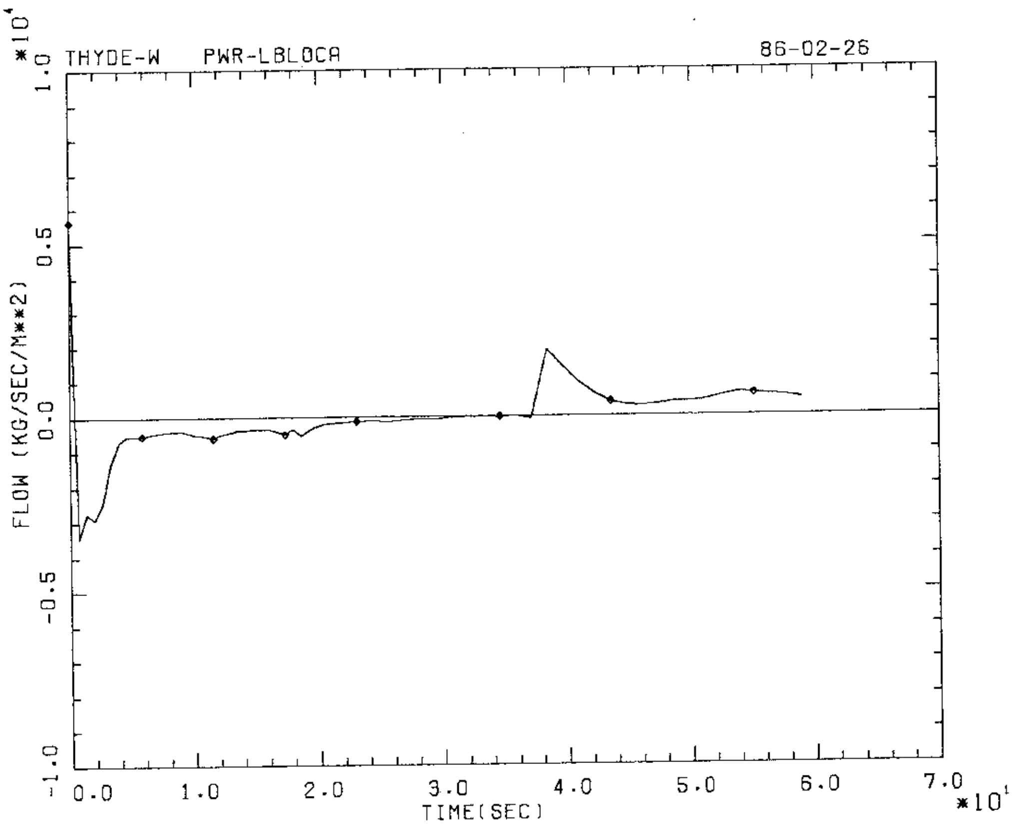

Fig. 10–1–23 Downcomer Flow (Sample Problem).

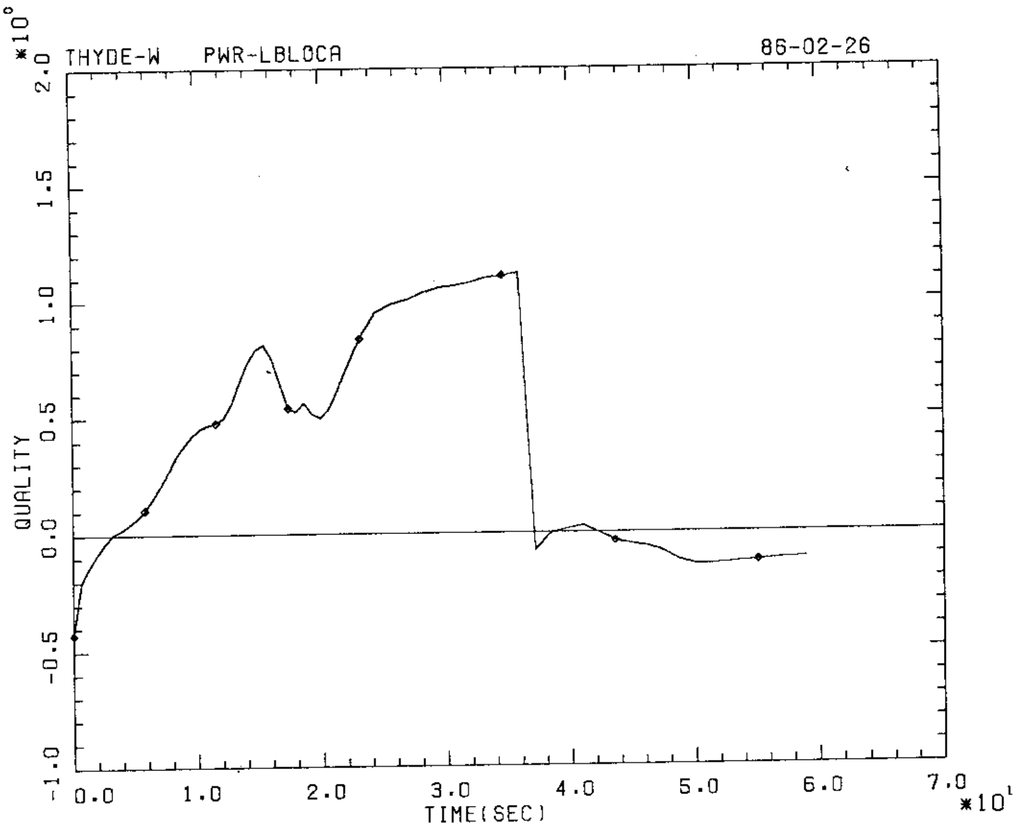

Fig. 10–1–24 Downcomer Quality (Sample Problem).

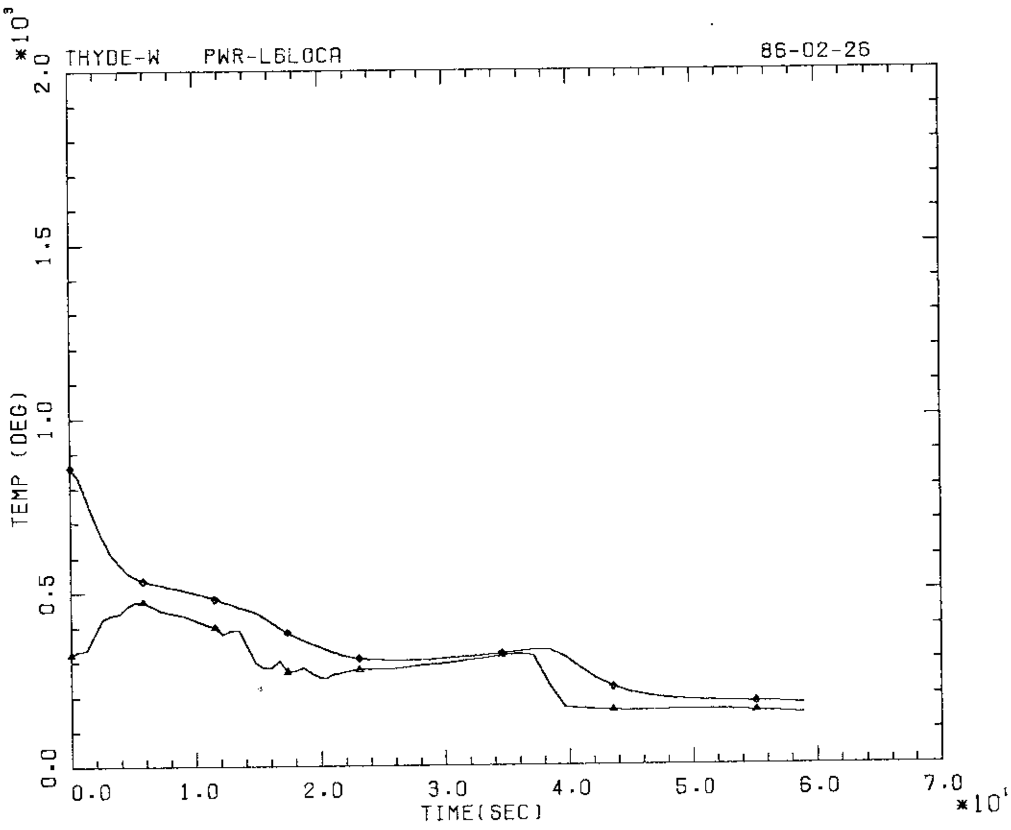

Fig. 10–1–25 Fuel Center and Clad Surface Temperatures (Node 26) (Sample Problem).

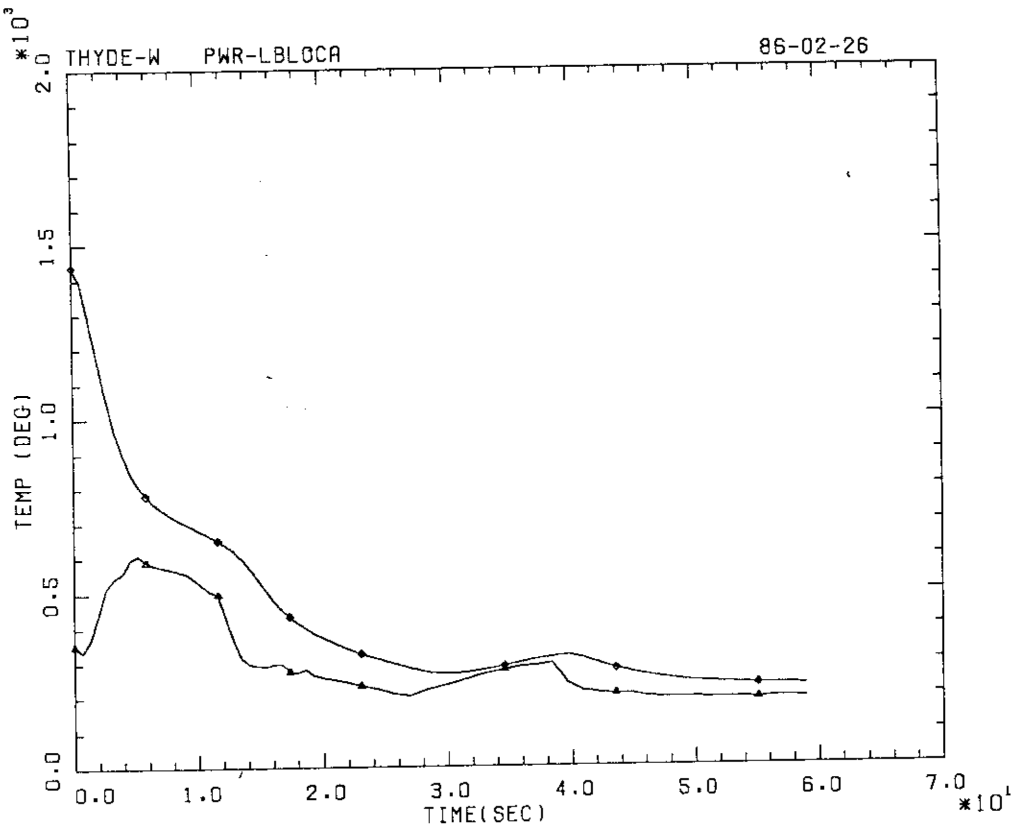

Fig. 10–1–26 Fuel Center and Clad Surface Temperatures (Node 27) (Sample Problem).

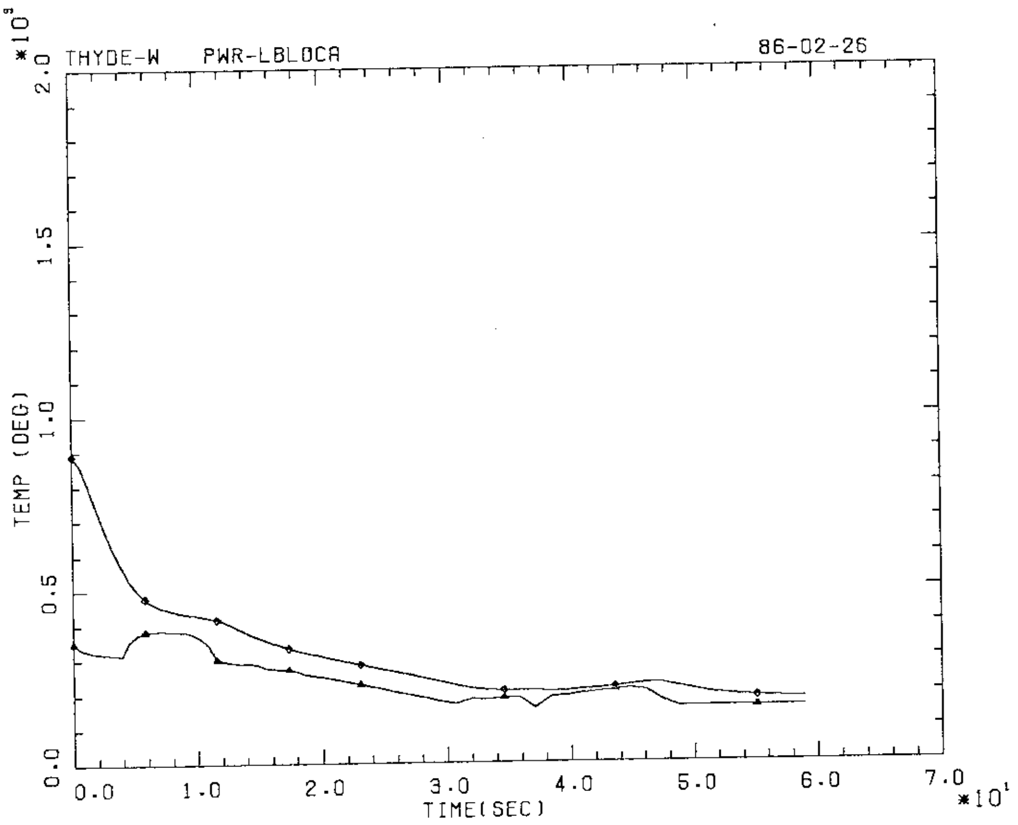

Fig. 10–1–27 Fuel Center and Clad Surface Temperatures (Node 28) (Sample Problem).

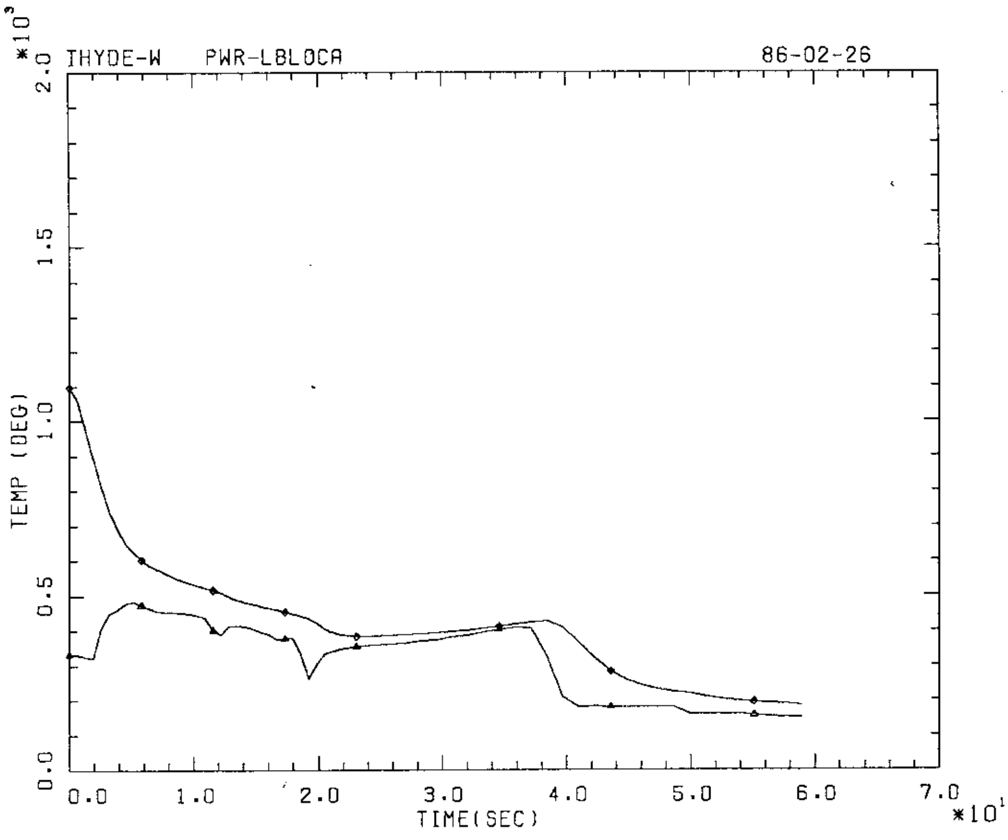

Fig. 10–1–28 Fuel Center and Clad Surface Temperatures (Node 31) (Sample Problem).

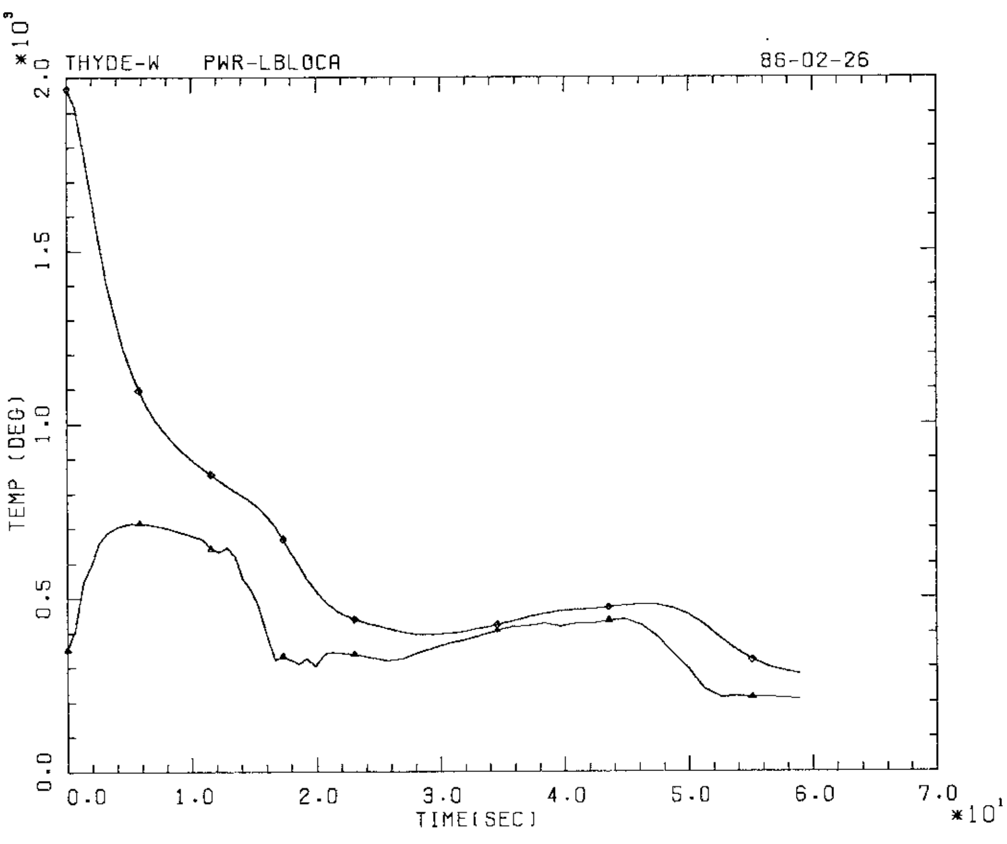

Fig. 10–1–29 Fuel Center and Clad Surface Temperatures (Node 32) (Sample Problem).

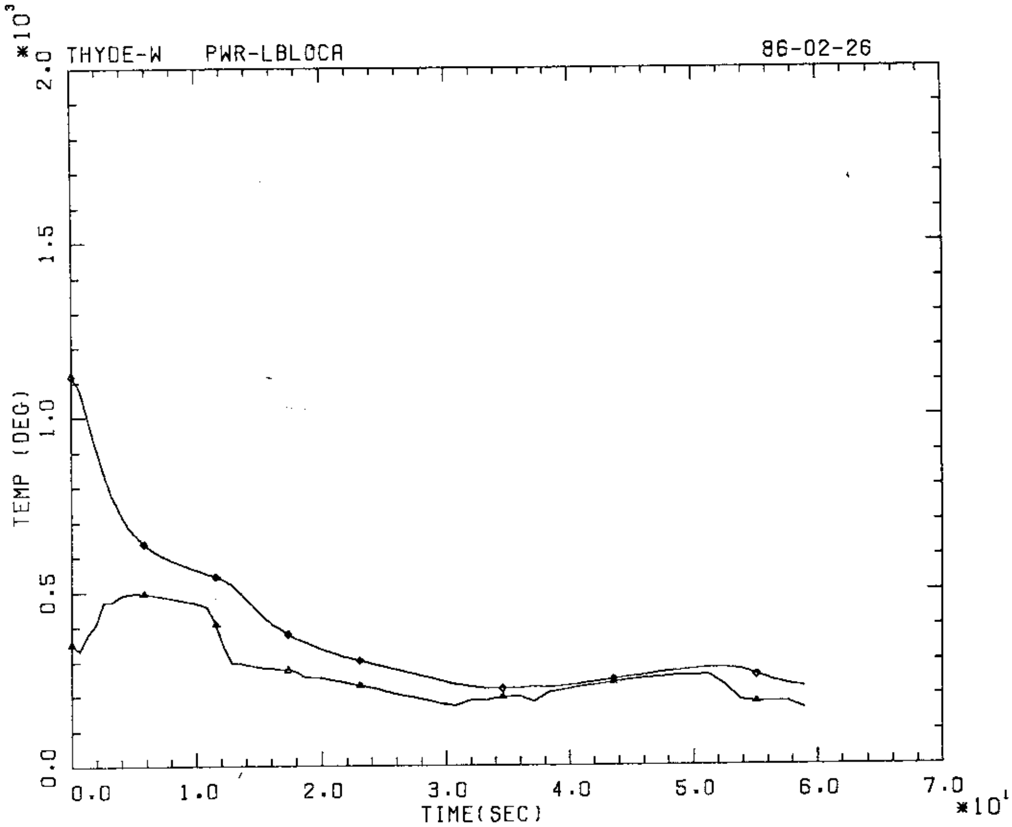

Fig. 10–1–30 Fuel Center and Clad Surface Temperatures (Node 33) (Sample Problem).

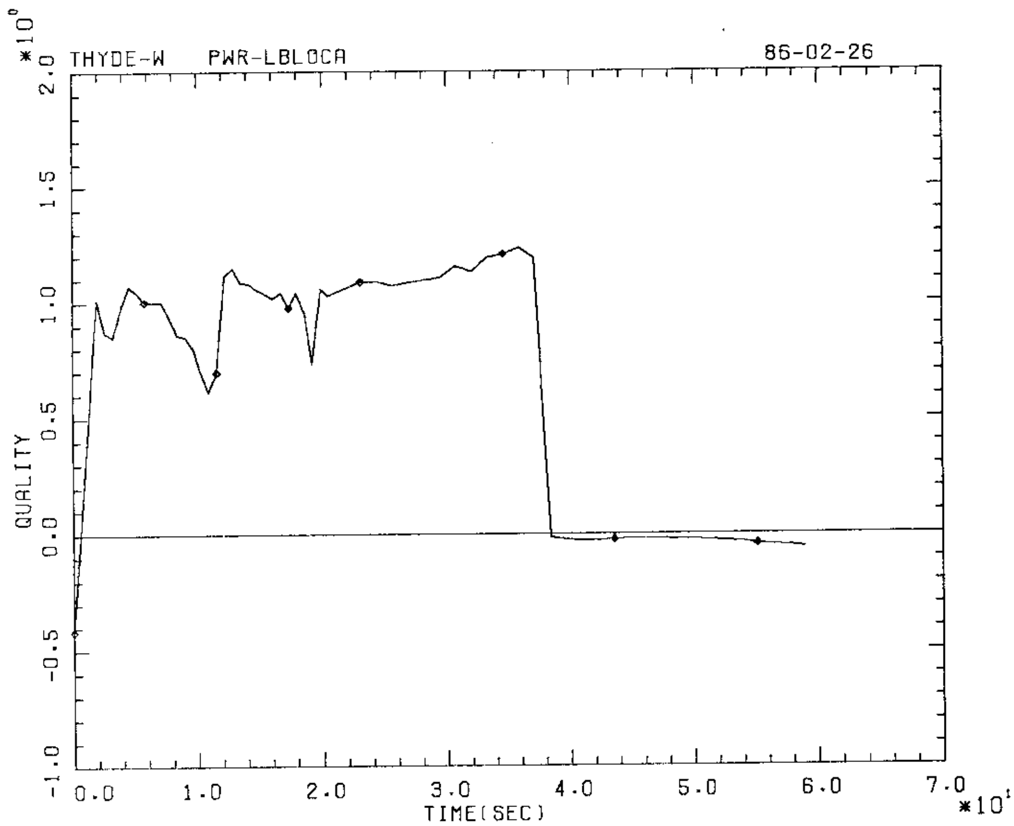

Fig. 10–1–31 Inlet Quality of Node 30 (Sample Problem).

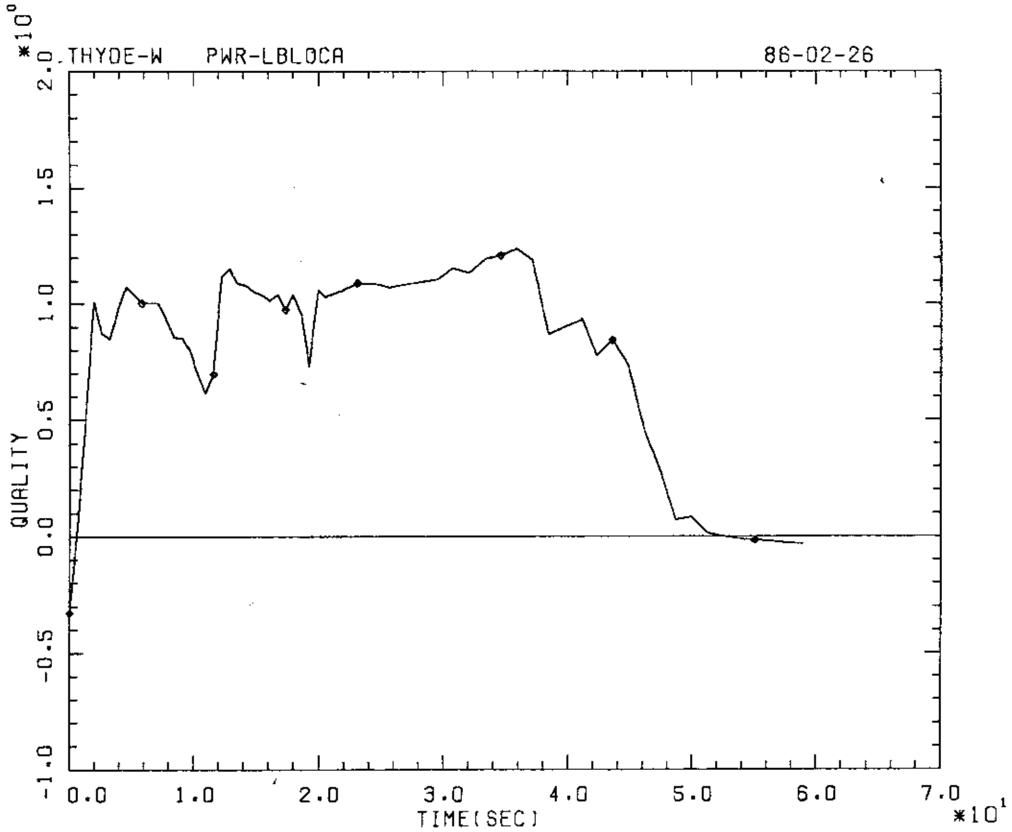

Fig. 10–1–32 Outlet Quality of Node 31 (Sample Problem).

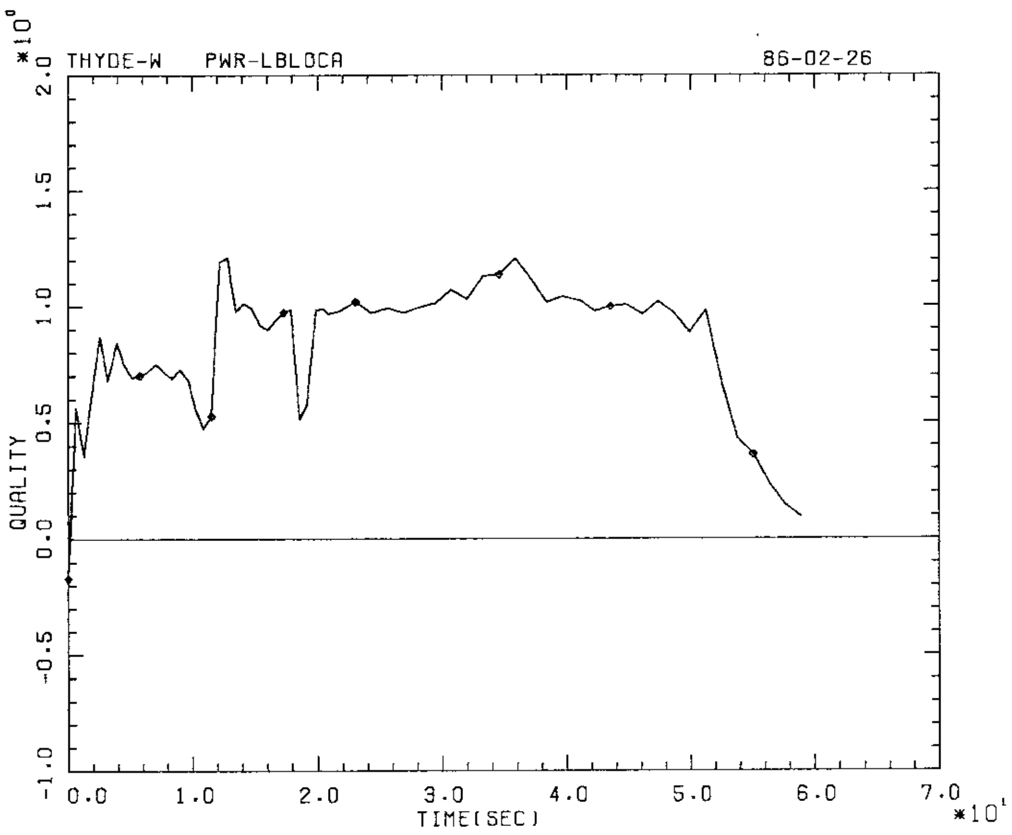

Fig. 10–1–33 Outlet Quality of Node 32 (Sample Problem).

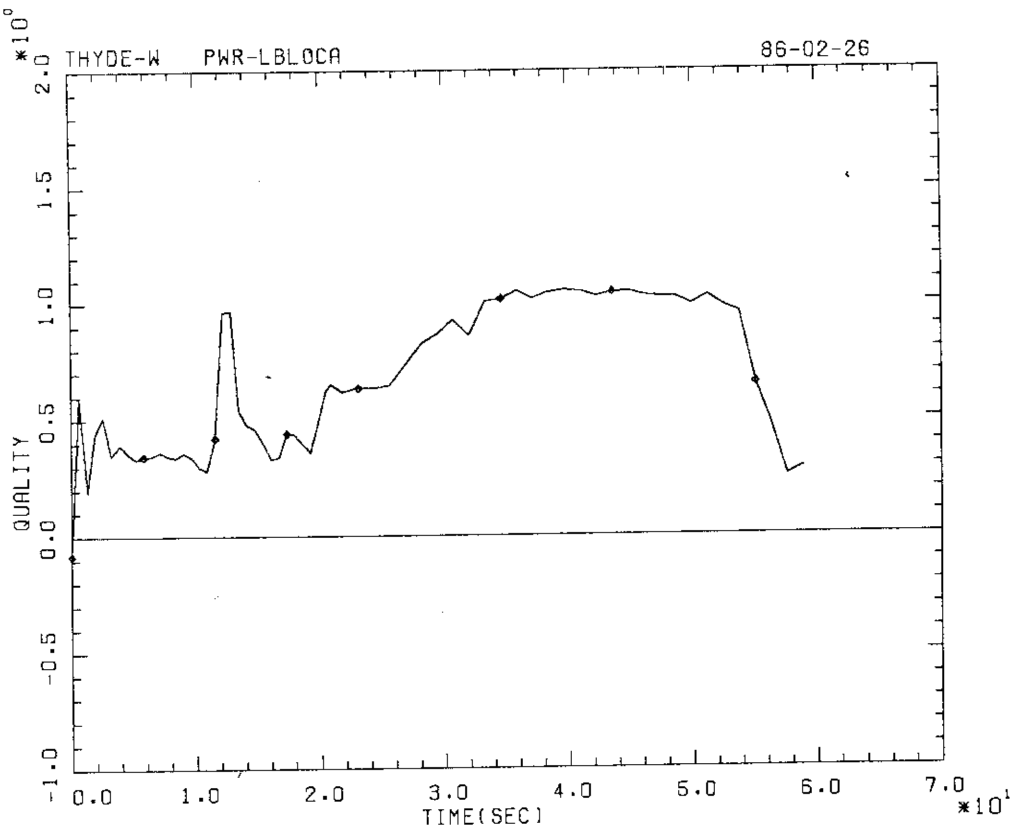

Fig. 10–1–34 Outlet Quality of Node 33 (Sample Problem).

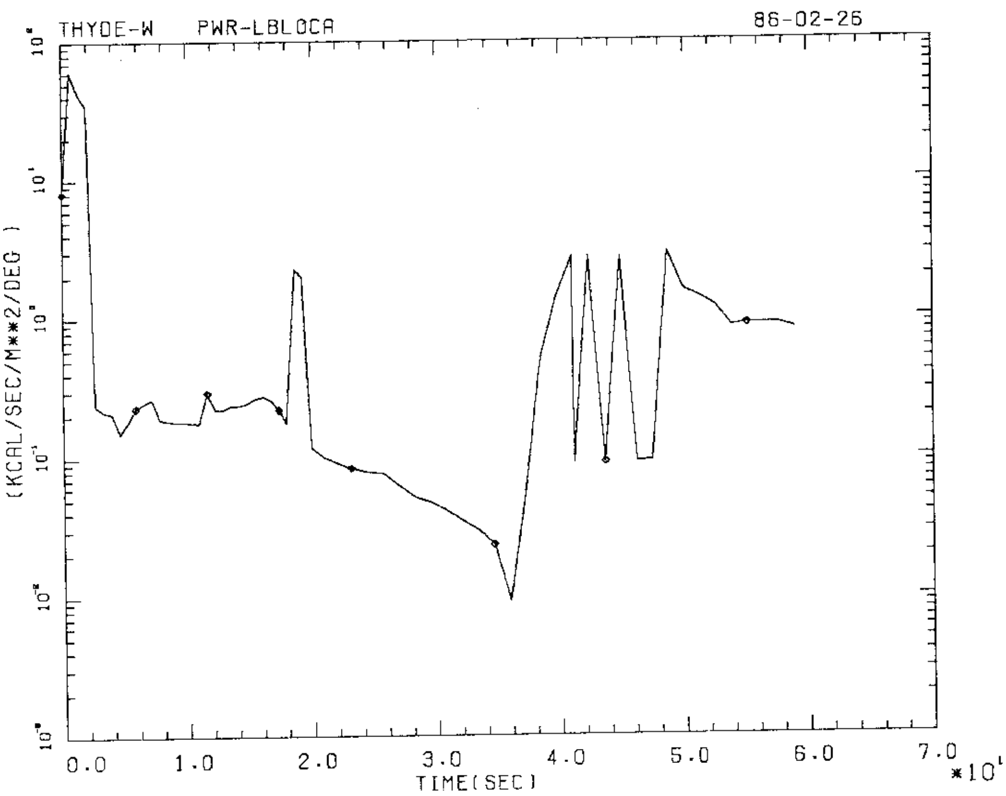

Fig. 10–1–35 Htc of Node 31 (Sample Problem).

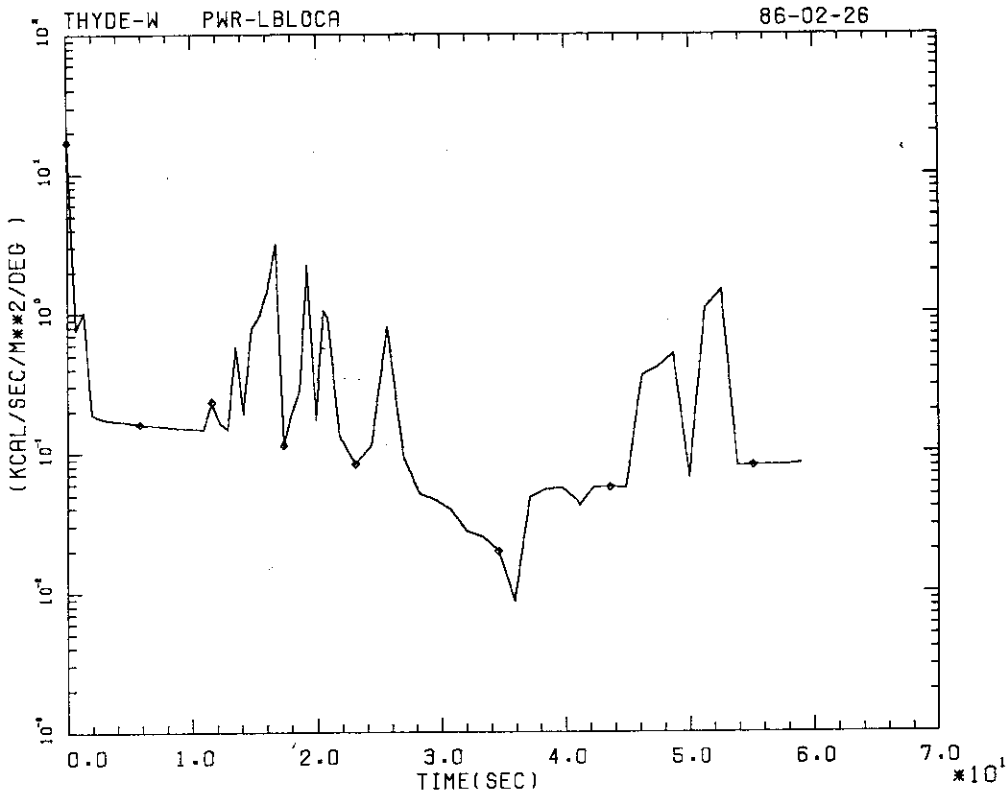

Fig. 10–1–36 Htc of Node 32 (Sample Problem).

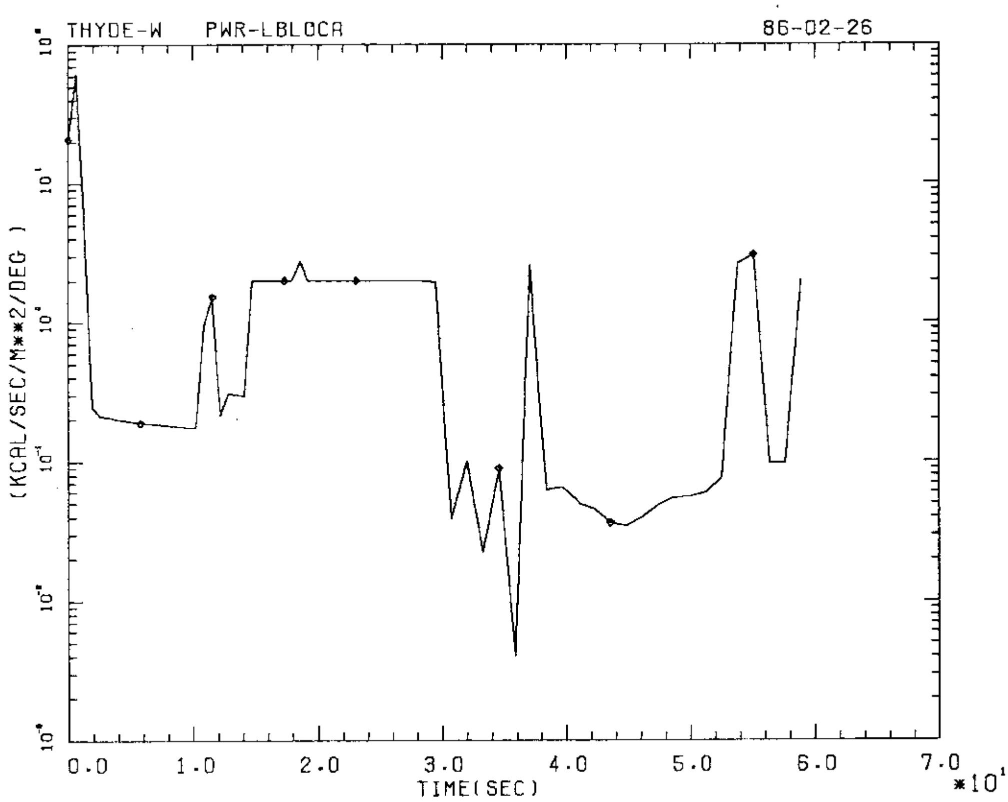

Fig. 10–1–37 Htc of Node 33 (Sample Problem).

11. Concluding Remarks

In RCS transients, coolant can be regarded as the medium which combines various phenomena, taking place in all parts of RCS. Since coolant behaviors are governed by the conservation laws, the validity of a RCS transient analysis code depends very much on how correctly one solves the conservation equations so that mass, energy and momentum conserve. To this end, two requirements must have been satisfied, i.e., the conservation equations must (1) be spatially differenced so that they retain conservative form, and (2) be solved "exactly". In order to satisfy these requirements, several model developments were needed.

The first requirement was satisfied by the new space differencing scheme, which led to the new thermal-hydraulic network model. It is new in that the conservation equations are reduced by three steps, each corresponding to the geometrical features of the system. Especially, it should be noted that the rank of the finally reduced equation is determined solely by the geometrical feature of the network. This is not the case with other models. Therefore, the programming of the three step reduction turned out be rather straightforward regardless of degree of network complexity.

The second was satisfied by applying the nonlinear implicit method on the basis of the three step reduction procedure. To be practical, the nonlinear implicit scheme must converge under any realistically possible circumstances. Therefore, first of all, it is necessary to ensure continuity of all the parameters contained in the conservation equations. Non-convergence of the nonlinear implicit scheme was solved not always by attainment of continuity by simple interpolation of the parameter in question, but sometimes only by development of new physical models. For example, the relaxation model for void fraction was developed under certain assumptions concerning thermal non-equilibrium between the two phases. This model is vitally needed to overcome what is sometimes called the "water packing" problem.

The main features of THYDE-P2 are mostly related to thermal-hydraulics. In order to help the readers modify the code, whenever necessary, however, this report also contains the methods and models in the other aspects for use in THYDE-P2. The correlations and assumptions for use in THYDE-P2 would be improved based on the progress in phenomenological understanding.

The capabilities of the new thermal-hydraulic network model built in THYDE-P2 is clearly shown in chapter 10, where the calculated result for 1,100 MWe PWR LB-LOCA is presented. The BE calculation was made by a FACOM VP100 computer untill 70 sec (physical time) when the reflooding of the core had been completed. It should be noted that a through calculation was successfully made without any artificial assumption, i.e., those cited in section 3.2. The overall tendency of the calculated result is very similar to that of LOFT L2-3[52] experiment, which was performed to simulate LB-LOCA of a commercial PWR. This is one of the few through calculations of LB-LOCA of a commercial PWR one can find in open literature. THYDE-P2 is also capable of what is called the EM calculation of LB-LOCA[48].

The CPU time and memory required by a VP100 FACOM computer are 13 minutes 45 seconds and 2,436 K bytes, respectively. The degrees of mass and energy imbalances are 1.32×10^{-8} % and 1.28×10^{-2} %, respectively, at the end of the calculation (70.0 seconds). Therefore, it can practically be concluded that mass and energy conserved in the calculation.

No other RCS transient analysis code solves the conservation equations so closely as THYDE-P2.

As shown in chapter 10 or in other literature[43,48], THYDE-P2 is capable of through calculation of LB-LOCA, which is regarded as the most critical for testing methods and models for thermal-hydraulics. Therefore, it is expected that there will be a great deal of possibilities[49,50] of THYDE-P2 application to various RCS transient analyses.

12. Aknowledgment

The authors would like to express their sincere thanks to the other members of their section Reactor Safety Evaluation Laboratory, with whom they enjoyed fruitful discussions in the course of the work. The authors' thanks are also due to the members of NEDAC, who made the programming of THYDE-P2, thereby scrutinizing the models in detail, especially the network model described in section 2.3.

13. References

1) "Keisui-Gata Doryoku-ro no Hizyo-yo Roshin-Reikyaku-kei no Anzen-Hyoka Shishin" (translated title, "Safety Evaluation Guide Line for Emergency Core Cooling Systems of Light-Water-Cooled Nuclear Power Reactors") Committee on Reactor Safety Examination, Japanese Atomic Energy Commission, May 24, 1974, (revised in April 15, 1975).
2) Esposito, V.J., Kesavan, K. and Maul, B., "WFLASH – A FORTRAN-IV Computer Program for Simulation of Transients in a Multi-Loop PWR", (Rev. 2), WCAP-8200, Westinghouse Electric Corporation (June, 1974).
3) Porsching, T.A., Murphy, J.H., Redfield, J.A. and Davis, V.C., "FLASH-4: A Fully Implicit FORTRAN-IV Program for the Digital Simulation of Transients in a Reactor Plant", WAPD-TM-840, Bettis Atomic Power Laboratory (March, 1969).
4) Bordelon, F.M., et al., "SATAN-IV Program: Comprehensive Space-Time Dependent Analysis of Loss-of-Coolant", WCAP-8302 (June, 1974).
5) Bordelon, F.M., et al., "LOCTA-IV Program: Loss-of-Coolant Transient Analysis", WCAP-8305 (June, 1974).
6) Collier, G., et al., "Calculational Model for Core Reflooding after a Loss of Coolant Accident (WREFLOOD Code)", WCAP-8170 (June, 1974).
7) "TRAC-P1A : An Advanced Best Estimate Computer Program for PWR LOCA Analysis", Safety Code Develop. Group, Energy Div., Los Alamos Sci. Lab., LA-7777-MS, NUREG/CF-0665 (1979).
8) Steinhoff, F., "DRUFAN-02 Interim Program Description", GRS-A685; GRS-A714 (1982).
9) "WREM : Water Reactor Evaluation Model (Rev. 1)", NUREG-75/056, USNRC (May, 1975).
10) "General Electric Company Analytical Model for Loss-of-Coolant Analysis in Accordance with 10 CFR 50 Appendix K", NEDO-20566 (1976).
11) Zuber, N. and Staub, F.W., Nucl. Sci. and Eng., 30, 268 (1967).
12) Harmathy, T., AIChE Journal, 6, 281 (1960).
13) Peebles, F.N. and Garber, H.J., Chem. Eng. Sci., 49, 88 (1953).
14) Bordelon, F.M. and Murphy, E.T., "Containment Pressure Analysis Code (COCO)", WCAP-8326 (June, 1974).
15) Zaloudek, F.R., "Steam-Water Critical Flow High Pressure Systems", HW-68936, Hanford Works (1964).
16) Zaloudek, F.R., "The Critical Flow of Hot Water through Short Tubes", HW-77594, Hanford Works (1963).
17) Moody, F.J., "Maximum Flow Rate of Single Component, Two-Phase Mixture", ASME, Paper No. 64-HT-35.
18) Porsching, T.A., Murphy, J.H. and Redfield, J.A., "Stable Numerical Integration of Conservation Equations for Hydraulic Networks", Nucl. Sci. Eng., 43, 218-225 (1971).
19) Baron, R.C., "Digital Model Simulation of a Nuclear Pressurizer", Nucl. Sci. Eng., 52, 283-291 (1973).
20) Boyd, G.M., Jr., Rosser, R.M. and Cardwell, B.B., Jr., "Transient Flow Performance in a Multiloop Nuclear Reactor System", Nucl. Sci. Eng., 9, 442-454 (1961).
21) Streeter, V.L. and Wylie, F.B., "Hydraulic Transients", McGraw-Hill, New York (1967).
22) Shure, K., "Fission Product Decay Energy", Report WAPD-BT-24, Westinghouse Atomic Power Division (1961).
23) Proposed American Nuclear Society Standard – "Decay Energy Release Rates Following Shutdown of Uranium-Fueled Thermal Reactors", approved by Subcommittee ANS-5, ANS Standard Committee, (October 1971, revised October 1973).
24) Perkins, J.F. and King, R.W., "Energy Release from Decay of Fission Products", Nucl. Sci. Eng., 3, 726-746 (1958).
25) Stehn, J.R. and Clancy, E.F., "Fission Product Radioactivity and Heat Generation" in "Proceedings of the Second United Nations International Conference on the Peaceful Uses of Atomic Energy, Geneva 1958", vol.13, pp.49-54, United Nations, Geneva (1958).
26) Baker, L. and Just, L.C., "Studies of Metal Water Reactions at High Temperatures, iii. Experimental and Theoretical Studies of the Zirconium-Water Reaction", ANL-6548 (May, 1962).
27) Dean, R.A., "Thermal Contact Conductance Between UO_2 and Zircaloy-2", CVNA-127 (1962).
28) Ross, A.M. and Stoute, R.L., "Heat Transfer Coefficient Between UO_2 Zircaloy-2", Report AECL-1552, (CRFD-1075), Chalk River, Ontario (June, 1962).
29) Brokaw, R.S., "Alignment Charts for Transport Properties, Viscosity, Thermal Conductivity and Diffusion Coefficients for Nonpolar Gases and Gas Mixtures at Low Density", Report NASA TR R-81 (1961).

30) Hottel, H.C., "Radiation Heat Transmission", Chapter 4 or "Heat Transmission", by W.H. McAdams, McGraw-Hill (1954).
31) Dittus, F.W. and Boelter, L.M.K., "Heat Transfer in Automobile Radiators of the Tubular Tube", 2, No.13, p.443-461 (1930).
32) Jens, W.H. and Lottes, "Analysis of Heat Transfer, Burnout, Pressure Drop and Density Data for High-Pressure Water", ANL-4627 (1951).
33) Slifer, B.C. and Hench, J.E., "Loss-of-Coolant Accident and Emergency Core Cooling Models for General Electric Boiling Water", Reactors, NEDO-10329, General Electric Company, Equation C-32 (April, 1971).
34) Groeneveld, D.C., "An Investigation of Heat Transfer in the Liquid Deficient Regime", Report AECL-3281, Chalk Rever, Ontario (December, 1968) (Revised December 1969 by E.O. Moeck).
35) McEligot, D.M., Ormand, L.W. and Perkins, H.C., Jr., Trans. Amer. Soc. Mech. Engrs., 88, Series C, p.239-245 (May, 1966).
36) McAdams, W.H., "Heat Transmission", 3rd Ed., p.337, McGraw-Hill, New York (1954).
37) Fishenden, M. and Saunders, O.A., "An Introduction to Heat Transfer", p.97, Oxford Univ. Press., London (1950).
38) Cadek, F.F., Dominicis, D.P. and Leyse, R.H., "PWR FLECHT (Full Length Emergency Cooling Heat Transfer) Final Report", WCAP 7665 (April, 1971).
39) Cadek, F.F., et al., 'PWR FLECHT Final Report Supplement", WCAP-7931 (October, 1972).
40) Henry, R.E., "A Correlation for the Minimum Film Boiling Temperature", American Institute of Chemical Engineers, Reprint 14, Presented at the 14th National Heat Transfer Conference Atlanta, GA (August, 1973).
41) Hardy, D.G., "High Temperature Expansion and Rupture Behavior of Zircaloy Tubing", National Topical Meeting on Water-Reactor Safety, Salt Lake City, Utah (March, 1973).
42) Weir, J.R., Jr., et al., "Certain Aspects of LWR Fuel Pins During a LOCA", ORNL-CF-72-11-1.
43) Asahi, Y. and Asaka, H., "New Non-Equilibrium Thermal-Hydraulic Model, (2) : Application to LOFT L2-3", J. Nucl. Sci. Tech., 21(10) (1984).
44) Asahi, Y., et al., "New Non-Equilibrium Thermal-Hydraulic Model; (II) Application to LOFT L2-3", J. of Nucl. Sci. Tech., 21(10), Oct. 1984.
45) Taylor, G.I., Proc. Roy. Soc., (London), A210, 192 (1950).
46) Biasi, L., et al., "Studies on Burnout", Part 3, Energ. Nucl. (Milan), 550-536 (1967).
47) Zuber, N., et al., "The Hydrodynamic Crisis in Pool Boiling of Saturated and Subcooled Liquids", International Developments in Heat Transfer, Part II, pp.230-236, 1961.
48) Kanazawa, M., et al., "A Through Calculation of 1,100 MWe PWR Large Break LOCA by THYDE-P1 EM Model", JAERI-M 84-132, 1984.
49) Harami, T., et al., "A Safety Analysis of Research Reactor JRR-3", Int. Meeting on Reduced Enrichment for Research and Test Reactors (RERTER), Petten, The Netherlands, 14-16 Oct. 1985.
50) Asahi, Y. and H. Wakabayashi, "Some Transient Characteristics of PIUS", Nuclear Technology, vol.72, pp.24-33, Jan. 1986.
51) Asahi, Y. and K. Tsuchihashi, "A Subroutine Reading Data in Free Format", JAERI-M4458, May 1971.
52) Prassions, P.G., "Experimental Data Report for LOFT Power Ascension Test L2-3", NUREG/CR-0792, TREE-1326 (1979).

Appendix A Jacobian Elements

A.1 Partial Derivatives of h_n^A and h_n^E

In order to obtain these quantities for h_n^A and h_n^E, we have to consider the type of the from-junction and the type of the to-junction, respectively, as can be seen from Eqs. (2–2–57) and (2–2–58).

A.1.1 Partial Derivatives of h_n^A

(1) If the from-junction is volumeless and open but break, then

$$\frac{\partial h_n^A}{\partial h_n^{av}}=0$$

$$\frac{\partial h_n^A}{\partial h_{from}^+}=1$$

and

$$\frac{\partial h_n^A}{\partial h_{to}^+}=0 .$$

(2) If the from-junction is a break, then

$$\frac{\partial h_n^A}{\partial h_n^{av}}=\eta_n^A$$

$$\frac{\partial h_n^A}{\partial h_{from}^+}=0$$

and

$$\frac{\partial h_n^A}{\partial h_{to}^+}=0 .$$

(3) If the from-junction is a mixing junction, then

$$\frac{\partial h_n^A}{\partial h^{av}}=\eta_n^A$$

$$\frac{\partial h_n^A}{\partial h_{from}^+}=1-\eta_n^A$$

and

$$\frac{\partial h_n^A}{\partial h_{to}^+}=0 .$$

(4) If the from-junction is closed, then

$$\frac{\partial h_n^A}{\partial h_n^{av}}=0$$

$$\frac{\partial h_n^A}{\partial h_{from}^+}=0$$

and

$$\frac{\partial h_n^A}{\partial h_{to}^+}=0$$

A.1.2 Partial Derivatives of h_n^E

(1) If the to-junction is volumeless and open but break, then

$$\frac{\partial h_n^E}{\partial h_n^{av}}=0$$

$$\frac{\partial h_n^E}{\partial h_{from}^+}=0$$

and

$$\frac{\partial h_n^E}{\partial h_{to}^+}=1.$$

(2) If the to-junction is a mixing junction, then

$$\frac{\partial h_n^E}{\partial h_n^{av}}=1-\eta_n^E$$

$$\frac{\partial h_n^E}{\partial h_{from}^-}=0$$

and

$$\frac{\partial h_n^E}{\partial h_{to}^+}=\eta_n^E$$

(3) If the to-junction is a boundary junction, then

$$\frac{\partial h_n^E}{\partial h_n^{av}}=1-\eta_n^E$$

$$\frac{\partial h_n^E}{\partial h_{from}^+}=0$$

and

$$\frac{\partial h_n^E}{\partial h_{to}^+}=0$$

(4) If the to-junction is closed, then always

$$\frac{\partial h_n^E}{\partial h_n^{av}}=0$$

$$\frac{\partial h_n^E}{\partial h_{from}^-}=0$$

and

$$\frac{\partial h_n^E}{\partial h_{to}^+}=0.$$

A.2 Node Jacobian

A.2.1 Derivatives of f_{n1}

$$(j_{11})_n=1$$

$$(j_{12})_n=-\frac{L_n}{2\Delta t}\left(\frac{\partial \rho}{\partial p}\right)_n^{av}$$

$$(j_{13})_n=-1$$

$$(j_{14})_n=-\frac{L_n}{2\Delta t}\left(\frac{\partial \rho}{\partial p}\right)_n^{av}$$

and

$$(j_{15})_n-\frac{L_n}{\Delta t}\left(\frac{\partial \rho}{\partial h}\right)_n^{av}$$

A.2.2 Derivatives of f_{n2}

If the to-junction is not a break,

$$(j_{21})_n = -(\xi_n^A)^2 \frac{G_n^A}{\rho_n^A} - \frac{1}{2}\left(\frac{\Phi^2}{\rho_f}\right)_n^A \frac{\partial}{\partial G_n^A}\kappa_n^A$$

$$(j_{22})_n = (\xi_n^A)^2\left[-1+\frac{1}{2}\left(\frac{G_n^A}{\rho_n^A}\right)^2\left(\frac{\partial \rho}{\partial p}\right)_n^A - \frac{1}{2}\left(\frac{\partial B}{\partial p}\right)_n^A\right] - \frac{\kappa_n^A}{2}\left(\frac{\partial}{\partial p}\frac{\Phi^2}{\rho_f}\right)_n^A$$

$$(j_{23})_n = 0$$

$$(j_{24})_n = 0$$

and

$$(j_{25})_n = \frac{(\xi_n^A)^2}{2}\left[\left(\frac{G_n^A}{\rho_n^A}\right)^2\left(\frac{\partial \rho}{\partial h}\right)_n^A - \left(\frac{\partial B}{\partial h}\right)_n^A\right]\frac{\partial h_n^A}{\partial h_n^{av}} - \frac{\kappa_n^A}{2}\left(\frac{\partial}{\partial h}\frac{\Phi^2}{\rho_f}\right)_n^A \frac{\partial h_n^A}{\partial h_n^{av}} .$$

If the to-junction is a break, then

$$(j_{21})_n = \frac{f_B(p_n^A, G_n^A + \Delta G_n^A, h_n^A) - f_B(p_n^A, G_n^A, h_n^A)}{\Delta G_n^A}$$

$$(j_{22})_n = \frac{f_B(p_n^A + \Delta p_n^A, G_n^A, h_n^A) - f_B(p_n^A, G_n^A, h_n^A)}{\Delta p_n^A}$$

$$(j_{23})_n = 0$$

$$(j_{24})_n = 0$$

and

$$(j_{25})_n = \frac{[f_B(p_n^A, G_n^A, h_n^A + \Delta h_n^A) - f_B(p_n^A, G_n^A, h_n^A)]\partial h_n^A/\partial h_n^{av}}{\Delta h_n^A} .$$

A.2.3 Derivatives of f_{n3}

There are two cases. Case 2 is when the to-junction is a break or a G-source. Case 1 includes all the other cases including p-sources.

Case 1

$$(j_{31})_n = 0$$

$$(j_{32})_n = 0$$

$$(j_{33})_n = (\xi_n^E)^2\left(\frac{G_n^E}{\rho_n^E} - \frac{\partial p_{to}^+}{\partial G_n^E}\right) - \frac{1}{2}\left(\frac{\Phi^2}{\rho_f}\right)_n^E \frac{\partial}{\partial G_n^E}\kappa_n^E$$

$$(j_{34})_n = (\xi_n^E)^2\left[1 - \frac{1}{2}\left(\frac{G^2}{\rho}\right)_n^E\left(\frac{\partial \rho}{\partial p}\right)_n^A + \frac{1}{2}\left(\frac{\partial B}{\partial p}\right)_n^E - \frac{\partial p_{to}^+}{\partial p_n^E}\right] - \frac{\kappa_n^E}{2}\left(\frac{\partial}{\partial p}\frac{\Phi^2}{\rho_f}\right)_n^E$$

$$(j_{35})_n = (\xi_n^E)^2\left[-\frac{1}{2}\left(\frac{G_n^E}{\rho_n^E}\right)^2\left(\frac{\partial \rho}{\partial h}\right)_n^E + \frac{1}{2}\left(\frac{\partial B}{\partial p}\right)_n^E - \frac{\partial p_{to}^+}{\partial h_n^E}\right]\frac{\partial h_n^E}{\partial h_n^{av}} - \frac{k_n^E}{2}\left(\frac{\partial}{\partial h}\frac{\Phi^2}{\rho_f}\right)_n^E \frac{\partial h_n^E}{\partial h_n^{av}}$$

In THYDE-P2, only $p(G)$- or $p(t)$-source is considered (see BB13) so that we can set in the above

$$\frac{\partial p_{to}^+}{\partial h_n^E} = 0$$

and

$$\frac{\partial p_{to}^-}{\partial p_n^E} = 0 .$$

Case 2a : break

If the to-junction is a break, then

$$(j_{31})_n = 0$$

$$(j_{32})_n = 0$$

$$(j_{33})_n = \frac{f_B(p_n^E,\ G_n^E + \Delta G_n^E,\ h_n^E) - f_B(p_n^E,\ G_n^E,\ h_n^E)}{\Delta G_n^E}$$

$$(j_{34})_n = \frac{f_B(p_n^E + \Delta p_n^E,\ G_n^E,\ h_n^E) - f_B(p_n^E,\ G_n^E,\ h_{nN}^E)}{\Delta p_n^E}$$

and

$$(j_{35})_n = \frac{[f_B(p_n^E,\ G_n^E,\ h_n^E + \Delta h_n^E) - f_B(p_n^E,\ G_n^E,\ h_n^E)]\ \partial h_n^E / \partial h_n^{av}}{\Delta h_n^E}$$

Case 2b : G-source

If the to-junction is a G-source given by Eq. (2–2–84), i.e.,

$$(f_3)_n = G_n^E - G(p_n^E) = 0$$

where G is a given function, then we have

$$(j_{31})_n = 0$$

$$(j_{32})_n = 0$$

$$(j_{33})_n = 1$$

$$(j_{34})_n = -\frac{\partial G}{\partial p_n^E}$$

and

$$(j_{35})_n = -\frac{\partial G}{\partial h_n^E}\ \frac{\partial h_n^E}{\partial h_n^{av}} \quad .$$

In THYDE-P2, we consider only $G(t)$- or $G(p)$-source (see BB13) so that we can set in the above

$$\frac{\partial G}{\partial h_n^E} = 0 \quad .$$

A.2.4 Derivatives of f_{n4}

$$(j_{41})_n = \frac{2G_n^A}{\rho_n^A} - \frac{1}{4}\left(\frac{\Phi^2}{\rho_f}\right)_n^{av} \frac{\partial}{\partial G_n^{av}}\left[\kappa_n^{av} + \frac{f_n^{av} L_n}{D_n} G_n^{av} | G_n^{av} |\right] - \frac{L_n}{2\Delta t} + \frac{g}{2}\left(\frac{\partial}{\partial G}\rho L_{head}\right)_n^{av}$$

$$(j_{42})_n = 1 - \left(\frac{G_n^A}{\rho_n^A}\right)^2 \left(\frac{\partial \rho}{\partial p}\right)_n^A + \left(\frac{\partial B}{\partial p}\right)_n^A - \frac{1}{4}\left(\kappa_n^{av} + \frac{f_n^{av} L_n}{D_n} G_n^{av} | G_n^{av} |\right)\left(\frac{\partial}{\partial p}\frac{\Phi^2}{\rho_f}\right)_n^{av}$$
$$+ \frac{g}{2}\left(\frac{\partial}{\partial p}\rho L_{head}\right)_n^{av}$$

$$(j_{43})_n = -\frac{2G_n^E}{\rho_n^E} - \frac{1}{4}\left(\frac{\Phi^2}{\rho_f}\right)_n^{av} \frac{\partial}{\partial G_n^{av}}\left(\kappa_n^{av} + \frac{f_n^{av} L_n}{D_n} G_n^{av} | G_n^{av} |\right) - \frac{L_n}{\partial \Delta t} + \frac{g}{2}\left(\frac{\partial}{\partial G}\rho L_{head}\right)_n^{av}$$

$$(j_{44})_n = -1 + \left(\frac{G_n^E}{\rho_n^E}\right)^2 \left(\frac{\partial \rho}{\partial p}\right)_n^E - \left(\frac{\partial B}{\partial p}\right)_n^{av} - \frac{1}{4}\left(\kappa_n^{av} + \frac{f_n^{av} L_n}{D_n} G_n^{av} | G_n^{av} |\right)\left(\frac{\partial}{\partial p}\frac{\Phi^2}{\rho_f}\right)_n^{av}$$
$$+ \frac{g}{2}\left(\frac{\partial}{\partial p}\rho L_{head}\right)_n^{av}$$

and

$$(j_{45})_n=\left[-\left(\frac{G_n^A}{\rho_n^A}\right)^2\left(\frac{\partial\rho}{\partial h}\right)_n^A+\left(\frac{\partial B}{\partial h}\right)_n^A\right]\frac{\partial h_n^A}{\partial h_n^{av}}-\left[-\left(\frac{G_n^E}{\rho_n^A}\right)^2\left(\frac{\partial\rho}{\partial h}\right)_n^E+\left(\frac{\partial B}{\partial h}\right)_n^E\right]\frac{\partial h_n^E}{\partial h_n^{av}}$$
$$-\frac{1}{2}\left(\kappa_n^{av}+\frac{f_n^{av}L_n}{D_n}G_n^{av}\,|\,G_n^{av}\,|\right)_n^{av}\left(\frac{\partial}{\partial h}\frac{\Phi^2}{\rho_f}\right)_n^{av}+g\left(\frac{\partial}{\partial h}\rho L_{head}\right)_n^{av}$$

A.2.5 Derivatives of f_{n5}

$$(j_{51})_n=\frac{h_n^A}{L_n}$$

$$(j_{52})_n=-\frac{h_n^{av}}{2\Delta t}\left(\frac{\partial\rho}{\partial h}\right)_n^{av}$$

$$(j_{53})_n=\frac{h_n^E}{L_n}$$

$$(j_{54})_n=-\frac{h_n^{av}}{2\Delta t}\left(\frac{\partial\rho}{\partial h}\right)_n^{av}$$

and

$$(j_{55})_n=\frac{G_n^A}{L_n}\frac{\partial h_n^A}{\partial h_n^{av}}-\frac{G_n^E}{L_n}\frac{\partial h_n^E}{\partial h_n^{av}}-\frac{\rho_n^{av}+h_n^{av}(\partial\rho/\partial h)_n^{av}}{\Delta t}$$

A.3 Matrix $(\boldsymbol{b}_{ij})_n$ (i, j = to, from)

To obtain matrix $(\boldsymbol{b}_{ij})_n$, we have to obtain matrices

$$\boldsymbol{r}_n=\begin{bmatrix}\partial\boldsymbol{f}_n/\partial\boldsymbol{x}_{from}^+\\ \partial\boldsymbol{f}_n/\partial\boldsymbol{x}_{to}^+\end{bmatrix}$$

and

$$\boldsymbol{l}_n=\begin{bmatrix}\partial\boldsymbol{f}_{from}^+/\partial\boldsymbol{x}_n\\ \partial\boldsymbol{f}_{to}^+/\partial\boldsymbol{x}_n\end{bmatrix}.$$

A.3.1 Matrix $\boldsymbol{r}_n$

$$\frac{\partial\boldsymbol{f}_n}{\partial\boldsymbol{x}_{from}^+}=\begin{bmatrix}\partial f_{n1}/\partial p_{from}^+ & \partial f_{n1}/\partial h_{from}^+\\ \partial f_{n2}/\partial p_{from}^+ & \partial f_{n2}/\partial h_{from}^+\\ \partial f_{n3}/\partial p_{from}^+ & \partial f_{n3}/\partial h_{from}^+\\ \partial f_{n4}/\partial p_{from}^+ & \partial f_{n4}/\partial h_{from}^+\\ \partial f_{n5}/\partial p_{from}^+ & \partial f_{n5}/\partial h_{from}^+\end{bmatrix}$$

$$=\begin{bmatrix}r_{11n} & r_{12n}\\ r_{21n} & r_{22n}\\ r_{31n} & r_{32n}\\ r_{41n} & r_{42n}\\ r_{51n} & r_{52n}\end{bmatrix}$$

and

$$\frac{\partial\boldsymbol{f}_n}{\partial\boldsymbol{x}_{to}^+}=\begin{bmatrix}\partial f_{n1}/\partial p_{to}^+ & \partial f_{n1}/\partial h_{to}^+\\ \partial f_{n2}/\partial p_{to}^+ & \partial f_{n2}/\partial h_{to}^+\\ \partial f_{n3}/\partial p_{to}^+ & \partial f_{n3}/\partial h_{to}^+\\ \partial f_{n4}/\partial p_{to}^+ & \partial f_{n4}/\partial h_{to}^+\\ \partial f_{n5}/\partial p_{to}^+ & \partial f_{n5}/\partial h_{to}^+\end{bmatrix}$$

$$= \begin{bmatrix} r_{13n} & r_{14n} \\ r_{23n} & r_{24n} \\ r_{33n} & r_{34n} \\ r_{43n} & r_{44n} \\ r_{53n} & r_{54n} \end{bmatrix}$$

where

$$r_{11} = \frac{\partial f_{n1}}{\partial p^+_{from}} = 0$$

$$r_{12} = \frac{\partial f_{n1}}{\partial h^+_{from}} = 0$$

$$r_{13} = \frac{\partial f_{n1}}{\partial p^-_{to}} = 0$$

$$r_{14} = \frac{\partial f_{n1}}{\partial h^+_{to}} = 0$$

$$r_{21} = \frac{\partial f_{n2}}{\partial p^+_{from}} = 0 \qquad \text{for break}$$

$$= \frac{\partial f_{n2}}{\partial p^+_{from}} = (\xi^A_n)^2 \qquad \text{otherwise}$$

$$r_{22} = \frac{\partial f_{n2}}{\partial^+_{from}} = 0 \qquad \text{for break}$$

$$= \frac{\partial f_{n2}}{\partial p^+_{from}} = (\xi^A_n)^2 \left[\left(\frac{G^A_n}{\rho^A_n} \right)^2 \left(\frac{\partial \rho}{\partial h} \right)^A_n - \left(\frac{\partial B}{\partial h} \right)^A_n \right] \frac{\partial h^A_n}{\partial h^+_{from}} - \frac{\kappa^A_n}{2} \left(\frac{\partial}{\partial h} \frac{\Phi^2}{\rho_f} \right)^A_n \frac{\partial h^A_n}{\partial h^+_{from}} \qquad \text{otherwise}$$

$$r_{23} = \frac{\partial f_{n2}}{\partial p^+_{to}} = 0$$

$$r_{24} = \frac{\partial f_{n2}}{\partial h^+_{to}} = 0$$

$$r_{31} = \frac{\partial f_{n3}}{\partial p^+_{from}} = 0$$

$$r_{32} = \frac{\partial f_{n3}}{\partial h^+_{from}} = 0$$

$$r_{33} = \frac{\partial f_{n3}}{\partial p^+_{to}} = 0 \qquad \text{for break or } G\text{-source}$$

$$= \frac{\partial f_{n3}}{\partial p^+_{to}} = (\xi^E_n)^2 \qquad \text{otherwise}$$

$$r_{34} = \frac{\partial f_{n3}}{\partial h^+_{to}} = \frac{\partial f_{n3}}{\partial h^E_n} \frac{\partial h^E_n}{\partial h^+_{to}}$$

with

$$\frac{\partial f_{n3}}{\partial h^E_n} = \frac{f_B(p^E_n, G^E_n, h^E_n + \Delta h^E_n) - f_B(p^E_n, G^E_n, h^E_n)}{\Delta h^E_n} \qquad \text{for break}$$

$$= -\frac{\partial G}{\partial h^E_n} \qquad \text{for } G\text{-source}$$

$$= (\xi^E_n)^2 \left[\frac{1}{2} \left(-\frac{G^E_n}{\rho^E_n} \right)^2 \left(\frac{\partial \rho}{\partial h} \right)^E_n + \frac{1}{2} \left(\frac{\partial B}{\partial h} \right)^E_n - \frac{\partial p^+_{to}}{\partial h^E_n} \right] - \frac{\kappa^E_n}{2} \left(\frac{\partial}{\partial h} \frac{\Phi^2}{\rho_f} \right)^E_n \qquad \text{otherwise}$$

$$r_{41}=\frac{\partial f_{n4}}{\partial p^{+}_{from}}=0$$

$$r_{42}=\frac{\partial f_{n4}}{\partial h^{+}_{from}}=\frac{\partial f_{n4}}{\partial h^{A}_{n}}\frac{\partial h^{A}_{n}}{\partial h^{+}_{from}}=\left[-\left(\frac{G^{A}_{n}}{\rho^{A}_{n}}\right)^{2}\left(\frac{\partial \rho}{\partial h}\right)^{A}_{n}+\left(\frac{\partial B}{\partial h}\right)^{A}_{n}-\frac{g}{2}\left(\frac{\partial}{\partial h}\rho L_{head}\right)^{av}_{n}\right.$$
$$\left.-\frac{1}{4}\left(\kappa^{av}_{n}-\frac{f^{av}_{n}L_{n}}{D_{n}}G^{av}_{n}\,|\,G^{av}_{n}\,|\right)\left(\frac{\partial}{\partial h}\frac{\Phi^{2}}{\rho_{f}}\right)^{av}_{n}\right]\frac{\partial h^{A}_{n}}{\partial h^{+}_{from}}$$

$$r_{43}=\frac{\partial f_{n4}}{\partial p^{-}_{to}}=0$$

$$r_{44}=\frac{\partial f_{n4}}{\partial h^{+}_{to}}=\frac{\partial f_{n4}}{\partial h^{E}_{n}}\frac{\partial h^{E}_{n}}{\partial h^{+}_{to}}=\left[-\left(\frac{G^{E}_{n}}{\rho^{E}_{n}}\right)^{2}\left(\frac{\partial \rho}{\partial h}\right)^{E}_{n}\quad\left(\frac{\partial B}{\partial h}\right)^{E}_{n}-\frac{1}{4}\left(\kappa^{av}_{n}\right.\right.$$
$$\left.\left.-\frac{f^{av}_{n}L_{n}}{D_{n}}G^{av}_{n}\,|\,G^{av}_{n}\,|\right)\left(\frac{\partial}{\partial h}\frac{\Phi^{2}}{\rho}\right)^{av}_{n}+\frac{g}{2}\left(\frac{\partial}{\partial h}\rho L_{head}\right)^{av}_{n}\right]\frac{\partial h^{E}_{n}}{\partial h^{+}_{to}}$$

$$r_{51}=\frac{\partial f_{n5}}{\partial p^{+}_{from}}=0$$

$$r_{52}=\frac{\partial f_{n5}}{\partial h^{+}_{from}}=\frac{\partial f_{n5}}{\partial h^{A}_{n}}\frac{\partial h^{E}_{n}}{\partial h^{+}_{from}}=\frac{G^{A}_{n}}{L_{n}}\frac{\partial h^{A}_{n}}{\partial h^{+}_{from}}$$

$$r_{53}=\frac{\partial f_{n5}}{\partial p^{-}_{to}}=0$$

and

$$r_{54}=\frac{\partial f_{n5}}{\partial h^{-}_{to}}=\frac{\partial f_{n5}}{\partial h^{E}_{n}}\frac{\partial h^{E}_{n}}{\partial h^{+}_{to}}=-\frac{G^{E}_{n}}{L_{n}}\frac{\partial h^{E}_{n}}{\partial h^{+}_{to}}$$

Thus, in general, matrices $\partial \boldsymbol{f}_{n}/\partial \boldsymbol{x}^{+}_{from}$ and $\partial \boldsymbol{f}_{n}/\partial \boldsymbol{x}^{-}_{to}$ have the following forms,

$$\frac{\partial \boldsymbol{f}_{n}}{\partial \boldsymbol{x}^{+}_{from}}=\begin{bmatrix} 0 & 0 \\ r_{21} & r_{22} \\ 0 & 0 \\ 0 & r_{42} \\ 0 & r_{52} \end{bmatrix}$$

and

$$\frac{\partial \boldsymbol{f}_{n}}{\partial \boldsymbol{x}^{+}_{to}}=\begin{bmatrix} 0 & 0 \\ 0 & 0 \\ r_{33} & r_{34} \\ 0 & r_{44} \\ 0 & r_{54} \end{bmatrix}.$$

A.3.2 Matrix $\boldsymbol{l}_{n}$

Let

$$\frac{\partial \boldsymbol{f}^{+}_{from}}{\partial \boldsymbol{x}_{n}}=\begin{bmatrix} l_{11n} & l_{12n} & l_{13n} & l_{14n} & l_{15n} \\ l_{21n} & l_{22n} & l_{23n} & l_{24n} & l_{25n} \end{bmatrix}$$

and

$$\frac{\partial \boldsymbol{f}^{+}_{to}}{\partial \boldsymbol{x}_{n}}=\begin{bmatrix} l_{31n} & l_{32n} & l_{33n} & l_{34n} & l_{35n} \\ l_{41n} & l_{42n} & l_{43n} & l_{44n} & l_{45n} \end{bmatrix}.$$

If the from-junction is normal, then

$$(l_{11})_{n}=A_{n}$$

$$(l_{21})_n = 0$$

and

$$(l_{25})_n = -\eta_n^A \quad .$$

If the from-junction is a mixing junction, then

$$(l_{11})_n = A_n$$

$$(l_{21})_n = A_n h_n^A$$

and

$$(l_{25})_n = A_n G_n^A \frac{\partial h_n^A}{\partial h_n^{av}} \quad .$$

If the from-junction is a break, then

$$(l_{11})_n = 0$$

$$(l_{21})_n = 0$$

and

$$(l_{25})_n = 0 \quad .$$

If the to-junction is normal, then

$$(l_{33})_n = -A_n$$

$$(l_{43})_n = 0$$

and

$$(l_{45})_n = -1 + \eta_n^E \quad .$$

If the to-junction is a mixing junction, then

$$(l_{33})_n = -A_n$$

$$(l_{43})_n = -A_n h_n^E$$

and

$$(l_{45})_n = -A_n G_n^E \frac{\partial h_n^E}{\partial h_n^{av}} \quad .$$

Thus, we can see that in general

$$\frac{\partial \boldsymbol{f}_{from}^+}{\partial \boldsymbol{x}_n} = \begin{bmatrix} l_{11} & 0 & 0 & 0 & 0 \\ l_{21} & 0 & 0 & 0 & l_{25} \end{bmatrix}$$

and

$$\frac{\partial \boldsymbol{f}_{to}^+}{\partial \boldsymbol{x}_n} = \begin{bmatrix} 0 & 0 & l_{33} & 0 & 0 \\ 0 & 0 & l_{43} & 0 & l_{45} \end{bmatrix} \quad .$$

A.3.3 Matrix $(\boldsymbol{b}_{ij})_n$ (i, j = to, from)

Let

$$J_n^{-1}=\begin{bmatrix} r_{11n} & r_{12n} & r_{13n} & r_{14n} & r_{15n} \\ r_{21n} & r_{22n} & r_{23n} & r_{24n} & r_{25n} \\ r_{31n} & r_{32n} & r_{33n} & r_{34n} & r_{35n} \\ r_{41n} & r_{42n} & r_{43n} & r_{44n} & r_{45n} \\ r_{51n} & r_{52n} & r_{53n} & r_{54n} & r_{55n} \end{bmatrix} .$$

Then

$$(\boldsymbol{b}_{from,\ from})_n$$

$$=\begin{bmatrix} l_{11}\gamma_{12}r_{21} & l_{11}(\gamma_{12}r_{22}+\gamma_{14}r_{42}-\gamma_{15}r_{52}) \\ (l_{21}\gamma_{12}+l_{25}\gamma_{52})r_{21} & l_{21}(\gamma_{12}r_{22}+\gamma_{12}r_{42}+\gamma_{15}r_{52}) \\ & +l_{25}(\gamma_{52}r_{22}+\gamma_{54}r_{42}+\gamma_{55}r_{52}) \end{bmatrix}_n$$

$$(\boldsymbol{b}_{from,\ to})_n$$

$$=\begin{bmatrix} l_{11}\gamma_{13}r_{33} & l_{11}(\gamma_{13}r_{34}+\gamma_{14}r_{44}+\gamma_{15}r_{54}) \\ (l_{21}\gamma_{13}+l_{25}\gamma_{53})\gamma_{33} & l_{21}(\gamma_{13}r_{34}+\gamma_{14}r_{44}+\gamma_{15}r_{54}) \\ & +l_{25}(\gamma_{53}r_{34}+\gamma_{54}r_{44}+\gamma_{55}r_{54}) \end{bmatrix}_n$$

$$(\boldsymbol{b}_{to,\ from})_n$$

$$=\begin{bmatrix} l_{33}\gamma_{32}r_{21} & l_{33}(\gamma_{32}r_{22}+\gamma_{34}r_{42}-\gamma_{35}r_{52}) \\ (l_{43}\gamma_{32}+l_{45}\gamma_{52})r_{21} & l_{43}(\gamma_{32}r_{22}+\gamma_{34}r_{42}-\gamma_{35}r_{52}) \\ & +l_{45}(\gamma_{52}r_{22}+\gamma_{54}r_{42}+\gamma_{55}r_{52}) \end{bmatrix}_n$$

and

$$(\boldsymbol{b}_{to,\ to})_n$$

$$=\begin{bmatrix} l_{33}\gamma_{33}r_{33} & l_{33}(\gamma_{33}r_{34}+\gamma_{34}r_{44}+\gamma_{35}r_{54}) \\ (l_{43}\gamma_{33}+l_{45}\gamma_{53})r_{33} & l_{43}(\gamma_{33}r_{34}+\gamma_{34}r_{44}+\gamma_{35}r_{54}) \\ & +l_{45}(\gamma_{53}r_{34}+\gamma_{54}r_{44}+\gamma_{55}r_{54}) \end{bmatrix}_n$$

A.4 Matrix $\boldsymbol{m}_j$

If junction j is a normal junction, then

$$\boldsymbol{m}_j=\begin{bmatrix} 0 & 0 \\ 0 & 1 \end{bmatrix} .$$

If junction j is a break, then

$$\boldsymbol{m}_j=\begin{bmatrix} 1 & 0 \\ 0 & 1 \end{bmatrix} .$$

If junction j is a mixing junction, then

$$\boldsymbol{m}_j=\frac{V_j}{\Delta t}\begin{bmatrix} (\partial\rho/\partial p)_j^+ & (\partial\rho/\partial h)_j^+ \\ h_j^+(\partial\rho/\partial p)_j^+ & \rho_j^+ + h_j^+(\partial\rho/\partial h)_j^+ \end{bmatrix} .$$

A.5 $\boldsymbol{F}_{j,\ from}$ and $\boldsymbol{F}_{j,\ to}$

$$\boldsymbol{F}_{j,\ from}=\begin{bmatrix} c_2 \\ c_1 \end{bmatrix}$$

and

$$\boldsymbol{F}_{j,\ to}=\begin{bmatrix} c_3 \\ c_4 \end{bmatrix}$$

where

$$c_1=(l_{33}\sum^{5}\gamma_{3i}f_i)_{from}$$

$$c_2=(l_{43}\sum_{i=1}^{5}\gamma_{3i}f_i+l_{45}\sum_{i=1}^{5}\gamma_{5i}f_i)_{from}$$

$$c_3=(l_{11}\sum_{i=1}^{5}\gamma_{1i}f_i)_{to}$$

and

$$c_4=(l_{21}\sum_{i=1}^{5}\gamma_{1i}f_i+l_{45}\sum_{i=1}^{5}\gamma_{2i}f_i)_{to}\quad .$$

Appendix B Nomenclature

In the following, the symbols for use in this report will be shown along with their units, e.g., kcal/m²/sec. In general, a unit written as $A/B/C/\cdots/H$ should be understood to be

$$\frac{A}{BC\ \cdots\ H}$$

For example, we have

$$\mathrm{k\,cal/m^2/sec} = \frac{\mathrm{k\,cal}}{\mathrm{m^2 \times sec}}$$

B.1 Alphabetic Symbols

a	Normalized pump speed (–)
A	Cross-sectional area of flow (m^2)
A_g	Flow area of the 3 × 3 fuel rod matrix (m^2)
b	Normalized hydraulic pump torque (–)
b_i	See **Fig. 3–2–2**
B	Momentum flux due to u_{rel} defined by Eq. (2–2–12)
$\boldsymbol{B}$	Matrix defined by Eq. (2–2–20)
BL	Percent blockage (–)
c_c	Convertion ratio (–)
c_D	Discharge coefficient for critical flow (–)
c_{eff}	Discharge coefficient for non-critical flow
c_i	Normalized concentration of i-th delayed neutron group (–)
c_p	Specific heat (kcal/m³/°C)
$\boldsymbol{C}$	Matrix defined by Eq. (2–3–53)
c_{VH}	Sign of L_H (–)
d	Effective diameter of the shell (m)
d_b	Diameter of the burst rod node (m)
d_n	Diameter of the non-burst rod node (m)
D	Hydraulic diameter (m)
e	$= r_{CL}^{ino}/r_R^o$
e_i	Factor defined by Eq. (3–2–21)
E_i	Heat transfer rate from pressurizer heater i (kcal/sec)
E_{loss}	Heat loss from Tank (kcal/sec)
E_y	Young's modulus for cladding (kg/m/sec²)
E_I	Quantity defined in conjunction with Eq. (2–4–2) (kcal/sec)
E_{II}	Quantity defined in conjunction with Eq. (2–4–3) (kcal/sec)
$\boldsymbol{f}$	Friction factor (–)
$(f_1^+)_j$	Function defined by Eq. (2–3–11) for junction j
$(f_2^+)_j$	Function defined by Eq. (2–3–12) for junction j
$(f_1)_n$	Function defined by Eq. (2–3–4) for node n
$(f_2)_n$	Function defined by Eq. (2–3–5) for node n
$(f_3)_n$	Function defined by Eq. (2–3–6) for node n
$(f_4)_n$	Function defined by Eq. (2–3–7) for node n

$(f_5)_n$	Function defined by Eq. (2–3–8) for node
g	Gravitational acceleration (m/sec^2)
g_M	Critical mass velocity by Moody (kg/m^2/sec)
G	Mass velocity (kg/m^2/sec)
$\boldsymbol{G}$	Function vector defined by Eq. (2–3–54)
G_r	Grashof number (–)
G_t'	= 273 kg/m^2/sec (transition mass flux)
G_r	Specific enthalpy (kcal/kg)
h	Rod-to-rod rediative heat transfer coefficient for burst rod (kcal/m^2/sec/°C)
h_b	Conventional heat transfer coefficient (kcal/m^2/sec/°C)
h_{cvn}	Gap conductivity without radiation (kcal/m^2/sec/°C)
h^t_{gap}	Total gap conductivity (kcal/m^2/sec/°C)
h_n	Rod-to-rod radiative heat transfer coefficient for non-burst rod (kcal/m^2/sec/°C)
h_{rad}	Radiative heat transfer coefficient between pellet and cladding (kcal/m^2/sec/°C)
h^c_{tr}	Coefficient of heat transfer from cladding coolant (kcal/m^2/sec/°C)
h^{cs}_{tr}	Coefficient of total heat transfer from non-burst cladding node (kcal/m^2/sec/°C)
h^{cs*}_{tr}	Coefficient to total heat transfer from burst cladding node (kcal/m^2/sec/°C)
h_{w-c}	Rod-to-coolant radiative heat transfer coefficient (kcal/m^2/sec/°C)
H^F_Q	Head-discharge curve for positive speeds (–)
H^R_Q	Head-discharge curve for negative speeds (–)
H^F_W	Head-speed curve for forward flow (–)
H^R_W	Head-speed curve for reverse flow (–)
I	Enthalpy flux due to u_{rel} defined with Eq. (2–2–13)
I_m	Moment of inertia (kg·m^2/rad^2)
IS	Water state index
IST	Tank state index
J	Number of normal junctions
$\boldsymbol{J}$	Jacobian matrix of thermal-hydraulic network
J_e	Mechanical equivalent of heat (kg·m^2/sec^2/kcal)
$\boldsymbol{J}_n$	Jacobian matrix associated with node n
k	Loss coefficient (–)
l	Neutron life (sec)
l_k	Size of junction group k
l_p	Fuel cell pitch (m)
l_w	Wetted perimeter (m)
L	Length of node (m)
L_H	Height of node (m)
L_{head}	Pump head (m)
L_i	Height of the pressurizer heater i (i = 1, 2 and 3) (m)
$\boldsymbol{L}_n$	Jacobian matrix defined in Eq. (2–3–23)
m	Mass flow rate (kg/sec)
M	Mass (kg)
M_i	Molecular weight of the i-th component of gap gas mixture
M_b	Number of non-burst off-diagonal rods of the 3×3 rod matrix when the center rod is burst
M_n	Number of non-burst off-diagonal rods of the 3×3 rod matrix when the center rod is non-burst
N	Mols of gas in fuel rod

N	Number of normal nodes
n	Normalized neutron density (–)
N_f	Number of radial nodes in fuel pellet
n_{gap}	Number of component gases in the gap gas
N_R	Number of radial nodes in fuel rod
n_{SG}	Number of SG U-tubes
N_b	Number of non-burst diagonal rods when the center rod is burst
N_n	Number of non-burst diagonal rods when the center rod is not burst
$NPSH_r$	Required net positive suction head (m)
p	Pressure (kgw/m²)
p_{flow}	Coolant flow pressure (kgw/m²)
p_{gc}	Contact pressure between pellet and cladding
p_{head}	Normalized pump head (–)
p_{ref}	Container pressure (kgw/m²)
Pr	Prandtl number (–)
q	Number of chains with at least one normal junction
$q_{rad,b}$	Rod-to-rod radiative heat flux from the burst rod (kcal/m²/sec)
$q_{rad,n}$	Rod-to-rod radiative heat flux from the non-burst rod (kcal/m²/sec)
Q	Heat transfer rate (kcal/sec)
q'''	Power density (kcal/sec/m³)
r_c	Cladding thickness (m)
r_{CL}^{in}	Cladding inner radius (m)
r_F	Fuel pellet radius (m)
r_m	Average clad radius (m)
r_{gap}	Average clad radius (m)
r_R	Fuel rod diameter (m)
r^*_{Rmax}	Maximum radius of burst rod (m)
R_{ACT}	Normalized actinides power decay (–)
Re	Reynolds number (–)
Re_t	Transition Reynolds number (–)
R_g	Perfect gas constant (kcal/sec)
R_{FP}	Normalized power decay from fission products (–)
$\boldsymbol{R}_n$	Jacobian matrix defined in Eq. (2–3–23)
R_{29}	Normalized power decay from (–)
R_{39}	Normalized power decay from (–)
s_n	Area of radial node of fuel rod (m²)
S	Plastic/burst hoop strain at middle point of clad (–)
S_{in}	Plastic/burst strain of clad inner surface (–)
S_{int}	Interfacial area between gas and liquid (m²)
S_{out}	Plastic/burst strain of clad outer surface (–)
S_p	Elastic strain of cladding inner radius due to pressure change
S_t	Elastic strain of cladding inner radius due to temperature change (m)
S_α	Function of defined in conjunction with Eq. (2–1–5)
T	Temperature (°C)
$\langle T \rangle$	Average temperature (°C)
T_b	Coolant bulk temperature (°C)
T_{burst}	Burst temperature (°C)
$T_{C,k}$	Temperature of coolant region k (°C)

$T_{F,k}$	Temperature of fuel region k (°C)
T_R^b	Clad surface temperature of burst node (°C)
T_R^n	Clad surface temperature of non-burst node (°C)
Te	Electric torque (kg·m²/sec²/rad)
T_h	Hydraulic torque (kg·m²/sec²/rad)
T_r	Rated torque (kg·m²/sec²/rad)
T_Ω^F	Torque-discharge curve for positive speed (–)
T_Ω^R	Torque-discharge curve for negative speed (–)
T_w^F	Torque-speed curve for forward flow (–)
T_w^R	Torque-speed curve for reverse flow (–)
u	Velocity (m/sec)
u_{gj}	Drift velocity (m/sec)
u_{rel}	Relative velocity between vapor and liquid (m/sec)
U	Internal energy (kcal/sec)
v	Specific volume (m³/kg)
V	Volume (m³)
w	Normalized volumetric flow rate (–)
W	Volumetric flow rate (m³/sec)
x	Mass quality (–)
$\boldsymbol{x}$	State vector defined by Eq. (2–3–1)
$\boldsymbol{x}_n$	State vector of normal node n (n = 1, 2, ... N)
$\boldsymbol{x}_{N+1}$	Junctions vector defined by Eq. (2–3–3)
y_i	Molecular fraction of the i-th component to gas gas (–)
z_w	Water level (m)
z	Coordinate along initial coolant flow (m)

B.2 Greek and Russian Symbols

α	Void fraction (–)
α	Linear coefficient of thermal expansion (°C⁻¹)
β	Delayed neutron fraction (–)
β_i	Delayed neutron fraction of the i-th group (–)
γ	Isentropic exponent (–)
$\gamma_{T,k}$	Temperature coefficient of reactivity in fuel region k (°C⁻¹)
$\gamma_{\alpha,k}$	Void coefficient of reactivity in coolant region k (–)
$(\gamma_{ij})_n$	(i, j) component of the inverse of the node Jacobian matrix J_n
Γ_{tot}	Total reactivity ($)
Γ_{ex}	External reactivity ($)
$\Gamma_{f,k}$	Reactivity coefficient for fuel temperature of region k ($/°C)
Γ_g	Gas generation rate (kg/m³/sec)
$\Gamma_{c,k}$	Reactivity coefficient for void fraction of region k ($)
Δh_{reac}	Heat of metal-water reaction (kcal/kg)
ΔT_{sub}	Subcooling (°C)
ε_{cl}	Emissivity of cladding (–)
ε_1	Emissivity of the center rod surface of the 3 × 3 rod matrix (–)
ε_2	Equivalent emissivity of the shell surface (–)
η	Delay factor (–)
η_α	Function of defined in conjunction with Eq. (3–5–14) (–)

Ⓗ	Thickness of zircaloy reacted (m)
θ	Clad thickness (m)
κ	Quantity defined by Eq. (2–2–4) ($kg^2/m^4/sec^2$)
Λ	Enthalpy flux defined by Eq. (2–2–11) ($kcal/m^2/sec$)
λ_i	Decay constant of delayed neutron precursor of the i-th group (sec^{-1})
λ	Thermal conductivity (kcal/m/°C/sec)
μ	Viscosity (kg/m/sec)
μ_p	Poisson's ratio for cladding (–)
Ξ	Heat source in the fuel rod ($kcal/m^3/sec$)
Ξ_{MW}	Heat source due to metal-water reaction ($kcal/m^3/sec$)
Π	Normalized total power (–)
ρ	Density (kg/m^3)
σ	Surface tension (m/sec^2)
σ_h	Plastic hoop strain (kgw/m^2)
Σ_a	Macroscopic neutron absorption cross section of fissile material (cm^{-1})
Σ_f	Macroscopic neutron fission cross section of fissile material (cm^{-1})
τ_I	Time constant defined by Eq. (3–2–16) (sec)
τ_{II}	Time constant defined by Eq. (3–2–17) (sec)
	Normalized electric torque (–)
φ	Heat flux ($kcal/m^2/sec$)
Φ^2	Two-phase multiplier (–)
Φ_{ij}	Quantity defined by Eq. (3–3–17) (–)
Ψ	Momentum flux defined by Eq. (2–2–7) ($kg/m/sec^2$)
Ψ_{ij}	Quantity defined by Eq. (3–3–16)
Ω	Pump speed (rpm)

B.3 Subscripts

A	Refers to A point of a node or a chain.
AC	Refers to accumulator condition.
ACD	Refers to the portion of the accumulator duct between AC and the (check) valve.
cd	Refers to crack and dish.
CL	Refers to cladding.
CL	Refers to cold leg.
core	Refers to core.
cs	Refers to condensates.
CHF	Refers to critical heat flux.
d	Refers to falling condensates.
E	Refers to E point of a node or a chain.
en	Refers to pellet envelope.
eye	Refers to pump "eye".
f	Refers to liquid.
from	Refers to from-node or from-junction
F	Refers to fuel pellet or fuel pellet surface.
	Refers to subcooled water.
fb	Refers to fallback effect.
feed	Refers to feed water line to SG.
fg	Refers to change in fluid property when condition changes from saturated water

	to saturated steam.
fs	Refers to liquid especially when it is saturated.
g	Refers to vapor condition.
G	Refers to super heated steam.
gap	Refers to gap between pellet and cladding.
gs	Refers to vapor especially when is saturated.
H_2O	Refers to accumulator water condition.
inj	Refers to injection flow.
j	Refers to loop junction or axial clad node.
L	Refers to laminar film condition corresponding to the temperature T_{SGW} $T_{SG}/2$.
lpl	Refers to lower plenum condition.
n	Refers to loop node or radial fuel node.
n_p	Refers to pump node.
N	Refers to inertial flow.
N_2	Refers to accumulator nitrogen condition.
M	Refers to critical flow.
opn	Refers to valve completely open.
out	Refers to outer surface.
p	Refers to pressurizer as a tank.
pb	Refers to phase boundary of tank.
pD	Refers to the pressurizer duct loop.
r	Refers to rated value.
R	Refers to fuel rod surface.
re	Refers to relief valve condition.
$recirc$	Refers to recirculation flow.
s	Refers to saturated value.
set	Refers to prescribed value.
SG	Refers to SG or to equivalent channel of SG secondary flow.
shr	Refers to SG shroud.
sp	Refers to spray of pressurizer.
$steam$	Refers to steam line flow out of SG.
su	Refers to surge flow.
T	Refers to tank.
to	Refers to to-junction or to-node.
TSG	Refers to entire SG secondary system as a tank.
upl	Refers to upper plenum.
w	Refers to wall condition.
I	Refers to region I of tank.
II	Refers to region II of tank.
o	Refers to initial steady state condition.

B.4 Superscripts

A	Refers to A point of a node or a chain.
E	Refers to E point of a node or a chain.
in	Refers to inner surface.
new	Refers to present time.
NC	Refers to natural convection.

old	Refers to time which is one-time step past.
o	Refers to initial steady state.
out	Refers to outer surface.
*	Refers to cladding condition after burst.
I	Refers to region I of tank.
II	Refers to region II of tank.
+	Refers to junction condition.

Appendix C Symbol Table for Plotter Output

The symbols of plotter output have the following format

XXX – YY

where XXX and YY stand for a variable and an index, respectively. Index YY is used to indicate the number of the node unless specified otherwise. In the following, the symbols as well as their units, the title along the abscissa, the default values for YM1 and YM2 (see subsection 6.2.3) and the type of the ordinate (1 = linear and 2 = logarithmic) will be shown.

***** NORMAL NODE DATA *****

Variable	UNIT	RANGE (MAX/MIN)		TYPE
1 PRA	PRESSURE (PASCAL)	2.000E+07	0.0	1
2 PRA	PRESSURE (PASCAL)	2.000E+07	0.0	1
3 PRA	PRESSURE (PASCAL)	2.000E+07	0.0	1
4 GLA	FLOW (KG/SEC/M**2)	1.000E+05	-1.000E+05	1
5 GLE	FLOW (KG/SEC/M**2)	1.000E+05	-1.000E+05	1
6 GLV	FLOW (KG/SEC/M**2)	1.000E+05	-1.000E+05	1
7 HLA	ENTHALPY (KCAL/KG)	1.500E+03	0.0	1
8 HLE	ENTHALPY' (KCAL/KG)	1.500E+03	0.0	1
9 HLV	ENTHALPY (KCAL/KG)	1.500E+03	0.0	1
10 RHA	DENSITY (KG/M**3)	1.000E+03	0.0	1
11 RHE	DENSITY (KG/M**3)	1.000E+03	0.0	1
12 RHV	DENSITY (KG/M**3)	1.000E+03	0.0	1
13 XLA	QUALITY (-)	2.000E+00	-1.000E+00	1
14 XLE	QUALITY (-)	2.000E+00	-1.000E+00	1
15 XLV	QUALITY (-)	2.000E+00	-1.000E+00	1
16 ALA	VOID FRACTION (-)	1.200E+00	-8.000E-01	1
17 ALE	VOID FRACTION (-)	1.200E+00	-8.000E-01	1
18 ALV	VOID FRACTION (-)	1.200E+00	-8.000E-01	1
19 QQQ	Q (KCAL/SEC/M**3)	1.000E+05	-1.000E+05	1
20 TMP	BULK TEMP (DEG)	1.500E+03	0.0	1

***** PUMP DATA *****

Variable	UNIT	RANGE (MAX/MIN)		TYPE
21 HDP	PUMP HEAD (M)	2.000E+02	0.0	1
22 AAA	PUMP SPEED	1.000E+01	-1.000E+01	1
23 BBB	PUMP TORQUE	1.000E+01	-1.000E+01	1
24 WWW	PUMP FLOW	1.000E+01	-1.000E+01	1

The variables 22 to 24 are relative values with respect to the steady state values.

***** ACCUMULATOR DATA *****

Variable	UNIT	RANGE (MAX/MIN)		TYPE
25 PAC	PRESSURE (PASCAL)	2.000E+07	0.0	1
26 GAJ	FLOW (KG/SEC)	5.000E+04	-5.000E+04	1
27 HAC	ENTHALPY (KCAL/KG)	1.000E+03	0.0	1
28 VAG	GAS VOLUME (M**3)	2.000E+02	0.0	1
29 MAL	LIQUID MASW (KG)	2.000E+02	0.0	1

For variables 25 to 29, index YY should indicate the accumulator number (input subblock number).

***** SG TANK MODEL DATA *****

Variable	UNIT	RANGE(MAX/MIN)		TYPE
30 PSG	PRESSURE (PASCAL)	2.000E+07	0.0	1
31 MUG	FLOW (KG/SEC)	1.000E+04	0.0	1
32 MRG	FLOW (KG/SEC)	1.000E+04	0.0	1
33 WLS	WATER LEVEL (M)	3.000E+01	0.0	1
34 HS1	ENTHALPY (KCAL/KG)	1.000E+03	0.0	1
35 HS2	ENTHALPY (KCAL/KG)	1.000E+03	0.0	1
36 MG1	MASS (KG)	1.000E+05	0.0	1
37 MG2	MASS (KG)	1.000E+05	0.0	1
38 HT1	(KCAL/SEC/M**2/DEG)	1.000E+02	1.000E-03	2
39 HT2	(KCAL/SEC/M**2/DEG)	1.000E+02	1.000E-03	2
40 TW1	WALL TEMP (DEG)	5.000E+02	0.0	1
41 TW2	WALL TEMP (DEG)	5.000E+02	0.0	1

For variables 30 to 37, XX1 and XX2 refer to Regions I and II, respectively. For variables 38 to 41, XX1 and XX2 refer to the primary and secondary sides, respectively. For variables 38 to 41, YY is the number of the corresponding primary node.

***** PRESSURIZER TANK MODEL DATA *****

Variable	UNIT	RANGE(MAX/MIN)		TYPE
42 PPP	PRESSURE (PASCAL)	2.000E+07	0.0	1
43 GPR	FLOW (KG/SEC)	5.000E+04	-5.000E+04	1
44 WLP	WATER LEVEL (M)	3.000E+01	0.0	1
45 MSP	FLOW (KG/SEC)	1.000E+04	0.0	1
46 HP1	ENTHALPY (KCAL/KG)	1.000E+03	0.0	1
47 HP2	ENTHALPY (KCAL/KG)	1.000E+03	0.0	1
48 MS1	MASS (KG)	1.000E+05	0.0	1
49 MS2	MASS (KG)	1.000E+05	0.0	1

Variable XX1 and XX2 refer to Regions I and II, respectively. For variables 42 to 49, YY must be 01.

***** CORE AND FUEL DATA *****

Variable	UNIT	RANGE(MAX/MIN)		TYPE
50 QCR	RELATIVE POWER	2.000E+00	1.000E-03	2
51 PG1	PRESSURE (PASCAL)	2.000E+07	0.0	1
52 PG2	PRESSURE (PASCAL)	2.000E+07	0.0	1
53 HE1	HTR COEFF (KCAL/SEC/M**2/DEG)	1.000E+02	1.000E-03	2
54 HE2	HTR COEFF (KCAL/SEC/M**2/DEG)	1.000E+02	1.000E-03	2
55 HC1	HTR COEFF (KCAL/SEC/M**2/DEG)	1.000E+02	1.000E-03	2
56 HC2	HTR COEFF (KCAL/SEC/M**2/DEG)	1.000E+02	1.000E-03	2
57 HG1	HTR COEFF (KCAL/SEC/M**2/DEG)	1.000E+02	1.000E-03	2
58 HG2	HTR COEFF (KCAL/SEC/M**2/DEG)	1.000E+02	1.000E-03	2
59 LI1	ZR-REACTED IN (M)	1.000E-04	0.0	1
60 LI2	ZR-REACTED IN (M)	1.000E-04	0.0	1
61 LO1	ZR-REACTED OUT (M)	1.000E-04	0.0	1
62 LO2	ZR-REACTED OUT (M)	1.000E-04	0.0	1
63 QM1	Q-MW (KCAL/M**3)	1.000E+06	0.0	1
64 QM2	Q-MW (KCAL/M**3)	1.000E+06	0.0	1
65 TS1	CLAD SURFACE TEMP (DEG)	2.000E+03	0.0	1
66 TS2	CLAD SURFACE TEMP (DEG)	2.000E+03	0.0	1
67 TC1	FUEL CENTER TEMP (DEG)	2.000E+03	0.0	1
68 TC2	FUEL CENTER TEMP (DEG)	2.000E+03	0.0	1
69 STR	PLASTIC HOOP STRESS (KG/M**2)	1.000E+03	0.0	1
70 HST	HOOP STRAIN(-)	1.000E+00	0.0	1
71 BTE	BURST TEMP (DEG)	2.000E+03	0.0	1

Variables XX1 and XX2 refer to non-burst and burst rods, respectively. Heat transfer coefficients HC and HE refer to values obtained from correlations and values obtained by smoothing HC, respectively. For the core and fuel variables except variables 65 to 68, YY must be 01.

```
***** HEAT CONDUCTOR DATA *****

Variable     UNIT                             RANGE(MAX/MIN)              TYPE
 72 BHR   HTR COEFF  (KCAL/SEC/M**2/DEG) 1.000E+02      1.000E-03      2
 73 BHL   HTR COEFF  (KCAL/SEC/M**2/DEG) 1.000E+02      1.000E-03      2
 74 BTR   SURFACE TEMP  (DEG)            2.000E+03      0.0            1
 75 BTL   SURFACE TEMP  (DEG)            2.000E+03      0.0            1
```

In variables 72 to 74, XXR and XXL stand for the right and left of the heat conductor, respectively, and index YY is to be used to show the heat conductor number. Plotting for fuel with gap can be made not by heat conductor variables 72-75, but by core and fuel variables 53-56 and 65-68.

Appendix D Input Data of Sample Problem (PWR LB-LOCA)

D.1 Input Data for First Job

```
  --- THYDE-P2 -------------------------------------------------------------
/
/
/============== ALPHA-DELAY MODEL ( INNER CALC. OPTION ) ===============
/                                                          85/06/10
/
/  **** PROBLEM CONTROL DATA ****
BB01
  0  9  4  18  1  0  5  0  0  90.0
  0
/ 4
/ 43 44 45 46
/
/  **** MINOR EDIT DATA ****
BB02
PRE-11  PRA-12  GLE-25  GLA-25  PRE-32  GLE-36  GLA-37  GLE-11  GLA-12
/
/  **** TIME STEP CONTROL DATA ****
BB03
SB0301
   -2
SB0302
   10  30  50   0   1.0E-3   1.0E-6     0.004
SB0303
   10  40  50   0  64.0E-3   1.0E-6   200.0
SB0304
   50  20  50   0   4.0E-3   1.0E-6    10.0
SB0305
   50  20  50   0  16.0E-3   1.0E-6  1000.0
/
/  **** TRIP CONTROL DATA ****
BB04
SB0401
  1   0   1   0  1000.000 0.0
SB0402
  5  47   1   0      0.4   0.0
SB0403
  5  48   1   0      0.4   0.0
SB0404
  2  10   1   0      0.1   0.0
SB0405
  2  21   1   0      0.1   0.0
SB0406
  3   0   1   0      0.1   0.0
SB0407
  4   1   1   0    20.01   0.0
SB0408
 -4   1   1   0   1000.0   0.0
SB0409
  4   2   1   0    20.01   0.0
SB0410
 -4   2   1   0   1000.0   0.0
SB0411
  4   5   1   0   1000.0   0.0
SB0412
 -4   5   1   0   2000.0   0.0
```

```
SB0413
 6   1  -3   1   240.0   0.005
SB0414
 6   2  -3   1   250.0   0.0
SB0415
 6   3  -3   1   360.0   0.0
SB0416
-6   1   3   1   350.0   0.0
SB0417
-6   2   3   1   305.0   0.0
SB0418
-6   3   3   1   380.0   0.0
/
/  **** PROBLEM OPTION DATA ****
BB07
 0  1  0  2  2  3  1  1
/
/  **** DIMENSION DATA ****
BB08
 51  43  9  2  2  2  1  2  3  2  10  5  24  2  5  5
/
/ ** FLOW AJUST DATA ****
BB09
 1  9000.0  360.0
/
/  **** NODE DATA ****
BB10
SB1001
 1  1 29  1      1  158.42       4.300840E-1  0.0  0.0  0.0
  5.2   0.0    0.0  0.0 -1.0  0.0
SB1002
 2  1  1  2      1  158.60       6.939778E-1  0.0  0.0  0.0
  1.0   0.0    0.0  0.0 -1.0  0.0
SB1003
 3  1  2  3      1  158.68       1.002875E0   0.0  0.0  0.0
  1.5   0.0    0.0  0.0 -1.0  0.0
SB1004
 4  1  3  4      1  158.71       1.306981E0   0.0  0.0  0.0
  2.0   1.6    0.0  0.0 -1.0  0.0
SB1005
 5  7  4  5   3248  158.55       3.141593E-4  0.0  0.0  0.0
  5.0   5.0    0.0  0.0 -1.0  0.0
SB1006
 6  7  5  6   3248  157.8        3.141593E-4  0.0  0.0  0.0
  6.8   5.3    0.0  0.0 -1.0  0.0
SB1007
 7  7  6  7   3248  156.84       3.141593E-4  0.0  0.0  0.0
 11.8 -10.3    0.0  0.0 -1.0  0.0
SB1008
 8  1  7  8      1  157.0        1.306981E0   0.0  0.0  0.0
  1.6  -1.6    0.0  0.0 -1.0  0.0
SB1009
 9  1  8  9      1  156.65       5.026548E-1  0.0  0.0  0.0
 12.9  -3.5    0.0  0.0 -1.0  0.0
SB1010
10  8  9 33      1  155.2        3.848451E-1  0.0  0.0  0.0
  6.6   3.5    0.0  0.0  0.0  1.E2
SB1011
11  1 33 10      1  161.85       3.848451E-1  0.0  0.0  0.0
  1.5   0.0    0.0  0.0 -1.0  0.0
SB1012
12  1 10 32      1  161.6        3.848451E-1  0.0  0.0  0.0
  3.0   0.0    0.0  0.0  0.0  0.0
SB1013
13  1 29 30      3  158.42       4.300840E-1  0.0  0.0  0.0
  2.0   0.0    0.0  0.0  0.0  0.0
```

```
SB1014
14  1 30 11      3  158.4        4.300840E-1  0.0  0.0  0.0
  3.2   0.0    0.0  0.0  0.0  0.0
SB1015
15  1 11 12      3  158.71       1.306981E0   0.0  0.0  0.0
  4.5   1.6    0.0  0.0 -1.0  0.0
SB1016
16  7 12 13   9744  158.55       3.141593E-4  0.0  0.0  0.0
  5.0   5.0    0.0  0.0 -1.0  0.0
SB1017
17  7 13 14   9744  157.8        3.141593E-4  0.0  0.0  0.0
  6.8   5.3    0.0  0.0 -1.0  0.0
SB1018
18  7 14 15   9744  156.84       3.141593E-4  0.0  0.0  0.0
 11.8 -10.3    0.0  0.0 -1.0  0.0
SB1019
19  1 15 16      3  157.0        1.306981E0   0.0  0.0  0.0
  1.6  -1.6    0.0  0.0 -1.0  0.0
SB1020
20  1 16 17      3  156.65       5.026548E-1  0.0  0.0  0.0
 12.9  -3.5    0.0  0.0 -1.0  0.0
SB1021
21  8 17 31      3  155.2        3.848451E-1  0.0  0.0  0.0
  6.6   3.5    0.0  0.0  0.0  1.E2
SB1022
22  1 31 32      3  161.85       3.848451E-1  0.0  0.0  0.0
  4.5   0.0    0.0  0.0  0.0  0.0
SB1023
23  4 32 18      1  161.3        2.746459E0   0.0  0.0  0.0
  8.0  -8.0    0.0  0.0  0.0  0.0
SB1024
24  5 18 34      1  160.8        4.830513E0   0.0  0.0  0.0
  5.0   3.1    0.0  0.0  0.0  0.0
SB1025
25  2 34 19 39800  160.25        1.113829E-4  0.0  0.0  1.32292E-2
  0.3   0.3    0.0  0.0  0.0  0.0
SB1026
26  2 19 35 39800  160.12        1.113829E-4  0.0  0.0  1.32292E-2
  1.0   1.0    0.0  0.0  0.0  0.0
SB1027
27  2 35 20 39800  159.88        1.113829E-4  0.0  0.0  1.32292E-2
  1.0   1.0    0.0  0.0  0.0  0.0
SB1028
28  2 20 21 39800  159.64        1.113829E-4  0.0  0.0  1.32292E-2
  1.0   1.0    0.0  0.0  0.0  0.0
SB1029
29  2 21 37 39800  159.45        1.113829E-4  0.0  0.0  1.32292E-2
  0.3   0.3    0.0  0.0  0.0  0.0
SB1030
30  2 34 22    200  160.25       1.113829E-4  0.0  0.0  1.32292E-2
  0.3   0.3    0.0  0.0  0.0  0.0
SB1031
31  2 22 36    200  160.1200001  1.113829E-4  0.0  0.0  1.32292E-2
  1.0   1.0    0.0  0.0  0.0  0.0
SB1032
32  2 36 23    200  159.8800001  1.113829E-4  0.0  0.0  1.32292E-2
  1.0   1.0    0.0  0.0  0.0  0.0
SB1033
33  2 23 24    200  159.6400001  1.113829E-4  0.0  0.0  1.32292E-2
  1.0   1.0    0.0  0.0  0.0  0.0
SB1034
34  2 24 37    200  159.4500001  1.113829E-4  0.0  0.0  1.32292E-2
  0.3   0.3    0.0  0.0  0.0  0.0
SB1035
35  1 36 35    200  159.9628070  9.079203E-4  0.0  0.0  0.0
  0.1   0.0    5.0  5.0  5.0  5.0
```

```
SB1036
36  1 37 29     1   159.15       9.402473E0   0.0  0.0  0.0
  1.3   1.3   0.0  0.0  0.0  0.0
SB1037
37 13 29 38     1    -5.0        8.851005E0   0.0  0.0  0.0
  2.0   2.0  10.0 10.0  0.0  0.0
SB1038
38 13 30 25     1    -5.0        1.963495E-1  0.0  0.0  0.0
  6.0   3.0   1.0  1.0  0.0  0.0
SB1039
39 13 25 26     1    -5.0        1.963495E-1  0.0  0.0  0.0
  6.0   0.0   0.0  0.0 -1.0  0.0
SB1040
40 13 26 27     1    -5.0        1.963495E-1  0.0  0.0  0.0
  6.0   0.0   0.0  0.0 -1.0  0.0
SB1041
41 13 27 28     1    -5.0        1.963495E-1  0.0  0.0  0.0
  6.0   0.0   0.0  0.0 -1.0  0.0
SB1042
42 13 28 39     1    -5.0        1.963495E-1  0.0  0.0  0.0
  6.0   3.0   0.0  0.0  0.0  0.0
SB1043
43 13 31 40     1   -10.0        7.068583E-2  0.0  0.0  0.0
  0.1   0.0   1.0  0.0  0.0  0.0
SB1044
44 13 31 41     3   -10.0        3.870756E-2  0.0  0.0  0.0
  0.42 -0.42  1.0  0.0  0.0  0.0
SB1045
45 13 33 42     1   -10.0        7.068583E-2  0.0  0.0  0.0
  0.1   0.0   1.0  0.0  0.0  0.0
SB1046
46 13 33 43     1   -10.0        3.870756E-2  0.0  0.0  0.0
  0.42 -0.42  1.0  0.0  0.0  0.0
/
/  **** JUNCTION DATA ****
BB11
     1   1   0.0    0.     0.
     2   1   0.0    0.     0.
     3   1   0.0    0.     0.
     4   1   0.0    0.     0.
     5   1   0.0    0.     0.
     6   1   0.0    0.     0.
     7   1   0.0    0.     0.
     8   1   0.0    0.     0.
     9   1   0.0    0.     0.
    10   1   0.0    0.     0.
    11   1   0.0    0.     0.
    12   1   0.0    0.     0.
    13   1   0.0    0.     0.
    14   1   0.0    0.     0.
    15   1   0.0    0.     0.
    16   1   0.0    0.     0.
    17   1   0.0    0.     0.
    18   1   0.0    0.     0.
    19   1   0.0    0.     0.
    20   1   0.0    0.     0.
    21   1   0.0    0.     0.
    22   1   0.0    0.     0.
    23   1   0.0    0.     0.
    24   1   0.0    0.     0.
    25   1   0.0    0.     0.
    26   1   0.0    0.     0.
    27   1   0.0    0.     0.
    28   1   0.0    0.     0.
    29   2   0.10   0.     0.
    30   4   0.05   0.     0.
```

```
    31   4   0.15   0.      0.
    32   3   0.10   0.      0.
    33   4   0.05   0.      0.
    34   4   0.05   0.      0.
    35   4   0.01   0.      0.
    36   4   0.01   0.      0.
    37   4   0.01   0.      0.
    38   8   0.0    0.      0.
    39   6   0.0    0.      0.
    40   7   0.0    0.      0.
    41   5   0.0    0.      0.
    42   7   0.0    0.      0.
    43   5   0.0    0.      0.
/
/  **** MIXING JUNCTION DATA ****
BB12
SB1201
    29   3    1   13   37   0     0.25   0.75   0.0   0.0
SB1202
    30   2   14   38    0   0     1.0    0.0    0.0   0.0
SB1203
    31   3   22   43   44   0     1.0    0.0    0.0   0.0
SB1204
    32   1   23    0    0   0     1.0    0.0    0.0   0.0
SB1205
    33   3   11   45   46   0     1.0    0.0    0.0   0.0
SB1206
    34   2   25   30    0   0   199.0    1.0    0.0   0.0
SB1207
    35   1   27    0    0   0     1.0    0.0    0.0   0.0
SB1208
    36   2   32   35    0   0     1.0    0.01   0.0   0.0
SB1209
    37   1   36    0    0   0     1.0    0.0    0.0   0.0
/
/  **** HYDRAULIC SOURCE DATA ****
BB13
SB1301
     1     40    1    35.0
   2
   0.0     700.0     1000.0     700.0
SB1302
     2     42    1    35.0
   2
   0.0     700.0     1000.0     700.0
/
/  **** PUMP DATA ****
BB14
SB1401
   10 1 0 1185.0 5.58 4.33E4 105.0 749.0 1150.0 3460.0  0.5 0.0 0.05
SB1402
   21 1 0 1185.0 5.58 4.33E4 105.0 749.0 1150.0 3460.0  0.5 0.0 0.05
/
/  **** PUMP DATA TABLE ****
BB15
SB1501
   1
  14
  -1.0    1.56     -0.85  1.33     -0.80  1.28     -0.72  1.30
  -0.62   1.35     -0.50  1.36     -0.34  1.34     -0.21  1.29
  -0.11   1.23      0.0   1.22      0.25  1.16      0.50  1.13
   0.75   1.07      1.0   0.98
  14
  -1.0    0.18     -0.85  0.34     -0.80  0.40     -0.72  0.48
  -0.62   0.556    -0.50  0.67     -0.34  0.77     -0.21  0.84
  -0.11   0.89      0.0   0.95      0.25  1.16      0.50  1.35
```

```
 0.75  1.62      1.0   1.94
11
-1.0   0.18     -0.75 -0.13     -0.50 -0.32     -0.32 -0.40
-0.16 -0.42      0.0  -0.39      0.16 -0.28      0.32 -0.16
 0.50  0.01      0.75  0.40      1.0   0.98
11
-1.0   1.56     -0.75  1.12     -0.50  0.90     -0.32  0.82
-0.16  0.76      0.0   0.71      0.16  0.71      0.32  0.76
 0.50  0.90      0.75  1.33      1.0   1.94
14
-1.0   0.70     -0.90  0.70     -0.80  0.68     -0.70  0.63
-0.60  0.53     -0.50  0.47     -0.40  0.46     -0.30  0.45
-0.20  0.45      0.0   0.48      0.25  0.55      0.50  0.66
 0.75  0.83      1.0   1.02
14
-1.0  -1.42     -0.90 -1.32     -0.80 -1.23     -0.70 -1.14
-0.60 -1.07     -0.50 -0.99     -0.40 -0.91     -0.30 -0.84
-0.20 -0.77      0.0  -0.64      0.25 -0.49      0.50 -0.34
 0.75 -0.20      1.0  -0.10
12
-1.0  -1.42     -0.80 -1.12     -0.60 -0.82     -0.50 -0.68
-0.40 -0.55     -0.20 -0.28      0.0  -0.08      0.11  0.0
 0.25  0.12      0.50  0.33      0.75  0.61
 1.0   1.02
13
-1.0   0.70     -0.80  0.50     -0.60  0.40     -0.50  0.39
-0.40  0.38     -0.20  0.33      0.0   0.28      0.11  0.25
 0.25  0.22      0.50  0.14      0.75  0.03      0.92  0.01
 1.0  -0.10
 12
 -1.0  -1.15     -0.90 -1.24     -0.60 -2.80     -0.50 -2.90
 -0.40 -2.70      0.0   0.0       0.12  0.85      0.20  1.10
  0.50  1.02      0.70  1.0       0.90  0.95      1.0   1.0
  4
 -1.0   0.0       0.0   0.0       0.5  -0.80      1.0  -1.46
  7
 -1.0   0.0       0.0   0.0       0.1  -0.02      0.2   0.0
  0.3   0.1       0.9   0.78      1.0   1.0
 12
 -1.0  -1.15     -0.8  -0.50     -0.6  -0.20     -0.4   0.03
 -0.2   0.04      0.0   0.10      0.2   0.15      0.4   0.12
  0.6   0.05      0.8  -0.50      0.9  -0.90      1.0  -1.46
  0
  0
  0
  0
 13
  0.0   0.0       0.05  0.0       0.10  0.025     0.15  0.075
  0.20  0.18      0.30  0.475     0.40  0.625     0.50  0.74
  0.60  0.82      0.70  0.87      0.80  0.84      0.90  0.72
  1.0   0.08
 11
  0.0   0.0       0.1   0.0       0.2   0.13      0.3   0.24
  0.4   0.31      0.5   0.33      0.6   0.3       0.7   0.23
  0.8   0.16      0.9   0.08      1.0   0.0
  6    6
        0.0  0.2         0.4         0.6         0.8         1.0
  0.0   0.0  0.0         0.0         0.0         0.0         0.0
  0.2   0.0  3.0650E-5   7.7239E-5   1.3263E-4   1.9460E-4   2.6207E-4
  0.4   0.0  4.8660E-5   1.2261E-4   2.1053E-4   3.0996E-4   4.1602E-4
  0.6   0.0  6.3760E-5   1.6066E-4   2.7587E-4   4.0485E-4   5.4514E-4
  0.8   0.0  7.7239E-5   1.9463E-4   3.3419E-4   4.9044E-4   6.6037E-4
  1.0   0.0  8.9628E-5   2.2585E-4   3.8780E-4   5.6910E-4   7.6631E-4
/
/  **** ACCUMULATOR DATA ****
BB16
```

```
SB1601
    50    41    70.    30.    35.0    44.    1.0
  75.0  3.0    0.5
SB1602
    51    43    23.3  10.    35.0    44.    1.0
  75.0  1.0    0.5
/
/  **** BREAK POINT DATA ****
BB17
  10  2.001E-3  0.8  0.6  0.6  0.8  0.6  0.6  0.0  1.0  0.0  1.0
  1.0  1.0
   6
   0.0 1.0  7.5 2.7  15.0 4.0  30.0 4.0  60.0 4.0  1000.0 4.0
/
/  **** PRESSURIZER DATA ****
BB18
  49   39   11   3.58  15.56  9.0  0.99  0.1  2.0  370.0
  50.0  1.0  0.1  0.0  0.0
  0.915  0.915  0.915  1.525  3.05  4.58
  0.564  0.67   0.619
  2
  0.0  1.0 1.0 1.0   1000.0  1.0 1.0 1.0
/
/  **** STEAM GENERATOR DATA ****
BB19
SB1901
  47   3248   5    7    3    1
  5.5    18.9    0.7    0.5    5.858407E-4   1.0E-2   10.4   4.0
  222.1  474.5   0.1    0.95   62.0          0.2      0.1
  -46.  -30.   -15.
  0.001   80.   0.5    0.5    0.5
   3
  0.0 1.0 1.0 1.0 1.0 1.0 1.0 1.0 1000.0 1.0 1.0 0.0
SB1902
  48   9744  16   18    3    1
  16.5   18.9    2.1    0.5    5.858407E-4   1.0E-2   10.4   4.0
  222.1  1423.5  0.1    0.95   62.0          0.2      0.1
  -46.  -30.   -15.
  0.003   80.   0.5    0.5    0.5
   3
  0.0 1.0 1.0 1.0 1.0 1.0 1.0 1.0 1000.0 1.0 1.0 0.0
/
/  **** CORE DATA ****
BB20
/
/  **** AVERAGE CHANNEL DATA ****
SB2001
 1  39800   25   29   1    5   1   1   5  3
/
/  **** HOT CHANNEL DATA ****
SB2002
 2    200   30   34   6    10  1   1
/
/  **** REACTIVITY DATA ****
BB21
 1.0E-04
 0.0124   0.0212E-2  0.0305   0.1402E-2
 0.1110   0.1254E-2  0.3010   0.2529E-2
 1.1300   0.0736E-2  3.0000   0.0269E-2
 0.6      1.2
/ ****  TABLE  DATA  ****
 3
 0.0 0.0 0.5 -5.0 1.0 -25.0
 5
 18.0 3.56E-3 538.0 0.0 1093.0 -3.08E-3 1649.0 -2.70E-3 2760.0 -2.44E-3
 5
```

```
0.01 0.0 1.0 -0.1 1.5 -0.2 2.0 -3.0 1000.0 -8.0
/
/  **** METAL-WATER REACTION DATA ****
BB22
SB2201
 2
 1  2
 1.54E+3  0.775E-4  2.29E+4  4.7268E-7   4.7268E-7
/
/  **** FUEL GAP DATA ****
BB23
SB2301
 2
 1  2
 0.0301  0.0      5.0E-05    1.235E-5  0.0  0.0     0.0  100.0
 0.6     0.6      0.0
 0.9495  0.0157   0.0028     0.0   0.032  0.0  0.0
/
/  **** BURST DATA ****
BB24
SB2401
 2
 1  2
 2  2
 5.0E+7   6.96E-8  2.87E+4    2.86E-3  1.15     1.528
 1.49E-7  2.0E-8   1.25E-16   1.85E-1  8.0E+9   3.3E-3  0.1
 6.0E-01
/
/ **** CONTROL DATA FOR HEAT SLAB ****
BB25
 1  1
/
/ **** HEAT SLAB DATA ****
BB26
SB2601
1       0    2       1        39800       2
0.0     5.36E-03    0.0     0.0
1       -1     3       -1
4.69E-03     0.0
2     -2     2     0
6.2E-04      0.0
0     25     3.0E-01
/
SB2602
2       0    2       1        39800       2
0.0     5.36E-03    0.0     0.0
1  -1      3      -1
4.69E-03     81242.76575
2  -2      2      0
6.2E-04      0.0
0     26     1.0
/
SB2603
3       0    2       1        39800       2
0.0     5.36E-03    0.0     0.0
1     -1     3       -1
4.69E-03     141090.466
2     -2     2     0
6.2E-04      0.0
0     27     1.0
/
SB2604
4       0    2       1        39800       2
0.0     5.36E-03    0.0     0.0
1     -1     3       -1
4.69E-03     81242.76575
```

```
2      -2    2      0
6.2E-04      0.0
0      28      1.0
/
SB2605
5      0     2      1      39800      2
0.0    5.36E-03    0.0    0.0
1      -1    3      -1
4.69E-03     0.0
2      -2    2      0
6.2E-04      0.0
0      29      3.0E-01
/
SB2606
6      0     2      1      200      2
0.0    5.36E-03    0.0    0.0
1      -1    3      -1
4.69E-03     0.0
2      -2    2      0
6.2E-04      0.0
0      30      3.0E-01
/
SB2607
7      0     2      1      200      2
0.0    5.36E-03    0.0    0.0
1      -1    3      -1
4.69E-03     108047.5175
2      -2    2      0
6.2E-04      0.0
0      31      1.0
/
SB2608
8      0     2      1      200      2
0.0    5.36E-03    0.0    0.0
1      -1    3      -1
4.69E-03     187681.9981
2      -2    2      0
6.2E-04      0.0
0      32      1.0
/
SB2609
9      0     2      1      200      2
0.0    5.36E-03    0.0    0.0
1      -1    3      -1
4.69E-03     108047.5157
2      -2    2      0
6.2E-04      0.0
0      33      1.0
/
SB2610
10     0     2      1      200      2
0.0    5.36E-03    0.0    0.0
1      -1    3      -1
4.69E-03     0.0
2      -2    2      0
6.2E-04      0.0
0      34      3.0E-01
/
SB2611
11     0     1      0      1      1
3.7E-01      8.0E-02 0.0    0.0
1      1     5      0
8.0E-02      0.0
1      0     5.2
/
```

```
SB2612
12      0      2      0         1            1
4.7E-01     5.7E-01  0.0        0.0
1     1      5      0
1.0E-01     0.0
2     0      1.0
/
SB2613
13      0      1      0         1            1
5.65E-01     1.1E-01         3.0E01    5.0E-02
1     1      5      0
1.1E-01     0.0
3     -1     1.5
/
SB2614
14      0      2      0         1            1
6.45E-01     7.75E-01           30.0         5.0E-02
1     1      5      0
1.3E-01     0.0
4     -1     2.0
/
SB2615
15      0      1      0         1            1
6.45E-01     1.3E-01           2.890594E02    0.0
1     1      5      0
1.3E-01     0.0
8     -2     1.6
/
SB2616
16      0      2      0         1            1
4.0E-01     4.8E-01    2.890491E2      0.0
1     1      5      0
8.0E-02     0.0
9     -2     12.9
/
SB2617
17      0      1      0         1            1
3.5E-01     8.0E-02  0.0        0.0
1     1      5      0
8.0E-02     0.0
0     10     6.6
/
SB2618
18      0      2      0         1            1
3.5E-01     4.3E-01  0.0        0.0
1     1      5      0
8.0E-02     0.0
0     11     1.5
/
SB2619
19      0      1      0         1            1
3.5E-01     8.0E-02  3.0E01   5.0E-02
1     1      5      0
8.0E-02     0.0
-1    12     3.0
/
SB2620
20      0      2      0         1            1
3.7E-01     4.5E-01   30.0      5.0E-02
1     1      5      0
8.0E-02     0.0
-1    13     2.0
/
SB2621
21      0      1      0         1            1
3.7E-01     8.0E-02  3.2828E02      0.0
```

```
1     1     5        0
8.0E-02    0.0
-2   14-    3.2
/
SB2622
22    0    2     0         1         1
6.45E-01    7.75E-01          3.282953E2  0.0
1     1     5        0
1.3E-01    0.0
-2    15    4.5
/
SB2623
23    0    1     0         1         1
1.19E-01    1.0E-01     .0.0        0.0
1     1     5        0
1.0E-01    0.0
25    23    0.3
/
SB2624
24    0    2     0         1         1
1.19  1.29      0.0      0.0
1     1     5        0
1.0E-01    0.0
26    23    1.0
/
/   **** MATERIAL DATA ****
BB27
SB2701
 1
 STAINLESS STEEL ( 18CR 8NI )
 2
 20.0 7820.0  1000.0 7820.0
 2
 20.0 0.118   1000.0 0.118
 5
 20.0 3.5E-3  100.0 3.8E-3  200.0 4.0E-3  400.0 4.7E-3  600.0 5.5E-3
/
/  **** RELATIVE POWER DATA FOR HEAT SLAB ****
BB28
SB2801
 1
 2
 0.0 0.0  1000.0 0.0
/
/  **** VALVE DATA ****
BB29
SB2901
  1   -2   43   5.0   5.0
SB2902
  2   -2   45   0.1   1.0
SB2903
  3   -3   44   0.1   1.0
SB2904
  4   -3   46   0.1   1.0
SB2905
  5    2   35   0.1   1.0
BEND
```

D.2 Input Data for Restart Job

```
  --- THYDE-P2 ------------------------------------------------------
/
/
/============== ALPHA-DELAY MODEL ( INNER CALC. OPTION ) ===============
/                                                   85/06/10
```

```
/
/  **** PROBLEM CONTROL DATA ****
BB01
 2  9  4  18  1  0  5  0     0   99.0
 0
/ 4
/ 43 44 45 46
/
/  **** MINOR EDIT DATA ****
BB02
PRE-11  PRA-12  GLE-25  GLA-25  GLE-35  GLE-36  GLA-37  GLE-11  GLA-12
/
/  **** TIME STEP WIDTH CONTROL DATA ****
BB03
SB0301
   -2
SB0302
   10  30  50   0   1.0E-3   1.0E-6      0.004
SB0303
   20  40  50   0  64.0E-3   1.0E-6    200.0
SB0304
   50  20  50   0   4.0E-3   1.0E-6     10.0
SB0305
   50  20  50   0  16.0E-3   1.0E-6   1000.0
/
/  **** TRIP CONTROL DATA ****
BB04
SB0401
  1   0   1   0  1000.000 0.0
SB0402
  5  47   1   0     0.4   0.0
SB0403
  5  48   1   0     0.4   0.0
SB0404
  2  10   1   0     0.1   0.0
SB0405
  2  21   1   0     0.1   0.0
SB0406
  3   0   1   0     0.1   0.0
SB0407
  4   1   1   0    20.01  0.0
SB0408
 -4   1   1   0  1000.0   0.0
SB0409
  4   2   1   0    20.01  0.0
SB0410
 -4   2   1   0  1000.0   0.0
SB0411
  4   5   1   0  1000.0   0.0
SB0412
 -4   5   1   0  2000.0   0.0
SB0413
  6   1  -3   1   240.0   0.005
SB0414
  6   2  -3   1   250.0   0.0
SB0415
  6   3  -3   1   360.0   0.0
SB0416
 -6   1   3   1   350.0   0.0
SB0417
 -6   2   3   1   305.0   0.0
SB0418
 -6   3   3   1   380.0   0.0
/
BEND
```